NATIONAL
URANIUM
TAILINGS
PROGRAM

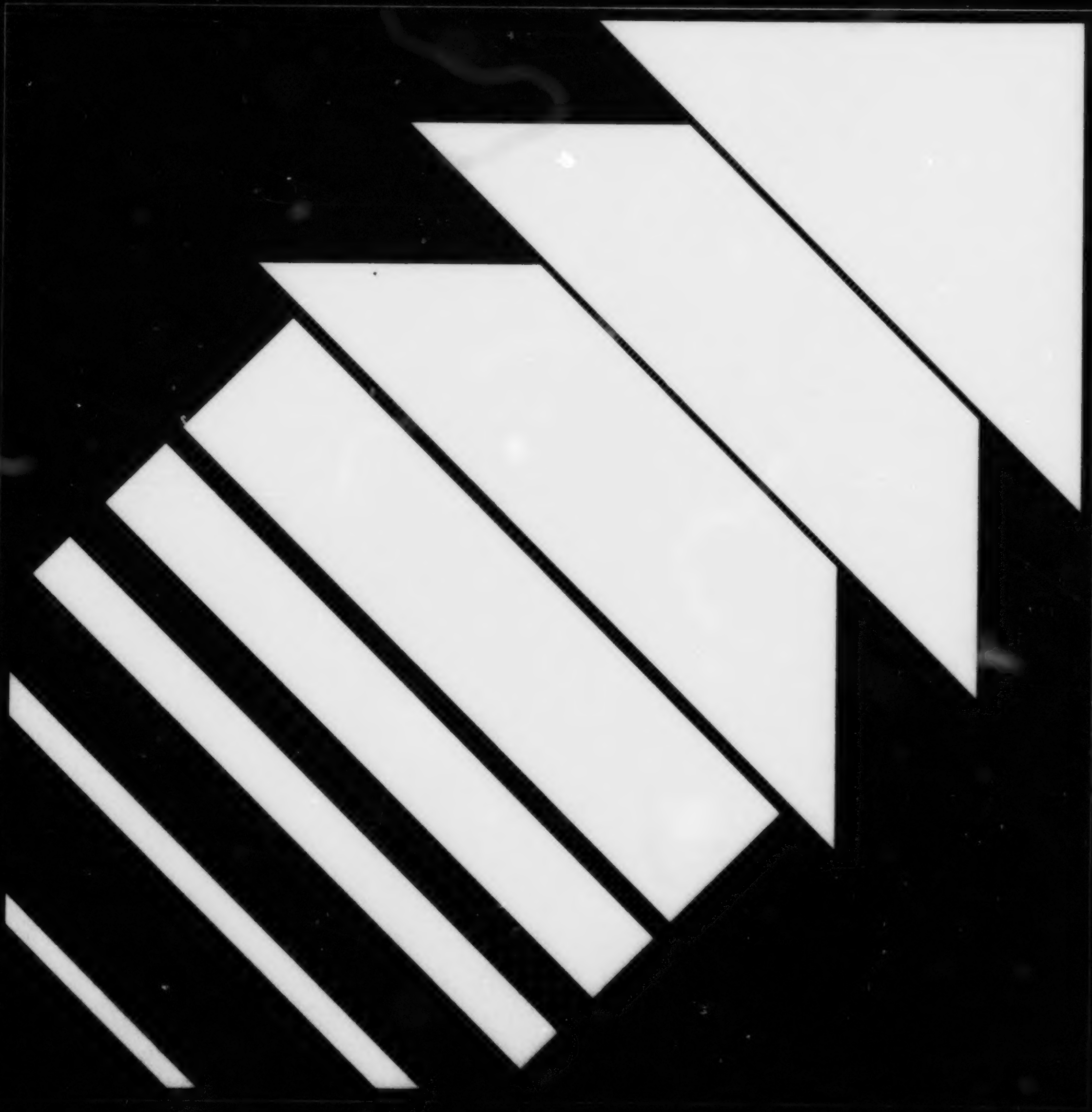

Canada

AN EXPERIMENTAL INVESTIGATION OF WIND-GENERATED SUSPENSIONS OF PARTICULATE MATTER FROM TAILINGS DISPOSAL AREAS

DSS File # 14SQ.23241-3-1667
Contract # 1SQ83-00268

A Research Report Prepared for:

The National Uranium Tailings Program
Canada Centre for Mineral and Energy Technology
Energy, Mines and Resources Canada
555 Booth Street
Ottawa, Ontario
K1A 0G1

by

Atmospheric Environment Research
Box 65
Oakville, Ontario
L6J 4Z5

March 1986

MICROMEDIA
APR 23 1986

176 pp

TABLE OF CONTENTS

Page

ABSTRACT i

LIST OF TABLES ii

LIST OF FIGURES iii

1.0 INTRODUCTION 1

2.0 PROGRAM DESCRIPTION 2

- 2.1 Background 2
- 2.2 Objective and Activities 2

3.0 PROBLEM ANALYSIS 5

- 3.1 Introduction 5
- 3.2 Soil Transport Models 5
  - 3.2.1 Wind Erosion 6
  - 3.2.2 Saltation Flux 9
  - 3.2.3 Suspension Flux 14
  - 3.2.4 Suspension Factor & Mass-Loading 14
  - 3.2.5 Suspension Rate 15
- 3.3 Suspension Rate as a Function of Saltation 17

4.0 EXPERIMENTAL CONIDERATIONS 21

- 4.1 General 21
- 4.2 Test Slab and Mini Wind Tunnel 22
- 4.3 Data Acquisition 23
  - 4.3.1 Particle Sampling Trains 24
  - 4.3.2 Digital Image Analysis System 25
  - 4.3.3 Turbulent Flow Measurements 27

5.0 RESULTS AND MODEL SPECIFICATIONS 28

- 5.1 Concentration and Saltation Measurements 28
- 5.2 Turbulent Wind Velocity Measurements 30
- 5.3 Particle Size Analysis 31
- 5.4 Model Development 33

TABLE OF CONTENTS CONT'D

6.0 SUMMARY AND CONCLUSIONS 40

REFERENCES 41

NOMENCLATURE

APPENDIX A HOT WIRE CALIBRATION PROCEDURE A1

APPENDIX B PARTICLE DISTRIBUTION OF PARENT SURFACE SAMPLES AND SALTATION SAMPLES B1

APPENDIX C PARTICLE DISTRIBUTION OF SELECTED FILTERS C1

APPENDIX D PARTICLE DISTRIBUTION OF VERTICAL FLUXES D1

APPENDIX E CHEMICAL CHARACTERISTICS OF TAILINGS SAMPLES E1

TABLES

FIGURES

ABSTRACT

An investigation of the wind erosion of uranium mine tailing material has been performed. This involved a detailed literature survey of previous work in the area to provide necessary background and a concomitant wind tunnel experiment to determine the effect of various parameters on the mechanism by which the tailing particulates become airborne. The analysis of the experimental data has yielded mathematical models for predicting the net mass fluxes in the case of dry and moist tailings.

LIST OF TABLES

TABLE	
3.1	Enviromental Variables and Model Parameters for the Wind Erosion Equations
3.2	Variables Which Influence Suspension
4.1	Experimental Runs and Nomenclature
4.2	Postion and Nomenclature of Particle Samplers
4.3	Location of Hot Wire Probes
5.1	Saltation Fluxes
5.2	Variation of Surface Friction Velocity with Distance
5.3	Dry Saltation Flux Particle Distribution
5.4	Wet Saltation Flux Particle Distribution
5.5	Dry and Wet Concentration Particle Distribution
5.6a	Slope of Dry Concentration Profiles
5.6b	Slope of Wet Concentration Profiles
5.7	Dry Net Vertical Flux-- Fine and Coarse Fractions
5.8	Wet Net vertical Flux-- Fine and Coarse Fractions

LIST OF FIGURES

Figure

3.1 Force diagram for an individual particle

3.2 Variation of threshold velocity

3.3 Wind Speed in moving saltation

3.4 Hypothetical energy and suspension factor curve

3.5 Size distribution of soil particles

4.1 Tailings Test Section and Sampling Configuration

4.2 Average Particle Distribution of Tailings

4.3 Rough " Flat Plate "

4.4 Hot Wire Anemometry Equipment

5.1 Concentration Profile for
Surface: Dry Turbulence: Low Wind: 4.5 m/s Rep # 1&2

5.2 Concentration Profile for
Surface: Wet Turbulence: Low Wind: 4.5 m/s Rep # 1&2

5.3 Concentration Profile for
Surface: Dry Turbulence: High Wind: 4.5 m/s Rep # 1&2

5.4 Concentration Profile for
Surface: Wet Turbulence: High Wind: 4.5 m/s Rep # 1&2

5.5 Concentration Profile for
Surface: Dry Turbulence: Low Wind: 7.5 m/s Rep # 1&2

5.6 Concentration Profile for
Surface: Wet Turbulence: Low Wind: 7.5 m/s Rep # 1&2

5.7 Concentration Profile for
Surface: Dry Turbulence: High Wind: 7.5 m/s Rep # 1&2

5.8 Concentration Profile for
Surface: Wet Turbulence: High Wind: 7.5 m/s Rep # 1&2

5.9 Concentration Profile for
Surface: Dry Turbulence: Low Wind: 9.5 m/s Rep # 1
Surface: Dry Turbulence: High Wind: 9.5 m/s Rep # 1

5.10 Concentration Profile for
Surface: Wet Turbulence: Low Wind: 9.5 m/s Rep # 1
Surface: Wet Turbulence: High Wind: 9.5 m/s Rep # 1

LIST OF FIGURES (Cont'd)

Figure

5.11 Wind and Turbulence Profiles for Turbulence: Low Wind Speed: 4.5 m/s
5.12 Wind and Turbulence Profiles for Turbulence: High Wind Speed: 4.5 m/s
5.13 Wind and Turbulence Profiles for Turbulence: Low Wind Speed: 7.5 m/s
5.14 Wind and Turbulence Profiles for Turbulence: High Wind Speed: 7.5 m/s
5.15 Wind and Turbulence Profiles for Turbulence: Low Wind Speed: 9.5 m/s
5.16 Wind and Turbulence Profiles for Turbulence: High Wind Speed: 9.5 m/s.
5.17 Average Particle Distribution for Surface: Dry Turbulence: Low Wind: 4.5 m/s
5.18 Average Particle Distribution for Surface: Dry Turbulence: High Wind: 4.5 m/s
5.19 Average Particle Distribution for Surface: Dry Turbulence: Low Wind: 7.5 m/s
5.20 Average Particle Distribution for Surface: Dry Turbulence: High Wind: 7.5 m/s
5.21 Average Particle Distribution for Surface: Dry Turbulence: Low Wind: 9.5 m/s
5.22 Average Particle Distribution for Surface: Dry Turbulence: High Wind: 9.5 m/s
5.23 Average Particle Distribution for Surface: Wet Turbulence: Low Wind: 4.5 m/s
5.24 Average Particle Distribution for Surface: Wet Turbulence: High Wind: 4.5 m/s
5.25 Average Particle Distribution for Surface: Wet Turbulence: Low Wind: 7.5 m/s
5.26 Average Particle Distribution for Surface: Wet Turbulence: High Wind: 7.5 m/s
5.27 Average Particle Distribution for Surface: Wet Turbulence: Low Wind: 9.5 m/s

LIST OF FIGURES (Cont'd)

Figure

5.28 Average Particle Distribution for
Surface: Wet Turbulence: High Wind: 9.5 m/s

5.29 Dry and Wet Median Particle Size vs. u_*

5.30 Average Particle Distribution on filters
Surface: Dry Turbulence: Low Wind: 7.5 m/s
Surface: Dry Turbulence: Low Wind: 9.5 m/s

5.31 Average Particle Distribution on filters
Surface: Dry Turbulence: High Wind: 7.5 m/s
Surface: Dry Turbulence: High Wind: 9.5 m/s

5.32 Average Particle Distribution on filters
Surface: Wet Turbulence: Low Wind: 7.5 m/s
Surface: Wet Turbulence: Low Wind: 9.5 m/s

5.33 Average Particle Distribution on filters
Surface: Wet Turbulence: High Wind: 7.5 m/s
Surface: Wet Turbulence: High Wind: 9.5 m/s

5.34 Mean Vertical Flux Profile for
Surface: Dry Turbulence: Low Wind: 4.5 m/s
Surface: Dry Turbulence: High Wind: 4.5 m/s

5.35 Mean Vertical Flux Profile for
Surface: Dry Turbulence: Low Wind: 7.5 m/s
Surface: Dry Turbulence: High Wind: 7.5 m/s

5.36 Mean Vertical Flux Profile for
Surface: Dry Turbulence: Low Wind: 9.5 m/s
Surface: Dry Turbulence: High Wind: 9.5 m/s

5.37 Mean Vertical Flux Profile for
Surface: Wet Turbulence: Low Wind: 4.5 m/s
Surface: Wet Turbulence: High Wind: 4.5 m/s

5.38 Mean Vertical Flux Profile for
Surface: Wet Turbulence: Low Wind: 7.5 m/s
Surface: Wet Turbulence: High Wind: 7.5 m/s

5.39 Mean Vertical Flux Profile for
Surface: Wet Turbulence: Low Wind: 9.5 m/s
Surface: Wet Turbulence: High Wind: 9.5 m/s

5.40 Dry Vertical Flux @ 2.5 cm vs. u_*

5.41 Wet Vertical Flux @ 2.5 cm vs. u_*

5.42 Dry Vertical Flux, Saltation Flux and
Suspension Factor vs. u_*

LIST OF FIGURES (Cont'd)

Figure

5.43 Wet Vertical Flux, Saltation Flux and Suspension Factor vs. u_*

5.44 Dry Net Vertical Flux Profiles

5.45 Wet Net Vertical Flux Profiles

5.46 Average Mass Flux Particle Distribution
Surface: Dry Turbulence: Low Wind: 7.5 m/s
Surface: Dry Turbulence: Low Wind: 9.5 m/s

5.47 Average Mass Flux Particle Distribution
Surface: Dry Turbulence: High Wind: 7.5 m/s
Surface: Dry Turbulence: High Wind: 9.5 m/s

5.48 Average Mass Flux Particle Distribution
Surface: Wet Turbulence: Low Wind: 7.5 m/s
Surface: Wet Turbulence: Low Wind: 9.5 m/s

5.49 Average Mass Flux Particle Distribution
Surface: Wet Turbulence: High Wind: 7.5 m/s
Surface: Wet Turbulence: High Wind: 9.5 m/s

5.50 Average Net Mass Flux Particle Distribution
Surface: Dry Turbulence: Low Wind: 7.5 m/s
Surface: Dry Turbulence: Low Wind: 9.5 m/s

5.51 Average Net Mass Flux Particle Distribution
Surface: Dry Turbulence: High Wind: 7.5 m/s
Surface: Dry Turbulence: High Wind: 9.5 m/s

5.52 Average Net Mass Flux Particle Distribution
Surface: Wet Turbulence: Low Wind: 7.5 m/s
Surface: Wet Turbulence: Low Wind: 9.5 m/s

5.53 Average Net Mass Flux Particle Distribution
Surface: Wet Turbulence: High Wind: 7.5 m/s
Surface: Wet Turbulence: High Wind: 9.5 m/s

1.0 INTRODUCTION

Atmospheric Environment Research (AER) has carried out a two-year project under a contract with the Department of Supply and Services (DSS), Government of Canada, for the National Uranium Tailings Program (NUTP), CANMET. This project concerns the investigation of wind-generated suspensions of particulate matter from uranium tailing disposal sites, and involves a detailed literature survey and an experimental program in which advanced techniques of data acquisition and analysis are used. The present document is the final project report.

2.0 PROGRAM DESCRIPTION

2.1 Background

Assessing the air quality contribution to a local airshed by a mining and milling operation is a difficult and, often, subjective task. Recommendation of cost-effective abatement strategies requires adequate review and evaluation of all potential fugitive emissions. Algorithms are readily available to estimate the downwind impact of stack released emissions to the local airshed. However, the physics associated with wind induced suspension and transport of fugitive emissions from flat surfaces such as tailings areas are currently not well understood.

The following serves to place the problem in perspective. In 1976, the U.S. EPA estimated that 52% of the 247 Air Quality Control Regions would not meet the U.S. ambient air quality standard (75 $\mu g/m^3$) for suspended particulate matter, even after controls were invoked. Fugitive emissions were estimated to contribute an annual average of 10 $\mu g/m^3$ to levels within a heavily industrialized locale. Generally, these emissions contribute significantly to an airshed's fine particulate mass loading and are of a greater health concern than process emissions.

2.2 Objective and Activities

The objective of the present study is to provide a set of models which characterize wind induced suspension of tailings particulate matter. The study involves updating and documenting recent advances in the field and carrying out wind erosion experiments.

On the basis of a thorough inspection of a typical uranium tailings disposal site (Stanrock, Elliot Lake) and consideration of field-experiment requirements, AER concluded that it would not be feasible to conduct field experiments to obtain the requisite experimental data. It was essential that tailings samples be collected at a number of streamwise locations and heights over a given tailings area under known wind conditions. And it was decided that this could be done most efficaciously by carrying out laboratory wind tunnel simulations of tailings emission events.

In order to make optimum use of available financial and manpower resources, a two-phase program was instituted.

The first phase consisted of a wind tunnel investigation of the creep, saltation and suspension of particulate matter obtained from real tailings sites. Factors investigated were:

- particle size distribution
- moisture content
- turbulence intensity of the wind for smooth and rough boundary layer conditions

The material used for the tests was taken from the Elliot Lake region and results for these tests are presented later in the report (Section 5).

For the second phase of the study, a comprehensive statistical analysis of the data for smooth and rough upstream boundaries has been carried out. This yielded information on the three basic mechanisms of creep, saltation and suspension. As well, correlation of the wind data and the particulate data has allowed basic mathematical models for predicting tailings mass fluxes to be developed.

It should be mentioned that in order to extend the analysis and aid in the development of models of the erosion process, experiments have been initiated with artificial particles by the Turbulence Research Group in the Department of Mechanical Engineering, University of Toronto. The data from these ancillary experiments, which are not part of the present contract, will be analyzed by means of sophisticated digital image processing techniqes and the results will be made available to CANMET at some future time.

3.0 PROBLEM ANALYSIS

3.1 Introduction

Suspension of a contaminant from a natural or man-made source is defined as a mass-transfer process across an air-surface interface. The mass is typically composed of respirable size particulate matter which is subsequently transported into an airshed and contributes to the deterioration of its air quality. Once airborne, aerosols from a suspension process cannot be distinguished from elevated point-source material or from previously-deposited material that has been re-entrained.

Initially, wind induced emissions were studied by the nuclear industry to quantify the impact of long-lived radionuclides on the environment. While there appears to be a great deal of qualitative knowledge about the mechanism of suspension, few quantitative results have been deduced (Travis, 1974). The variability of reported suspension rates from field measurements under similar conditions has underlined the need for insight into the fundamental principles governing this mechanism. A desirable generic model, simulating the suspension process as a vertical mass flux function, would include the particle distribution, the soil surface characteristics, the vegetation cover, and the meteorological variables (Anspaugh, et al, 1975; Sehmel, 1980). Although no model currently exists with the above features, some progress has been achieved in developing quantitative knowledge of the various functions.

3.2 Soil Transport Models

Particulate movement by wind shear stresses has been studied in deserts (Bagnold, 1941) and in agricultural lands (Gillette, 1973-1978, Chepil and Woodruff, 1959-1963). These studies demonstrate that soil movement occurs under three distinct modes of transport:

- surface creep - grains too heavy to be airborne roll or slide along the ground due to forces of the wind or the impact of other grains
- saltation - dislodged particles, ejected into the air stream, gain horizontal momentum from the wind and descend (because of their relatively large masses) to impact with the soil causing soil movement.
- suspension - dislodged particles with light masses follow the turbulent actions of the surface wind.

Nominal particle size (diameter) ranges for each transport mode are (Sehmel, 1980, Anspaugh et al, 1975, Horst, 1977, Travis, 1974):

Surface Creep	1000 - 2000 μm
Particle Saltation	100 - 1000 μm
Suspension	$\leq$ 100 μm

The greatest mass movement occurs by saltation and quantitative studies in soil erosion have been restricted to analyzing the horizontal flux of large particles. Suspension, the vertical particle flux, is much smaller than saltation and has not been studied in depth. However, a correlation between saltation and suspension has been deduced - "suspension of particles does not occur without saltation" (Bagnold, 1959, Gillette et al, 1972).

Various models have been developed to quantitatively estimate the saltation and suspension fluxes. The following provides a description of the physics associated with each mode of transport.

3.2.1 Wind Erosion

A wind erosion equation was designed by agricultural scientists to evaluate potential soil losses on an annual basis

(Chepil and Woodruff, 1963). The 11 key variables known to govern wind erosion are presented in Table 3.1 and result in five equivalent parameters used in the wind erosion equation as

$$E = E(I', C', K', L', V) \qquad (3.1)$$

where E is the potential average annual soil loss,
I' is a soil erodibility index,
C' is a local climate factor,
K' is a soil ridge roughness factor,
L' is a field length,
V is a vegetative cover factor.

The relationship between variables is complex and a single equation to express E as a function of the five parameters is not available. Graphs and charts have been used to solve the equation in a stepwise fashion (Skidmore, et al, 1970). A description of each variable follows.

Soil erodibility or ease of detachment and transport was developed from wind tunnel simulations (Chepil, 1957). The dimensionless soil erodibility index (I) is a relative measure based on the percentage of non-erodible particles exceeding 840 μm. This percentage is typically determined by dry sieving techniques. The index is expressed as

$$I = X_2/X_1 \qquad (3.2)$$

where X_1 is the mass of material eroded from soil containing a non-erodible percentage of 60% and X_2 is the quantity eroded from soil containing a test percentage under the same wind tunnel conditions. Intuitively, as the percentage of non-erodible material increases, the erodibility effectively decreases. Thus, I represents a field which is smooth, bare, wide, unsheltered and non-crusted. Further, to account for increasing erodibility of knolls on the windward slopes, I is multiplied by a factor I_s to produce the field erobility index I' in the wind erosion equation.

A climatic factor (C') was introduced to determine annual soil loss for conditions other than those simulated in the wind tunnel tests. It is an index of the average rate of soil movement as influenced by surface moisture content and average windspeed. Tests have shown that erosion varies inversely with the moisture content (M) (Chepil, 1957) and is proportional to windspeed ($\bar{u}$) cubed. Recent investigations have upgraded the climate factor by introducing the effect of precipitation and evaporation (Blackwood and Wachter, 1978). They show that erosion is inversely proportional to the square of the surface moisture content.

The ridge roughness factor (K') is a function of the physical width, height and spacing of ridges in the surface of the soils. This factor is determined empirically by comparision to a set of standard photographs. Field data have shown that increasing roughness decreases the quantity of mass flow. The U.S. Soil Conversion Service evaluates fields as either smooth, semi-ridged or ridged, depending on the ridge roughness, and assigns numerical values of 1.0, 0.75 and 0.5 respectively as the ridge-roughness factor.

The field length (L') is regarded as the length of field in the prevailing wind direction (D_f) minus the wind sheltered distance (D_b). The wind sheltered distance represents the length of field which is fully protected from wind erosion by a barrier. The mass flow rate was subsequently shown to be proportional to the field length.

The equivalent vegetative cover (V) is a function of three variables including quantity of cover (R'), type of vegetation (S), and orientation of cover (K_o). Empirical properties of vegetative covers influencing erosion have been quantified (Siddoway, Chepil and Armburst, 1965) and expressed in a relative manner. The type of vegetation (S) pertains to the total cross-sectional surface area and is assigned a value of 1 for small grain stubble. The finer the vegetation the greater its surface area, thus providing greater protection from the wind. The orientation factor (K_o) is assigned a value of 1 for flat, small grain stubble aligned parallel to the wind. It can be regarded as a vegetative surface roughness. Erect material will reduce surface windspeeds and thus lower the rate of mass transport. The equivalent vegetative cover is the product of R', S and K_o, and is inversely proportional to the erosion rate.

The general relationship among parameters, variables and the potential soil loss is summarized as follows

$$\begin{aligned} &E \propto I' \propto I \cdot I_s \\ &E \propto C' \propto \frac{\overline{u}^3}{M^2} \\ &E \propto K' \\ &E \propto L' \propto (D_f - D_b) \\ &E \propto \frac{1}{V} \propto \frac{1}{R'SK_o} \end{aligned} \qquad (3.3)$$

The quantities predicted by the wind erosion equation are for net soil loss, with no information on particle size or amount in saltation or suspension. It provides a general quantity of material available for mass transport.

3.2.2 Saltation Flux

Soil erosion occurs by saltation. The most erodible particles become dislodged as the wind approaches the fluid threshold velocity. This threshold wind speed is found by equating the moment due to the particle weight to that of the drag force about the particle pivot point (Bagnold, 1959). As illustrated in Fig. 3.1, and assuming the grain to be spherical, the resulting equation is

$$m\bar{g}(\sin\alpha)\,\frac{d_i}{2} = D_F(\cos\alpha)\,\frac{d_i}{2} \qquad (3.4)$$

$$(\rho_s - \rho_a)\,\frac{\pi}{6}\,d_i^3\bar{g} = D_F\,\frac{\cos\alpha}{\sin\alpha} \qquad (3.5)$$

where D_F is the drag force, m is the mass of a particle with diameter d_i and density ρ_s, α is the pivot angle, ρ_a is the density of air and $\bar{g}$ is gravity.

Since the drag force acting on the particle is proportional to the mean surface stress ($\rho_a u_*^2$) and the particle area normal to the flow,

$$D_F = \beta\,\rho_a\,u_*^2 d_i^2 \qquad (3.6)$$

where β is a coefficient depending on the shape and position of the particle and u_* is the surface friction velocity. Substituting (3.6) into (3.5), an expression for the fluid threshold friction velocity is obtained,

$$u_{*ti} = n\left(\frac{(\rho_s - \rho_a)}{\rho_a}\,\bar{g}d_i\right)^{\frac{1}{2}} \qquad (3.7)$$

where $n = \left(\frac{\pi}{6}\,\frac{\tan\alpha}{\beta}\right)^{\frac{1}{2}} \sim 0.1$ (Bagnold, 1959).

The mean wind profile is expressed as $\bar{u} = \frac{u_*}{k}\ln(z/z_o)$, thus, the mean wind to initiate saltation is expressed in logarithmic form as

$$\bar{u}_{ti}(z) = \frac{n}{k}\sqrt{\frac{\rho_s - \rho_a}{\rho_a}\,\bar{g}d_i}\;\ln\left(\frac{z}{z_o}\right) \qquad (3.8)$$

and represents the wind profile prior to entrainment of particles where k is von Karman's constant.

As illustrated in Fig. 3.2, the minimum fluid threshold velocity occurs for particles of 80 μm in diameter. As saltation continues, particles smaller and larger than the initial erodible size begin to saltate and the system moves into a dynamic state where saltation is maintained as long as the wind velocity is greater than the particle impact threshold velocity, V_{ti} (Fig. 3.2) which is less than the fluid threshold velocity ($\bar{u}_{ti}$).

Bagnold observed, during the wind tunnel studies, that once the air has attained the fluid threshold velocity and particles begin to move, particle drag reduces the wind velocity. Further, the wind velocity at height z' did not change with increasing vertical wind gradients, Fig. 3.3. Bagnold expressed the wind profile in the presence of saltation as

$$\bar{u}(z) = \frac{u'_*}{k} \ln \frac{z}{z'} + V_t(z'), \quad z > z' \qquad (3.9)$$

where u'_* = average friction velocity in the presence of saltation

V_t = average impact threshold velocity

z' = height where $\bar{u} = V_t$: $(z' >> z_o)$

The above expression may be extended to specific size classes. Wind tunnel experiments show that V_{ti} follows the same square root law as $\bar{u}_{ti}$ (Fig. 3.2) and is expressed as,

$$V_{ti}(z') = \frac{n'}{k} \sqrt{\frac{\rho_s - \rho_a}{\rho_a} g d_i} \ln \left(\frac{z'}{z_o}\right) \qquad (3.10)$$

where n' is equal to 0.08 (Fig. 3.2). The drag imposed on the air by the saltating particle is

$$\lambda'_i = \rho_a u'^2_{*i} \qquad (3.11)$$

and, rewriting (3.9), the saltation friction velocity is

$$u'_{*i} = [\bar{u}(z) - V_{ti}(z'_*)] \, k \, [\ln (\frac{z}{z'})]^{-1} \qquad (3.12)$$

Assuming the momentum lost by the air is completely transmitted to the saltating particle, the horizontal mass flow per size class is expressed as,

$$q_{si} = \frac{\rho_a}{g} \, u'^{2}_{*i} w_i \qquad (3.13)$$

where q_{si} = saltation flux, mass per unit width per unit time
w_i = initial vertical velocity

Bagnold postulates that w_i is proportional to the friction velocity (i.e., $w_i = \varepsilon_i u'_{*i}$); thus

$$q_{si} = \varepsilon_i \frac{\rho_a}{g} u'^{3}_{*i} \qquad (3.14)$$

where ε_i is an empirical constant varying according to the particle size distribution and was derived from wind tunnel and field studies. The functional dependence of q_{si} on u^{3}_{*i} was confirmed by wind tunnel and field measurements (Sehmel and Lloyd, 1975). Further, experimental evidence shows that q_{si} varies approximately as the square root of the particle diameter. Bagnold (1941) used 250 μm diameter particles as a standard; thus

$$q_{si} = \varepsilon_i \frac{\rho_a}{g} \left(\frac{d_i}{d_{250}}\right)^{\frac{1}{2}} u'^{3}_{*i} \qquad (3.15)$$

and substituting u'_{*i} from (2.9)

$$q_{si} = \varepsilon_i \frac{\rho_a}{g} \left(\frac{d_i}{d_{250}}\right)^{\frac{1}{2}} (\bar{u}(z) - V_{ti}(z'))^3 \left(\frac{k}{\ln(z/z')}\right)^3$$

$$\text{if} \quad \bar{u}(z) > V_{ti}(z')$$

or

$$q_{si} = 0 \quad \text{if } \bar{u}\,(z) < V_{ti}(z') \tag{3.16}$$

where d_{250} = standard particle diameter (250 μm)

ε_i = 1.5 for nearly uniform sand
= 1.8 for naturally graded sand
= 2.8 for wide range of particle size

Gillette (1976) carried out wind tunnel simulations to evaluate the total horizontal mass flux. Measured parameters comprised soil moisture content, ridge roughness, vegetative residue and soil erodibility, which are included in the wind erosion equation. Work carried out by Chepil and Woodruff (1959) state that the "wind tunnel erodibility" is given as

$$X = \frac{I}{(K_r\ V)^{1.26}} \tag{3.17}$$

where X is the "wind tunnel erodibility"
I' is the erodibility index
K_r is the ridge roughness
V is the equivalent vegetative cover

The moisture content was used to reduce the wind shear stress and, subsequently, the friction velocity. Gillette determined that the horizontal mass flux was also a function of the friction velocity cubed. The resulting equation was

$$q_s = 0.16\ \frac{L'X}{16500}\ \left(\frac{u_*}{78}\right)^3 \tag{3.18}$$

$$\text{for } \frac{L'X}{16500} \leq 1$$

and

$$q_s = 0.16\ \left(\frac{u_*}{78}\right)^3 \tag{3.19}$$

$$\text{for } \frac{L'X}{16500} > 1$$

where u_* is the friction velocity and L' is the effective length of field parallel to the wind. Gillette modified the above equation to include the average fluid threshold velocity (u_{*t}) by replacing u_*^3 with $u_*^2(u_* - u_{*t})$ (Gillette and Cowherd, 1980).

Gillette's equations for saltation do not contain information regarding particle size but, as in the previous equations, show a strong dependence on the friction velocity cubed. The above equations are similar to the concept of the erosion equation (Chepil and Woodruff, 1957) but does distinguish between saltation and suspension.

3.2.3 Suspension Flux

Soil erosion studies have been able to identify many factors which influence suspension (Table 3.2). It is evident that the suspension process is time dependent and very complex. Faced with a need to estimate air concentrations from suspensions, researchers have developed three primary methods of calculations: the suspension factor, the mass-loading of air and the suspension rate[1].

3.2.4 Suspension Factor & Mass-Loading

The suspension factor (S_f) is the ratio of air contaminant concentration to the quantity of contaminant per unit area below the location where the air is sampled (Healy, 1976).

$$S_f(m^{-1}) = \frac{\text{Airborne Concentration (units/m}^3\text{)}}{\text{Surface Contamination (units/m}^2\text{)}} \quad (3.20)$$

This simple approach neglects many factors which contribute to suspension. Its deficiencies include 1) airborne concentrations for inhalation are assumed to be related to the surface concentration on the soil at a person's feet rather than upwind, 2) it is applicable only to conditions where measurements took place and, 3) there is a lack of built-in classification of source characteristics and causes of suspension. Tabulated data, from a variety of experiments, illustrate the uncertainty associated with this concept. The magnitude of the suspension factor ranges from 10^{-10} to 10^{-4} (m^{-1}) for freshly deposited material in arid and semi-arid climates. This wide variation in factors is the result of different measurement heights and particle size distributions.

---

[1] Suspension factor and suspension rate are also known as the resuspension factor and resuspension rate in the literature.

Mass-loading estimates of contaminant airborne concentration (i.e., $g^{137}Cs/m^3$) are obtained by multiplying the airborne gravimetric concentration (g soil/m^3) by the soil contamination ($g^{137}Cs$/g soil). This is not a predictive tool, but a scaling technique initially used by the nuclear industry for determining local airborne contamination. Both the suspension factor and mass loading approach are adequate in calculating the air contamination in the vicinity of the breathing zone from local sources. The mass loading approach cannot be used in evaluating the particulate vertical fluxes and subsequent transport downwind. The suspension factor has been historically adopted for evaluating the air concentration in post dispersion scenarios. Another application of the suspension factor will be discussed later.

3.2.5 Suspension Rate

The suspension rate describes the fraction of material on the ground that becomes airborne under the influence of a given action. The vertical suspension flux from the ground to the air is expressed as,

$$Q_v = \frac{dG}{dt} = \nabla G \qquad (3.21)$$

where G = amount of surface contamination (g/m^2)
Q_v = vertical suspension flux (g/m^2-s)
∇ = suspension rate (s^{-1})

This flux would represent a source term or boundary condition for downwind diffusion, transport and subsequent deposition. Like the suspension factor, ∇ is influenced by many factors.

A very limited number of measurements of ∇ have been made. Healy and Fuquay (1958) obtained rates from 10^{-8} to 10^{-7} s^{-1} at wind speeds of 3 m/s for suspension of desert soil. Sehmel and Lloyd (1976) found values from 10^{-10} to 10^{-8} s^{-1} for respirable particles and 10^{-11} s^{-1} for large particles in lightly vegetated areas. Anspaugh, et al (1975) calculated values between 10^{-12} and 10^{-10} s^{-1} downwind of plutonium deposits. As in the case of the suspension factor, a lack of uniform measuring techniques (height above ground, particle size and soil contamination) is apparent; thus a wide variation in reported data is found. One result has evolved from this data - suspension is dependent on the wind speed.

Shinn, et al (1974) found plutonium dust fluxes to be proportional to $u_*^{3.09}$ and the associated concentration (flux ÷ wind) to be proportional to $u_*^{2.09}$ at the USAEC's Nevada Test Site. This agrees well with the Sehmel and Orgill (1973) results that plutonium concentrations at Rocky Flats are a function of $\bar{u}^{2.1}$ and subsequently that the vertical flux is a function of $\bar{u}^3$. Similarly, Anspaugh, et al (1975), found that the suspension rate correlates with u_*^3 with a confidence level of 99.95%.

Wind tunnel experiments carried out by Fairchild and Tillery (1982), suggest that the suspension rate increases with the wind velocity, not only because of the increase in wind energy but because of a more efficient utilization of the wind energy by the saltation mechanism, i.e., the saltating particles carry amounts of energy directly to the surface. This energy is the combination of the kinetic energy of the saltating particles and the wind. Gillette (1976) noted that the vertical flux of aerosols increased with wind speed at about the same rate as the horizontal sand flux for coarse soil. For finer soils, the vertical aerosol flux increased at a greater rate. This rate increase can be regarded as a higher energy transfer from saltation to suspension caused by the "sand blasting" effect of the saltating particles into a reservoir of fine particles.

3.3 Suspension Flux As a Function of Saltation

As illustrated in sections 3.1 and 3.2, the fluxes of saltation and suspension are both proportional to the wind-speed cubed. A dimensional argument for determining the relationship between saltation and suspension is possible (Mills, et al, 1974).

In the presence of a large saltation flux, the chance of a particle impacting the ground is also large. If the distance between impacts is large, particles will stay aloft longer. This implies that the number of ground impacts of saltating particles per unit area per unit time will be directly proportional to the saltation rate and inversely proportional to the distance between ground impacts. Since saltating particles are energy carriers, the number of bonds which are broken between small and large particles should be proportional to the kinetic energy ($\frac{1}{2} m \overline{u}^2$) of the saltating particles. Thus,

$$Q_v = \Omega q_s \tag{3.22}$$

where Q_v is the suspension flux, q_s is the 'unit width' saltation flux (3.16) and Ω is a dynamic suspension factor with units m^{-1} similar to the suspension factor (S_f) of section 3.2. It represents the energy transfer from the saltating particle to the suspended particle. Hypothetical curves of Ω and particle energy required for uplift versus particle size are illustrated in Fig.

3.4. As particles increase in size, a corresponding increase in energy is needed to overcome the inertial forces and Ω becomes small. As the particle size decreases, the energy required for uplift diminishes and Ω increases to a maximum value. The Ω curve now begins to decrease with particle size because of the increase in energy required to overcome the Brownian forces acting on these smaller particles.

Gillette (1972-1978) reported the change in the mass size distribution of particles in the parent soil and airborne particles in the first 1.3 cm, 1 m and 1.5 m above the ground, for two different soils at two wind speeds (Fig. 3.5). For both soils, the size distribution at 1.3 cm is similar to the parent soil and reflects the availability of particles to be entrained. At 1 m, the mass of particles greater than 40 μm is reduced because of their high sedimentation velocities and particles smaller than 20 μm become important for Soil I. The peak at 100 μm for Soil I is caused by the agglomeration of smaller particles and can therefore be considered an anomaly. Soil II best illustrates the spectral change from saltation (1.3 cm) to suspension (1.5 m).

Dust suspension as a function of saltation has been incorporated into various computer models used by the U.S. Nuclear Regulatory Commission (NRC) including UDAD and MILDOS, as well as part of NRC's Final Generic Environmental Impact Statement (FGEIS). These algorithms are based on a model developed by Travis (1974). Here the horizontal mass flux is calculated using

$$F_h = X\left(\frac{u_{*e}}{u_{*r}}\right)^2\left(\frac{U_{*e}}{U_{*r}} - \frac{u_{*t}}{u_{*r}}\right) \qquad (3.23)$$

where F_h is the horizontal mass flux (in $g/cm^2.s$)
X is the "wind tunnel" erodability
u_{*e} is the effective friction velocity
u_{*r} is the reference friction velocity for conditions used to determine X and
u_{*t} is the average fluid threshold velocity

As in previous discussions, the horizontal mass flux is proportional to the friction velocity cubed,

$$F_h = C_h\, u_*^3 \tag{3.24}$$

or

$$\frac{F_h}{C_h u_*^3} = 1 \tag{3.25}$$

where C_h is a constant equal to $1 \times 10^{-6} (g \cdot s^2/cm^4)$ (Gillette, 1973).

The vertical flux of line particulate was calculated using

$$F_v = C_v\left(\frac{u_*}{u_{*t}}\right)^{p/3 + 3} \tag{3.26}$$

where F_v is the vertical flux
C_v is a constant (2×10^{-10} g/cm^2.s)
p is the mass percent of particles < 20 μm

Travis developed this equation from data collected by Gillette and carried out a regression analysis. Equations (3.24) and (3.26) are combined to give

$$F_v = F_h\left(\frac{C_v}{C_h\ u_{*t}}\right)\left(\frac{u_*}{u_{*t}}\right)^{p/3} \tag{3.27}$$

Two limiting cases were noted by Travis: (1) the vertical mass flux goes to zero as the surface friction velocity approaches the fluid threshold velocity, (2) the vertical flux goes to zero as p approaches zero. The first case is satisfied by (3.23). Travis satisfies the second by subtracting 1 as follows,

$$F_v = F_h\left(\frac{C_v}{C_h\ u_{*t}}\right)\left(\left[\frac{u_*}{u_{*t}}\right]^{p/3} - 1\right) \tag{3.28}$$

thus forcing the vertical flux to zero for the second case.

Travis' equations are of great interest since they link suspension and saltation and also contain particle size information.

4.0 EXPERIMENTAL CONSIDERATION

4.1 General

As mentioned earlier, a series of controlled wind tunnel tests were carried out to investigate various aspects of the wind erosion of tailings disposal areas. These tests were conducted in the UTME micro-meteorological wind tunnel with a simulated tailings area comprising a slab of tailings material obtained from the Stanrock tailings disposal site located in Elliot Lake on the property of Denison Mines Ltd. This slab is referred to as the "test slab".

The primary objective of the investigation was to measure the amount of tailings material eroded from the surface of the test slab under known surface and wind conditions, and hence develop a mathematical model for the mass flux, which would serve to provide the source term in a higher order model describing the total wind erosion process.

The following measurements were obtained:

- particle concentrations at four elevations above the test slab, for three downwind stations along the test slab,
- saltation rates at the trailing edge of the test slab,
- particle size distributions of the tailings before and after the tests,
- particle size distributions of selected filters,
- particle size distributions of saltation samples,
- moisture content of the tailings, and
- mean wind velocity and turbulence intensities.

These measurements were carried out for three different wind velocities (4.5 m/s, 7.5 m/s and 9.5 m/s), two different boundary layer conditions (smooth and rough) and two different surface moisture conditions (0% and ~ 5%). As well, two replicates of the measurements pertaining to the 4.5 m/s and 7.5 m/s wind conditions were made. Thus, a total of 20 tests were conducted - 10 "dry tests" (i.e., tests with dry tailings) and 10 "wet tests" (i.e., tests with moist tailings). Table 4.1 presents a list of the various experimental runs and the nomenclature used.

With respect to the "wet" tests, it was decided not to consider air humidity as a parameter. This was beyond the scope of the investigation. It could be speculated that if the air stream was saturated, the saltation of particles would be reduced. It is difficult however to assess with certainty the mass transfer from the stream to the surface without extensive testing.

4.2 Test Slab and Mini Wind Tunnel

The test slab, which is depicted in Fig. 4.1, was 38 mm thick, 1.82 m long and 0.92 m wide, and was formed in an open plexiglass channel, which is referred to as the "mini wind tunnel". The latter was positioned in the UTME micro-meteorological wind tunnel, which is a variable-speed, open-circuit tunnel with maximum and minimum speed capabilities of about 0.5 m/s and 18 m/s respectively and a 9 m long, 1.22 m by 2.44 m rectangular test section.

The tailings were placed in the mini wind tunnel and smoothed to give a level surface. After each test, the surface was replenished with new tailings and again smoothed to maintain a consistent, level surface. In the case of the wet tests, the surface was moistened with distilled water. Surface samples weighing about 5 g were taken before and after each test to determine parent particle distribution and moisture content. The average particle distribution of the tailings is shown in Fig. 4.2.

The mini wind tunnel was 3.66 m long with a square cross-section, 0.92 m by 0.92 m. It was made of plexiglass and mounted on a 0.46 m high metal frame to elevate it above the boundary layer of the micro-meteorological tunnel. Mean wind velocity and turbulence intensity data obtained in this tunnel established that the flow within it was reasonable two-dimensional over an adequately large span and that boundary layer growth along the floor was consistent with smooth flat-plate boundry-layer growth.

For the purpose of evaluating the effects of various wind conditions, two boundary-layer generators were used upstream of the test slab. The first was a smooth flat plexiglass plate (0.92 m by 0.92 m) which produced low turbulence intensities and surface-friction velocities. The second was a rough "flat plate" comprising a 0.92 m by 0.92 m section of plexiglass on which styrofoam blocks measuring about 25 mm by 25 mm by 25 mm and occupying 30% of the plate's surface were attached (Fig. 4.3). Mean velocity and turbulence intensity measurements taken over this plate established that it generated a typical rough flat-plate boundary layer.

4.3 Data Acquisition

Particle samples were collected at selected locations along and above the test slab (Fig. 4.1 and Table 4.2). In addition, an open-faced wedge was placed at the trailing edge of the test slab to collect saltation samples during the tests. Pitot tubes were placed in the vicinity of the leading edge of the test slab also to monitor the mean wind speeds during the tests. The mean velocity, root-mean-square (rms) and Reynolds shear stress distributions over the test slab were evaluated from hot-wire measurements taken with the test slab replaced by a styrofoam sheet whose surface roughness was approximately the same as that of the test slab. It was not possible to carry out these hot-wire measurements with the test slab in place since the hot-wire would sustain damage on impact by airborne tailing particles.

It should be noted that suspended particles within a boundary layer act as momentum sinks and therefore cause an increase in the rate of transfer of momentum from the free stream to the bounday layer, as a result of which the boundary layer becomes thicker. Accordingly, the boundary-layer characteristics for the styrofoam sheet were not precisely identical to those for the test slab. Nevertheless, any differences between the characteristics of the two boundary layers could be considered insignificant, since the dominant factor governing these characteristics was the surface roughness (which was effectively the same for both layers).

4.3.1 Particle Sampling Trains

Three individual particle sampling trains were used at three stations along the test slab to obtain the particle concentration measurements. Each of these trains consisted of four stream-lined sampling probes, four nucleopore filters held in standard 3.7 cm Millipore samplings cassettes, a heavy duty vacuum pump capable of drawing 40.7 lpm of free air, and a cylindrical dividing-flow manifold to distribute the pump flow among the four sampling-probe/filter-cassette combinations.

The position of each sampling probe relative to the leading edge of the test slab is specified in Table 4.2. The probes at the third station (#3) were located along the centre-plane of the mini wind tunnel, and those at the first and second stations (#1 and #2) were located 0.15 m from the centre-plane, on either side of the latter, to prevent the wakes of upstream samplers from affecting downstream samplers.

It was initially proposed to meter the air drawn by each of the three pumps using rotometers individually. Unfortunately it was found that the pressure drop across the rotometer was too great and the units themselves were not very accurate. An alternative technique was found to be effective. The internal diameters of the streamlined sampling probes were varied for each specific wind velocity tested.

Three sets of 12 sampling probes were constructed from glass tubes tapered at the inlet ends to 5 mm, 4mm and 3.5 mm pertaining to wind speeds of 4.5 m/s, 7.5 m/s and 9.5 m/s, respectively.

Each sampling probe/filter cassette combinations, referred to as a "sampler", was calibrated prior to each test by means of a bubble meter and a timer. The bubble meter was attached to each sampler in turn and, with the vacuum pump in operation, the flow rate through the sampler determined.

To function as isokinetic sampling, the individual receptors were positioned according to their flow rates, with the samplers having the highest flow rates placed at the highest elevations (since the mean flow velocity in a boundary layer increases with increasing elevation).

Standard nucleopore filters which can trap particles > 2 μm were chosen as the filtering medium. These were all desiccated and pre-weighed at the University of Toronto, Occupational Health Group's facilities. After the wind tunnel simulations were completed, the exposed filters were again desiccated and weighed at these facilities. Over 240 filters were treated in the above fashion. Of these, 40 had collected a sufficient number of particles to enable a particle size analysis to be carried out on the UTME digital image analysis system (DIAS).

For each test, the surface moisture content was determined. Surface samples were taken along the centerline of the test slab, weighed, oven-dried and weighed again to evaluate the surface moisture content.

4.3.2 Digital Image Analysis System

The classical dry and wet sieving techniques for evaluating particle size distribution could not be used here because of the small amount of mass caught by the filters (< 1 g). An alternative method was thus devised, which involved attaching particles to slides, measuring and counting them with the UTME/DIAS.

The UTME/DIAS includes a Bausch & Lomb Omnicom 3000 unit that is designed to detect "features" within an illuminated image (e.g., dark particles on a white background) that have light intensity levels that are lower or higher than a specific level (e.g. the background level). Several measurements (such as area, perimeter, width, projected length, etc.) and various statistical data analyses (e.g., mean, standard deviation, mode and probability distribution functions) can be carried out with respect to the aforementioned "features" via specific built-in hardware. This unit was used in conjunction with a microscope to determine the size distributions of the particle samples.

Particles from the surface samples, nucleopore filters and saltation samples (Section 4.3.1) were attached to microscope slides following the method of Perrie and Peach (1973) and subsequently modified by Nickling (1983). In this technique, a small portion of an aqueous dispersion of a sample is placed on a gelatin-coated slide by means of a micropipette. The water is quickly absorbed by the gelatin, leaving individual particles dispersed and cemented on the slide. The slide was then placed under the DIAS microscope for analysis. With class limits set, the DIAS was programmed to measure the largest particle diameter and to count the number of particles within these classes.

Over 200 particles were counted on individual slides pertaining to initial and final surface conditions, saltation samples and various elevated sampling positions. In all, over 100 slides were digitized. These slides have been stored for possible future analysis.

Six particle size classes were chosen, ranging from 25-50 μm, 50-100 μm, 100-200 μm, 200-400 μm, 400-800 μm and 800-1600 μm. Size class distributions based on particle count and equivalent weight were calculated. The distributions based on the latter used the class mid-point as the equivalent diameter for each size class to determine the class and total volume and subsequently the weight. Particle diameters below 25 μm could not be distinguished from background. Cleaning of the open circuit wind tunnel air supply was not feasible for the present investigation.

4.3.3 Turbulent Flow Measurements

Turbulent-flow measurements were obtained by means of a combination of normal and cross hot-wire probes, in conjunction with three DISA 55 M constant temperature anemometers. DC and rms voltmeters were used to measure the mean and rms values of the anemometer voltage signals corresponding to the turbulent flow signals (Fig. 4.4). These values were subsequently converted to mean velocities, rms streamwise and lateral velocities, and Reynolds shear stresses, with the aid of anemometer response equations based on hot-wire calibration data. The hot-wire calibration procedure and typical calibration data are given in Appendix A, and the locations at which the measurements were taken are specified in Table 4.3.

5.0 RESULTS AND MODEL SPECIFICATIONS

As mentioned in Section 4.0, airborne particulate samples were collected for three wind velocities under two different turbulence conditions and two different surface moisture conditions. Sampling was carried out over a 30 minute period in each test case to avoid an unnecessary loss of tailings material.

5.1 Concentration and Saltation Measurements

The concentration profiles are shown on log-log axes in Figs. 5.1 to 5.10 and the saltation flux values obtained for the various experimental runs are presented in Table 5.3.

For both dry and wet surface conditions, at wind velocities of 4.5 m/s, the concentration profiles (Figs. 5.1-5.4) are variables but in most cases, show an increase with elevation, i.e., a positive gradient. This is contrary to what is expected. The apparent anomaly is the result of not having a long enough fetch for the system to reach a steady state condition. Very little particle movement was observed during the test run at this wind velocity, as can be verified by the saltation results. In fact, inspection of the test slab showed that most of the saltation samples came from the very end of the test slab. This observation was made for both high and low turbulence conditions. We can thus conclude that a threshold wind speed can be defined below which significant erosion does not take place. The present test results establish this threshold at about 4.5 m/s.

At 7.5 m/s, a definitive pattern begins to develop (Figs. 5.5 -5.8). Concentration at the lower elevations are substantially greater than those at the higher elevations, implying that the vertical concentration gradient is negative. As well, there is an increase in concentration with streamwise distance, which suggests that the horizontal (or streamwise) gradient is positive. Note that the concentration profile for station #1 is effectively flat and can be considered as representing a background level.

With respect to the dry tests (Figs. 5.5 and 5.7), the concentration profiles have similar functional shapes, but at station #3, the concentrations for the high turbulence case are slightly higher than those for the low turbulence case. The reverse is true at station #2, where concentrations for the low turbulence case are greater than those for the high turbulence case. Of interest are the concentration changes between stations. This aspect will be expanded in section 5.4. It was observed during the tests that significant particle movement occurred just ahead of station #2 and continued until the end of the test slab. This occurred in both the high and low turbulence tests and suggests the presence of transition and steady state regions. This concept is consistent with the wind analysis results which indicate that a steady surface friction velocity was not reached until midway over the test slab.

With respect to the wet tests (Figs. 5.6 and 5.7), the vertical gradients are again negative but generally smaller in magnitude cf. the dry test results. There is a substantial difference between the results at station #2 and those at #3. It was observed during these tests that significant particle movement did not occur until midway through the test and only between stations #2 and #3. It is clear that the wind passing over the tailing material results in marked evaporation, with conditions approaching those of the dry tests.

It should be noted that there is a significant difference between the dry and wet 7.5 m/s results, as can be seen from Figs. 5.5 to 5.8. (The replicate #1 concentration levels for the high turbulence, wet test at station #3 are higher than expected. This is considered an anomaly.)

As shown in Table 5.1, there is also a substantial difference between the 7.5 m/s saltation fluxes for the dry and wet cases. The wet fluxes are almost an order of magnitude lower than the dry fluxes. This illustrates the effectiveness of moisture in decreasing erosion.

Figs. 5.9 and 5.10 show the concentration profiles for the dry and wet 9.5 m/s tests. Again the profiles are similar to those shown earlier but with substantially higher concentrations. It is of interest to note that in the higher turbulence cases, the profiles at station #1 also begin to show negative vertical gradients although these gradients are not as steep as those at the other stations. This is expected, since significant particle movement occurred 7.5 cm from the leading edge of tailings slab and upstream of station #1. In the dry tests, particle movement occurred immediately upon the onset of the wind and continued at a relatively steady rate. In the wet tests, however, particle movement did not occur until some time after the wind velocity was brought up to full speed. The saltation flux can again be taken as a measure of particle movement (Table 5.1). Note that the wet fluxes are approximately half the dry fluxes.

5.2 Turbulent Wind Velocity Measurements

Wind velocity measurements were carried out using the hot-wire anemometer techniques described earlier. A normal wire probe was used to measure the mean streamwise wind velocity (U) and the streamwise rms velocity (up). In addition a cross wire was used to determine the vertical rms velocity (vp) and the Reynolds shear stress ($\overline{uv}$).

The profiles of U, up, vp and $\overline{uv}$ for all test conditions are presented in Figs. 5.11 - 5.16. As expected, the rough upstream surface conditions caused greater rms velocities as well as larger Reynolds shear stresses.

Of interest is the change in mean velocity profiles with streamwise distance. Table 5.2 gives the surface friction velocities determined from a log-normal fit of the mean velocity profiles. In the 7.5 m/s and 9.5 m/s high-turbulence cases, where a rough surface precedes a smooth surface, the friction velocity decreases more rapidly over the first half of the test slab than it does over the second half. With a smooth surface preceeding a rough surface, as is the case in the low-turbulence tests, there is a decrease in the friction velocity followed by a sudden increase in this velocity which gradually decreases with distance. These results are consistent with those obtained by Rao, Wyngaard and Cote (1974), and can be explained as follows. In the case of the rough/smooth situation, the gradient of the boundary layer velocity profile at any elevation decreases monotonically with streamwise distance, and hence u_* decreases initially, increases rapidly near the transition point and then decreases monotonically with distance; thus u_* increases initially.

The above results indicate that there are two distinct flow regions over the test slab, viz, a transition region and steady state region. The first half of the slab is arbitrarily defined as the transition region and the latter half the steady state region. This is consistent with the concentration profiles given in the previous section.

5.3 Particle Size Analysis

The particle size analysis was carried out using the UTME/DIAS equipment as outlined in the previous section. Six particle size classes ranging from 25 μm to 1600 μm were used to determine the particle size distribution by count and by weight for initial and final surface material, for saltation samples obtained during each test, and for particle concentrations greater than 10 mg/m^3.

Figures 5.17 - 5.22 show the average initial and final particle distributions for the dry tailings slab material (or parent distributions) and the distributions for the saltation samples. Figures 5.23 - 5.28 present similar results for the wet conditions. The distribution for each replicate is provided in Appendix B in tabular form.

As shown in the above figures, there is a significant difference between distribution based on count and those based on weight. Those based on count show a skewed distribution toward the smaller size classes while the other shows a distribution skewed to the larger particle size classes. To evaluate the total amount of particles in saltation or suspension, a particle size distribution based on weight is the appropriate choice.

Using the median diameter as an indicator, a comparison between initial, final and saltation distribution versus friction velocity can be realized. For the dry cases, the initial median diameter is typically greater than the final, indicating that the larger diameter particles have been removed (Figure 5.29). These particles should show up in the saltation results, but as can be seen in Fig. 5.29, the saltation median diameter is typically smaller than the initial or final. This suggests that a sufficient amount of the smaller diameter particles have also been removed. As friction velocity increases, the saltation median diameter also increases indicating that the larger particles are more susceptible to the action of the friction velocity. It appears that at the higher surface friction velocities, the saltation median diameter is greater than either of the other two diameters. This trend would be expected since the larger diameter particles protrude into the fluid boundary layer to a greater extent and therefore subjected to a greater drag force.

Figure 5.29 also shows the median particle diameter versus friction velocity for the wet cases. There is little difference between initial, final and saltation cases as can be verified by the actual distributions (Appendix B). The moisture in the surface tailings test slab has caused the particles to resist the effects of the wind to a greater degree. As the friction velocity increases, there is a general decrease in the median diameter, which is somewhat surprising vis-á-vis the dry cases.

The rate of particle movement in saltation was obtained by multiplying the saltation rate by the size class weight percent in each test. Replicate and average values are presented in Tables 5.3 and 5.4 for both dry and wet conditions.

The distributions by count of particles on selected filters (i.e., _23 to _34) and saltation samples are presented in Figs. 5.30 - 5.33 and in tabular form in Appendix C. Table 5.5 presents the mean concentration distributions for each filter on a weight basis for both dry and wet conditions. The distribution for each replicate is also presented in Appendix C.

Table 5.5 shows that there is an increase in the concentration of each size class in the streamwise direction as well as in the downward vertical direction. Note that for the dry tailings, at 7.5 m/s, there are concentrations of particles in the 800 - 1200 μm range which do not appear at 9.5 m/s. This suggests that the vertical lift force on the particles is suppressed at the higher wind speed. From the distributions given in Appendix C (Tables C2 and C4), the particle median diameter on a weight basis decreases with elevation as would be expected.

5.4 Model Development

From Section 3.0, it is apparent that both the vertical flux and the saltation flux are proportional to the surface friction velocity cubed (u_*^3), and the ratio of one to the other is given by a modified suspension factor (S^*). From the concentration gradients presented in section 5.1, the vertical flux values can be determined and correlated with the friction velocity.

The vertical flux can be expressed as

$$F_v = -K \, dC(z)/dz \qquad (5.1)$$

where F_v is the vertical mass flux (mg/m^2-s), K is the eddy diffusivity (m^2/s) and, C(z) is the concentration at height z (mg/m^3).

The concentration gradient is determined by noting that the concentration profiles from section 5.1 follow a power law with respect to z. Therefore,

$$C(z) = az^b \tag{5.2}$$

$$dC(z)/dz = abz^{b-1} \tag{5.3}$$

and substituting 5.2 and 5.3 results in

$$dC(z)/dz = bC(z)/z \tag{5.4}$$

where b is the slope of a log C versus log z plot. What is required to complete the model is a value for the eddy diffusivity (K). The eddy diffusivity can be interpreted as a combination of a turbulent length scale and velocity scale. In boundary layer flows, approximate length and velocity scales are taken as the height above ground (z) and surface shear velocity (u_*), respectively. An improvement can be made if the surface shear velocity is replaced with the square root of the Reynolds shear stress ($\overline{uv}$) at each elevation. Thus the eddy diffusivity can be effectively expressed as

$$K = kz[\overline{uv}(z)]^{1/2} \tag{5.5}$$

where k is the von Kármán constant (0.4) and $\overline{uv}(z)$ is the turbulent shear stress at z (m^2/s^2).

Thus, substitution of 5.5 and 5.4 into 5.1 results in

$$F_v = -bk[uv(z)]^{1/2}C(z). \tag{5.6}$$

The slopes of the concentration profiles were calculated using linear regression, and are presented in Table 5.6a and 5.6b for each replicate and mean profile. Only the lower three positions were used in the calculation since the uppermost positions were appreciably out of the boundary layer. Concentrations at these positions were thus independent of the velocity shear and fairly constant. Shinn et. al (1982) reported a value of -0.3 for the slope for heights between 0.7 m to 2.0 m.

The mean dry and wet vertical fluxes calculated using equation (5.6) are presented Figures 5.34 - 5.39. Each curve indicates that the vertical flux consistently increases with streamwise distance. The flux at station #1 is always significantly lower than those at stations #2 and #3 and pertains to background concentration levels.

As discussed in Section 5.1 and 5.2, the tailings tests slab can be arbitrarily separated into two regions: a transition region and a steady state region. The net flux from the transition region was calculated from the difference in the fluxes at stations #2 and #1 and the net flux from the steady state region from the difference between the station #3 flux and the station #2 flux. The vertical flux at 2.5 cm is plotted against the average friction velocity for each region and is presented in Fig. 5.40 for dry conditions and Fig. 5.41 for wet conditions. The net flux over the entire region shows an inconsistancy, viz, decrease in the vertical flux with increase in u_*. By separating the region into its transition and steady state regions however, this apparent inconsistency can be resolved.

The final four points in the steady state region exhibit a linear fit given by

$$F_v(z=2.5\text{ cm}) = 5{,}000\ u_*^{2.3} \quad \text{(dry)} \qquad (5.7a)$$

$$F_v(z=2.5\text{ cm}) = 42{,}000\ u_*^{5.0} \quad \text{(wet)} \qquad (5.7b)$$

where u_* is the surface friction velocity in meters per second (and is less than 1.0 m/s).

This is consistent with the expectation that the flux would be proportional to u_*^3 in the dry case. The first data point represents a situation where the velocity is below the threshold and is not used to determine the above curve.

Figures 5.42 - 5.43 show the vertical flux, saltation flux and modified suspension factor verus u_* over the steady state region. The saltation rate was calculated as

$$Q = 5{,}000\ u_*^{2.0} \qquad \text{(dry)} \qquad (5.8a)$$
$$Q = 30{,}500\ u_*^{4.4} \qquad \text{(wet)} \qquad (5.8b)$$

Thus, the dry saltation flux varies with $u_*^{2.0}$ and the wet flux varies with $u_*^{4.4}$. It should be noted that for both the dry and wet cases, the variation with u_* of the saltation flux is similar to that of the vertical flux (F_v). Thus, the ratio F_v/Q which is the modified suspension factor (S^*) is weakly dependent upon u_* and can be determined as

$$S^* = F_v/Q = 1.09\ u_*^{0.39} \qquad \text{(dry)} \qquad (5.9a)$$
$$S^* = F_v/Q = 1.35\ u_*^{0.6} \qquad \text{(wet)} \qquad (5.9b)$$

The average of the last four data points for both dry and wet cases yields a value of approximately 0.61. This is consistent with the value obtained for coal pile erosion by Hunt (1984).

Finally, Figs. 5.44 - 5.45 present the net vertical flux profiles for the various friction velocities. The functional profiles are similar for all data obtained at velocities in excess of the threshold velocity. It is possible to reduce these curves into a single curve described by

$$F_v(z) = F_{vn}\ (z/z_n)^{\alpha}$$

where F_{vn} is the flux at height z_n and α is the slope of the power curve.

With the vertical flux at 2.5 cm chosen for F_n, the following relationships between the friction velocity and the flux at any height can be obtained by means of multiple linear regression:

$$F_v(z)/F_{vn} = 0.67\ u_*^{-0.36}\ (z/z_n)^{-2.1} \qquad \text{(dry)} \qquad (5.10a)$$

$$F_v(z)/F_{vn} = 0.085\ u_*^{-1.6}\ (z/z_n)^{-1.8} \qquad \text{(wet)} \qquad (5.10b)$$

where $F_{vn} = F_v(z_n = 2.5\ \text{cm})$. The correlation coefficient for the dry and wet casesis calculated to be 0.991 and 0.951, respectively. The error associated with these equations is 29.3% for dry cases and 18% for the wet cases. The power coefficient, α, in both cases is similar and should be expected since the turbulent boundary layer is the same. Insufficient data between dry and wet cases are available to determine a general equation to include the effects of moisture.

With the aid of equations 5.8, 5.9 and 5.10, and prediction of the amount of tailings suspended can be made with adequate confidence.

The particle size distributions for the mean vertical fluxes were calculated using the particle distributions and equation 5.6 for each size class, assuming that the turbulence affected each size class equally. Figures 5.46 to 5.49 show the particle fluxes for the various runs along with the saltation fluxes. Tabulated data are presented in Appendix D. As in the total mass flux cases, the particle flux at each elevation of station #3 was reduced by the particle flux at station #2, thus removing any background contamination. These results which are presented in Figs. 5.50 - 5.53 show the net vertical flux over the steady state region of the tailings test slab. In these figures _2, _3 and _4 refer to elevations of 16.5 cm, 6.5 cm and 2.5 cm, respectively.

For the dry cases (Figs. 5.50 - 5.51), the maximum vertical flux occurs within the 400 - 800 μm range for three of the cases and within 200 - 400 μm range for the fourth (DS95). Only for DR95 do the maxima occur within the same size range of 400 - 800 μm. As mentioned previously, the increase of friction velocity causes an increase in the saltation particle diameter. This is further illustrated in these figures. Note that the size range pertaining to the maximum saltation flux shifts from the 200 - 400 μ range to the larger range, for the higher friction velocities, i.e., DS95 and DR95.

The wet cases, shown in Figs. 5.52 and 5.53, do form a pattern, with the maximum vertical fluxes and saltation flux occurring within the 400 -800 μm range for three of the cases. In the fourth case (WR95), the maximum saltation occurs within the 200 - 400 μm range while the maximum vertical flux occurs within the 800 - 1600 μm range.

The net vertical flux and saltation flux distributions were reduced to fine and coarse fractions, which refer to particle size ranges less than 100 μm and thos greater than 100 μm, respectively. Tables 5.7 and 5.8 present these fluxes along with the ratio of fine to coarse fractions and the total mass flux, i.e., vertical fluxes plus the saltation flux.

The saltation and total fine and coarse mass flux fractions in the dry cases show an increase with the friction velocity, but their ratio decreases with friction velocity; thus, the coarse-size particles are more susceptible to the drag force created by the wind. At the lower sampling points (_4), an increase in the fine fraction and the ratio of fine to coarse with the friction velocity is observed, except at the highest friction velocity where the ratio decreases. This decrease suggests that the coarse-size particles have a greater lift force applied to them to attain greater heights at the highest friction velocity. In addition, Table 5.7 shows a larger quantity of coarse-size particles at the higher elevations. With sufficient time, these coarse-size particles will fall out and leave only the fine size particles to be dispersed downwind.

The total wet fine and coarse mass flux fractions (table 5.8) show an increase with the friction velocity as well as an increase in their ratios, unlike the dry cases. At the higher friction velocities, the wet saltation fine fraction is greater than the corresponding dry cases. As the friction velocity increases, the rate of surface drying also increases, and since the smaller diameter particles have smaller surface area they are dried at a faster rate; thus, they are more susceptible to transport than the larger particles. This would explain the decrease in the median diameter with the friction velocity in the wet cases.

6.0 SUMMARY AND CONCLUSIONS

- Wind tunnel tests have provided quantitative information on the physics of the erosion of tailings material due to wind. Specific attention was paid to the characteristics of the turbulence and how this influenced the erosion, saltation and suspension of the material.

- Experiments have served to define transition and steady state regions for the erosion of the test slabs which were studied within the wind tunnel.

- The data have enabled the development of a model to describe the erosion process with respect to the various aspects of the oncoming wind.

- Specifically, the vertical mass flux and the saltation flux of tailings material have been found to be proportional to the third power of the surface friction velocity of the oncoming wind.

- The ratio between the vertical flux and the saltation flux is described in terms of a modified suspension factor.

- These models are in agreement with published theoretical analyses of the problem and as well are consistent with experimental studies which have been carried out for similar situations.

- Particle size analysis has indicated that the larger particles reach higher elevations, during saltation, than anticipated.

- Through the drying process, the finer particles are more susceptible to movement.

REFERENCES

1. Anspaugh, L.R., Shinn, J.H., Phelps, P.L. and Kennedy, N.C., 1975: Resuspension and Redistribution of Plutonoim in Soils, Health Physics. 29: 571-582.

2. Bagnold, R.A., 1941: The Physics of Blown Sand and Desert Dunes. Metheun and Co. Ltd., London.

3. Blackwood, T.R. and Wachter, R.A., 1978: "Source Assessment Coal Storage Piles", Report EPA/600/2-78-004K, U.S. Environmental Protectio Agency.

4. Chepil, W.S., 1957: Width of Field Strips to Control Wind Erosion, Tech. Bull, 92, Kansas State College of Agriculture and Applied Science.

5. Chepil, W.S. and Woodruff, N.P., 1959: Estimations of Wind Erodibility of Farm Fields, Report #25, U.S. Dept. of Agriculture.

6. Chepil, W.S. and Woodruff, N.P., 1963: The Physics of Wind Erosion and its Control, pp. 1-301, Advances in Agronomy, Vol. 15, Academic Press, New York.

7. Fairchild, Charles I. and Tillery, Marvin I., 1982: Wind Tunnel Measurements of Resuspension of Ideal Particles, Atmospheric Environment. 16: 229-238.

8. Gillette, Dale, 1973: "On the Production of Soil WInd Erosion Aerosols Having the Potential For Long Range Transport", Journal de Recherches Atmospheriques, Ncie Symposium on the Chemistry of Sea Air Particulate Exchange Process, Nice, France.

9. Gillette, Dale, 1976: Fine Particulate Emissions Due To Wind Erosion, Proc. American Society of Agricultural Engineers. Lincoln, Ne, 27-30 June, 1976.

10. Gillette, Dale A., 1976: Production of Fine Durst By Wind Erosion of Soil: Effect of Wind and Soil Texture, Proc. Conf. on Atmospheric Surface Exchange of Particulate and Gaseous Pollutants. Richland, Wa. 4-6 Sept. 1974.

11. Gillette, Dale, 1977: Fine Particulate Emissions Due To Wind Erosion, Transaction of the ASAE. 890-897.

12. Gillette, Dale, 1978: Tests With a Portable Wind Tunnel For Determining Wind Erosion Threshold Velocities, Atmospheric Environment. 12: 2309-2313.

13. Gillette, Dale A., Blifford, Irving H., and Fenster, Charles R., 1972: Measurements of Aerosol Size Distributions and Vertical Fluxes of Aerosols on Land Subject to Wind Erosion, J. of Applied Meteorology. 11: 977-987.

14. Gillettee, Dale and Cowherd, C., 1980: "The Concept of Resuspension Rates Applied to Problems of Fugitive Dust Emissions and Wind Erosion", Precipitation Scavenging Dry Deposition and Resuspension.

15. Healy, J.W., 1976: A Review of Resuspension Models. LA-UR-76-2767. Los Alamos Scientific Laboratory, New Mexico.

16. Healy, J.W. and Faquay, J.J., 1958: Windpickup of Radioactive Particles From the Ground, Proc. Conf. of hte Second United Nations International Conference on the Peaceful Uses of Atomic Energy, Vol. 18.

17. Horst, Thomas ., 1977: The Estimation of Air Concentrations Due to the Diffusion, Deposition and Resuspension of Contaminants by the Wind. PNL-2426, Battelle Pacific Northwest Laboratories, Richland, WA.

18. Hunt, J. 1984, Personal Communications.

19. Mills, M.T., Dahlman, R.C. and Olson, J.S., 1974: Ground Level Air Concentrations of Dust Particles Downwind from A TAilings Area During a Typical Windstorm. ORNL-TM-4375 Oak Ridge National Laboratory, Oak Ridge, Te.

20. Nickling, W.G., 1982: Grain-Size Characteristics of Sediment Transport During Dust Storms. J. Sedimentary Petrology. 53: 1011-1024.

21. Peach, P.A. and Perrie, L.A., 1973: Gelation-Coated Microscope. Slides in Sedimentary Size Analysis. J. Sedimentary Petrology. 43: 1174-1175.

22. Rao, K.S., Wyngaard, J.C. and Cote, O.R., 1974: The Structure of the Two-dimensional Internal Boundary Layer Over a Sudden Change of Surface Roughness", J. Atmos. Sci. 31: 738-746.

23. Sehmel, G.A., 1980: Particle Resuspension: A Review, Environment International. 4: 107-127.

24. Sehmel, G.A. and Lloyd, R.D., 1975: Particle Resuspension Rates. Battelle, Pacific Northwest Laboratory, Richland, Wa.

25. Sehmel, G.A. and Orgill, M.M., 1973: Resuspension by Wind at Rocky Flats, BNWL-1751, Part 1. Battelle, Pacific Northwest Laboratory, 15-21.

26. Shinn, J.H., Kennedy, N.C. Koval, J.S., Clegg, B.R. and Porch, W.M., 1974: Observations of Dust Flux in the Surface Boundary Layer for Steady and Nonsteady Cases, Proc. Conf. on Atmospheric-Surface Exchange of Particulate and Gaseous Pollutants. Richland, Washington, 4-6 Sept.

27. Shinn, J.H. and Homan, D.N., 1982: Plutonium-Aerosol Emission Rates and Human Pulmonary Deposition Calculations for Nuclear Site 201, Nevada Test Site. UCRL-53301, Lawrence Livermore Laboratory.

28. Siddoway, F.H., Chepil, W.S. and Armbrust, D.V., 1965: "Effects of Kind, Amount, and Placement of Residue on Wind Erosion Control", Trans. American Society of Agricultural Engineers, 8: 327-331.

29. Skidmore, E.L., Fisher, P.S. and Woodruff, N.P. 1970: "Wind Erosion Equation: Computer Solution and Application", Proceedings of Soil Science Society, 34: 931-935.

30. Smith, W.J., Whicker, F.W. and Meyer, H.R., 1982: "Review and Catagorization of Saltation, Suspension and Resuspension Models", Nuclear Safety, 23: 685-699.

31. Travis, John R., 1974: A Model for Predicting the Redistribution of Particulate Contaminates From Soil, Proc. Conf. on Atmospheric Surface Exchange of Particulate and Gaseous Pollutants. Richland, Washington, 4-6 Sept.

NOMENCLATURE

C	Mass concentration (mg/m^3)
C_h	Horizontal mass flux constant ($C_h = 1x10^{-6}\ g \cdot s^2/cm^4$)
C_v	Vertical mass flux constant ($C_v = 2x10^{-10}\ g/cm^2 - \sigma$)
C'	Local climatic factor
D_b	Length of wind shelter distance (m)
D_f	Length of field in windward direction (m)
D_F	Drag force (N)
d_i	Particle diameter (m)
E	Potential annual average soil loss (tons/acre)
$\bar{g}$	Gravity acceleration (m^2/s)
F_H	Mass Horizontal Flux (g/cm^2-s)
F_v	Mass Vertical Flux (mg/m^2-s or g/cm^2-s)
G	Surface contamination (g/m^2)
I	Soil erodibility factor
I'	Effective Soil erodibility index
I_s	Knoll erodibility factor
k	von Karman's Constant ($k = 0.4$)

K'	Soil ridge roughness factor
K_o	Orientation of vegetation cover
L'	Effective field length
m	Mass of particle (g)
M	Soil moisture content
n	Constant (n 0.1)
n'	Constant ($n' = 0.08$)
p	Mass percent of particles < 20 μm(%)
Q_v	Vertical emission rate or flux ($g/m^2 \cdot s$)
q_{si}	Saltation flux of particle i ($g/m \cdot s$)
R'	Quantity of vegetation cover (lb/acre)
S	Type of vegetation cover
S_f	Suspension factor (m^{-1})
S^*	Modified suspension factor
t	Time(s)
$\bar{u}$	Mean wind speed (m/s)
u_*	Surface friction velocity (m/s)
u_*'	Saltation friction velocity (m/s)

u_{*i}	Threshold friction velocity (m/s)
$\bar{u}_{ti}$	Wind threshold velocity prior to saltation of particle i (m/s)
V	Vegetative cover
V_{ti}	Impact threshold velocity during saltation of particle i
w_i	Initial vertical velocity of particle i (m/s)
X	Wind tunnel erodibility (tons)
x,y,z	Cartesian coordiantes (m)
z'	Height where $\bar{u} = V_{ti}$ (m)
z_o	Roughness height (m)
β	Particle shape and position coefficient
ε_i	Empirical saltation constant
λ'_i	Drag imposed on particle i (N/m^2)
Ω	Dynamic suspension factor (m^{-1})
ρ_a	Atmospheric density (g/m^3)
ρ_s	Particle density (g/m^3)
∇	Suspension rate (s^{-1})

appendices

appendix a

HOT WIRE CALIBRATION PROCEDURE

HOT-WIRE CALIBRATION PROCEDURE

When the sensor of a constant temperature hot-wire anemometer system is placed in an isothermal flow, with its axis normal to the streamwise flow direction, the response of the system can be described by (Hinze 1959)

$$\frac{E^2(t)/R_w}{R_w-R_g} = A + B\, U^n(t),$$

where E(t) is the anemometer voltage corresponding to the instantaneous streamwise velocity U(t): R_w is the (constant) operating resistance of the anemometer; R_g is the resistance of the hot-wire at the flow temperature; and A, B and n are constants. Thus, once A, B and n are known, the streamwise velocity signals can be determined from the measured anemometer output signals.

In view of the fact that $E(t) = \bar{E} + e(t)$ and $U(t) = \bar{U} + u(t)$, where e(t) and u(t) are the fluctuating parts of the velocity and voltage signals respectively, the above response equation implies that

$$\frac{\bar{E}^2/R_w}{R_w-R_g} = A + B\, \bar{U}^n.$$

On the basis of this equation, A, B and n for a given system can be determined from a set of $\bar{E}$, $\bar{U}$ data. The latter can be obtained by placing the sensor in a flow whose velocity can be varied - a calibration flow - and simultaneously measuring $\bar{E}$ and $\bar{U}$. It should be noted that n depends on the velocity range in which the $\bar{E}$, $\bar{U}$ data are measured. This range should encompass that of the turbulent flow being investigated.

In the present investigation, the calibration flow was a round jet generated by a DISA calibration unit fed with pressurized air. This unit consists of three components viz. a DISA 55D44 pressure control unit, a DISA 55D45 nozzle unit and a DISA 55D46 pressure converter. It is capable of producing several velocity ranges within the limits of a velocity corresponding to Mach 1 (with compensation for compressibility) and 0.5 m/s. A maximum velocity reduction of 5 to 1 can be obtained either continuously over a period of approximately 25 s, by means of 'push-button' scanning device built into the pressure control unit, or discretely by altering the pressure control setting. It has a voltage output which is directly proportional to the jet velocity, the constant of proportionality depending upon the velocity range being used.

The following procedure was used in obtaining the $\bar{E}$, $\bar{U}$ data. The calibration unit was adjusted for a velocity range having an upper limit of about 15 m/s, and a lower limit of about 4 m/s.

The A, B and n were then determined from N pairs of $\bar{E}$, $\bar{U}$ data by means of a linear regression technique. With $X_i = \bar{U}_i^{n_j}$ and $Y_i = \bar{E}_i / R_w(R_w - R_g)$, i = 1, ..., N, the regression lines of Y on X for a range of n_j values and the corresponding A_j, B_j and the residue, i.e., the RMS relative error

$$\left\{ \sum_{i=1}^{N} \left[\frac{\bar{U}\text{ measured} - \bar{U}\text{ calculated}}{\bar{U}\text{ measured}}\right]^2_{ij} \right\}^{1/2} ,$$

were computed. The A_j, B_j and n_j corresponding to the minimum residue were the desired values of A, B and n.

29-AUG-85
****

TABLE A-1

** NORMAL WIRE: A1 *** CALIBRATION DATE: 3-JUL-85 ****

CONSTANTS
****

CALIBRATION CONSTANT Kc (M/S/BAR) : 1.600
PRESSURE TO SIGNAL CONSTANT C (BAR/V): 1.000
WIRE DECADE RESISTANCE Rdw (OHMS) : 5.780
GAS DECADE RESISTANCE Rdg (OHMS) : 3.482

INPUT DATA **********		CALCULATED DATA ***************	
EP (V)	EA (V)	UC (M/S)	UM (M/S)
10.02	4.441	16.075	16.032
9.72	4.422	15.579	15.552
9.17	4.386	14.670	14.672
8.65	4.351	13.824	13.840
8.22	4.322	13.151	13.152
7.97	4.303	12.723	12.752
7.34	4.257	11.730	11.744
7.08	4.237	11.316	11.328
6.64	4.202	10.618	10.624
6.30	4.174	10.083	10.080
6.13	4.158	9.786	9.808
5.88	4.137	9.406	9.408
5.37	4.090	8.594	8.592
5.15	4.068	8.232	8.240
4.79	4.032	7.664	7.664
4.58	4.011	7.346	7.328
4.31	3.981	6.909	6.896
4.14	3.962	6.642	6.624
3.93	3.936	6.288	6.288
3.69	3.906	5.897	5.904
3.39	3.867	5.416	5.424
3.04	3.820	4.874	4.864
2.84	3.789	4.538	4.544

FOR HWA RESPONSE EQUATION:

Ea*Ea/(Rdw-Rdg) = A+B*U**0.4

A= [illegible].011
B= 1.[illegible]
R^2= [illegible].0000
UR= 0.1[illegible]%

FIGURE A-1

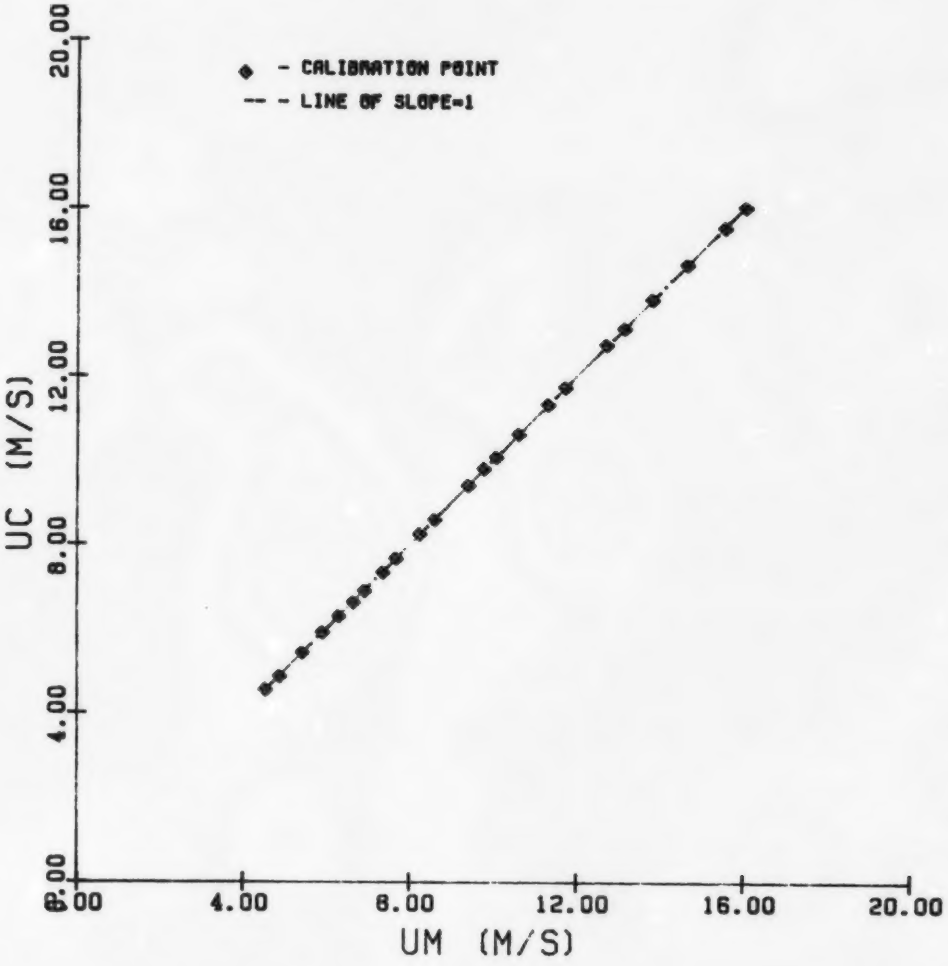

PLOT OF CALCULATED VS. MEASURED VELOCITY

**** NORMAL WIRE: A1 **** CALIBRATION DATE: 3-JUL-85 ****

```
         29-AUG-85                         TABLE A-2
         *********

   ** X-WIRE-1 (47 DEG): XP *CALIBRATION DATE: 8-JUL-85 ***

         CONSTANTS
         *********

         CALIBRATION CONSTANT Kc (M/S/BAR)     :  1.600
         PRESSURE TO SIGNAL CONSTANT C (BAR/V):  1.000
         WIRE DECADE RESISTANCE Rdw (OHMS)     :  6.500
         GAS DECADE RESISTANCE Rdg (OHMS)      :  4.043

            INPUT DATA                        CALCULATED DATA
            **********                        ***************

        EP                  EA                  UC                  UM
        (V)                 (V)               (M/S)               (M/S)
   ***************************************************************************
       9.66               4.311              15.508              15.456
       9.08               4.273              14.556              14.528
       8.42               4.227              13.463              13.472
       7.74               4.179              12.388              12.384
       7.06               4.124              11.236              11.296
       6.54               4.084              10.448              10.464
       6.09               4.046               9.739               9.744
       5.59               4.000               8.928               8.944
       5.12               3.955               8.183               8.192
       4.59               3.901               7.351               7.344
       4.07               3.843               6.527               6.512
       3.75               3.804               6.012               6.000
       3.31               3.745               5.290               5.296
       2.98               3.697               4.751               4.768
       2.72               3.660               4.363               4.352
       2.52               3.628               4.046               4.032
       2.32               3.592               3.710               3.712

         FOR HWA RESPONSE EQUATION:

          Ea*Ea/(Rdw-Rdg)= A+B*U**0.4

                    A=      2.2560
                    B=      1.7730
                  R^2=      1.0000
                   UR=      0.2357%
```

FIGURE A-2

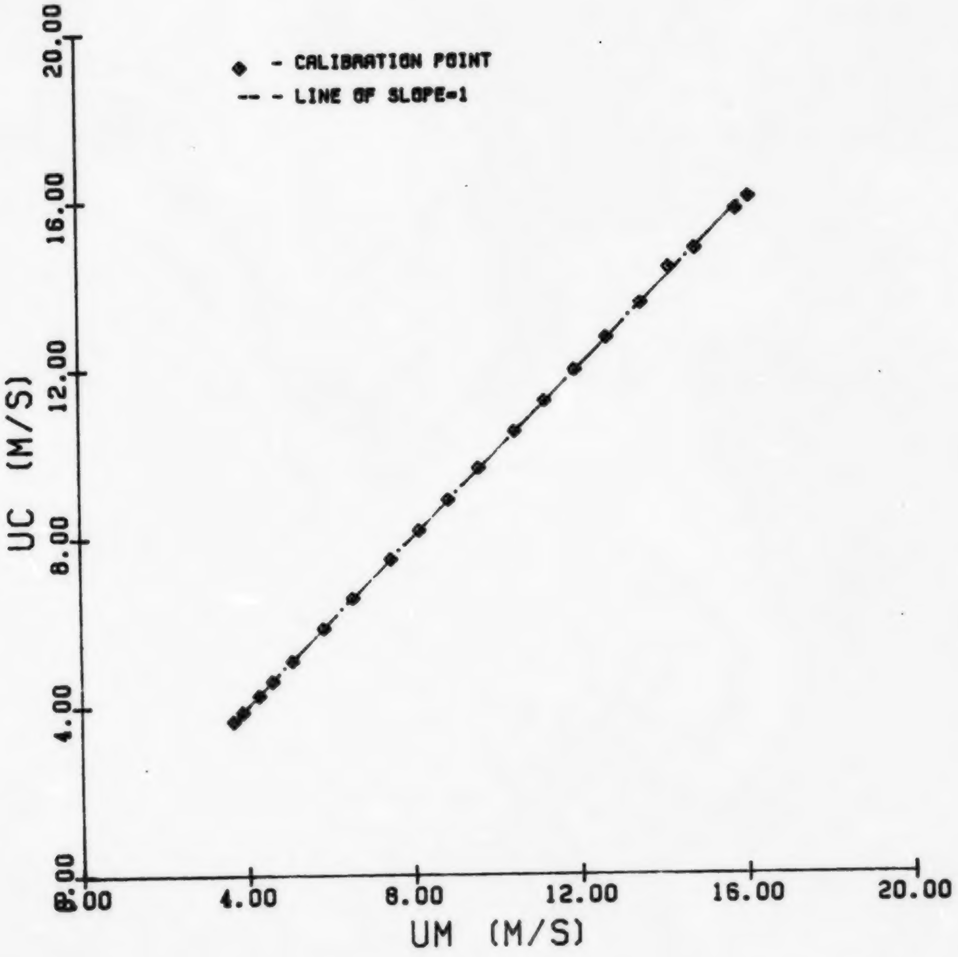

PLOT OF CALCULATED VS. MEASURED VELOCITY

*** X-WIRE-1 (45 DEG): XA *CALIBRATION DATE: 4-JUL-85 ***

29-AUG-85
****

TABLE A-3

** X-WIRE-2 (45 DEG): XA *CALIBRATION DATE 4-JUL-85 ***

CONSTANTS
****

CALIBRATION CONSTANT Kc (M/S/BAR) : 1.600
PRESSURE TO SIGNAL CONSTANT C (BAR/V): 1.000
WIRE DECADE RESISTANCE Rdw (OHMS) : 6.200
GAS DECADE RESISTANCE Rdg (OHMS) : 3.829

INPUT DATA		CALCULATED DATA	
EP (V)	EA (V)	UC (M/S)	UM (M/S)
10.02	4.267	16.109	16.032
9.82	4.255	15.784	15.712
9.26	4.219	14.841	14.816
8.58	4.173	13.697	13.728
7.91	4.122	12.619	12.656
7.23	4.077	11.519	11.568
6.62	4.031	10.571	10.592
6.06	3.984	9.663	9.696
5.50	3.935	8.778	8.800
4.96	3.884	7.921	7.936
4.57	3.845	7.308	7.312
4.08	3.792	6.531	6.528
3.70	3.747	5.919	5.920
3.38	3.707	5.412	5.408
3.04	3.662	4.879	4.864
2.65	3.604	4.249	4.240
2.41	3.566	3.869	3.856
2.24	3.536	3.587	3.584

FOR HWA RESPONSE EQUATION:

Ea*Ea/(Rdw-Rdg) A+B*U**0.4

A= 2.5528
B= [illegible]
R^2= 1.0000
UR= [illegible]%

FIGURE A-3

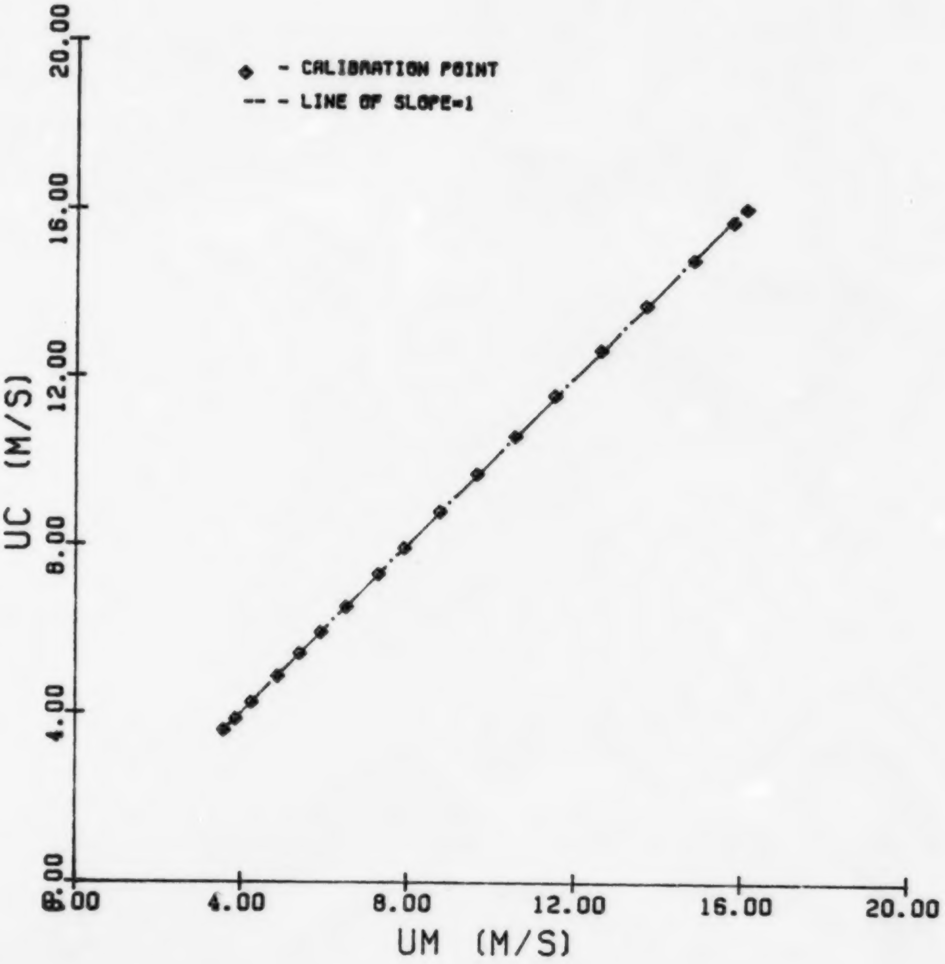

PLOT OF CALCULATED VS. MEASURED VELOCITY

*** X-WIRE-2 (45 DEG): XA *CALIBRATION DATE 4-JUL-85 ***

appendix b

PARTICLE DISTRIBUTION OF PARENT SURFACE SAMPLES AND SALTATION SAMPLES

TABLE B-1

PARTICLE DISTRIBUTION BY COUNT

	Particle Size Range (um)									
	25-50	50-100	100-200	200-400	400-800	800-1600	MEAN	STD DEV	MEDIAN	# of PARTICLES
MID. PT.	37.50	75.00	150.00	300.00	600.00	1200.00				
INITIAL										
DS451B	50.30	26.80	16.20	4.40	2.00	0.00	81.70	89.90	49.80	290.00
DS452B	62.50	18.30	11.60	4.40	1.70	1.30	82.10	125.90	45.00	224.00
DR451B	59.10	19.10	10.00	8.60	2.10	0.80	92.30	128.70	46.10	230.00
DR452B	56.90	24.80	11.00	6.60	0.60	0.00	47.00	79.00	47.00	318.00
DS751B	61.10	18.00	9.00	7.20	4.10	0.30	93.70	128.70	45.50	288.00
DS752B	77.00	13.90	3.20	3.20	1.60	0.80	64.80	114.40	41.20	244.00
DR751B	57.60	21.30	10.60	6.50	2.30	1.30	94.80	145.00	46.70	215.00
DR752B	57.30	18.00	13.10	7.70	3.20	0.40	46.80	119.40	46.80	244.00
DS951B	42.80	17.70	15.70	16.20	7.30	0.00	127.70	131.10	70.10	203.00
DR951B	55.70	18.00	17.60	7.70	0.80	0.00	80.20	79.50	47.40	244.00
FINAL										
DS451A	63.90	22.50	4.70	5.70	3.00	0.00	74.60	100.20	44.50	297.00
DS452A	70.70	18.00	3.80	5.10	1.90	0.30	69.80	104.00	42.70	311.00
DR451A	66.90	16.70	4.90	9.50	1.80	0.00	77.40	100.90	43.70	221.00
DR452A	62.60	17.50	9.90	8.10	1.30	0.40	80.40	104.90	45.00	222.00
DS751A	68.20	21.50	4.60	3.90	1.20	0.40	65.40	90.00	43.30	478.00
DS752A	67.20	13.00	5.80	8.90	4.90	0.00	92.40	139.50	43.60	223.00
DR751A	68.10	21.60	5.70	3.20	0.60	0.60	64.40	99.10	43.40	486.00
DR752A	64.40	16.90	8.80	8.40	1.40	0.00	78.10	92.70	44.40	284.00
DS951A	66.90	20.20	5.70	6.10	0.80	0.00	65.80	79.60	43.70	227.00
DR951A	65.40	13.80	13.80	5.50	1.10	0.00	74.70	85.20	44.10	252.00
SALTATION										
DS451	47.70	21.20	22.00	8.90	0.00	0.00	83.80	70.70	55.30	245.00
DS452	30.90	19.90	27.80	20.30	0.80	0.00	122.20	94.70	97.80	226.00
DR451	42.90	11.90	22.10	18.80	4.60	0.00	128.90	121.10	81.70	217.00
DR452	49.10	19.30	17.00	12.30	2.00	0.00	98.50	104.10	52.20	299.00
DS751	51.00	21.60	16.00	10.80	0.30	0.00	87.90	85.70	49.50	352.00
DS752	44.60	20.30	21.90	13.10	0.00	0.00	99.60	86.70	63.50	251.00
DR751	50.30	22.30	16.70	10.00	0.30	0.00	84.00	76.88	49.80	268.00
DR752	47.40	17.60	22.60	10.50	1.60	0.00	98.30	92.60	57.10	238.00
DS951	50.60	17.90	15.60	11.90	3.60	0.00	106.10	117.60	49.70	217.00
DR951	68.30	12.60	4.90	10.80	3.10	0.00	84.80	113.90	43.30	221.00

TABLE B-2

PARTICLE DISTRIBUTION BY WEIGHT

	Particle Size Range (um)								
	25-50	50-100	100-200	200-400	400-800	800-1600	MEAN	STD DEV	MEDIAN
MID. PT.	37.50	75.00	150.00	300.00	600.00	1200.00			
INITIAL									
DS451B	0.43	1.83	8.83	19.18	69.74	0.00	490.75	172.87	442.22
DS452B	0.12	0.28	1.41	4.27	13.20	80.73	94.35	210.22	990.65
DR451B	0.15	0.38	1.60	10.99	21.47	65.42	164.50	248.79	845.61
DR452B	0.84	2.92	10.36	49.72	36.16	0.00	384.18	173.63	338.58
DS751B	0.20	0.46	1.85	11.86	54.01	31.62	362.85	273.92	660.59
DS752B	0.22	0.32	0.59	4.71	18.83	75.33	128.32	239.16	958.63
DR751B	0.10	0.30	1.21	5.92	16.75	75.73	120.30	229.93	948.57
DR752B	0.18	0.46	2.69	12.64	42.01	42.01	294.45	279.00	698.27
DS951B	0.11	0.36	2.55	21.06	75.92	0.00	522.84	140.35	495.27
DR951B	0.65	1.69	13.18	46.14	38.35	0.00	389.76	176.16	344.23
FINAL									
DS451A	0.41	1.14	1.91	18.53	78.01	0.00	527.54	141.16	496.22
DS452A	0.34	0.70	1.18	12.63	37.63	47.53	266.07	278.73	734.08
DR451A	0.52	1.05	2.46	38.15	57.82	0.00	466.04	161.79	429.27
DR452A	0.27	0.60	2.71	17.71	22.74	55.98	194.19	249.07	738.64
DS751A	0.33	0.84	1.43	9.71	23.91	63.77	175.53	256.56	833.10
DS752A	0.27	0.41	1.47	18.10	79.74	0.00	535.38	131.38	510.30
DR751A	0.28	0.71	1.50	6.73	10.09	80.70	83.58	192.62	959.52
DR752A	0.60	1.25	5.22	39.83	53.11	0.00	447.11	169.29	405.85
DS951A	0.96	2.31	5.22	44.66	46.86	0.00	425.03	172.74	380.12
DR951A	0.78	1.32	10.54	33.60	53.76	0.00	440.47	180.43	391.07
SALTATION									
DS451	0.77	2.74	22.78	73.71	0.00	0.00	257.64	72.83	242.70
DS452	0.20	1.02	11.38	66.46	20.95	0.00	342.98	142.91	314.80
DR451	0.14	0.32	4.71	32.06	62.76	0.00	480.14	160.04	445.32
DR452	0.31	0.98	6.89	39.91	51.91	0.00	442.37	170.30	401.73
DS751	0.64	2.16	12.79	69.07	15.35	0.00	320.33	134.12	292.47
DS752	0.54	1.95	16.85	80.66	0.00	0.00	268.92	65.01	256.91
DR751	0.66	2.33	13.98	66.96	16.07	0.00	320.27	137.92	290.69
DR752	0.35	1.04	10.66	39.63	48.32	0.00	425.70	176.52	381.12
DS951	0.23	0.65	4.53	27.66	66.93	0.00	491.93	158.62	456.01
DR951	0.37	0.54	1.68	29.55	67.87	0.00	498.91	150.47	467.55

TABLE B-3

PARTICLE DISTRIBUTION BY COUNT

	Particle Size Range (um)									
	25-50	50-100	100-200	200-400	400-800	800-1600	MEAN	STD DEV	MEDIAN	# of Particles
MID. PT.	37.5	75.00	150.00	300.00	600.00	1200.00				
INITIAL										
WS451B	59.80	19.10	12.30	7.30	1.30	0.00	75.10	79.90	45.90	219.00
WS452B	59.80	24.80	8.70	5.60	0.80	0.00	67.60	69.00	45.90	229.00
WR451B	65.00	21.90	10.30	2.30	0.30	0.00	59.40	53.50	44.20	260.00
WR452B	72.20	17.80	6.90	2.10	0.70	0.00	54.90	58.50	42.30	274.00
WS751B	63.00	22.80	9.20	3.70	1.00	0.00	64.10	65.20	44.80	398.00
WS752B	70.30	17.90	7.90	3.40	0.30	0.00	56.70	52.90	42.80	290.00
WR751B	71.00	12.60	9.60	5.00	1.60	0.00	66.30	78.60	42.60	238.00
WR752B	67.30	20.60	5.70	4.40	1.90	0.00	68.80	87.80	43.60	315.00
WS951B	67.10	20.10	6.30	5.10	1.20	0.00	64.90	74.70	43.60	332.00
WR951B	67.20	17.80	8.10	6.30	0.30	0.00	66.60	78.00	43.60	269.00
FINAL										
WS451A	66.30	15.70	10.30	4.80	2.00	0.00	68.80	78.40	43.80	247.00
WS452A	68.20	19.30	7.40	4.00	0.80	0.00	61.60	66.90	43.30	347.00
WR451A	59.90	24.70	10.30	4.60	0.20	0.00	66.00	60.00	45.90	347.00
WR452A	54.50	27.90	8.70	7.80	0.80	0.00	74.60	76.40	47.90	229.00
WS751A	69.10	16.30	7.80	5.30	1.40	0.00	66.20	76.30	43.10	282.00
WS752A	67.60	20.90	7.90	1.90	1.50	0.00	61.20	80.60	43.50	263.00
WR751A	59.00	12.60	17.60	9.00	0.90	0.40	87.30	98.90	46.10	221.00
WR752A	64.60	20.00	7.10	7.10	1.00	0.00	72.00	84.60	44.30	294.00
WS951A	68.30	19.30	7.70	3.40	1.10	0.00	62.50	69.80	43.30	259.00
WR951A	56.10	19.70	15.70	7.30	0.90	0.00	79.70	77.00	47.30	203.00
SALTATION										
WS451	30.90	35.10	23.80	8.70	1.20	0.00	96.20	78.60	77.10	239.00
WS452	40.90	17.50	25.80	11.70	3.90	0.00	117.90	113.10	75.70	205.00
WR451	22.10	11.30	13.10	28.20	4.40	0.00	163.00	115.20	147.80	202.00
WR452	32.60	6.20	20.10	34.60	6.20	0.00	174.10	131.80	15.80	208.00
WS751	70.70	13.40	8.60	5.90	1.10	0.00	67.00	81.00	42.70	335.00
WS752	68.70	17.60	7.20	4.90	1.40	0.00	64.80	77.40	43.20	346.00
WR751	62.20	16.00	10.30	8.40	2.30	0.40	85.10	111.80	45.10	212.00
WR752	59.50	16.00	15.60	7.30	1.30	0.00	77.70	79.70	46.00	230.00
WS951	61.60	21.00	13.20	3.10	0.90	0.00	67.00	64.20	45.30	219.00
WR951	60.10	22.70	12.70	3.90	0.30	0.00	66.70	70.00	45.80	251.00

TABLE B-4

PARTICLE DISTRIBUTION BY WEIGHT

	Particle Size Range (um)								
	25-50	50-100	100-200	200-400	400-800	800-1600	MEAN	STD DEV	MEDIAN
MID. PT.	37.5	75.00	150.00	300.00	600.00	1200.00			
INITIAL									
WS451B	0.59	1.52	7.82	37.14	52.92	0.00	442.04	175.20	396.61
WS452B	0.86	2.85	8.00	41.20	47.09	0.00	420.59	178.86	371.41
WR451B	1.97	5.30	19.94	35.62	37.17	0.00	364.52	195.44	301.53
WR452B	1.57	3.10	9.60	23.38	62.35	0.00	461.56	187.55	400.94
WS751B	0.92	2.67	8.63	27.76	60.02	0.00	458.68	181.93	404.94
WS752B	1.91	3.88	13.71	47.19	33.31	0.00	365.64	179.89	313.01
WR751B	0.72	1.02	6.21	25.86	66.20	0.00	485.12	167.33	441.68
WR752B	0.63	1.55	3.43	21.19	73.20	0.00	509.30	155.91	469.99
WS951B	0.82	1.97	4.94	32.01	60.25	0.00	466.75	171.44	421.04
WR951B	1.30	2.75	10.00	62.24	23.71	0.00	346.54	154.75	309.12
FINAL									
WS451A	0.58	1.09	5.73	21.37	71.23	0.00	501.12	161.74	459.74
WS452A	1.13	2.56	7.87	34.01	54.42	0.00	442.73	181.07	390.48
WR451A	1.46	4.83	16.11	57.57	20.02	0.00	321.19	157.80	279.64
WR452A	0.67	2.75	6.87	49.27	40.43	0.00	403.02	171.67	359.33
WS751A	0.76	1.43	5.46	29.67	62.69	0.00	474.70	169.29	430.54
WS752A	0.86	2.13	6.43	12.38	78.20	0.00	517.89	162.12	470.50
WR751A	0.26	0.44	4.96	20.31	16.25	57.77	166.30	226.87	714.31
WR752A	0.77	1.90	5.40	43.22	48.70	0.00	431.71	171.72	388.22
WS951A	0.98	2.22	7.08	25.00	64.72	0.00	475.97	176.02	425.03
WR951A	0.65	1.82	11.63	43.25	42.65	0.00	404.72	178.12	357.84
SALTATION									
WS451	0.28	2.51	13.59	39.76	43.87	0.00	404.85	182.59	355.37
WS452	0.17	0.59	6.94	25.17	67.13	0.00	489.20	163.90	450.00
WR451	0.07	0.27	2.51	43.21	53.94	0.00	457.27	157.50	426.30
WR452	0.07	0.11	2.89	39.83	57.09	0.00	466.50	157.06	435.47
WS751	0.86	1.30	6.67	36.59	54.58	0.00	448.57	173.49	403.46
WS752	0.77	1.58	5.17	28.15	64.33	0.00	479.67	168.51	435.26
WR751	0.22	0.46	2.38	15.54	34.04	47.36	254.84	271.00	712.38
WR752	0.58	1.25	9.74	36.47	51.96	0.00	436.93	177.63	390.34
WS951	0.97	2.65	13.31	25.00	58.07	0.00	445.75	190.76	386.52
WR951	1.40	4.24	18.99	46.65	28.71	0.00	344.41	177.68	293.87

appendix c

PARTICLE DISTRIBUTION OF SELECTED FILTERS

TABLE C-1

PARTICLE SIZE DISTRIBUTION BY COUNT

	Particle Size Range (um)									
	25-50	50-100	100-200	200-400	400-800	800-1600	MEAN	STD DEV	MEDIAN	# of PARTICLE
MID. PT.	37.50	75.00	150.00	300.00	600.00	1200.00				
FILTER										
DS751_23	35.40	11.80	14.00	32.20	6.30	0.00	161.50	138.30	119.40	220.00
DS751_24	36.20	19.80	9.10	23.60	10.60	0.40	166.50	165.60	84.80	207.00
DS751_33	47.50	12.90	12.50	21.60	5.20	0.00	131.60	131.70	59.30	208.00
DS751_34	37.10	21.20	16.80	19.90	4.80	0.00	136.30	130.90	80.20	226.00
DS752_23	29.90	9.80	12.10	42.90	5.10	0.00	187.80	142.40	184.60	214.00
DS752_24	18.50	18.50	32.00	25.50	5.50	0.00	161.90	122.90	140.60	200.00
DS752_33	34.10	14.40	10.70	33.60	6.50	0.40	168.10	147.60	113.00	214.00
DS752_34	11.00	34.80	23.80	22.90	6.80	0.40	168.80	144.40	117.30	218.00
DR751_23	12.70	11.70	17.10	43.60	13.20	1.40	239.70	163.50	238.20	204.00
DR751_24	18.50	7.50	13.00	46.00	15.00	0.00	242.50	165.40	247.80	200.00
DR751_33	9.30	8.80	32.00	45.30	4.40	0.00	206.50	113.70	199.20	203.00
DR751_34	19.50	39.50	21.40	13.80	5.20	0.40	137.20	133.70	88.60	210.00
DR752_23	10.60	10.60	26.50	47.70	4.40	0.00	208.60	116.10	209.30	113.00
DR752_24	13.10	29.60	33.40	20.80	2.40	0.40	149.50	116.40	121.70	206.00
DR752_33	10.80	11.80	16.30	50.00	10.30	0.40	236.50	143.00	243.60	202.00
DR752_34	18.60	33.00	25.30	18.10	4.70	0.00	140.20	118.30	97.50	209.00
DS951_23	15.20	13.80	24.20	38.50	8.00	0.00	206.90	143.60	186.30	210.00
DS951_24	31.00	10.00	24.60	27.80	6.30	0.00	166.10	113.60	136.10	219.00
DS951_32	22.00	11.40	13.60	41.80	11.00	0.00	206.90	154.30	213.70	227.00
DS951_33	26.70	9.90	25.80	35.70	1.70	0.00	165.40	115.80	151.70	232.00
DS951_34	42.70	20.20	20.20	14.80	1.80	0.00	104.00	102.30	67.80	222.00
DR951_23	50.90	23.70	10.90	11.20	3.10	0.00	94.50	105.80	49.50	320.00
DR951_24	31.20	18.50	28.70	19.50	1.90	0.00	132.50	112.70	100.80	205.00
DR951_32	51.30	14.70	7.10	20.90	5.80	0.00	126.30	141.60	49.30	224.00
DR951_33	34.70	12.30	20.90	23.30	8.00	0.40	158.00	145.10	113.60	210.00
DR951_34	46.30	21.10	21.50	7.50	3.10	0.00	96.00	96.10	58.60	250.00

TABLE C-2

PARTICLE SIZE DISTRIBUTION BY WEIGHT

	Particle Size Range (um)								
	25-50	50-100	100-200	200-400	400-800	800-1600	MEAN	STD DEV	MEDIAN
MID. PT.	37.50	75.00	150.00	300.00	600.00	1200.00			
FILTER									
DS751_23	0.08	0.22	2.07	38.06	59.57	0.00	474.91	154.57	444.81
DS751_24	0.05	0.23	0.84	17.41	62.57	18.89	429.14	240.39	595.46
DS751_33	0.14	0.31	2.40	33.20	63.94	0.00	487.16	153.47	456.28
DS751_34	0.12	0.54	3.45	32.73	63.15	0.00	482.74	157.57	449.24
DS752_23	0.07	0.18	1.77	50.22	47.76	0.00	440.05	155.40	411.03
DS752_24	0.05	0.39	5.42	34.54	59.60	0.00	469.66	163.01	433.94
DS752_33	0.06	0.20	1.19	29.78	46.09	22.69	367.81	242.01	558.67
DS752_34	0.02	0.51	2.79	21.51	51.11	24.05	375.78	252.45	580.90
DR751_23	0.01	0.08	0.89	18.08	43.79	37.16	318.38	271.93	675.20
DR751_24	0.02	0.07	0.97	27.42	71.52	0.00	512.90	139.67	488.54
DR751_33	0.02	0.16	4.73	53.51	41.58	0.00	417.23	158.40	386.27
DR751_34	0.05	0.73	3.17	16.36	49.33	30.36	350.40	267.15	622.33
DR752_23	0.02	0.19	3.83	55.21	40.74	0.00	415.98	156.32	386.24
DR752_24	0.04	0.66	5.94	29.60	27.33	36.43	262.18	242.23	570.90
DR752_33	0.01	0.12	1.27	31.20	51.42	15.98	404.14	225.54	529.01
DR752_34	0.06	0.87	5.32	30.46	63.28	0.00	479.76	163.06	442.41
DS951_23	0.03	0.20	2.86	36.40	60.51	0.00	476.70	155.70	445.84
DS951_24	0.07	0.19	3.77	34.11	61.85	0.00	479.25	157.40	446.80
DS951_32	0.03	0.14	1.29	31.73	66.81	0.00	498.10	146.56	471.24
DS951_33	0.10	0.29	6.12	67.70	25.79	0.00	367.28	143.12	341.74
DS951_34	0.26	0.98	7.86	46.07	44.83	0.00	419.80	169.48	380.31
DR951_23	0.26	0.98	3.60	29.60	65.55	0.00	488.36	158.92	452.22
DR951_24	0.16	0.75	9.29	50.47	39.34	0.00	402.00	166.91	364.47
DR951_32	0.15	0.34	1.30	30.50	67.72	0.00	500.08	147.29	471.78
DR951_33	0.06	0.17	2.26	20.13	55.28	22.11	395.59	249.07	586.60
DR951_34	0.26	0.93	7.59	21.18	70.04	0.00	495.97	165.10	454.16

TABLE C-3

PARTICLE DISTRIBUTION BY COUNT

	Particle Size Range (um)									
	25-50	50-100	100-200	200-400	400-800	800-1600	MEAN	STD DEV	MEDIAN	# of Particles
MID. PT.	37.5	75.00	150.00	300.00	600.00	1200.00				
FILTER										
WS751_23	0.00	0.00	0.00	0.00	0.00	0.00	0.00	0.00	0.00	0.00
WS751_24	0.00	0.00	0.00	0.00	0.00	0.00	0.00	0.00	0.00	0.00
WS751_33	0.00	0.00	0.00	0.00	0.00	0.00	0.00	0.00	0.00	0.00
WS751_34	13.40	15.80	36.00	29.30	5.20	0.00	175.60	117.80	157.30	208.00
WS752_23	0.00	0.00	0.00	0.00	0.00	0.00	0.00	0.00	0.00	0.00
WS752_24	23.30	11.60	12.10	49.30	3.40	0.00	205.90	139.90	211.40	231.00
WS752_33	27.20	13.60	22.70	27.70	8.50	0.00	179.10	137.00	140.00	198.00
WS752_34	15.30	12.90	39.20	28.20	4.30	0.00	168.50	105.90	155.50	209.00
WR751_23	0.00	0.00	0.00	0.00	0.00	0.00	0.00	0.00	0.00	0.00
WR751_24	17.30	10.10	28.00	40.00	4.30	0.00	186.60	116.20	180.20	207.00
WR751_33	25.00	12.50	12.50	39.40	10.50	0.00	203.90	157.70	200.00	208.00
WR751_34	36.00	32.70	6.60	17.00	7.50	0.00	128.70	136.30	71.40	211.00
WR752_23	0.00	0.00	0.00	0.00	0.00	0.00	0.00	0.00	0.00	0.00
WR752_24	0.00	0.00	0.00	0.00	0.00	0.00	0.00	0.00	0.00	0.00
WR752_33	10.00	10.00	28.00	43.00	9.00	0.00	211.80	115.60	209.30	200.00
WR752_34	24.80	16.50	31.70	20.90	5.80	0.00	157.50	131.50	126.90	205.00
WS951_23	0.00	0.00	0.00	0.00	0.00	0.00	0.00	0.00	0.00	0.00
WS951_24	20.90	14.40	18.30	33.60	12.60	0.00	198.50	146.80	179.80	229.00
WS951_32	0.00	0.00	0.00	0.00	0.00	0.00	0.00	0.00	0.00	0.00
WS951_33	20.80	10.40	15.90	38.80	13.90	0.00	214.40	152.40	214.10	201.00
WS951_34	35.70	11.10	12.00	28.50	12.00	0.40	178.50	160.30	126.00	207.00
WR951_23	0.00	0.00	0.00	0.00	0.00	0.00	0.00	0.00	0.00	0.00
WR951_24	36.60	8.20	8.20	28.40	18.30	0.00	189.30	172.90	161.10	218.00
WR951_32	0.00	0.00	0.00	0.00	0.00	0.00	0.00	0.00	0.00	0.00
WR951_33	23.30	9.10	16.50	36.60	0.00	0.00	0.00	0.00	0.00	0.00
WR951_34	33.30	29.80	14.60	14.20	5.60	1.80	143.60	174.80	77.40	211.00

TABLE C-4

PARTICLE DISTRIBUTION BY WEIGHT

	Particle Size Range (um)								
MID. PT.	25-50	50-100	100-200	200-400	400-800	800-1600	MEAN	STD DEV	MEDIAN
FILTER	37.5	75.00	150.00	300.00	600.00	1200.00			
WS751_23	0.00	0.00	0.00	0.00	0.00	0.00	0.00	0.00	0.00
WS751_24	0.00	0.00	0.00	0.00	0.00	0.00	0.00	0.00	0.00
WS751_33	0.00	0.00	0.00	0.00	0.00	0.00	0.00	0.00	0.00
WS751_34	0.03	0.33	5.95	38.72	54.97	0.00	455.18	164.91	419.21
WS752_23	0.00	0.00	0.00	0.00	0.00	0.00	0.00	0.00	0.00
WS752_24	0.06	0.23	1.93	63.01	34.77	0.00	400.72	148.17	375.00
WS752_33	0.05	0.22	2.87	28.04	68.82	0.00	501.54	149.46	471.93
WS752_34	0.04	0.30	7.23	41.64	50.79	0.00	440.73	167.31	403.69
WR751_23	0.00	0.00	0.00	0.00	0.00	0.00	0.00	0.00	0.00
WR751_24	0.04	0.20	4.48	51.22	44.05	0.00	424.86	159.53	393.21
WR751_33	0.04	0.16	1.25	31.47	67.09	0.00	498.94	146.30	472.10
WR751_34	0.09	0.65	1.05	21.68	76.52	0.00	526.29	135.93	500.71
WR752_23	0.00	0.00	0.00	0.00	0.00	0.00	0.00	0.00	0.00
WR752_24	0.00	0.00	0.00	0.00	0.00	0.00	0.00	0.00	0.00
WR752_33	0.02	0.13	2.95	36.23	60.67	0.00	477.25	155.47	446.62
WR752_34	0.07	0.36	5.54	29.20	64.83	0.00	485.21	160.56	449.61
WS951_23	0.00	0.00	0.00	0.00	0.00	0.00	0.00	0.00	0.00
WS951_24	0.03	0.16	1.67	24.53	73.60	0.00	517.85	139.49	492.49
WS951_32	0.00	0.00	0.00	0.00	0.00	0.00	0.00	0.00	0.00
WS951_33	0.03	0.11	1.31	25.49	73.07	0.00	516.93	138.78	492.33
WS951_34	0.05	0.11	0.99	18.77	63.22	16.86	437.23	233.02	581.93
WR951_23	0.00	0.00	0.00	0.00	0.00	0.00	0.00	0.00	0.00
WR951_24	0.04	0.07	0.58	16.13	83.17	0.00	548.37	116.18	530.80
WR951_32	0.00	0.00	0.00	0.00	0.00	0.00	0.00	0.00	0.00
WR951_33	0.03	0.09	1.35	24.01	74.52	0.00	521.23	136.68	497.20
WR951_34	0.04	0.26	1.03	8.04	25.37	65.25	178.14	261.86	873.59

TABLE C-5

CONCENTRATION DISTRIBUTION BY SIZE CLASS (mg/m^3)

	Particle Size Range (um)						
	25-50	50-100	100-200	200-400	400-800	800-1600	MEASURED WEIGHT
MIDPOINT	37.50	75.00	150.00	300.00	600.00	1200.00	
FILTER							
DS751_23	0.04	0.12	1.10	20.29	31.75	0.00	53.30
DS751_24	0.41	1.81	6.65	138.06	496.07	149.76	792.76
DS751_33	0.24	0.53	4.09	56.51	108.83	0.00	170.20
DS751_34	1.80	8.22	52.11	493.80	952.87	0.00	1508.80
DS752_23	0.03	0.07	0.66	18.60	17.69	0.00	37.04
DS752_24	0.14	1.15	15.89	101.32	174.82	0.00	293.32
DS752_33	0.06	0.21	1.27	31.94	49.43	24.34	107.26
DS752_34	0.14	3.62	19.83	152.62	362.56	170.62	709.40
DR751_23	.00	0.03	0.37	7.58	18.37	15.59	41.95
DR751_24	0.09	0.29	4.01	113.44	295.94	0.00	413.77
DR751_33	0.04	0.27	7.79	88.18	68.52	0.00	164.79
DR751_34	0.63	10.20	44.20	228.04	687.41	423.02	1393.50
DR752_23	0.01	0.04	0.87	12.58	9.28	0.00	22.78
DR752_24	0.08	1.53	13.79	68.72	63.43	84.58	232.14
DR752_33	0.01	0.11	1.23	30.25	49.85	15.49	96.94
DR752_34	0.42	6.00	36.81	210.69	437.68	0.00	691.61
DS951_23	0.02	0.16	2.18	27.72	46.08	0.00	76.15
DS951_24	0.69	1.78	35.10	317.28	575.22	0.00	930.07
DS951_32	0.01	0.03	0.28	6.76	14.24	0.00	21.31
DS951_33	0.42	1.25	26.16	289.61	110.33	0.00	427.78
DS951_34	4.81	18.22	145.77	854.39	831.30	0.00	1854.50
DR951_23	0.49	1.82	6.68	54.93	121.64	0.00	185.56
DR951_24	1.69	8.03	99.61	541.43	422.04	0.00	1072.80
DR951_32	0.04	0.10	0.39	9.11	20.23	0.00	29.87
DR951_33	0.33	0.94	12.76	113.82	312.65	125.06	565.56
DR951_34	6.97	25.42	207.23	578.33	1912.34	0.00	2730.30

TABLE C-6

CONCENTRATION DISTRIBUTION BY SIZE CLASS (mg/m^3)

	Particle Size Class (um)						
	25-50	50-100	100-200	200-400	400-800	800-1600	MEASURED WEIGHT
MIDPOINT	37.50	75.00	150.00	300.00	600.00	1200.00	
FILTER							
WS751_23	0.00	0.00	0.00	0.00	0.00	0.00	4.44
WS751_24	0.00	0.00	0.00	0.00	0.00	0.00	11.99
WS751_33	0.00	0.00	0.00	0.00	0.00	0.00	9.32
WS751_34	0.01	0.13	2.33	15.18	21.55	0.00	39.20
WS752_23	0.00	0.00	0.00	0.00	0.00	0.00	7.17
WS752_24	0.01	0.05	0.41	13.36	7.37	0.00	21.21
WS752_33	0.01	0.05	0.72	7.07	17.36	0.00	25.22
WS752_[illegible]	0.07	0.49	11.86	68.24	83.24	0.00	163.89
WR751_23	0.00	0.00	0.00	0.00	0.00	0.00	5.32
WR751_24	0.01	0.05	1.18	13.52	11.62	0.00	26.39
WR751_33	0.08	0.34	2.68	67.66	144.24	0.00	215.00
WR751_34	1.63	11.82	19.08	393.14	1387.54	0.00	1813.20
WR752_23	0.00	0.00	0.00	0.00	0.00	0.00	3.05
WR752_24	0.00	0.00	0.00	0.00	0.00	0.00	5.06
WR752_33	.00	0.02	0.48	5.91	9.90	0.00	16.31
WR752_34	0.13	0.68	10.51	55.45	123.10	0.00	189.87
WS951_23	0.00	0.00	0.00	0.00	0.00	0.00	10.68
WS951_24	0.03	0.15	1.55	22.82	68.46	0.00	93.01
WS951_32	0.00	0.00	0.00	0.00	0.00	0.00	4.70
WS951_33	0.01	0.03	0.42	8.17	23.42	0.00	32.06
WS951_34	0.17	0.41	3.58	67.99	229.02	61.07	362.24
WR951_23	0.00	0.00	0.00	0.00	0.00	0.00	10.34
WR951_24	0.01	0.02	0.20	5.47	28.19	0.00	33.90
WR951_32	0.00	0.00	0.00	0.00	0.00	0.00	2.92
WR951_33	0.02	0.06	0.88	15.66	48.61	0.00	65.24
WR951_34	0.24	1.69	6.63	51.61	162.84	418.73	641.74

appendix d

PARTICLE DISTRIBUTION OF VERTICAL FLUXES

TABLE D-1

MASS FLUX RATE DISTRIBUTION BY SIZE CLASS (mg/m^2-s)

	Particle Size Range (um)						
	25-50	50-100	100-200	200-400	400-800	800-1600	
MIDPOINT	37.50	75.00	150.00	300.00	600.00	1200.00	
FILTER							FLUX
DS751_23	0.01	0.02	0.16	2.88	4.50	0.00	7.56
DS751_24	0.08	0.37	1.37	28.33	101.78	30.73	162.65
DS751_33	0.04	0.10	0.74	10.21	19.66	0.00	30.75
DS751_34	0.36	1.64	10.39	98.48	190.02	0.00	300.89
DS752_23	.00	0.01	0.07	2.09	1.99	0.00	4.17
DS752_24	0.02	0.19	2.59	16.52	28.50	0.00	47.83
DS752_33	0.01	0.04	0.22	5.48	8.48	4.17	18.39
DS752_34	0.03	0.69	3.75	28.89	68.62	32.29	134.26
DR751_23	.00	0.01	0.07	1.36	3.28	2.78	7.50
DR751_24	0.02	0.06	0.78	21.99	57.36	0.00	80.20
DR751_33	0.01	0.07	2.07	23.50	18.26	0.00	43.91
DR751_34	0.16	2.67	11.58	59.74	180.09	110.82	365.07
DR752_23	.00	0.01	0.13	1.94	1.43	0.00	3.51
DR752_24	0.01	0.26	2.30	11.48	10.60	14.13	38.78
DR752_33	.00	0.03	0.30	7.24	11.93	3.71	23.20
DR752_34	0.10	1.41	8.66	49.58	103.00	0.00	162.76
DS951_23	.00	0.03	0.40	5.03	8.37	0.00	13.83
DS951_24	0.18	0.47	9.17	82.88	150.26	0.00	242.96
DS951_32	.00	0.01	0.06	1.58	3.33	0.00	4.98
DS951_33	0.11	0.31	6.53	72.33	27.55	0.00	106.83
DS951_34	1.28	4.84	38.75	227.10	220.97	0.00	492.94
DR951_23	0.16	0.58	2.14	17.56	38.88	0.00	59.31
DR951_24	0.60	2.84	35.29	191.84	149.54	0.00	380.11
DR951_32	0.02	0.04	0.14	3.35	7.43	0.00	10.97
DR951_33	0.12	0.34	4.58	40.86	112.24	44.90	203.04
DR951_34	2.44	8.89	72.51	202.35	669.10	0.00	955.29

TABLE D-2

AVERAGE MASS FLUX RATE DISTRIBUTION BY SIZE CLASS (mg/m^2-s)

	25-50	50-100	100-200	200-400	400-800	800-1600	
MIDPOINT	37.50	75.00	150.00	300.00	600.00	1200.00	
AVG FILTER							
DS75_23	.00	0.01	0.11	2.60	3.17	0.00	5.90
DS75_24	0.05	0.29	2.48	23.95	63.21	12.71	102.70
DS75_33	0.02	0.06	0.40	7.63	12.93	3.58	24.62
DS75_34	0.12	1.14	6.60	55.80	120.77	32.82	217.26
DR75_23	.00	0.01	0.07	1.32	2.36	1.69	5.45
DR75_24	0.02	0.15	1.45	16.55	34.31	6.47	58.95
DR75_33	0.01	0.04	0.83	13.04	16.08	3.49	33.49
DR75_34	0.14	2.07	10.65	58.17	144.50	46.81	262.33
DS951_23	.00	0.03	0.40	5.03	8.37	0.00	13.83
DS951_24	0.18	0.47	9.17	82.88	150.26	0.00	242.96
DS951_32	.00	0.01	0.06	1.58	3.33	0.00	4.98
DS951_33	0.11	0.31	6.53	72.33	27.55	0.00	106.83
DS951_34	1.28	4.84	38.75	227.10	220.97	0.00	492.94
DR951_23	0.16	0.58	2.14	17.56	38.88	0.00	59.31
DR951_24	0.60	2.84	35.29	191.84	149.54	0.00	380.11
DR951_32	0.02	0.04	0.14	3.35	7.43	0.00	10.97
DR951_33	0.17	0.49	6.61	58.98	162.00	64.80	293.04
DR951_34	2.44	8.89	72.51	202.35	669.10	0.00	955.29

TABLE D-3

MASS FLUX RATE DISTRIBUTION BY SIZE CLASS (mg/m^2-s)

	Particle Size Class (um)						
	25-50	50-100	100-200	200-400	400-800	800-1600	FLUX
MIDPOINT	37.50	75.00	150.00	300.00	600.00	1200.00	
FILTER							
WS751_23	0.00	0.00	0.00	0.00	0.00	0.00	0.17
WS751_24	0.00	0.00	0.00	0.00	0.00	0.00	0.67
WS751_33	0.00	0.00	0.00	0.00	0.00	0.00	0.86
WS751_34	.00	0.01	0.24	1.54	2.18	0.00	3.97
WS752_23	0.00	0.00	0.00	0.00	0.00	0.00	0.53
WS752_24	.00	0.01	0.04	1.44	0.79	0.00	2.29
WS752_33	.00	0.01	0.12	1.15	2.81	0.00	4.09
WS752_34	0.01	0.09	2.12	12.21	14.90	0.00	29.33
WR751_23	0.00	0.00	0.00	0.00	0.00	0.00	0.43
WR751_24	.00	.00	0.10	1.18	1.01	0.00	2.30
WR751_33	0.03	0.11	0.86	21.72	46.30	0.00	69.01
WR751_34	0.51	3.71	6.00	123.55	436.04	0.00	569.81
WR752_23	0.00	0.00	0.00	0.00	0.00	0.00	0.19
WR752_24	0.00	0.00	0.00	0.00	0.00	0.00	0.35
WR752_33	.00	.00	0.11	1.33	2.23	0.00	3.68
WR752_34	0.03	0.15	2.33	12.29	27.29	0.00	42.09
WS951_23	0.00	0.00	0.00	0.00	0.00	0.00	1.20
WS951_24	.00	0.02	0.25	3.70	11.09	0.00	15.07
WS951_32	0.00	0.00	0.00	0.00	0.00	0.00	1.07
WS951_33	.00	0.01	0.10	1.99	5.72	0.00	7.82
WS951_34	0.04	0.11	0.93	17.66	59.49	15.86	94.09
WR951_23	0.00	0.00	0.00	0.00	0.00	0.00	2.01
WR951_24	.00	0.01	0.04	1.18	6.08	0.00	7.31
WR951_32	0.00	0.00	0.00	0.00	0.00	0.00	1.28
WR951_33	0.01	0.03	0.38	6.72	20.87	0.00	28.01
WR951_34	0.10	0.71	2.78	21.59	68.13	175.19	268.49

TABLE D-4

AVERAGE MASS FLUX RATE DISTRIBUTION BY SIZE CLASS (mg/m^2-s)

	Particle Size Range (um)						
	25-50	50-100	100-200	200-400	400-800	800-1600	FLUX
MIDPOINT	37.50	75.00	150.00	300.00	600.00	1200.00	
AVG FILTER							
WS75_23	0.00	0.00	0.00	0.00	0.00	0.00	0.33
WS75_24	.00	.00	0.02	0.54	0.30	0.00	1.35
WS75_33	.00	.00	0.05	0.48	1.17	0.00	2.33
WS75_34	0.01	0.05	1.06	6.21	7.80	0.00	15.12
WR752_23	0.00	0.00	0.00	0.00	0.00	0.00	0.19
WR752_24	0.00	0.00	0.00	0.00	0.00	0.00	0.35
WR752_33	.00	.00	0.11	1.33	2.23	0.00	3.68
WR752_34	0.03	0.15	2.33	12.29	27.29	0.00	42.09
WS951_23	0.00	0.00	0.00	0.00	0.00	0.00	1.20
WS951_24	.00	0.02	0.25	3.70	11.09	0.00	15.07
WS951_32	0.00	0.00	0.00	0.00	0.00	0.00	1.07
WS951_33	.00	0.01	0.10	1.99	5.72	0.00	7.82
WS951_34	0.04	0.11	0.93	17.66	59.49	15.86	94.09
WR951_23	0.00	0.00	0.00	0.00	0.00	0.00	2.01
WR951_24	.00	0.01	0.04	1.18	6.08	0.00	7.31
WR951_32	0.00	0.00	0.00	0.00	0.00	0.00	1.28
WR951_33	0.01	0.03	0.38	6.72	20.87	0.00	28.01
WR951_34	0.10	0.71	2.78	21.59	68.13	175.19	268.49

appendix e

CHEMICAL CHARACTERISTICS OF THE TAILINGS SAMPLES

INTRODUCTION

As a part of the overall program of investigation, AER undertook the responsibility of obtaining a chemical analysis of dust samples from the tailings material used in the wind tunnel erosion study.

The original intention was to take the dust samples directly from the material collected during the wind tunnel runs. The amount of material impacting upon the samplers however, proved to be too little for an appropriate analysis. It was decided therefore to take the material for analysis directly from the untested tailings material. Although this would not provide information on the chemical composition of the eroded material directly, a correlation of the results with respect to particle size distribution after the fact would enable this information to be extracted. The subsequent steps involving such a correlation was not deemed to be part of the present investigation.

Monenco Analytical Laboratories of Calgary were contracted to provide the chemical analysis for a number of samples of the base, uneroded tailings material.

The Work Statement describing this part of the project was prepared by NUTP and is attached. The final report on the chemical analysis from Monenco follows. Through a misunderstanding, sample S-3 was not analysed in duplicate. An inspection of the results however, showed no abnormalitites in the data for this sample and after some discussion with Monenco, and given the limitations on time for meeting the contract, it was decided to present the results as is.

WORK STATEMENT FOR ANALYSIS OF DUST SAMPLES

Samples:

There are ten(10) solid test samples. Sample S-3 is to be analyzed in duplicate.

Analytical Requirements:

All samples except S-10 are to be analyzed for:

(1) calcium
(2) total iron
(3) total sulphur
(4) sulphate
(5) total uranium
(6) radium-226
(7) lead -210
(8) total thorium
(9) thorium-230
(10) thorium-232

Sample S-10 is to be analyzed for barium only.

Background:

All the samples were taken from uranium mill tailings in Elliot Lake, Ontario. The expected concentration of the constituents can therefore be approximated by:

Constituent	Conc'n	Constituent	Conc'n
Ca	100 -8000 µg/g	Ra-226	0.5 - 10 Bq/g
Fe	1000-30,000 µg/g	Pb-210	0.5 - 10 Bq/g
S	1 - 5 %	Th	100 - 400 µg/g
SO_4^{2-}	0.2 - 9 %	Th-230	0.5 - 10 Bq/g
U	5 - 150 µg/g	Th-232	0.05 - 2 Bq/g
Ba	0.01 - 100 µg/g		

Methodological Information:

The laboratory is to provide a brief summary of the methods used including an estimate of the limit of detection. The mass of test portion used is to be reported.

File

MONENCO ANALYTICAL LABORATORIES
A DIVISION OF MONENCO CONSULTANTS LIMITED

2023 - 2nd Avenue S.E.
Calgary, Alberta, Canada T2E 6K1

Telephone: (403) 273-2525 Telex: 038-22636

March 24, 1986

Dr. J.F. Keffer,
Atmospheric Environment Research,
Box 65,
Oakville, Ontario
L6J 4Z5

Dear Dr. Keffer:

The results of our analysis of the dust sample that you submitted are attached. Please note that we received only 10 samples from Henry Steger, so the cost is reduced.

In the course of our quality control program we analysed a CANMET standard, DL-1a, (Ref.: CANMET Report 84-14E). Those results are included. In addition, we analysed one of the samples, S4, in duplicate. Those results are included (in brackets).

The methodologies that we used are attached. The radiochemical methods quoted refer to the NUTP Analytical Methods Manual (soon to be published?).

If you have any questions concerning this report don't hesitate to contact me. I hope that we can have the opportunity to be of further service to you in the coming months.

Yours truly,

John R. Dean, Ph.D.
General Manager

JRD/ns
Attach.

DUST SAMPLE ANALYSIS

MONENCO NO.	SAMPLE DESCRIPTION	U µg/g	Ca %	Fe %	Th µg/g	Bq/gm					Total SO_4 mg/g	Total Sulfur as S, mg/g ±2
						Ra226	Th232	Th230	Th228	Pb210		
RS 6335	S-1	31 ±1	0.92	5.0	450	5.0 ±0.2	1.74 ±0.06	1.36 ±0.06	2.14 ±0.08	4.6 ±0.2	175	56
6336	S-2	35 ±1	1.23	4.1	315	6.2 ±0.2	1.23 ±0.08	1.07 ±0.08	2.06 ±0.10	4.7 ±0.2	149	45
6337	S-3	16 ±1	0.29	1.3	120	2.59 ±0.11	0.470±0.011	0.410±0.010	0.382±0.011	1.7 ±0.2	39 ±3	11 ±2
6338	S-4	9 ±1	(1.06) 1.07	(0.69) 0.69	(14) 11	(1.28 ±0.05) 1.23 ±0.06	(0.054±0.005) 0.043±0.009	(0.22 ±0.02) 0.18 ±0.02	(0.078±0.012) 0.061±0.011	(1.1 ±0.2) 1.3 ±0.2	(21 ±2) 24 ±2	(6 ±1) 6 ±1
6339	S-5	61 ±1	0.37	3.1	170	5.89 ±0.11	0.68 ±0.04	4.05 ±0.14	0.99 ±0.07	4.8 ±0.2	104 ±3	33 ±3
6340	S-6	34 ±1	2.8	3.6	205	8.48 ±0.10	0.82 ±0.05	1.30 ±0.06	1.50 ±0.07	5.6 ±0.2	124 ±3	31 ±3
6341	S-7	7.2±0.5	0.13	0.43	8	1.74 ±0.07	0.031±0.007	0.21 ±0.02	0.131±0.011	1.35±0.09	8.4 ±0.5	2.5 ±0.5
6342	S-8	30 ±1	0.64	3.8	325	4.01 ±0.10	1.25 ±0.12	0.80 ±0.09	1.60 ±0.14	3.2 ±0.2	142 ±4	40 ±3
6343	S-9	13 ±1	0.31	1.1	50	1.94 ±0.08	0.22 ±0.05	0.41 ±0.06	0.32 ±0.05	1.75±0.12	32 ±3	9 ±1
6344	S-10	-	0.27	1.3	-	-	-				39 ±	
CANMET STD												
DL-12 Found		-	0.25	0.97	-	1.30 ±0.08	-	-	-	1.6 ±0.2	14 ±2	-
	Present	-	Approx. 0.3	Approx. 0.9	-	1.40 ±0.04	-	-	-	1.4 ±0.02	-	4

Ra-226	KF/pyrosulfate fusion (Section 2.5.4) Coprecipitate Ra with $BaSO_4$ and HRAS (Section 5.1.5)
Th's	KF/pyrosulfate fusion. (Section 2.5.4) Extraction and coprecipitation with $Ce(OH)_3$ and HRAS (Section 9.5)
Pb-210	$HF/HNO_3/HClO_4$ Digestion and pyrosulfate fusion (Section 2.5.5) Extraction and coprecipitation of Bi-210 with BiOCl and beta count. (Section 7.5)
Ca/Fe/Sulfate	Total acid digestion ($HF/HNO_3/HClO_4$) ICAP (Ca/Fe) $BaSO_4$ turbidimetry (sulfate)
Total S	AOAC 2.148 (Ion chromatography finishing)
Uranium	Delayed neutron activation

HRAS = High Resolution Alpha Spectrometry

Official methods of Analysis of the Association of Official Analytical Chemists 14th edition

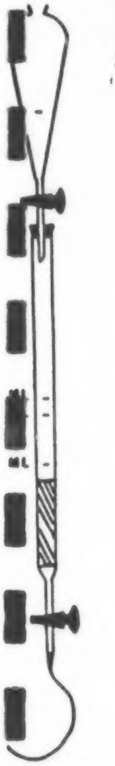

in column.

or to column.
mple soln to
s 0.5*N* HCl.
5 sec/drop.
h 20 ml 0.5*N*
in column.

tion of Zinc

, immediately
sec/drop until 1
M NH_4SCN.
rain resin and
oir thru elution
tubing and col-
ension as it is
n liq. reaches
g tube to vol.
k until flow just
rop remains in
d neither rises
eparator with
ck. Add 240 ml
opcock. Open
ml/min is sus-
e rate slightly
tinue overnight.
adjust rate as
mark. Finally,

---

lower flask, fill to 250 ml mark at convenient rate from dispensing tip, and mix. Detach hose and separator from column, and drain all 3. Reactivate resin, and stopper column as in 2.143.

2.145 ***Determination***

Pipet 20 ml eluate into 50 ml vol. flask contg small piece litmus paper. Make alk. with 0.3*N* NaOH, then just acidic with 0.25*N* HCl. Pipet in 2 ml more acid, 5 ml buffer, and 3 ml zincon soln. Dil. to vol. with H_2O. Similarly prep. 0, 1, 2, and 3 ppm std solns, using 0, 5, 10, and 15 ml std Zn working soln, resp. Using 0 ppm std soln as blank, det. *A* at 620 nm 15–45 min after zincon addn. Plot std curve of ppm against *A*.

% $Zn = (C \times F)/W$, where C = ppm from std curve; W = g sample; and $F = 0.0625$ for samples contg <0.14% Zn or 6.25/ml aliquot pipetted onto resin for samples contg ≥0.14% Zn.

2.146 ***Atomic Absorption Method***

See 2.096–2.100.

Total Sulfur (54)—Official Final Action

2.147 ***Reagents***

(a) *Barium chloride soln.*—10%. Dissolve 100 g $BaCl_2.2H_2O$ in 900 ml H_2O and filter thru Whatman No. 42 paper, or equiv. 1 ml = 14 mg S.

(b) *Bromine in carbon tetrachloride.*—10%. Add 10 g Br to 90 g reagent grade CCl_4. Stir until homogeneous. Store in g-s bottle. (*Caution: See* 51.047 and 51.049.)

2.148 ***Determination***

Weigh sample contg 50–150 mg S into 250 ml beaker, and add 20 ml 10% Br in CCl_4, (b). Mix by swirling beaker at 5 min intervals during 30 min. Add 15 ml HNO_3 and mix as before. Evap. to 1–2 ml on warm hot plate. Add 15 ml HCl and 10 ml H_2O. Evap. just to dryness on warm hot plate or steam bath. Add 10 ml HCl and 50 ml H_2O, heat to boiling, boil 5 min, and filter thru Whatman No. 42 paper, or equiv. Wash paper with ten 20 ml portions hot H_2O.

Heat filtrate to boiling. Add 5–6 drops 10% $BaCl_2$ soln, (a). After 1 min, add dropwise amt $BaCl_2$ soln equiv. to expected S content plus 5 ml excess. Digest at gentle boil 1 hr. Remove from hot plate and let ppt settle 15–20 min. Filter immediately thru prepd gooch, previously ignited and weighed. Wash with hot H_2O until 10 ml wash H_2O shows no ppt with 3 ml 1% $AgNO_3$. Dry and ignite at 800° to constant wt. Cool in desiccator over $MgClO_4$ and weigh.

% S = g $BaSO_4 \times 0.1374 \times 100$/g sample.

2.149 Free Sulfur (55)—Official Final Action

(*Caution: See* 51.011, 51.047, 51.048, and 51.049.)

Ext 1 g sample with CS_2 in Soxhlet app., letting extn thimble drain ≥12 times. Transfer ext to 250 ml beaker. Evap. CS_2 in draft at room temp. Heat in oven 20 min at 60–70°; then cool to room temp. Add 10 ml satd soln of Br in CCl_4, cover, and let stand ca 30 min, stirring several times. Add 15 ml HNO_3, cover, and let stand ca 30 min, stirring several times. Evap. on hot plate to ca 5 ml. Add 20 ml HCl and evap. to ca 5 ml. Add ca 50 ml H_2O; filter, and wash with HCl (1+49). Add 2 drops bromophenol blue, 6.018(f), and then NH_4OH to first color change. Add HCl dropwise until distinctly acid, then 5 drops excess; dil. to 150 ml, heat to bp, and add 10% $BaCl_2$ soln, 2.147(a), dropwise until ca 50% excess is present. Cover beaker and digest on steam bath ≥1 hr. Cool to room temp. and filter thru asbestos on gooch previously ignited at 800° and weighed. Wash 10 times with hot H_2O. Ignite in furnace at 800° ≥20 min. Cool in desiccator and weigh as $BaSO_4$. Calc. as S as in 2.148.

2.150 ★ Acid-Forming or Nonacid-Forming ★ Quality (56)—Official Final Action

Fusion with std amt Na_2CO_3 followed by neutzn of melt with excess acid and back-titrn with std NaOH. *See* 2.141–2.142, 11th ed.

PEAT—OFFICIAL FIRST ACTION

(Moss, humus, and reed-sedge types)

2.151 Sampling (57)—Procedure

Use slotted single or double tube or slotted tube and rod, all with pointed ends and min. 1" diam. Pennsylvania State Forage Sampler (NASCO, Fort Atkinson, WI 53538) is satisfactory core sampler.

Take representative sample from lot or shipment as follows:

(a) *Packaged or baled peats.*—Lay bag or bale horizontally and remove core diagonally from end to end. From lots of 1–10 bags, sample all bags; from lots of ≥11, sample 10 bags. Take 1 core from each bag sampled; except for lots of 1–4 bags, take diagonal cores from each bag and addnl cores to total ≥5 cores.

(b) *Bulk samples.*—Draw ≥10 cores from different regions.

(c) *Small containers (10 lb or less).*—Take entire package. Working rapidly to prevent moisture losses, reduce composite sample to ≤500 g (by wt) or 2 L (by vol.) by mixing on clean oilcloth or paper and quartering. Place sample in air-tight container.

Sampling by random "grab" procedure is necessary if particle size range is to be detd or if representative sample cannot be taken with core sampler as above.

2.152 Preparation of Sample (58)—Official First Action

Place representative field sample on square rubber sheet, paper, or oilcloth. Reduce sample to amt required by quartering and place in moisture-proof container. *Work rapidly to prevent moisture losses.*

Moisture (58)—Official First Action

2.153 ***Method I***

Mix sample thoroly and place 10–12 g in ignited and weighed (with fitted heavy-duty Al foil cover) Vycor

---

★ Surplus method—see inside front cover.

ADDENDUM TO APPENDIX E

This Addendum to Appendix E was prepared by H.F. Steger, Project Manager, Measurements, NUTP.

DISCUSSION OF ANALYTICAL RESULTS

The particle size distribution of the tailings sample used in this study of wind-generated dust suspensions is shown in Table E-2 and was determined at the Mineral Sciences Laboratories of the Canada Centre for Mineral and Energy Technology using Rotap Sieves.

Ten tailings samples, including the eight particle size fractions in Table E-2, were assigned a random sample number between one and ten and submitted to Monenco Analytical Laboratories. Samples S-3 and S-9 were replicates of the 75 - 150 µm fraction. Sample S-5 was a test portion of UTS-2, a reference uranium tailings sample(1). The analytical results for the particle size fractions are reported in Tables E-3 and E-4. The duplicate results for the 75-150 µm fraction are in acceptable agreement except for total thorium. Unfortunately since Monenco Analytical Laboratories did not analyze S-3 in duplicate as requested, it is not possible to assign this discrepancy to analytical error or sample inhomogeneity. A comparison of total thorium values for larger and smaller particle size ranges also does not provide any evidence as to which value is more reasonable.

The results for S-5, the test portion of UTS-2, are shown together with the recommended values in Table E-5. The good agreement observed attests to the accuracy of the analytical results. Sample S-10 represents that fraction of the tailings which passes a 212 µm sieve, and was to have been analyzed for barium only. Monenco Analytical Laboratories did not do this but provided instead results for Ca, Fe and SO_4^{2-}. These values may be used to check the overall accuracy of these constituents by comparing these values with calculated values based on the sum of the constituent concentrations times the mass fraction for all particle size fractions. The reported values for Ca, Fe and SO_4^{2-} of 0.27 %, 1.3% and 39 mg/g compare very well with the calculated values of 0.38%, 1.43% and 42 mg/g, respectively.

---

(1) C.W. Smith, H.F. Steger and W.S. Bowman, "Uranium Tailings Reference Materials", NUTP-2E, CANMET, Energy, Mines and Resources Canada, 1984.

The constituents of interest in these tailings samples exhibit two types of behaviour with decreasing particle size. Iron, total Th, SO_4^{2-}, total S, Th-232 and Th-228 increase in concentration in a particle size fraction reaching a maximum for 45 - 53 µm. This behaviour is expected where the particle size distribution is determined by comminution, and is reasonable for thorium containing minerals and pyrite which do not necessarily undergo extensive leaching. The sulphate containing minerals however are reprecipitation products during leaching and neutralization and are expected to increase in concentration with decreasing particle size. No explanation can be given at this time.

Uranium and its daughters, thorium-230, radium-226 and lead-210, show a continuous increase in concentration with decreasing particle size. For uranium, the effect of comminution on particle size distribution has been largely countered by extensive leaching. The daughter radionuclides are present as reprecipitation products such as thorium hydroxide and lead and radium sulphates. Calcium also follows this behaviour, as is to be expected, since it is mostly present as gypsum formed in neutralization after leaching.

Although the particle size distribution measured at CANMET is based on different size ranges from those used to characterize dust suspensions in this study, the trends observed in mass fraction and element or radionuclide concentration with particle size are characteristic of the tailings sample. It can be concluded therefore that dust dispersion of tailings material favours the movement of smaller particles having higher uranium decay chain radioactivity.

Table E-2 Particle Size Distribution

Particle Size Fraction, µm	Mass Fraction of Tailings	Code
> 212	0.212	S-4
< 212	0.788	S-10
150 - 212	0.376	S-7
75 - 150	0.266	S-3, S-9
53 - 75	0.081	S-8
45 - 53	0.014	S-1
38 - 45	0.025	S-2
< 38	0.027	S-6

TABLE E-3 ANALYTICAL RESULTS FOR NON-RADIONUCLIDES

Size Fraction	U	Ca	Fe	Th	SO_4^{2-}	S
µm	µg/g	mg/g		µg/g	mg/g	
> 212	9	1.07	0.69	13	23	6
< 212		0.27	1.3		39	
150 - 212	7	0.13	0.43	8	8.4	25
75 - 150	16	0.29	1.3	120	39	11
	13	0.31	1.1	50	32	9
53 - 75	30	0.64	3.8	325	142	40
45 - 53	31	0.92	5	450	175	56
38 - 45	35	1.23	4.1	315	149	45
< 38	34	2.8	3.6	205	124	31

TABLE E-4 ANALYTICAL RESULTS FOR RADIONUCLIDES

Size Fraction	Ra-226	Th-232	Th-230	Th-228	Pb-210
µm			Bq/g		
> 212	1.27	0.048	0.20	0.069	1.2
150 - 212	1.74	0.031	0.21	0.131	1.35
75 - 150	2.59	0.470	0.41	0.382	1.7
	1.94	0.22	0.41	0.32	1.75
53 - 75	4.01	1.25	0.80	1.60	3.2
45 - 53	5.0	1.74	1.36	2.14	4.6
38 - 45	6.2	1.23	1.07	2.06	4.7
< 38	8.5	0.82	1.30	1.50	5.6

TABLE E-5 RESULTS FOR REFERENCE URANIUM TAILINGS SAMPLE UTS-2

Constituent		Value Found	Value Recommended
U	, µg/g	61	56
Ca	, %	0.37	0.42
Fe	, %	3.1	3.2
Th	, µg/g	170	174
SO_4^{2-}	, mg/g	104	84
S	, mg/g	33	32.3
Ra-226	, Bq/g	5.89	5.6
Th-232	, Bq/g	0.68	0.88
Th-230	, Bq/g	4.05	4.4
Th-228	, Bq/g	0.99	1.0
Pb-210	, Bq/g	4.8	4.4

TABLES

TABLE 3.1 ENVIRONMENTAL VARIABLES AND MODEL PARAMETERS FOR THE WIND EROSION EQUATIONS (SMITH, ET AL, 1982)

Primary wind erosion variables	Equivalent erosion equation parameters
Soil erodibility index, I (function of soil particle size distribution; read from a table) Knoll erodibility, I_s (function of knoll slope steepness; read from a graph)	Soil and knoll erodibility, I' (the product of I and I_s)
Surface crust stability, F_r	Disregarded—crust is transient
Soil ridge roughness, K_r (function of height, width, and spacing of clods and furrows)	Soil ridge roughness factor, K' (estimated by comparison to a set of standard photographs)
Annual average wind velocity, v (read from map) Surface soil moisture, M [estimated using Thornthwaite's (Ref. 12) precipitation-evaporation index]	Local wind erosion climatic factor, C' (may be calculated but commonly read from maps of C')
Distance across field, D_f (field width in direction of primary erosive wind) Sheltered distance, D_b (calculated from barrier height upwind of field)	Field length, L' (the difference between D_f and D_b)
Quantity of vegetative cover, R' (mass of standing or fallen vegetative residue per unit area) Kind of vegetative cover, S (factor related to erosion-reducing effectiveness of residues from different crops) Orientation of vegetative cover, K_0 (factor relating erosion reduction to standing vs. fallen crop residues)	Equivalent vegetative cover, V (the product of R', S, and K_0)

Table 3.2 Variables Which Influence Suspension (Sehmel, 1980)

Pollutant particle properties	Soil properties	Particle-soil interaction	Surface properties	Topography	Meteorological variables
Chemical reactivity	Moisture content	Attraction forces	Areas of erodible surface	Agricultural	Air density, affected by
Density	Ratio of erodible to non-erodible fractions	• Molecular forces: Van-der-Waals forces	Cohesiveness of particles	Broken	• Humidity
Hydrophobic		• Chemical binding forces (Valence forces)	• Binding action of materials	Desert	• Pressure
Hydrophilic					
Particle diameter	Soil size frequency distribution	• Electrostatic forces	• Surface moisture	Diurnal	• Temperature
• Respirable	Specific gravity	• Magnetic forces	Cover	Flat	Soil burden carried
• Nonrespirable	Structure	Capillary forces at the surface of aggregates filled with liquid	Obstructions	Forested	• Influence on air velocity
• Frequency distribution	• Organic matter	Chemical reaction	Roughness, large scale	Hills	•Avalanching
Shape	• Lime content	Contact area effect on adhesion	• Mechanical turbulence	Humidity	• Saltation
Surface roughness	• Texture	• Particle shape	• Overall sheltering	Seasonal	Surface moisture content
	Temperature	• Particle size	Roughness, small scale	Temperature	• Dew
		• Nature of particle and surface	• Orientation of obstacles	Undulating	• Frost upheaval
		• Surface roughness	• Percent of area covered by non-erodible aggregates or obstacles	Uniform	Relative humidity
		• Adhesion of agglomerates vs individual particles		Urban	Temperature
		Crystallization of dissolved substances	• Sheltering of individual particles	Valley	• Surface dry
		Deposition of suspended colloidal particle	• Stability of aggregates against abrasion and disintegration by moisture and watering	Water	• Surface drying
		Hardening binders			• Surface frozen
					• Wind speed
		Liquid bridges	Temperature		Wind removal forces
		Mineral bridges	Topographic features		• Mean wind speed
		Relative humidity	• Broken		• Frequency, period, and intensity of gusts penetrating to the surface
		Temperature	• Uniform		
		Time of contact	Vegetative cover		• Transient and steady drag
		Viscous surface coating	• Live vegetation		• Verticle wind profile
			• Plant residue		• Stability
					• Vertical turbulent exchange
					• Surface roughness
					• Temperature stratification
					• Wind direction

Table 4.1 Experiment Runs and Nomenclature

Code	Tailings Surface	Turbulence	Wind Speed (m/s)	Replicate #
DS451	DRY	LOW	4.5	1
DS452	DRY	LOW	4.5	2
DR451	DRY	HIGH	4.5	1
DR452	DRY	HIGH	4.5	2
DS751	DRY	LOW	4.5	1
DS752	DRY	LOW	4.5	2
DR751	DRY	HIGH	4.5	1
DR752	DRY	HIGH	4.5	2
DS951	DRY	LOW	4.5	1
DR951	DRY	HIGH	4.5	1
WS451	WET	LOW	4.5	1
WS452	WET	LOW	4.5	2
WR451	WET	HIGH	4.5	1
WR452	WET	HIGH	4.5	2
WS751	WET	LOW	4.5	1
WS752	WET	LOW	4.5	2
WR751	WET	HIGH	4.5	1
WR752	WET	HIGH	4.5	2
WS951	WET	LOW	4.5	1
WR951	WET	HIGH	4.5	1

Table 4.2 Position and Nomenclature of Particle Samplers

Elevation (cm)	Station #1	Station #2	Station #3
40	_11	_21	_31
16	_12	_22	_32
6.5	_13	_23	_33
2.5	_14	_24	_34
Streamwise Distance (m)	0.305	1.006	1.830
Offset from Centerline (m)	-0.15	+0.15	0.00

notes: Particle samplers and samples will be refered to in some cases as DR752_23 which refers to the sampler located at position _23 during test DR752.

Table 4.3 Location of Hot Wire Probes

	Streamwise Distance (m)					
Elevation (cm)	-0.12	0.46	0.88	1.15	1.49	1.75
	10.0	9.2	9.6	9.3	9.3	9.6
	5.0	4.2	4.6	4.3	4.3	4.6
	2.5	1.7	2.1	1.8	1.8	2.1
	1.0	0.8	0.9	0.8	0.8	0.4

¦-----Transition Region----¦----Steady State Region--¦

Table 5.1 Saltation Fluxes

Test	Saltation Flux (mg/m^2-s)	Average (mg/m^2-s)
DS451	3.92	2.47
DS452	1.01	
DR451	3.54	2.33
DR452	1.11	
DS751	242.	200.
DS752	158.	
DR751	288.	332.
DR752	377.	
DS951	481.	481.
DR951	753.	753.
WS451	0.22	0.431
WS452	0.639	
WR451	0.167	0.125
WR452	0.0833	
WS751	11.	23.9
WS752	36.9	
WR751[1]	174.	83.5
WR752	83.5	
WS951	112.	112.
WR951	353.	353.

note: 1) WR751 is considered an anomoly and not considered in the final assessment.

Table 5.2 Variation of Surface Friction Velocity with Distance

Streamwise Distance (m)	Wind (m/s) Turbulence	Friction Velocity (u_*) (cm/s)					
		4.5 Low	4.5 High	7.5 Low	7.5 High	9.5 Low	9.5 High
-0.12		11.8	26.7	20.8	51.6	29.9	61.6
0.46		9.4	25.9	19.1	38.5	29.6	50.0
0.87		11.1	21.5	26.6	34.4	37.6	43.9
1.15		8.3	21.7	19.1	30.6	30.8	38.6
1.49		5.9	18.5	21.9	27.7	28.5	37.4
1.75		3.18	14.0	16.1	21.6	26.1	28.5
	Average	8.3	21.4	20.6	34.1	30.4	43.4
	Transition	10.8	24.7	22.2	41.5	32.3	51.8
	Steady State	5.8	18.1	19.0	26.6	28.5	34.8

Table 5.3 Dry Saltation Flux Particle Distributiion

SALTATION RATE DISTRIBUTION BY SIZE CLASS (mg/m^2-s)

	Particle Size Range (um)						
	25-50	50-100	100-200	200-400	400-800	800-1600	MEASURED
MIDPOINT	37.50	75.00	150.00	300.00	600.00	1200.00	WEIGHT
SALTATION							
DS451	0.03	0.11	0.89	2.89	0.00	0.00	3.92
DS452	.00	0.01	0.11	0.67	0.21	0.00	1.01
DR451	0.01	0.01	0.17	1.14	2.22	0.00	3.54
DR452	.00	0.01	0.08	0.44	0.58	0.00	1.11
DS751	1.54	5.22	30.95	167.14	37.14	0.00	242.00
DS752	0.85	3.09	26.63	127.44	0.00	0.00	158.00
DR751	1.89	6.72	40.26	192.85	46.28	0.00	288.00
DR752	1.32	3.91	40.20	149.42	182.15	0.00	377.00
DS951	1.10	3.13	21.80	133.03	321.94	0.00	481.00
DR951	2.75	4.06	12.62	222.54	511.03	0.00	753.00

AVERAGE SALTATION RATE DISTRIBUTION BY SIZE CLASS (mg/m^2-s)

	25-50	50-100	100-200	200-400	400-800	800-1600	MEASURED
MIDPOINT	37.50	75.00	150.00	300.00	600.00	1200.00	WEIGHT
AVG SALT							
DS45	0.02	0.06	0.50	1.78	0.11	0.00	2.47
DR45	.00	0.01	0.12	0.79	1.40	0.00	2.33
DS75	1.19	4.15	28.79	147.29	18.57	0.00	200.00
DR75	1.61	5.32	40.23	171.13	114.22	0.00	332.00
DS95	1.10	3.13	21.80	133.03	321.94	0.00	481.00
DR95	2.75	4.06	12.62	222.54	511.03	0.00	753.00

Table 5.4 Wet Saltation Flux Particle Distribution

SALTATION FLUX DISTRIBUTION BY SIZE CLASS (mg/m^2-s)

Particle Size Range (um)

	25-50	50-100	100-200	200-400	400-800	800-1600	MEASURED WEIGHT
MIDPOINT	37.50	75.00	150.00	300.00	600.00	1200.00	
SALTATION							
WS451	.00	0.01	0.03	0.09	0.10	0.00	0.22
WS452	.00	.00	0.04	0.16	0.43	0.00	0.64
WR451	.00	.00	.00	0.07	0.09	0.00	0.17
WR452	.00	.00	.00	0.03	0.05	0.00	0.08
WS751	0.09	0.14	0.73	4.03	6.00	0.00	11.00
WS752	0.28	0.58	1.91	10.39	23.74	0.00	36.90
WR751	0.39	0.80	4.14	27.04	59.22	82.40	174.00
WR752	0.48	1.04	8.13	30.45	43.38	0.00	83.50
WS951	1.09	2.96	14.91	28.00	65.04	0.00	112.00
WR951	4.96	14.98	67.04	164.69	101.34	0.00	353.00

AVERAGE SALTATION FLUX DISTRIBUTION BY SIZE CLASS (mg/m^2-s)

Particle Size Range (um)

	25-50	50-100	100-200	200-400	400-800	800-1600	MEASURED WEIGHT
MIDPOINT	37.50	75.00	150.00	300.00	600.00	1200.00	
AVG SALT							
WS45	.00	.00	0.04	0.12	0.26	0.00	0.43
WR45	.00	.00	.00	0.05	0.07	0.00	0.13
WS75	0.19	0.36	1.32	7.21	14.87	0.00	23.95
WR75	0.48	1.04	8.13	30.45	43.38	0.00	83.50
WS95	1.09	2.96	14.91	28.00	65.04	0.00	112.00
WR95	4.96	14.98	67.04	164.69	101.34	0.00	353.00

Table 5.5 Dry and Wet Concentration Particle Distributions

AVERAGE DRY CONCENTRATION DISTRIBUTION BY SIZE CLASS (mg/m^3)

	Particle Size Range (um)						
	25-50	50-100	100-200	200-400	400-800	800-1600	MEASURED
MIDPOINT	37.50	75.00	150.00	300.00	600.00	1200.00	WEIGHT
DS75_23	0.03	0.09	0.87	19.91	24.27	0.00	45.17
DS75_24	0.28	1.55	13.13	126.64	334.24	67.21	543.04
DS75_33	0.12	0.33	2.25	43.02	72.83	20.17	138.73
DS75_34	0.63	5.81	33.72	284.88	616.53	167.53	1109.10
DR75_23	.00	0.03	0.44	7.84	14.01	10.04	32.37
DR75_24	0.08	0.80	7.97	90.67	187.97	35.46	322.96
DR75_33	0.02	0.17	3.23	50.96	62.83	13.66	130.87
DR75_34	0.54	8.21	42.31	231.20	574.26	186.04	1042.56
DS951_23	0.02	0.16	2.18	27.72	46.08	0.00	76.15
DS951_24	0.69	1.78	35.10	317.28	575.22	0.00	930.07
DS951_32	0.01	0.03	0.28	6.76	14.24	0.00	21.31
DS951_33	0.42	1.25	26.16	289.61	110.33	0.00	427.78
DS951_34	4.81	18.22	145.77	854.39	831.30	0.00	1854.50
DR951_23	0.49	1.82	6.68	54.93	121.64	0.00	185.56
DR951_24	1.69	8.03	99.61	541.43	422.04	0.00	1072.80
DR951_32	0.04	0.10	0.39	9.11	20.23	0.00	29.87
DR951_33	0.33	0.94	12.76	113.82	312.65	125.06	565.56
DR951_34	6.97	25.42	207.23	578.33	1912.34	0.00	2730.30

AVERAGE WET CONCENTRATION DISTRIBUTION BY SIZE CLASS (mg/m^3)

	Particle Size Range (um)						
	25-50	50-100	100-200	200-400	400-800	800-1600	MEASURED
MIDPOINT	37.50	75.00	150.00	300.00	600.00	1200.00	WEIGHT
WS75_23	0.00	0.00	0.00	0.00	0.00	0.00	5.81
WS75_24	0.01	0.02	0.20	6.68	3.69	0.00	16.60
WS75_33	0.01	0.03	0.36	3.54	8.68	0.00	17.27
WS75_34	0.04	0.31	7.09	41.71	52.39	0.00	101.55
WR752_23	0.00	0.00	0.00	0.00	0.00	0.00	3.05
WR752_24	0.00	0.00	0.00	0.00	0.00	0.00	5.06
WR752_33	.00	0.02	0.48	5.91	9.90	0.00	16.31
WR752_34	0.13	0.68	10.51	55.45	123.10	0.00	189.87
WS951_23	0.00	0.00	0.00	0.00	0.00	0.00	10.68
WS951_24	0.03	0.15	1.55	22.82	68.46	0.00	93.01
WS951_32	0.00	0.00	0.00	0.00	0.00	0.00	4.70
WS951_33	0.01	0.03	0.42	8.17	23.42	0.00	32.06
WS951_34	0.17	0.41	3.58	67.99	229.02	61.07	362.24
WR951_23	0.00	0.00	0.00	0.00	0.00	0.00	10.34
WR951_24	0.01	0.02	0.20	5.47	28.19	0.00	33.90
WR951_32	0.00	0.00	0.00	0.00	0.00	0.00	2.92
WR951_33	0.02	0.06	0.88	15.66	48.61	0.00	65.24
WR951_34	0.24	1.69	6.63	51.61	162.84	418.73	641.74

Table 5.6a Slope of Dry Concentration Profiles

Test	Station #1	Station #2	Station #3
DS451	-0.07	-0.80	0.05
DS452	-0.06	0.66	0.49
DR451	0.33	0.10	-0.47
DR452	-0.13	-0.08	-0.09
DS751	0.09	-2.6	-2.6
DS752	0.31	-2.1	-2.5
DR751	-0.1	-2.0	-2.6
DR752	-0.08	-1.8	-2.3
DS951	0.04	-2.5	-2.4
DR951	-1.1	-2.6	-2.4
Mean			
DS45	-0.07	-0.54	0.25
DR45	-0.77	-0.002	-0.32
DS75	0.18	-2.4	-2.5
DR75	-0.09	-1.9	-2.5
DS95	0.04	-2.5	-2.4
DR95	-1.1	-2.6	-2.4

Table 5.6b Slope of Wet Concentration Profiles

Test	Station #1	Station #2	Station #3
WS451	0.4	-0.18	-0.17
WS452	-0.47	-0.05	0.01
WR451	0.26	-0.20	-0.44
WR452	-0.09	-0.01	-0.09
WS751	0.14	-0.72	-1.3
WS752	0.30	-1.4	-2.3
WR751	-0.02	-0.90	-3.1
WR752	-1.2	-0.72	-2.2
WS951	-1.3	-1.5	-2.3
WR951	-0.15	-1.6	-2.9
Mean			
WS45	-0.14	-0.12	-0.09
WR45	0.07	-0.1	-0.25
WS75	0.24	-1.04	-1.9
WR751	-1.2	-0.72	-2.2
WS95	-1.3	-1.5	-2.3
WR95	-0.15	-1.6	-2.9

Table 5.7 Dry Net Vertical Flux-- Fine And Coarse Fraction

Sample	Fine	Coarse	Ratio	Friction Velocity	Elevation
	mg/m^2-s			cm/s	cm
DS75_3	0.06	18.66	0.35%		6.50
DS75_4	0.92	113.64	0.81%		2.50
DS75	5.35	194.65	2.75%	19.00	Salt
Total	6.33	326.95	1.94%		
DR75_3	0.04	28.00	0.16%		6.50
DR75_4	2.04	201.34	1.01%		2.50
DR75	6.92	325.58	2.13%	26.60	Salt
Total	9.01	554.92	1.62%		
DS95_2	0.01	4.97	0.17%		16.50
DS95_3	0.39	92.62	0.42%		6.50
DS95_4	5.48	244.50	2.24%		2.50
DS95	4.23	476.77	0.89%	28.50	Salt
Total	10.10	818.86	1.23%		
DR95_2	0.05	10.92	0.48%		16.50
DR95_3	0.02	233.81	0.01%		6.50
DR95_4	7.89	567.29	1.39%		2.50
DR95	6.81	746.19	0.91%	34.80	Salt
Total	14.77	1558.21	0.95%		

Table 5.8 Wet Net Vertical Flux-- Fine And Coarse Fraction

Sample	Fine	Coarse	Ratio	Friction Velocity	Elevation
	mg/m^2-s			cm/s	cm
WS75_3	0.01	1.99	0.56%		6.50
WS75_4	0.04	13.71	0.32%		2.50
WS75	0.55	23.40	2.36%	19.00	Salt
Total	0.61	39.10	1.55%		
WR75_3	0.01	3.67	0.15%		6.50
WR75_4	0.18	41.56	0.43%		2.50
WR75	1.53	81.97	1.86%	26.60	Salt
Total	1.71	127.20	1.35%		
WS95_3	0.01	6.60	0.16%		6.50
WS95_4	0.12	78.90	0.15%		2.50
WS95	4.05	107.95	3.75%	28.50	Salt
Total	4.18	193.45	2.16%		
WR95_3	0.03	25.96	0.13%		6.50
WR95_4	0.80	260.38	0.31%		2.50
WR95	19.93	333.07	5.99%	34.80	Salt
Total	20.77	619.41	3.35%		

FIGURES

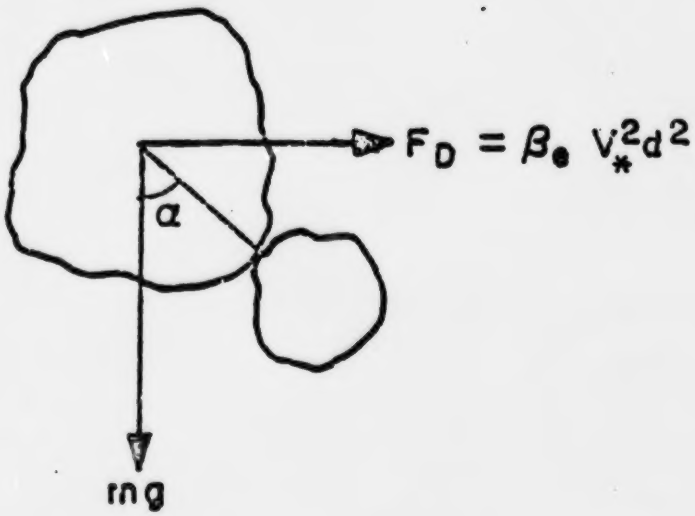

$F_D = \beta_e V_*^2 d^2$
α
mg

Figure 3.1 Force diagram for an individual particle (Mill et al, 1974).

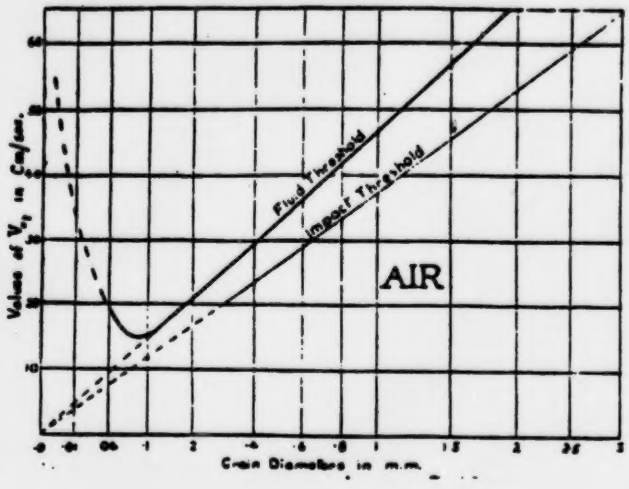

FIGURE 3.2 VARIATION OF THRESHOLD VELOCITY (BAGNOLD, 1941)

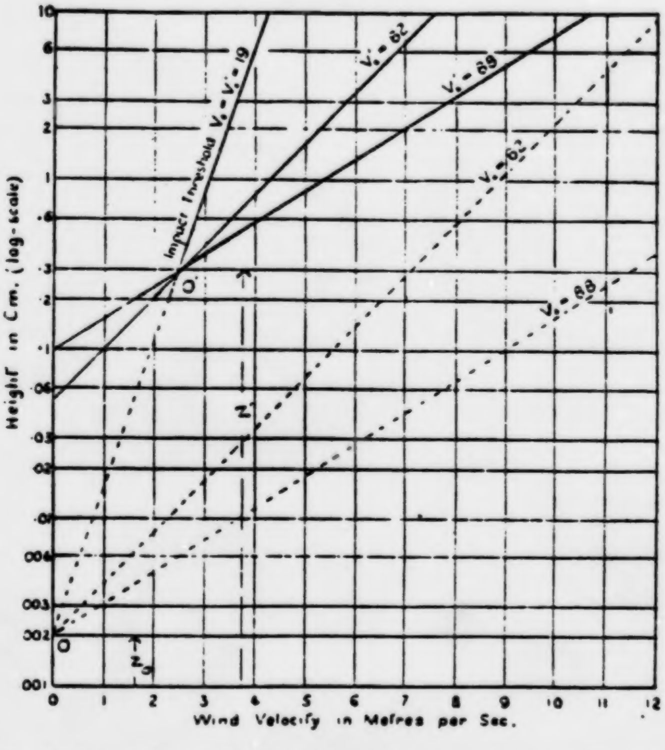

FIGURE 3.3 WIND SPEED IN MOVING SALTATION (BAGNOLD,1941)

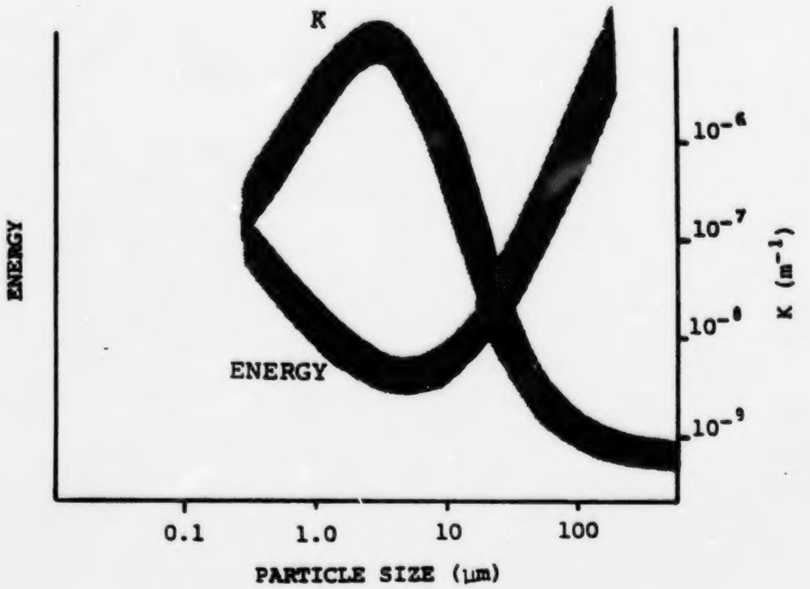

Figure 3.4 Hypothetical Energy and Suspension Factor Curves

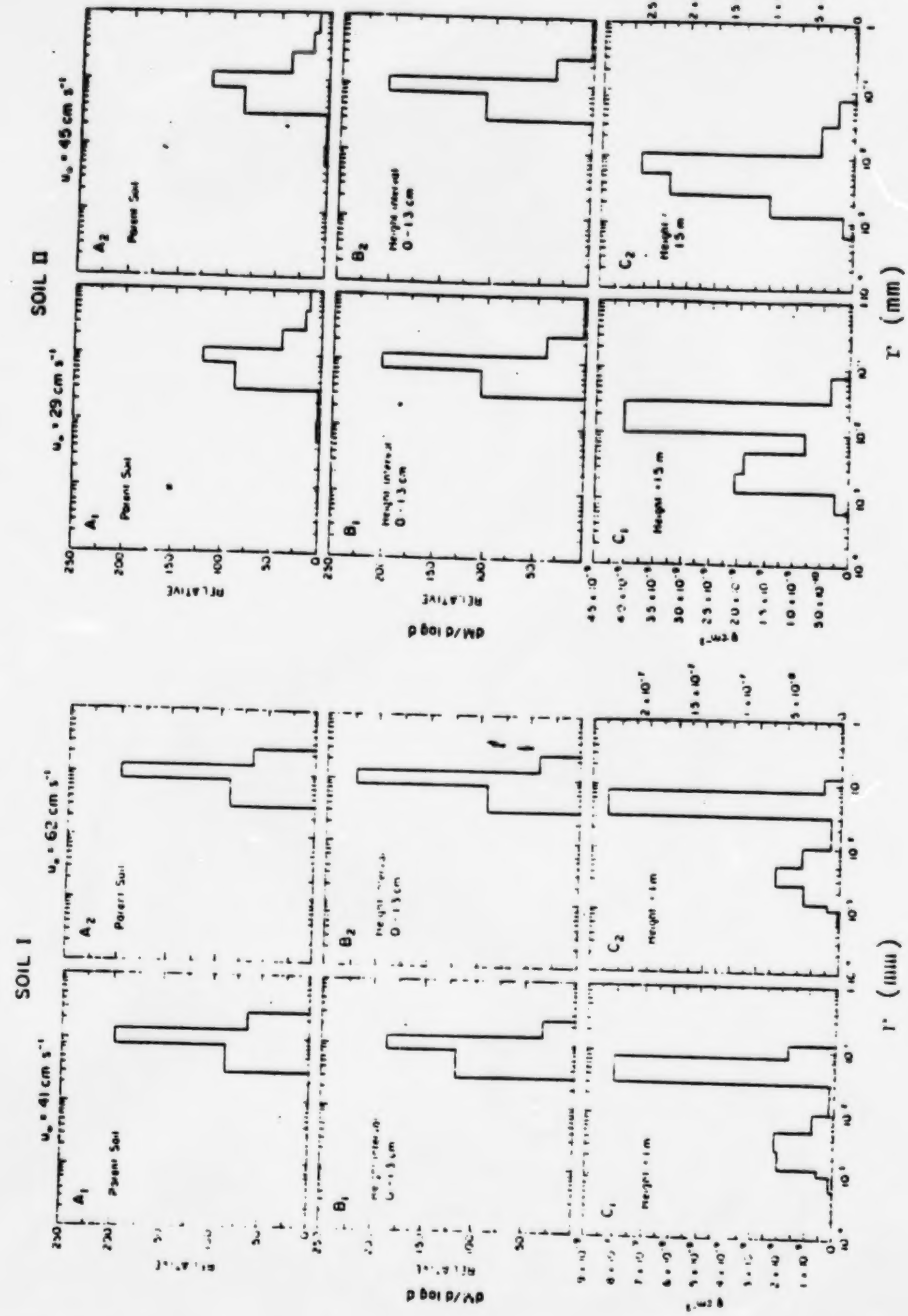

Figure 3.5 Size distributions of soil particles eroded from two soils. Soil I has a surface texture fine sand and soil II has a surface texture loamy fine sand. For each soil for the labelled wind friction velocities 1 and 2, A is the relative size distribution of the dry parent soil, determined by dry sieving; B is the relative size distribution of particles moving between the heights 0 - 1.3 cm above ground, and C is the mass size distribution for airborne particles at 1 m above the ground (Gillette, 1976).

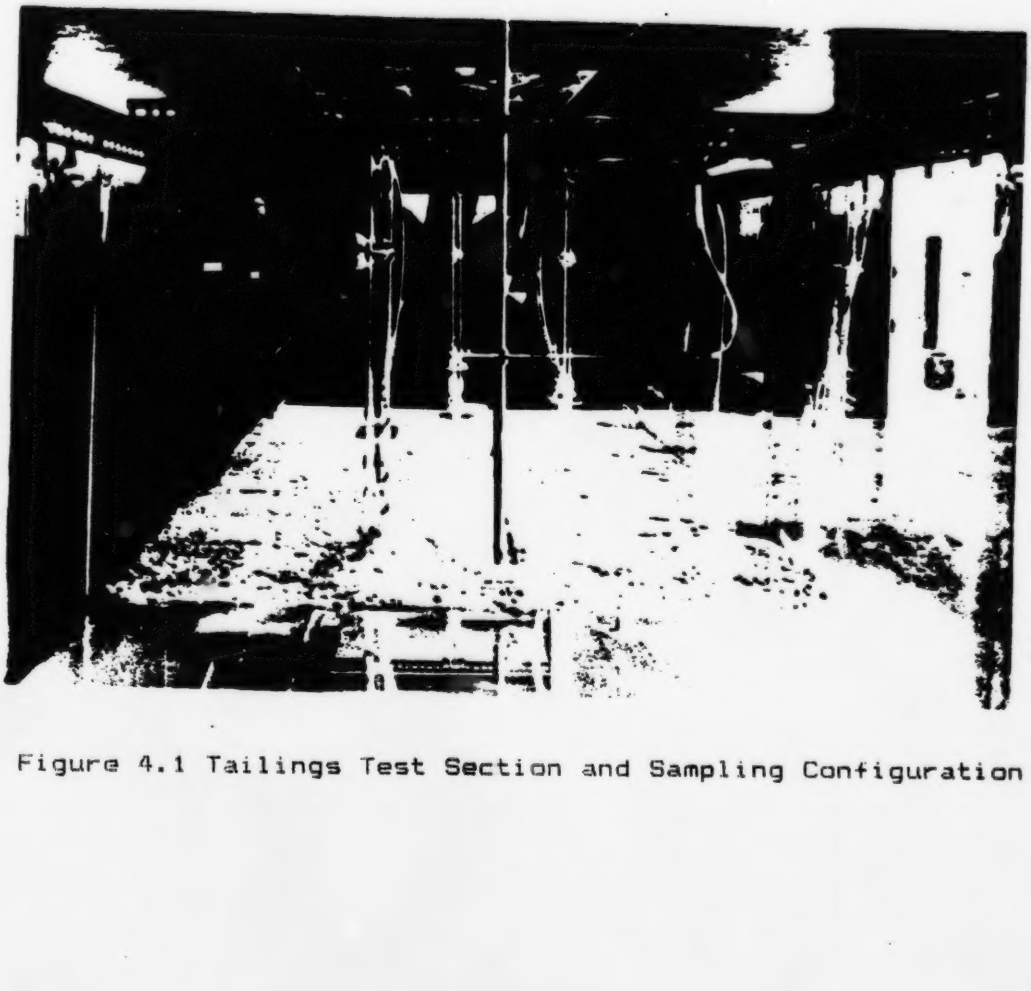

Figure 4.1 Tailings Test Section and Sampling Configuration

Figure 4.2 Average Particle Distribution of Tailings

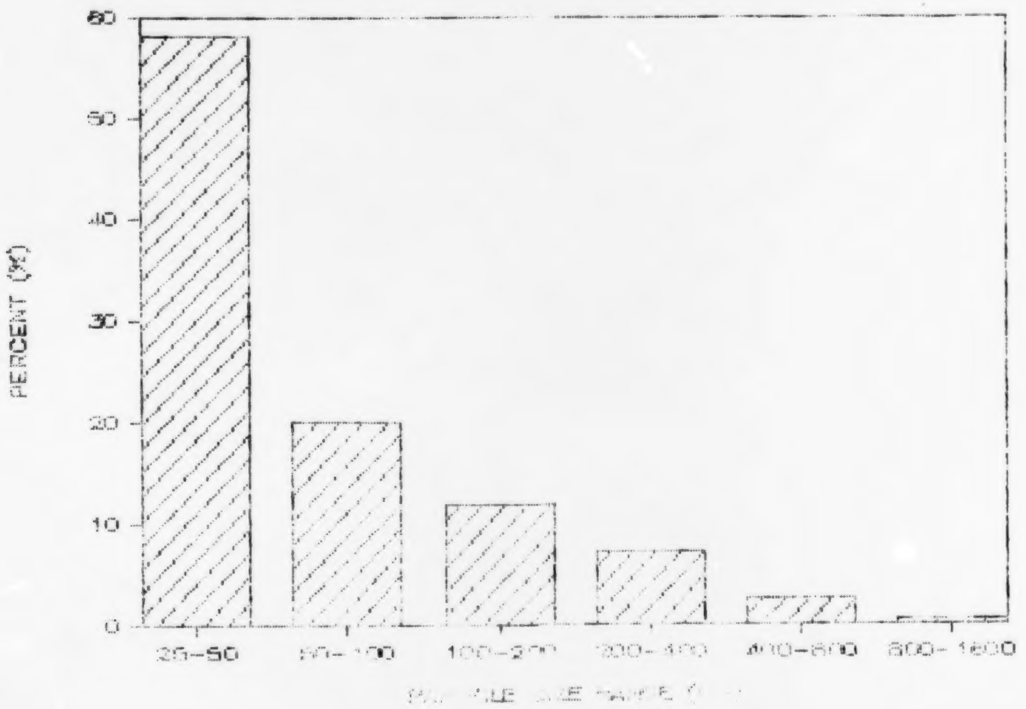
AVERAGE PARTICLE DISTRIBUTION BY COUNT

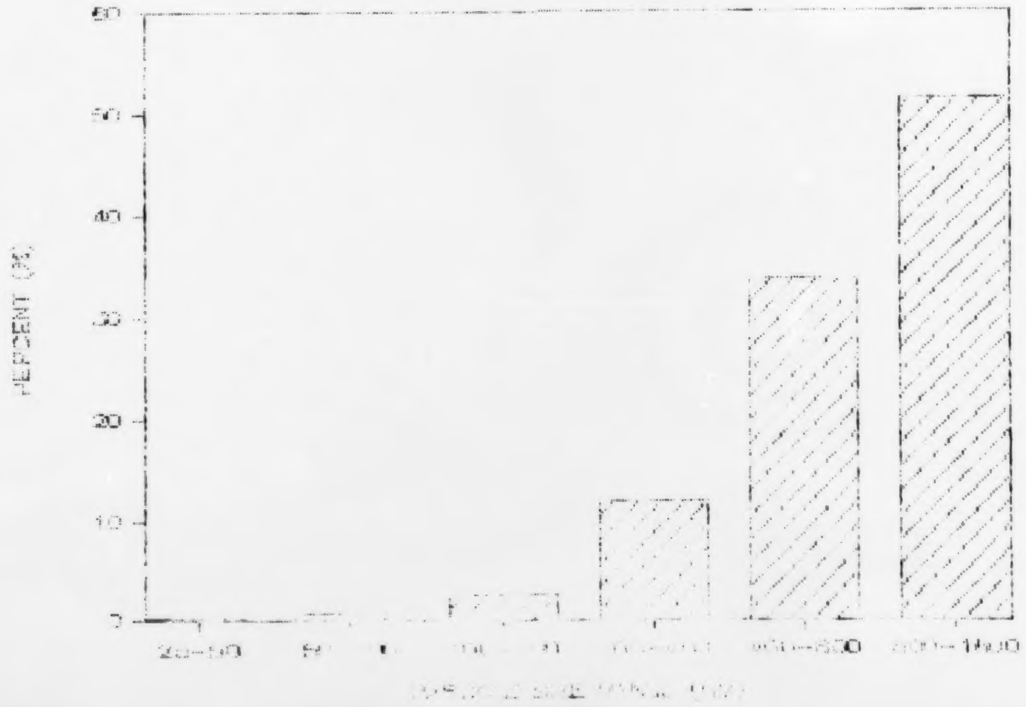
AVERAGE PARTICLE DISTRIBUTION BY WEIGHT

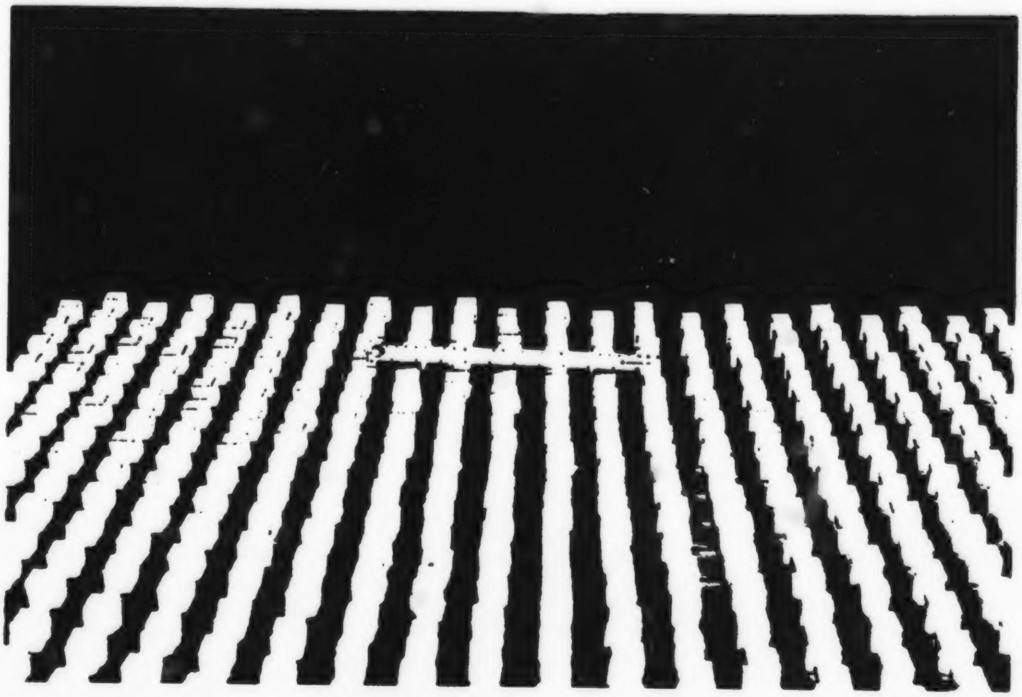

Figure 4.3 Rough " Flat Plate"

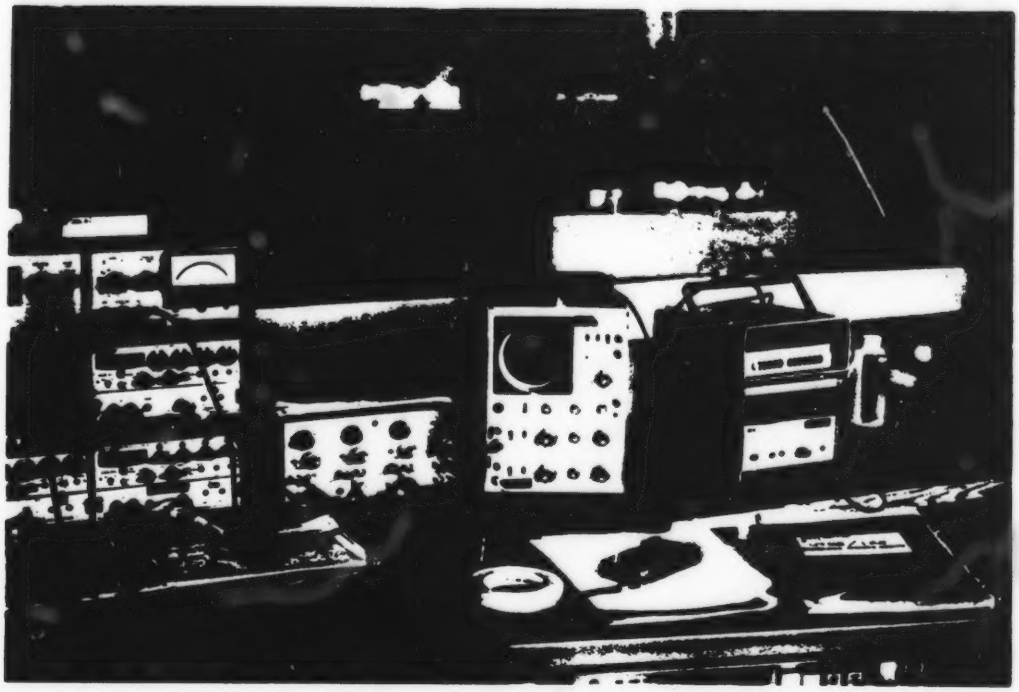

Figure 4.4 Hot Wire Anemometry Equipment

FIGURE 5.1 CONCENTRATION PROFILES FOR

TURBULENCE LOW SURFACE DRY NOMINAL WIND 4.5 M/S REP # 1

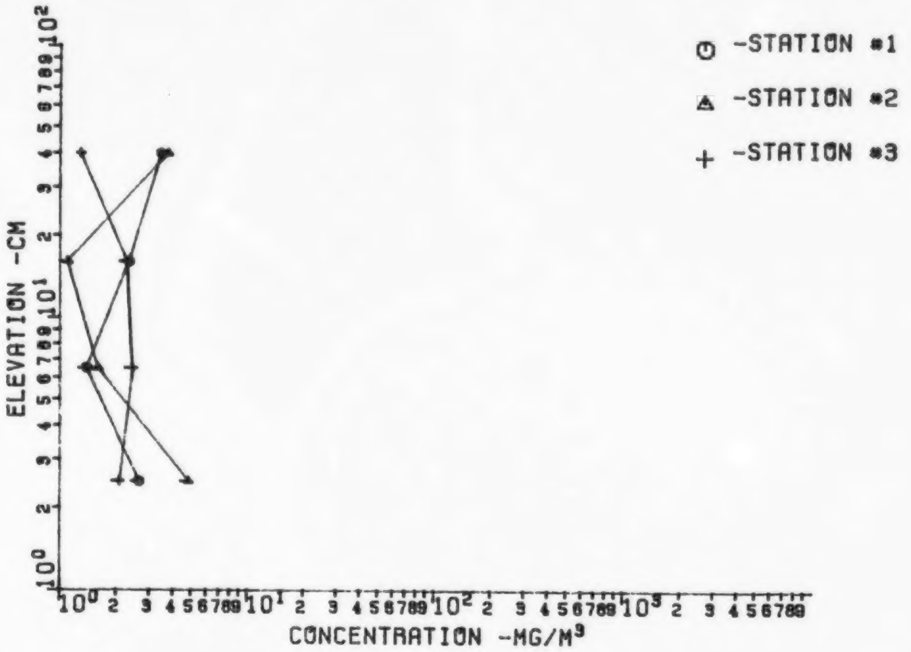

TURBULENCE LOW SURFACE DRY NOMINAL WIND 4.5 M/S REP # 2

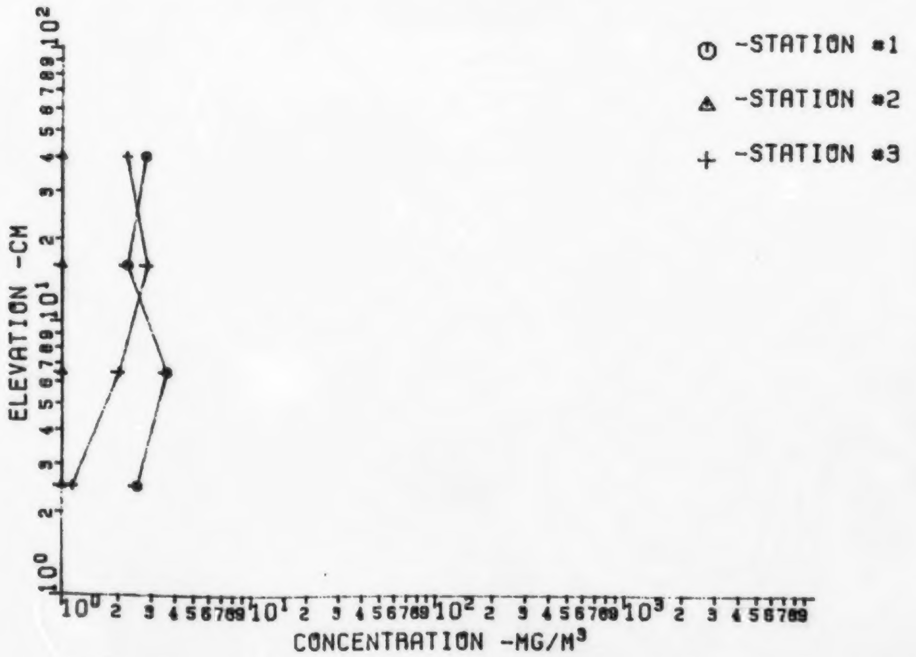

FIGURE 5.2 CONCENTRATION PROFILES FOR

TURBULENCE LOW SURFACE WET NOMINAL WIND 4.5 M/S REP # 1

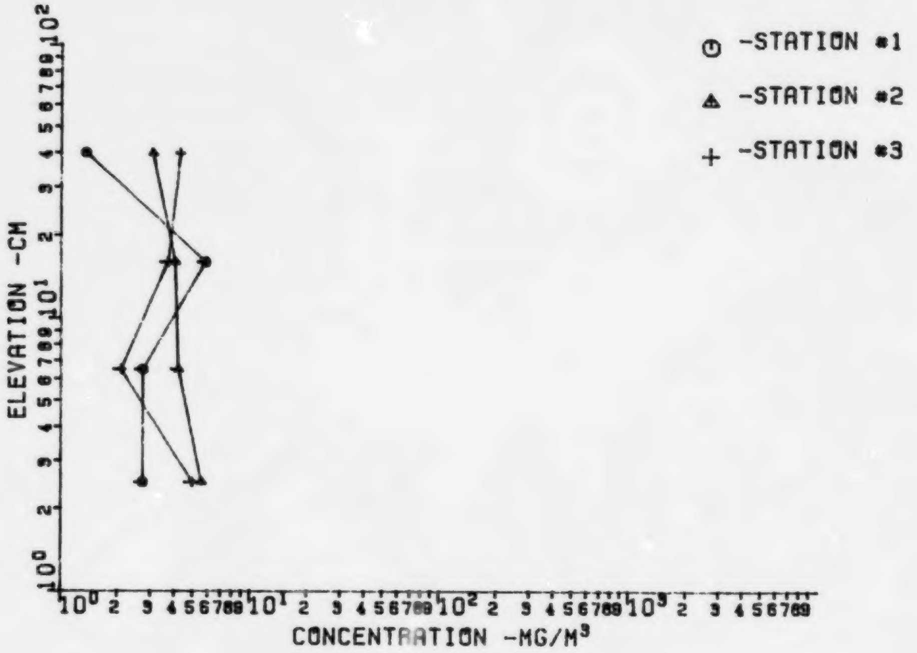

TURBULENCE LOW SURFACE WET NOMINAL WIND 4.5 M/S REP # 2

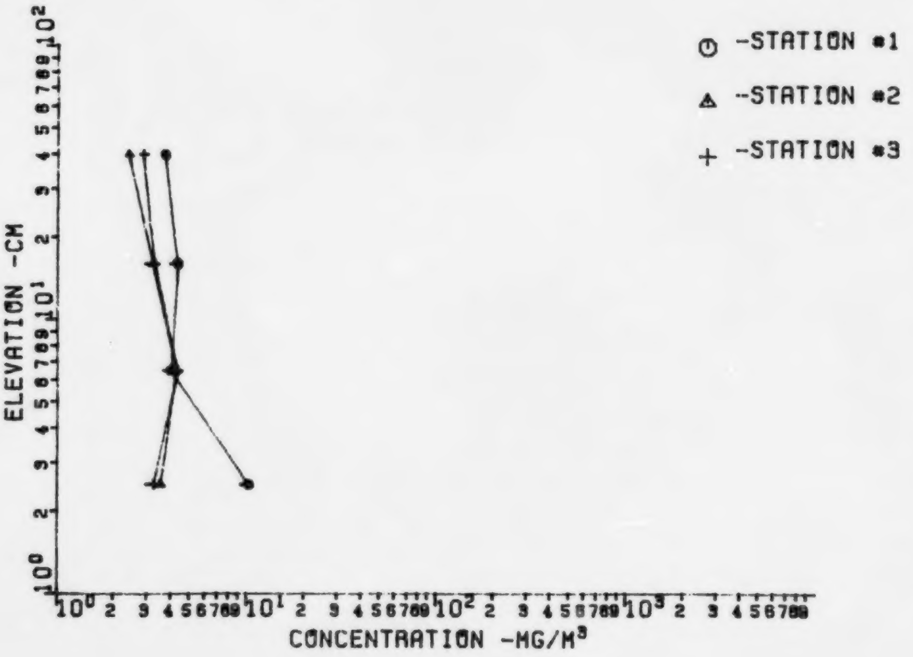

FIGURE 5.3 CONCENTRATION PROFILES FOR

TURBULENCE HIGH SURFACE DRY NOMINAL WIND 4.5 M/S REP # 1

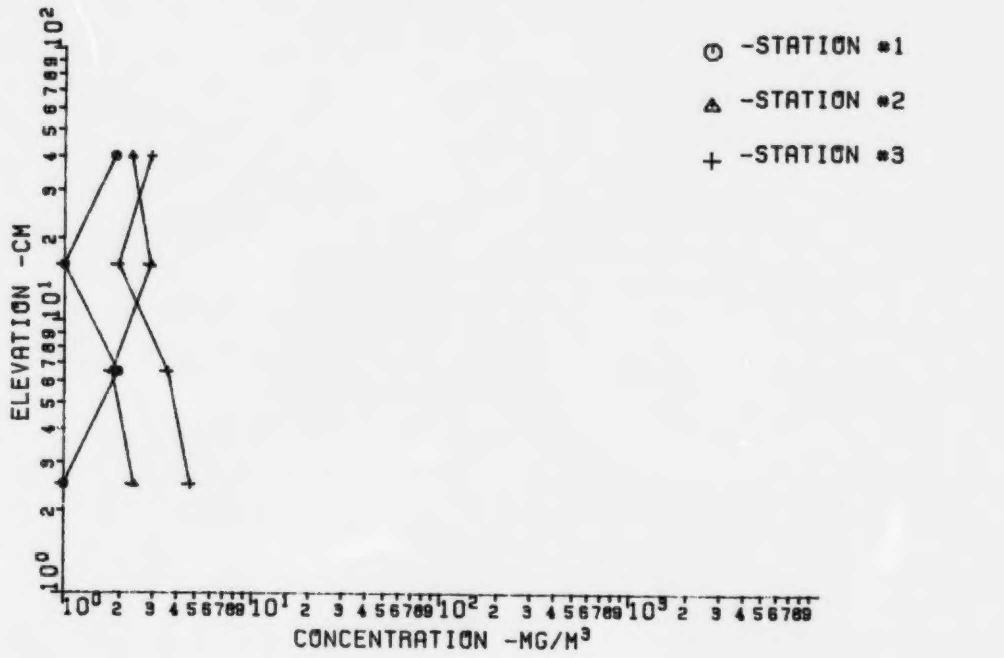

TURBULENCE HIGH SURFACE DRY NOMINAL WIND 4.5 M/S REP # 2

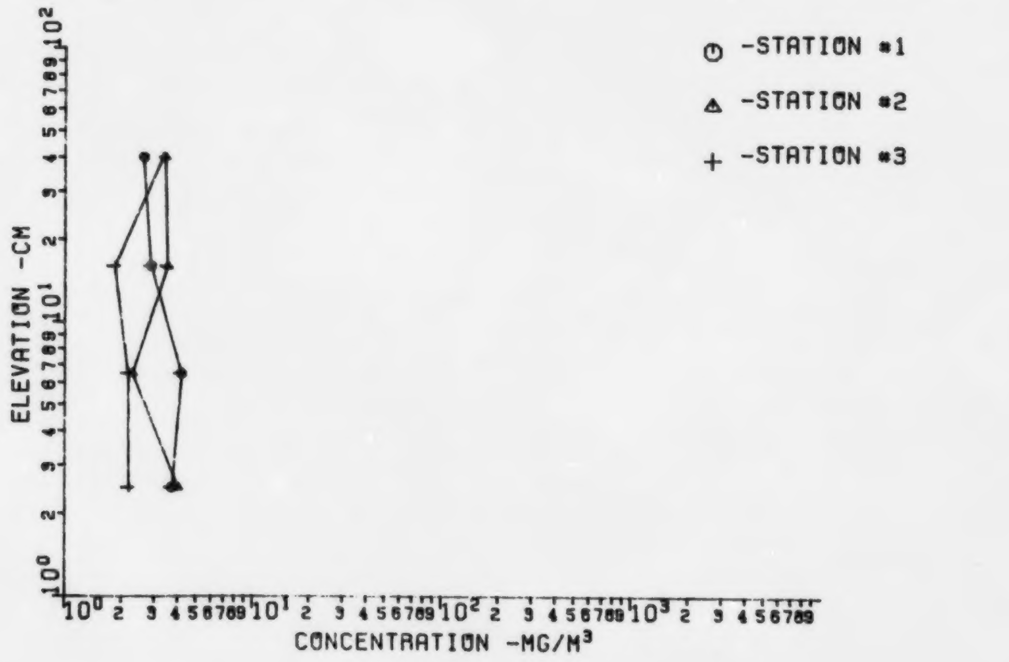

FIGURE 5.4 CONCENTRATION PROFILES FOR

TURBULENCE HIGH SURFACE WET NOMINAL WIND 4.5 M/S REP # 1

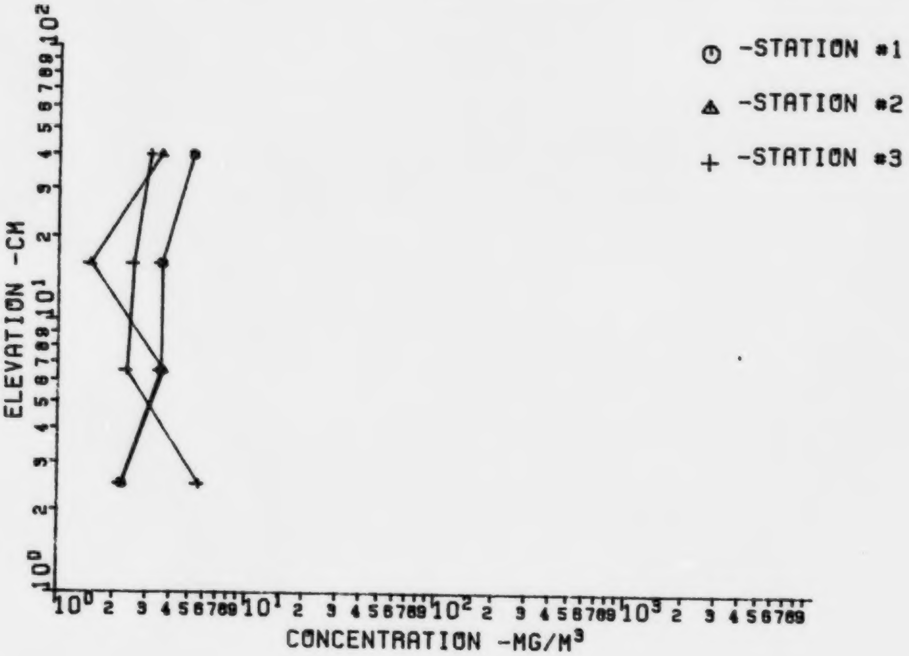

TURBULENCE HIGH SURFACE WET NOMINAL WIND 4.5 M/S REP # 2

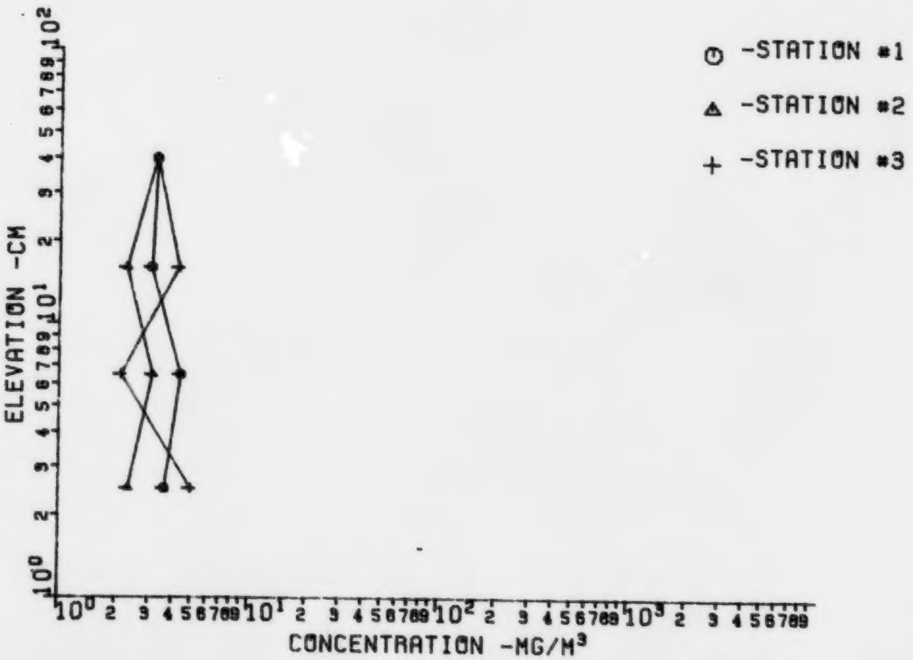

FIGURE 5.5 CONCENTRATION PROFILES FOR

TURBULENCE LOW SURFACE DRY NOMINAL WIND 7.5 M/S REP # 1

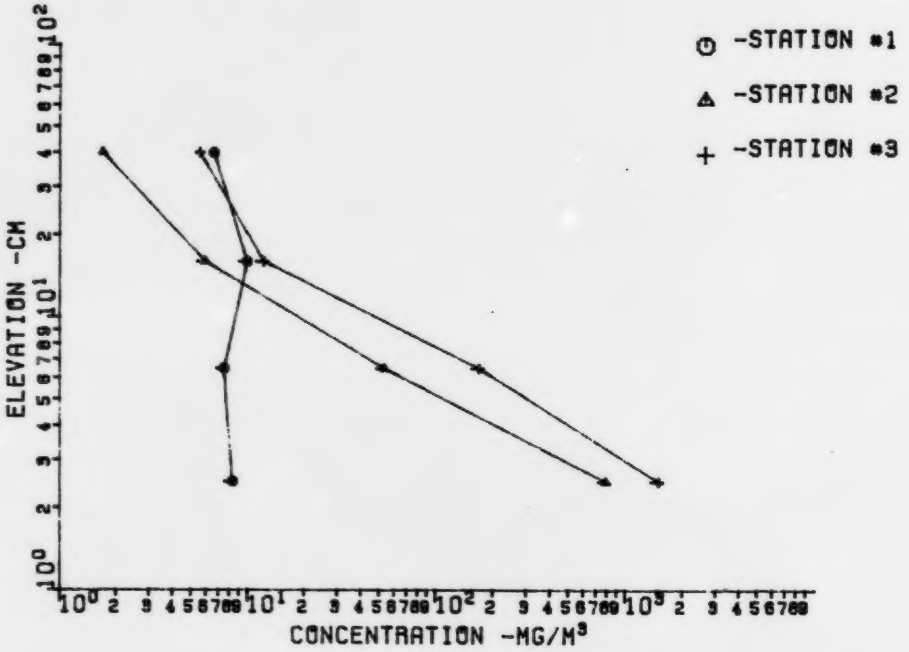

TURBULENCE LOW SURFACE DRY NOMINAL WIND 7.5 M/S REP # 2

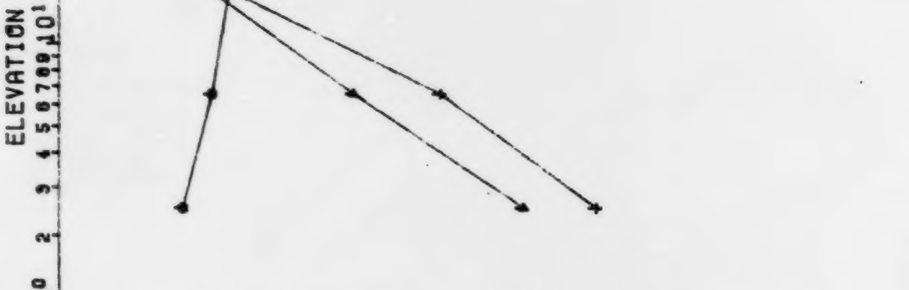

FIGURE 5.6 CONCENTRATION PROFILES FOR

TURBULENCE LOW SURFACE WET NOMINAL WIND 7.5 M/S REP # 2

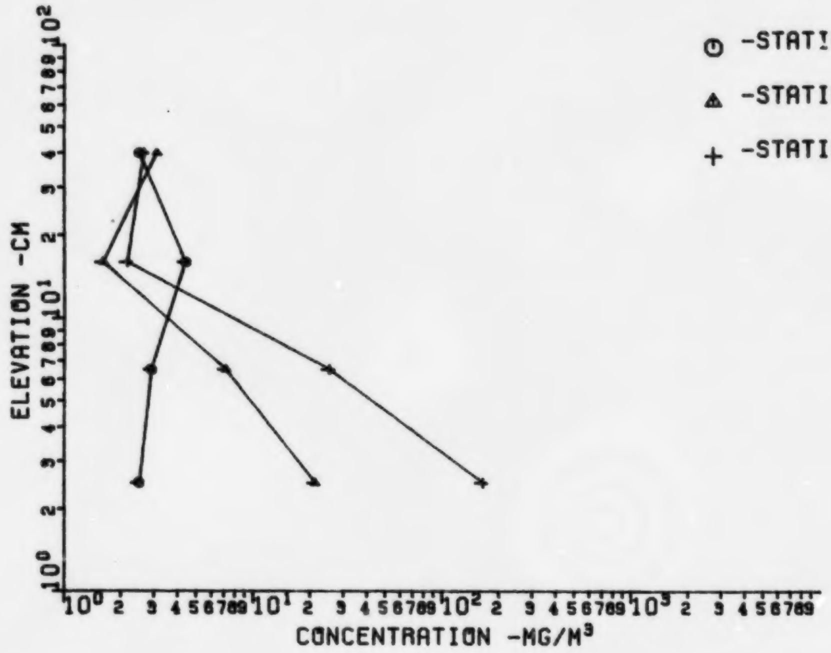

TURBULENCE LOW SURFACE WET NOMINAL WIND 7.5 M/S REP # 1

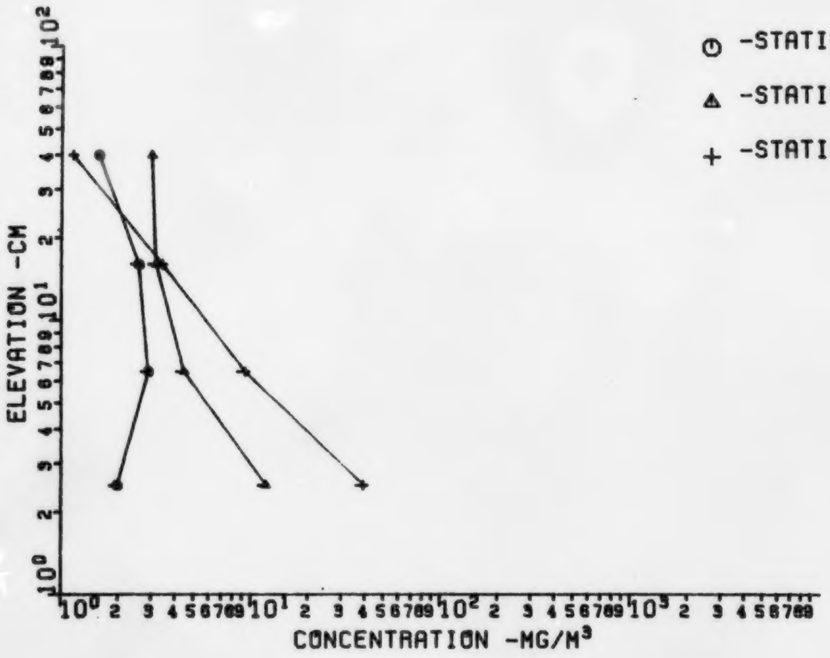

FIGURE 5.7 CONCENTRATION PROFILES FOR

TURBULENCE HIGH SURFACE DRY NOMINAL WIND 7.5 M/S REP # 1

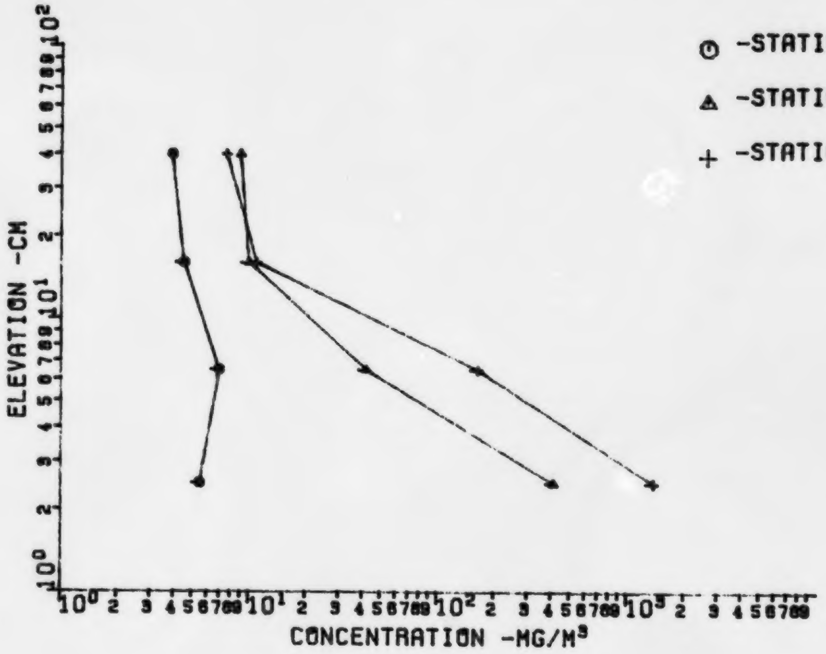

TURBULENCE HIGH SURFACE DRY NOMINAL WIND 7.5 M/S REP # 2

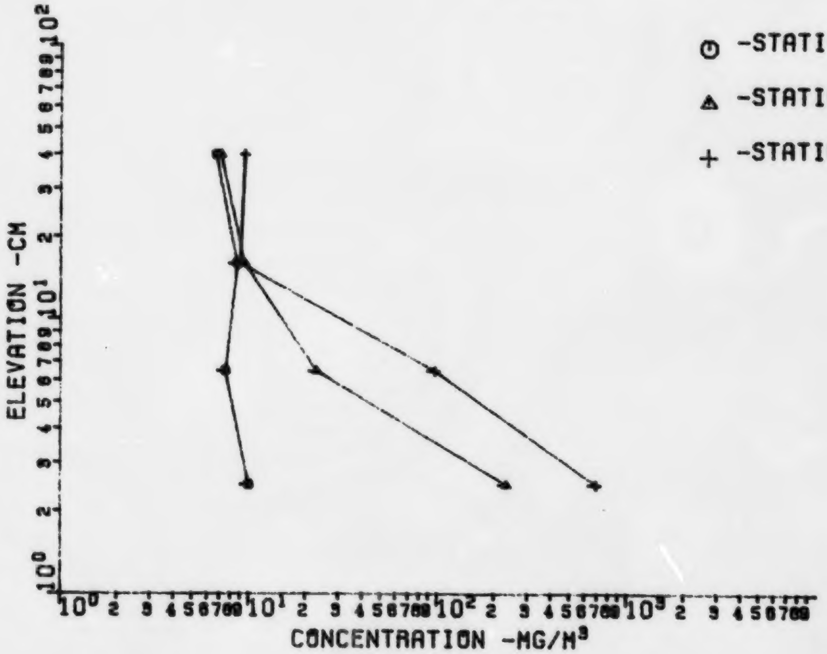

FIGURE 5.8 CONCENTRATION PROFILES FOR

TURBULENCE HIGH SURFACE WET NOMINAL WIND 7.5 M/S REP # 1

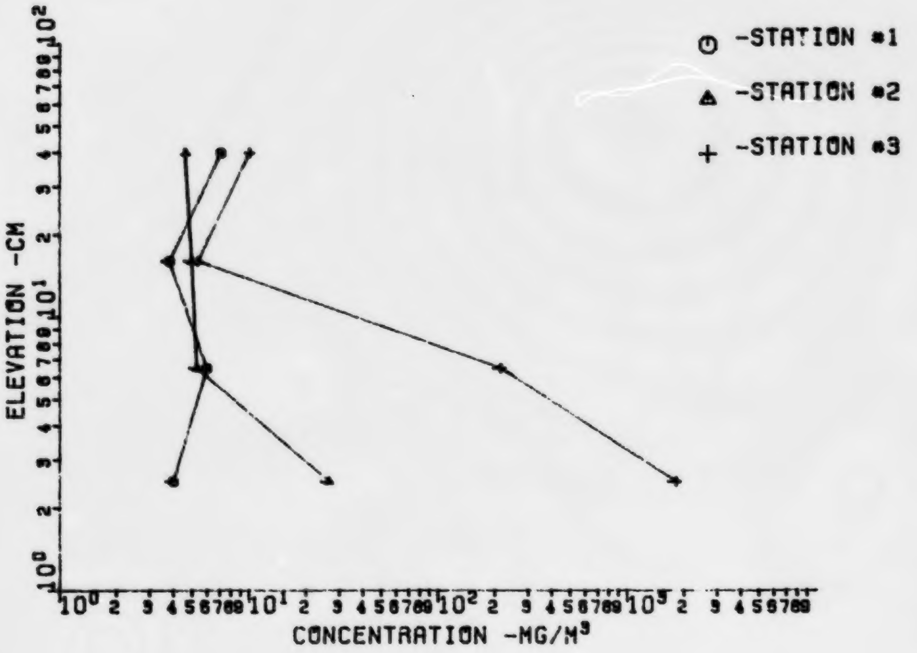

TURBULENCE HIGH SURFACE WET NOMINAL WIND 7.5 M/S REP # 2

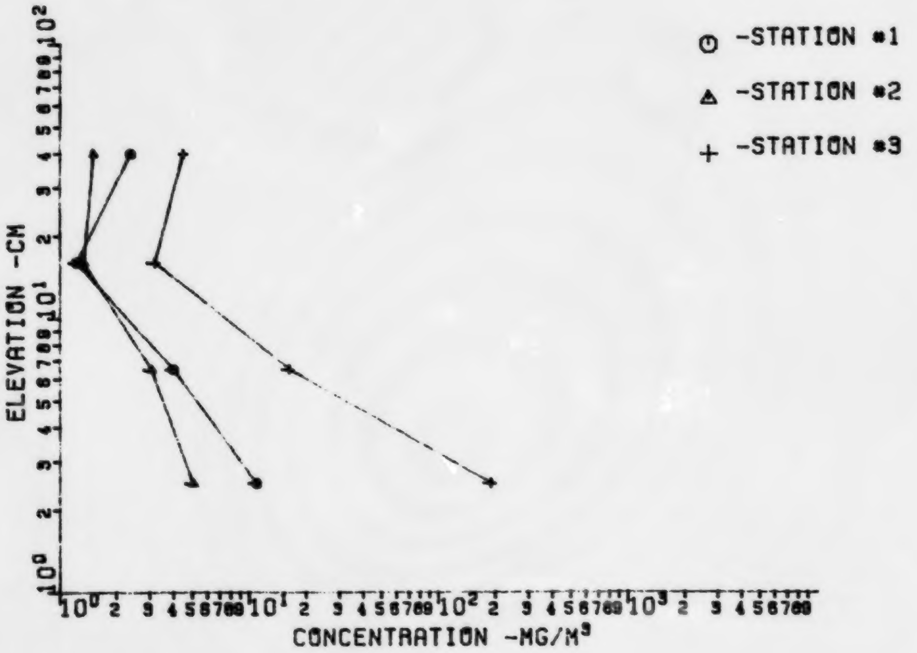

FIGURE 5.9 CONCENTRATION PROFILES FOR

TURBULENCE LOW SURFACE DRY NOMINAL WIND 9.5 M/S REP # 1

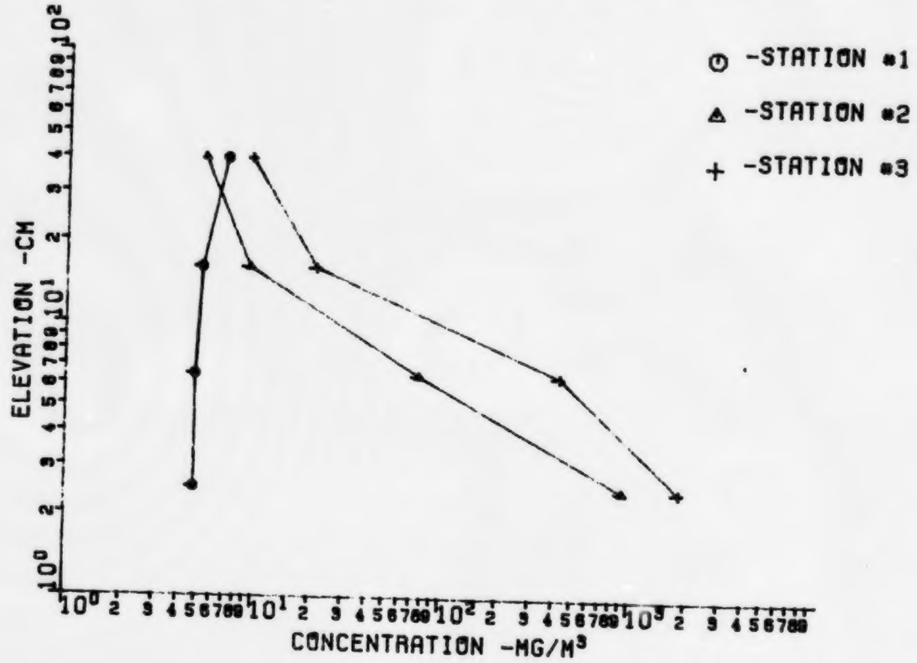

TURBULENCE HIGH SURFACE DRY NOMINAL WIND 9.5 M/S REP # 1

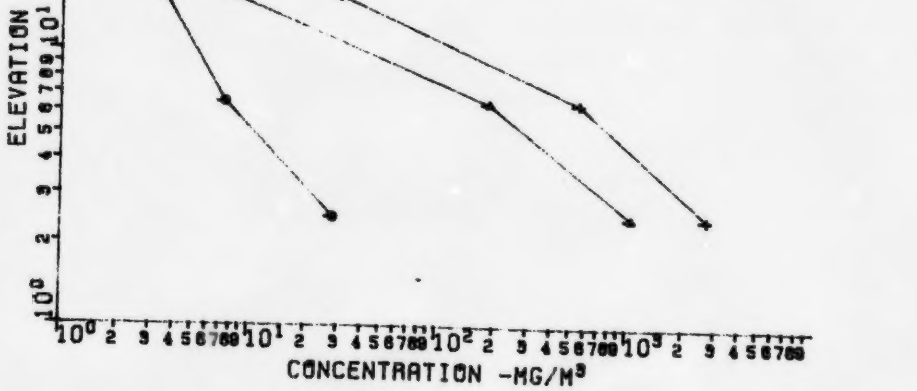

FIGURE 5.10 CONCENTRATION PROFILES FOR

TURBULENCE LOW SURFACE WET NOMINAL WIND 9.5 M/S REP # 1

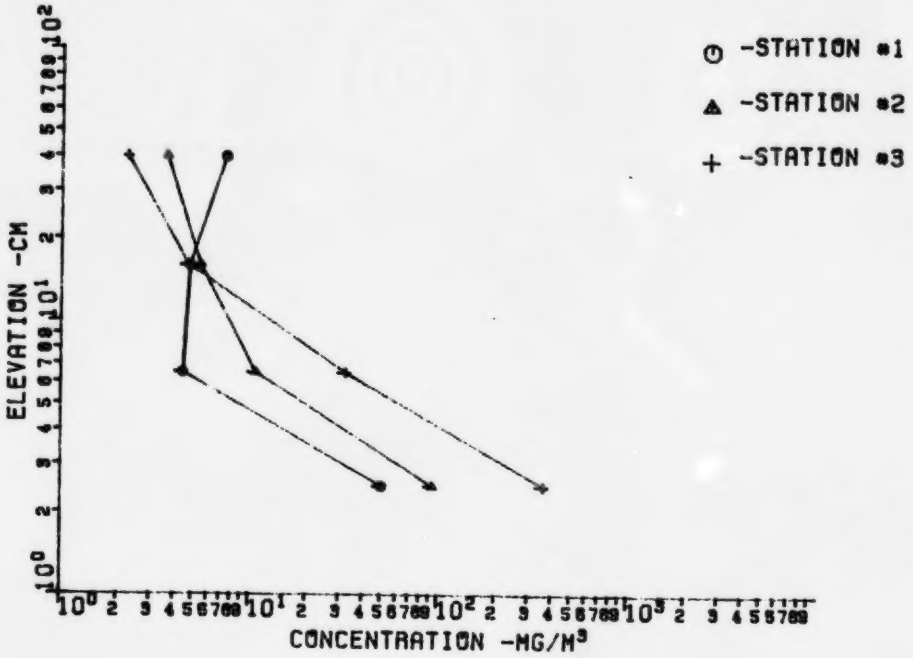

TURBULENCE HIGH SURFACE WET NOMINAL WIND 9.5 M/S REP # 1

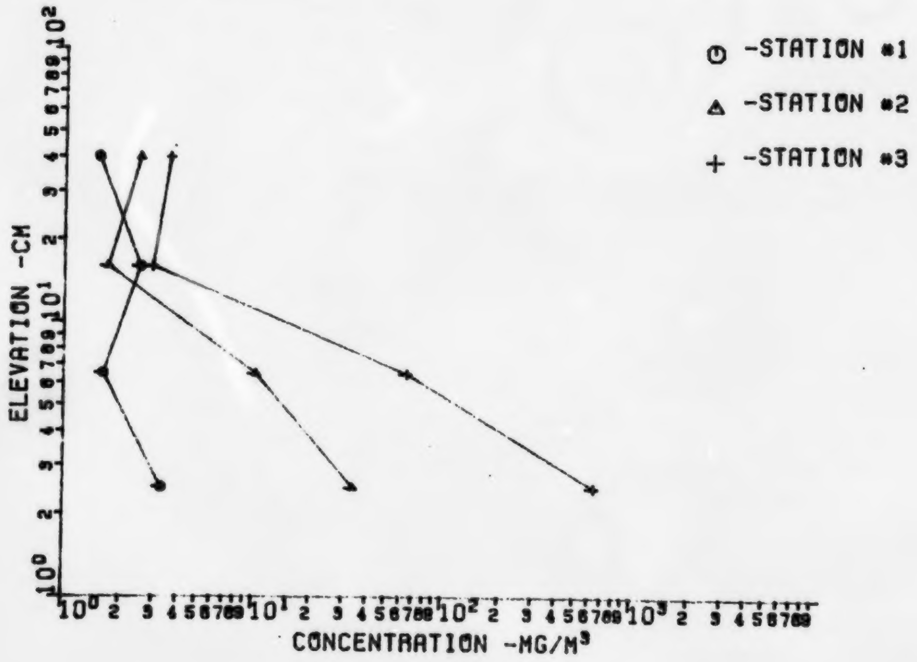

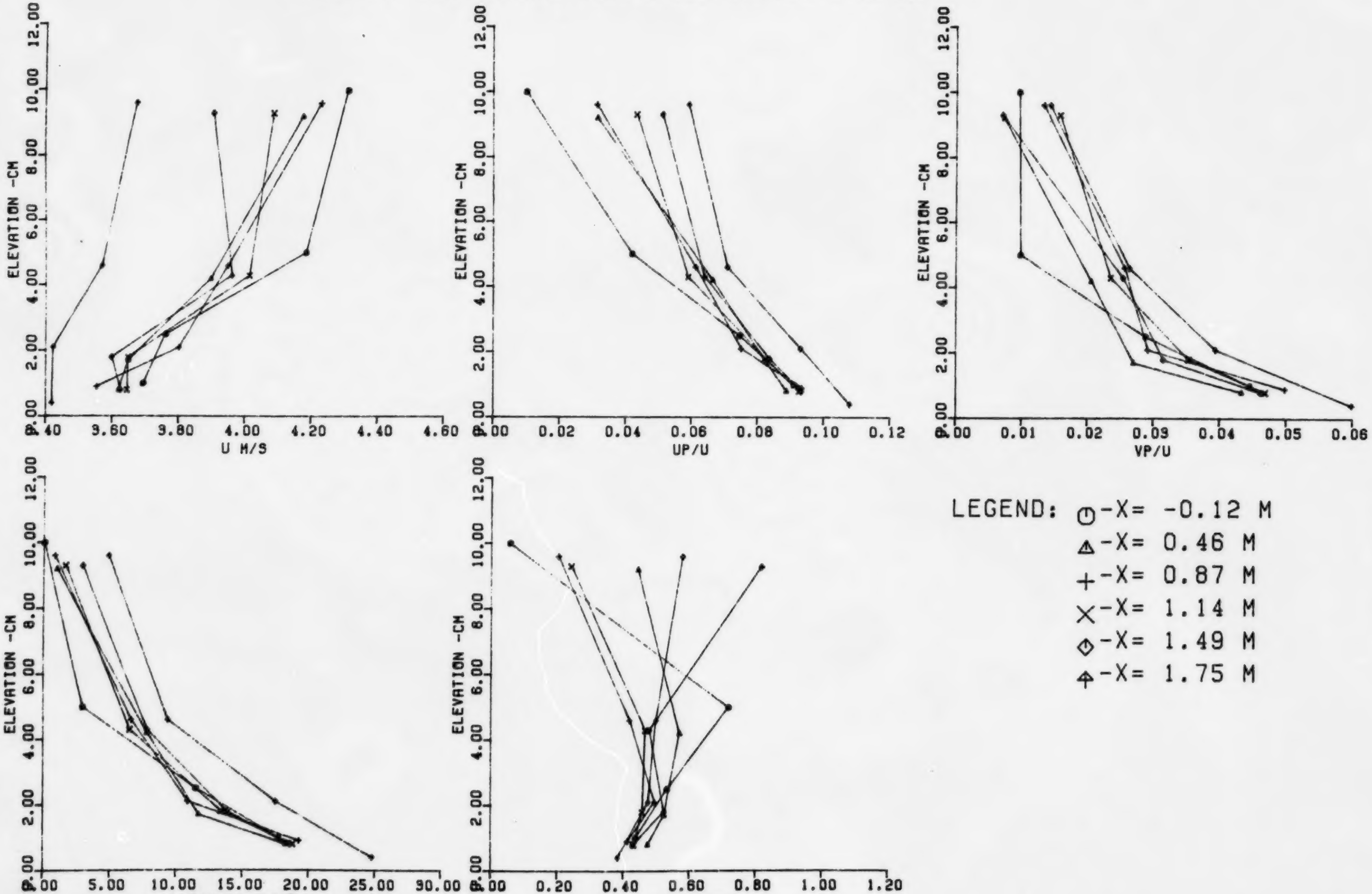
FIGURE 5.11 WIND & TURBULENCE PRØFILES
TURBULENCE LØW NØMINAL WIND SPEED 4.5 M/S @ 40 CM

FIGURE 5.12 WIND & TURBULENCE PRØFILES
TURBULENCE HIGH NØMINAL WIND SPEED 4.5 M/S @ 40 CM

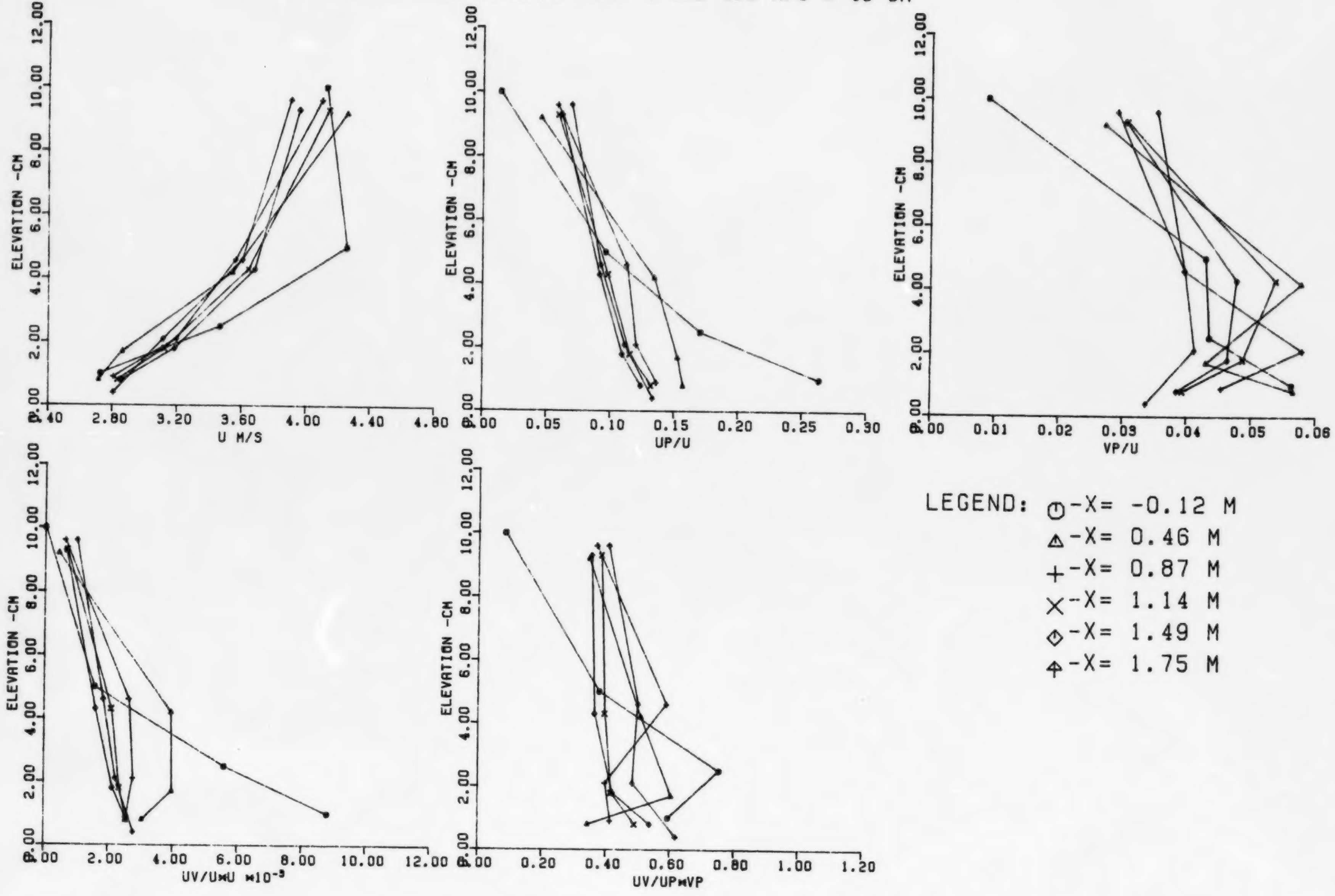

FIGURE 5.13 WIND & TURBULENCE PRØFILES
TURBULENCE LØW NØMINAL WIND SPEED 7.5 M/S @ 40 CM

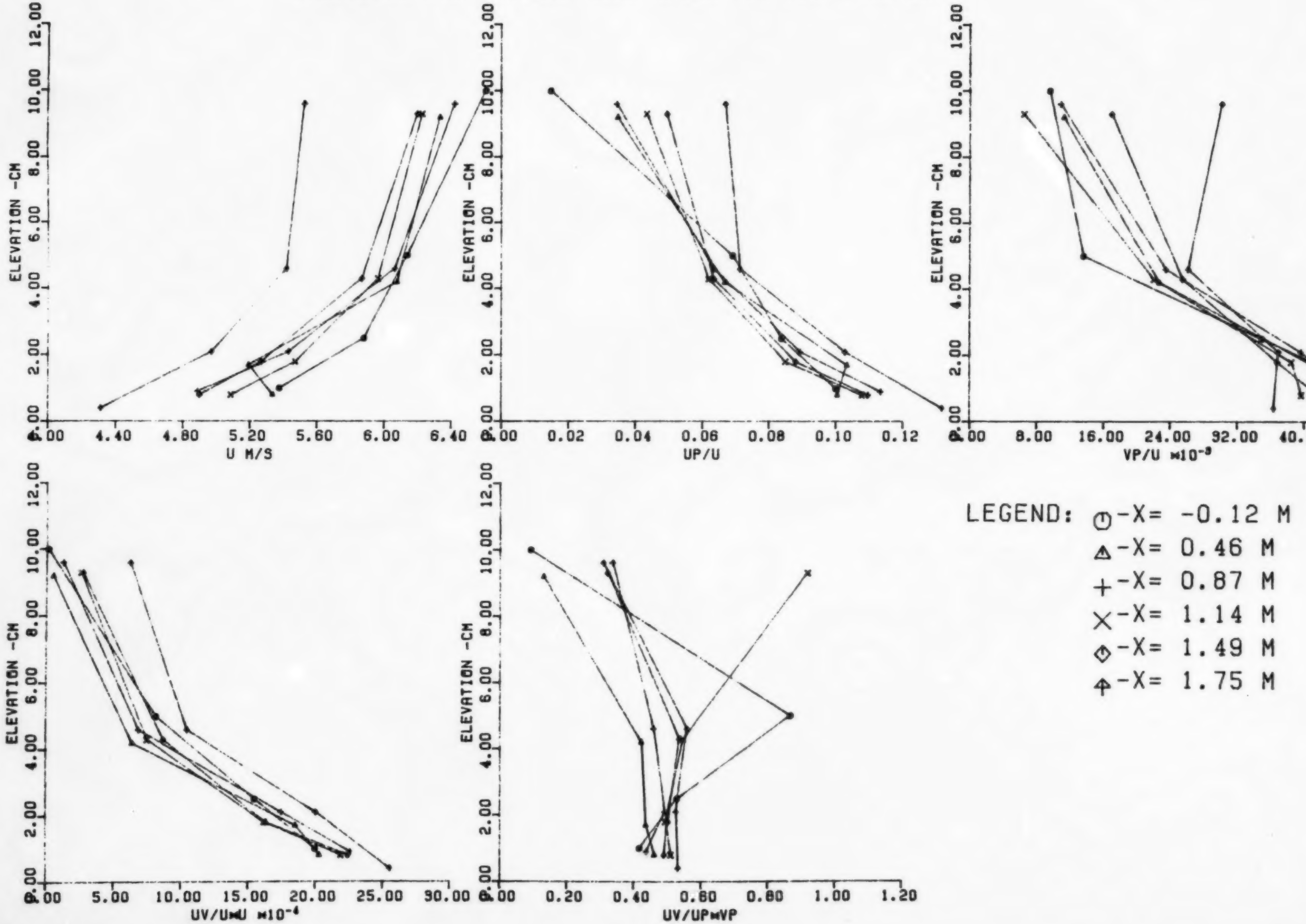

FIGURE 5.14 WIND & TURBULENCE PRØFILES

TURBULENCE HIGH NØMINAL WIND SPEED 7.5 M/S @ 40 CM

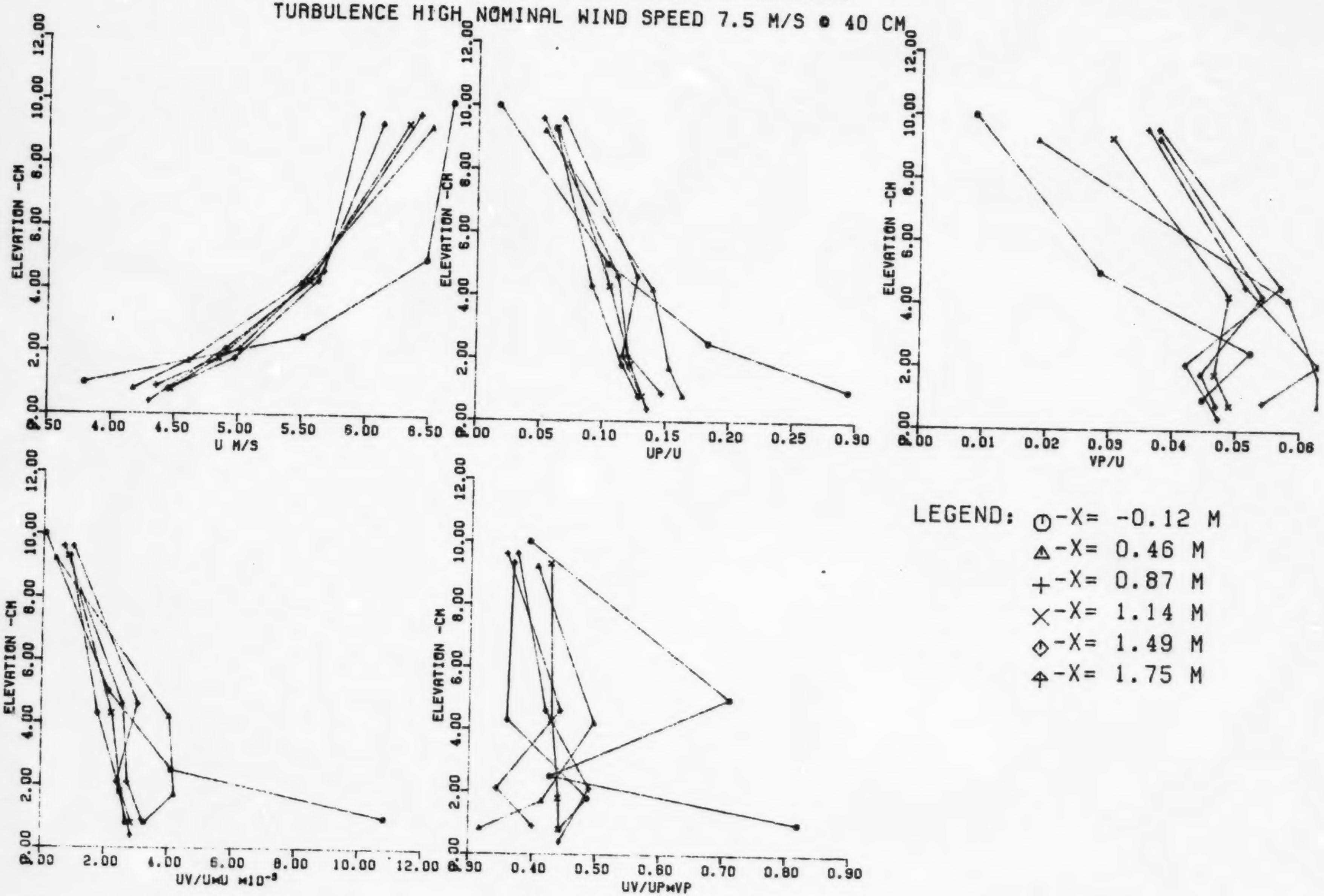

FIGURE 5.15 WIND & TURBULENCE PRØFILES

TURBULENCE LØW NØMINAL WIND SPEED 9.5 M/S @ 40 CM

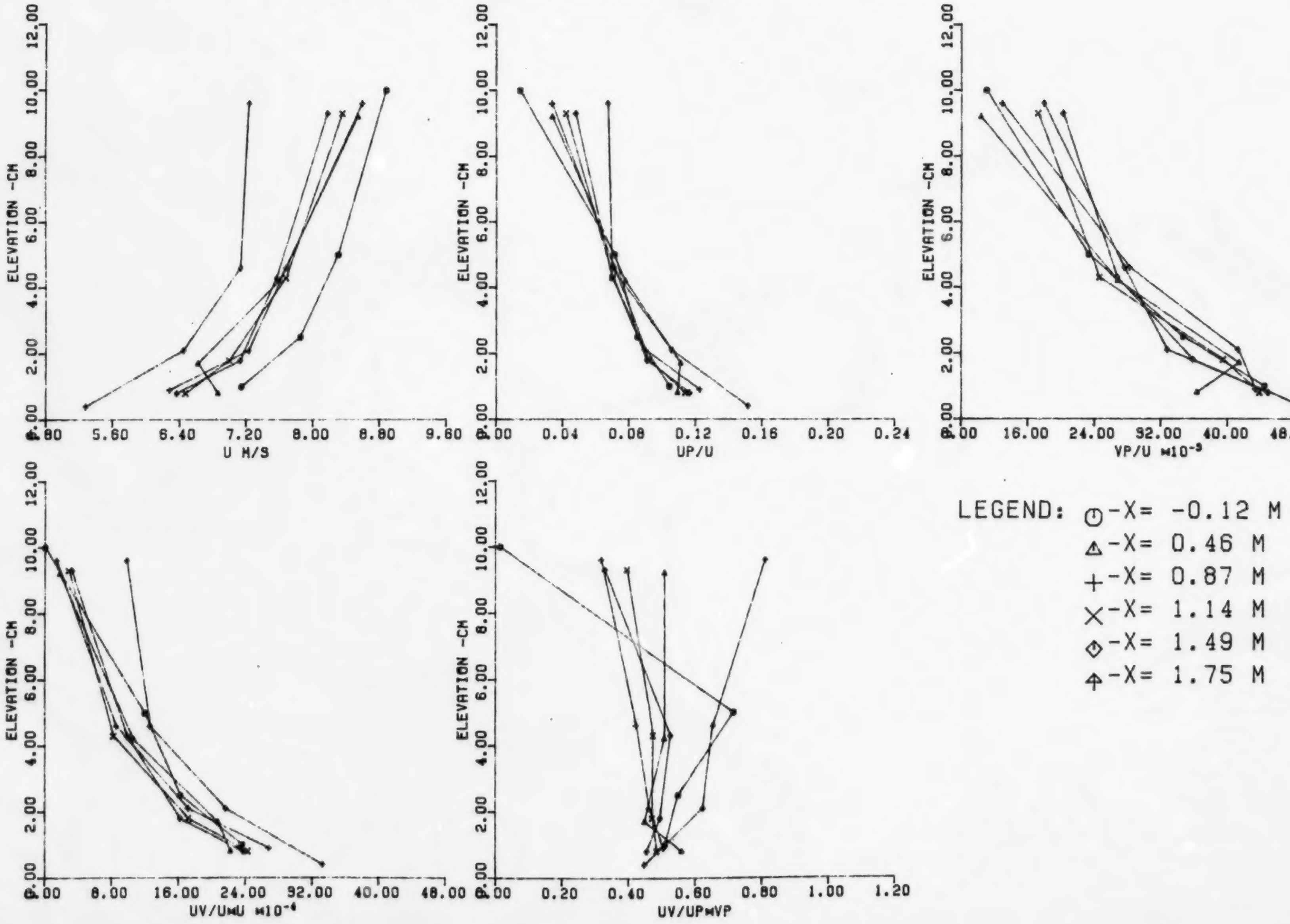

FIGURE 5.16 WIND & TURBULENCE PROFILES

TURBULENCE HIGH NOMINAL WIND SPEED 9.5 M/S @ 40 CM

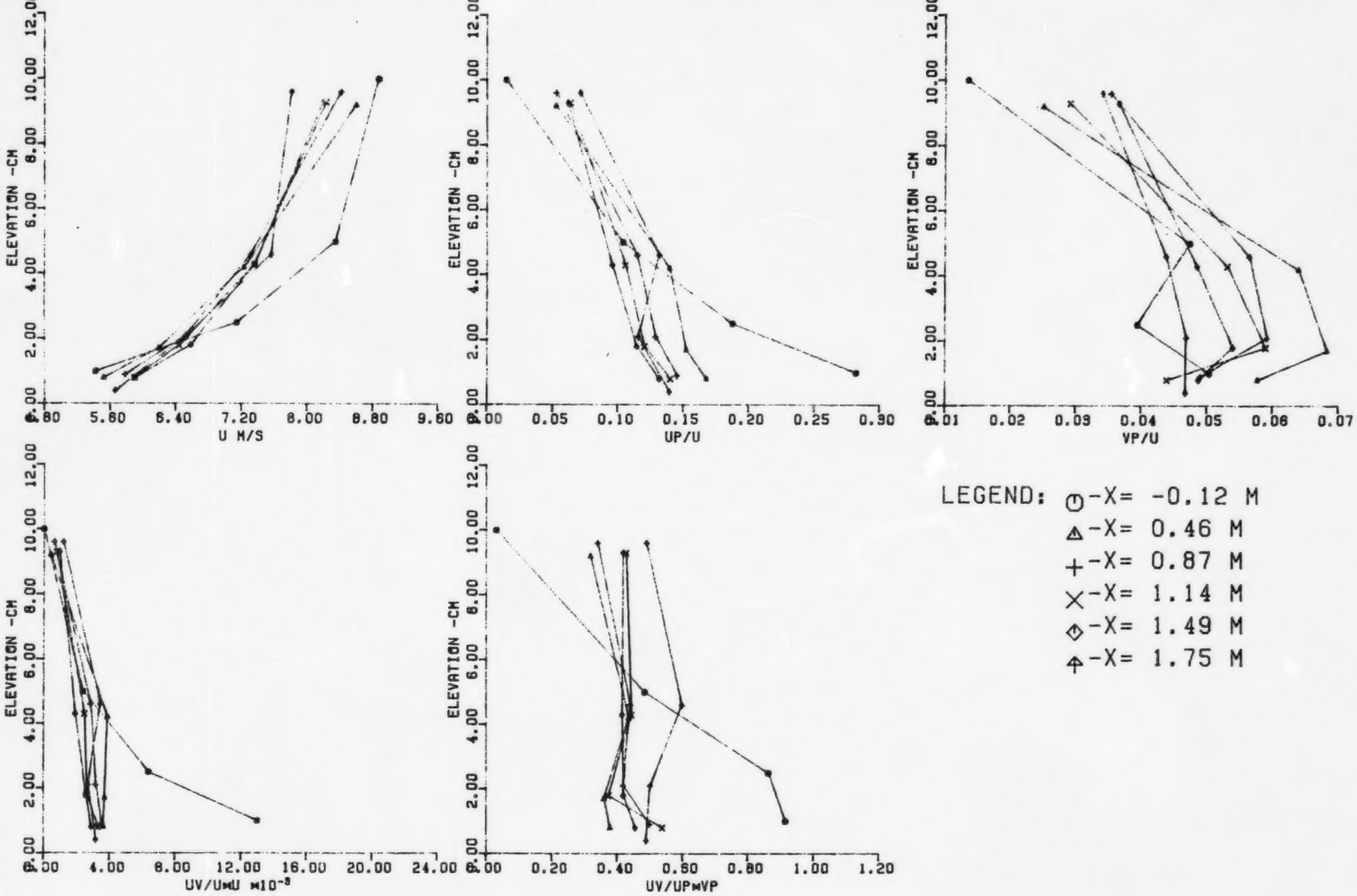

FIGURE 5.17

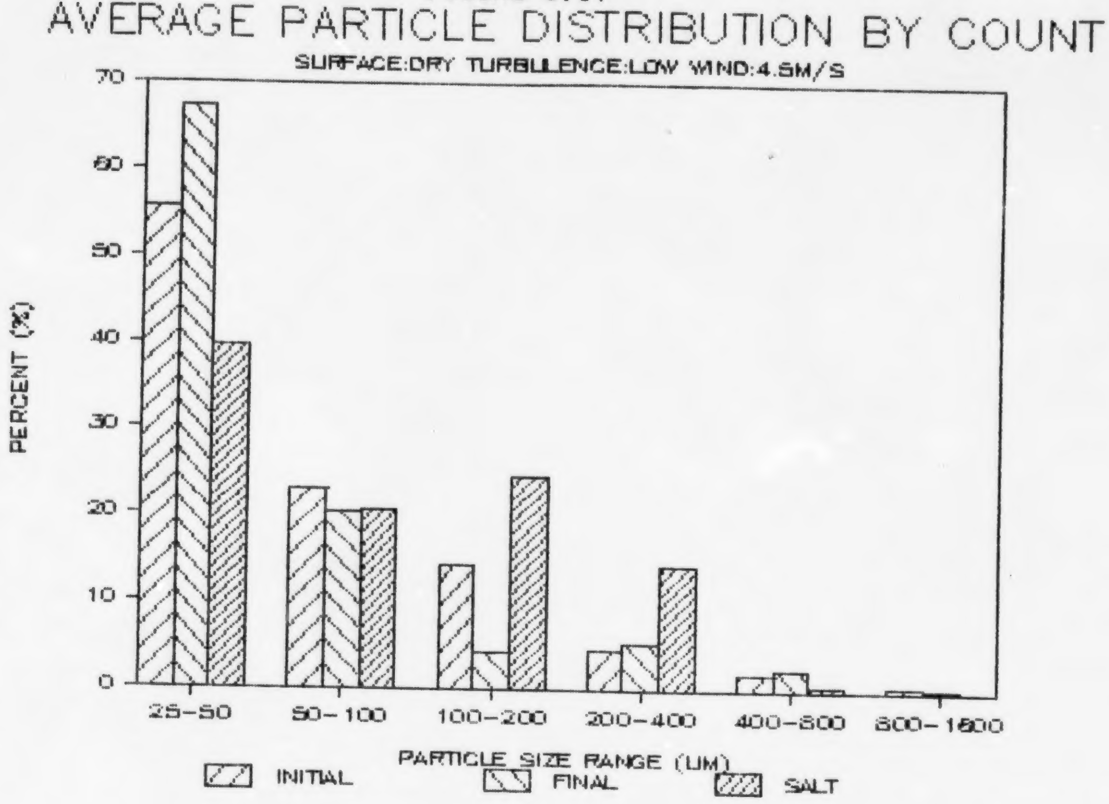
AVERAGE PARTICLE DISTRIBUTION BY COUNT

SURFACE:DRY TURBULENCE:LOW WIND:4.5M/S

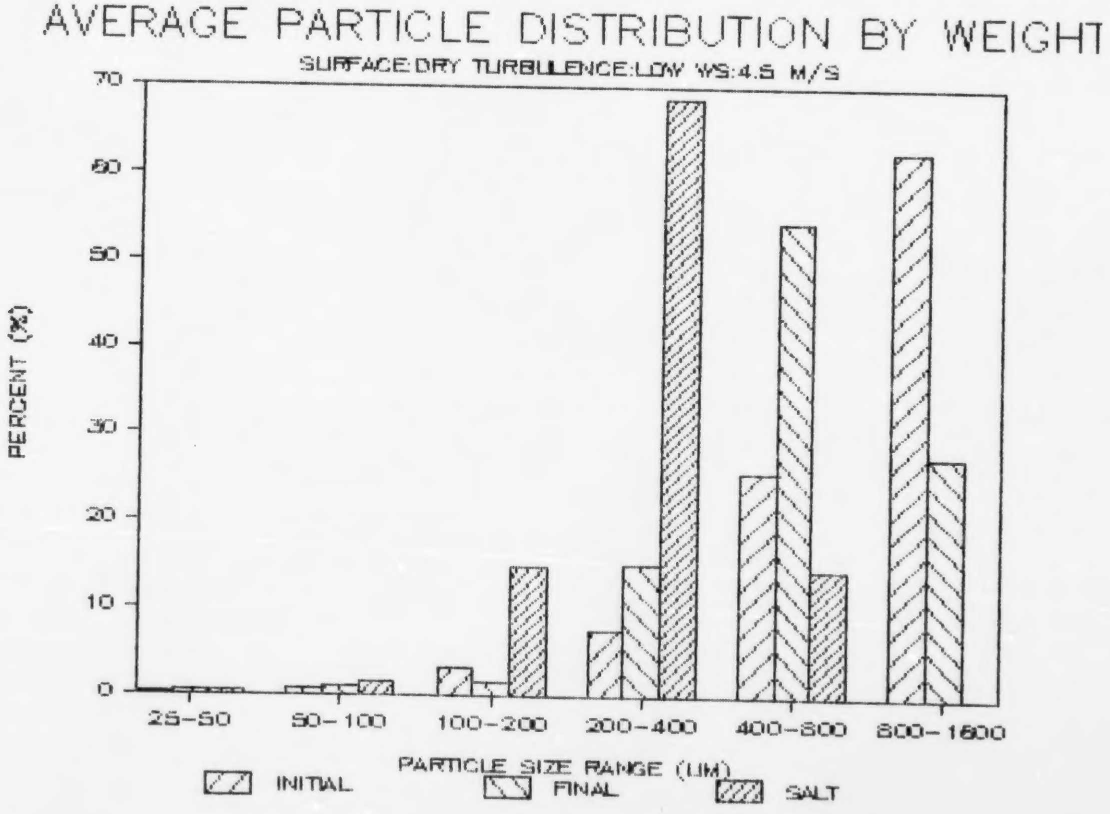
AVERAGE PARTICLE DISTRIBUTION BY WEIGHT

SURFACE:DRY TURBULENCE:LOW WS:4.5 M/S

FIGURE 5.18

AVERAGE PARTICLE DISTRIBUTION BY COUNT

SURFACE:DRY TURBULENCE:HIGH WS:4.5M/S

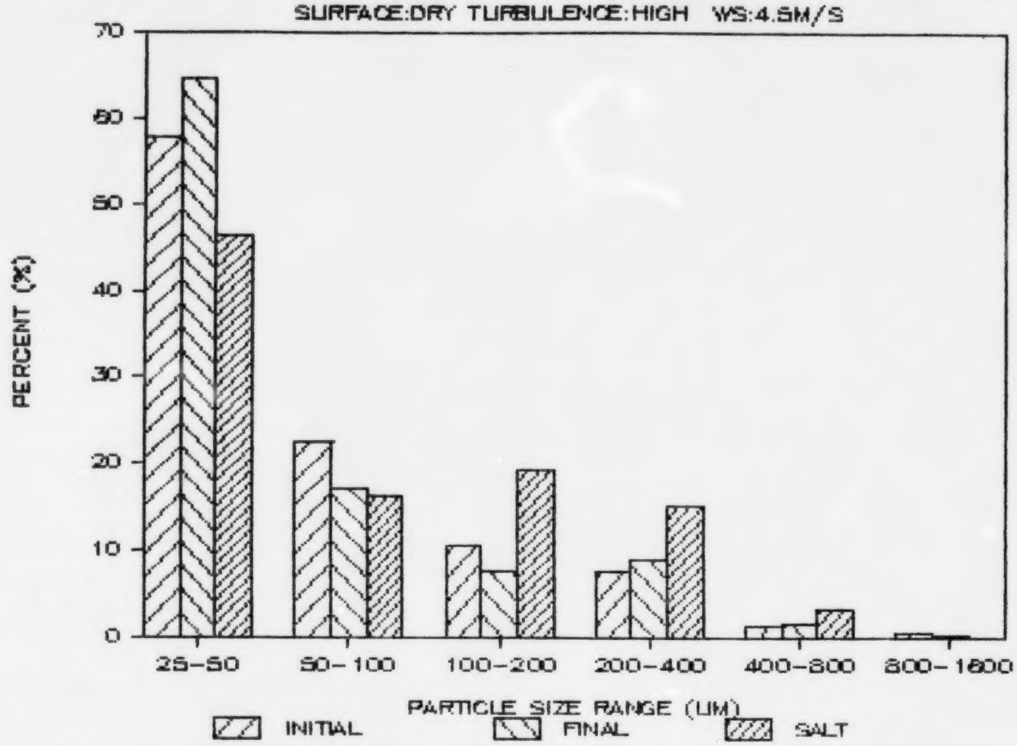

AVERAGE PARTICLE DISTRIBUTION BY WEIGHT

SURFACE:DRY TURBULENCE:HIGH WS:4.5 M/S

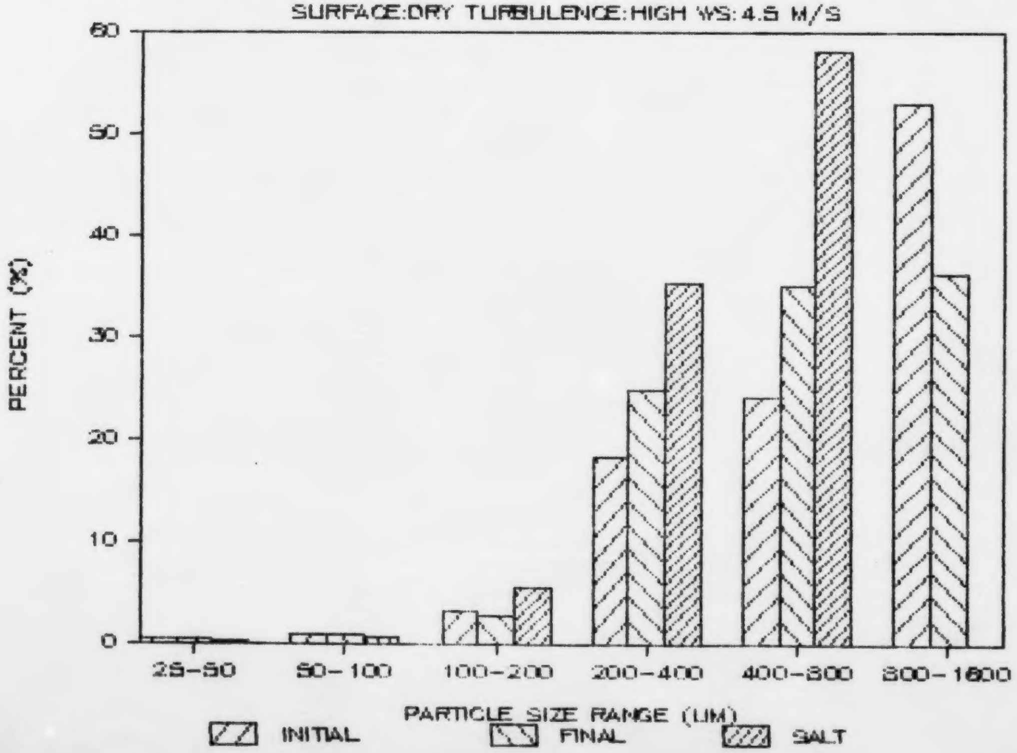

FIGURE 5.19

AVERAGE PARTICLE DISTRIBUTION BY COUNT

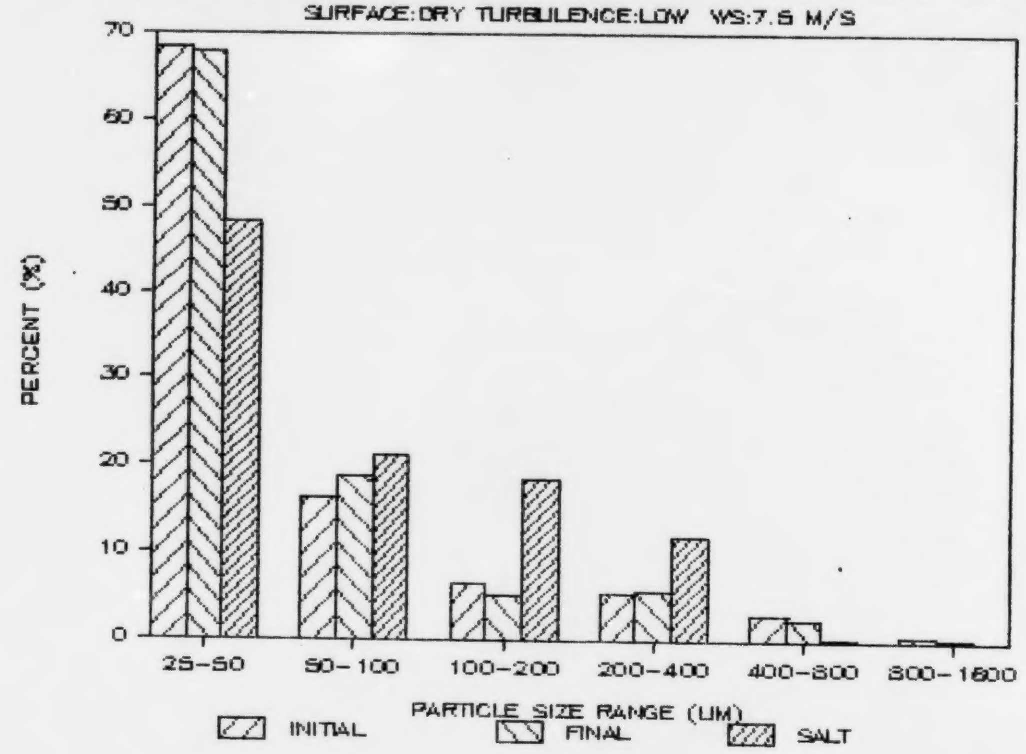

AVERAGE PARTICLE DISTRIBUTION BY WEIGHT

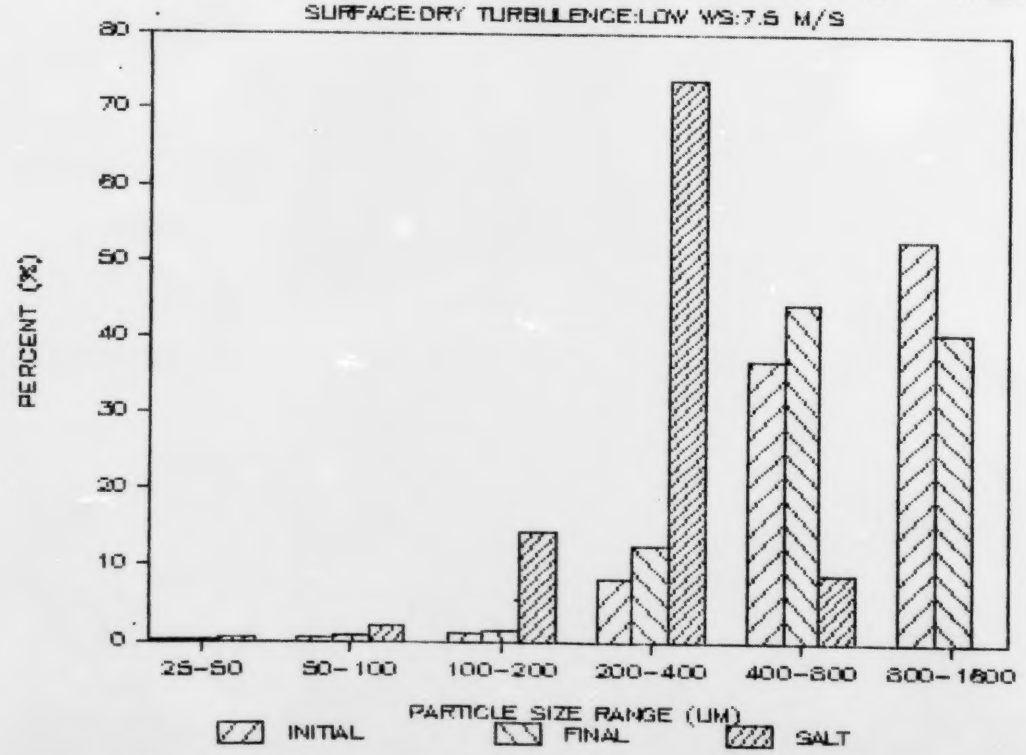

FIGURE 5.20

AVERAGE PARTICLE DISTRIBUTION BY COUNT

SURFACE:DRY TURBULENCE:HIGH WS:7.5 M/S

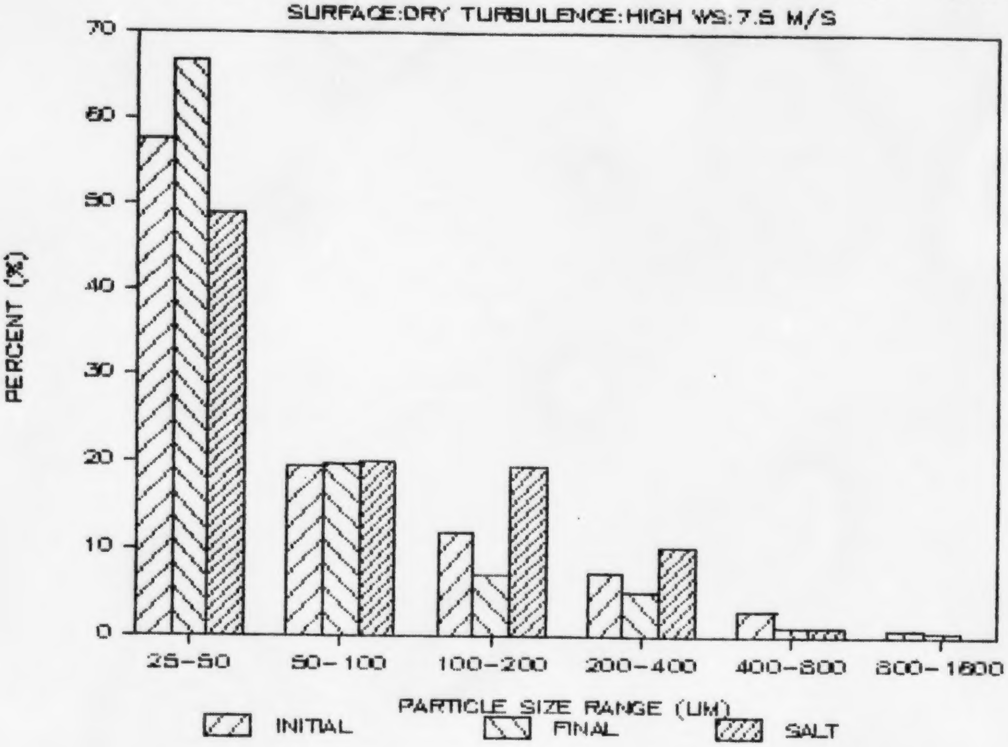

AVERAGE PARTICLE DISTRIBUTION BY WEIGHT

SURFACE:DRY TURBULENCE:HIGH WS:7.5 M/S

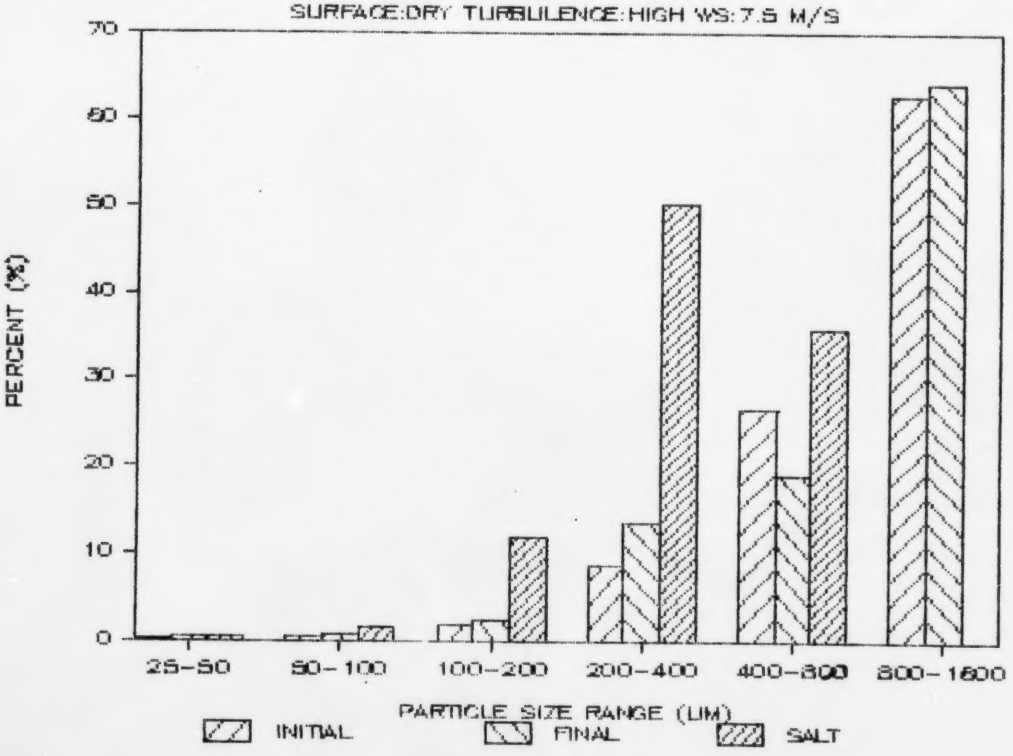

FIGURE 5.21

AVERAGE PARTICLE DISTRIBUTION BY COUNT

SURFACE:DRY TURBULENCE:LOW WS:9.5 M/S

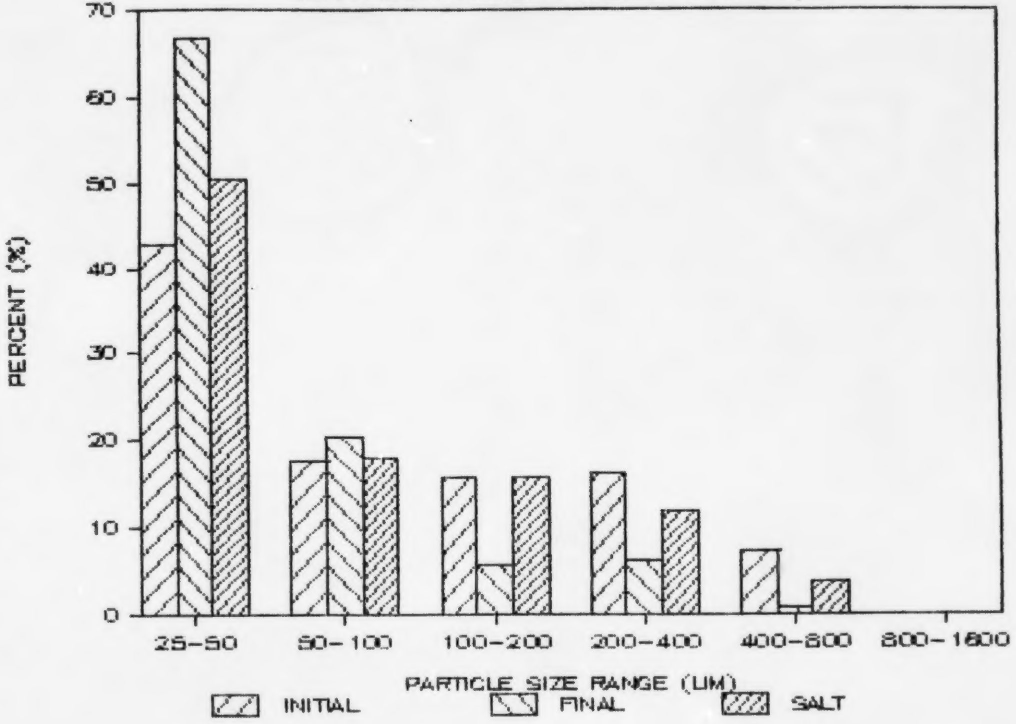

AVERAGE PARTICLE DISTRIBUTION BY WEIGHT

SURFACE:DRY TURBULENCE:LOW WS:9.5 M/S

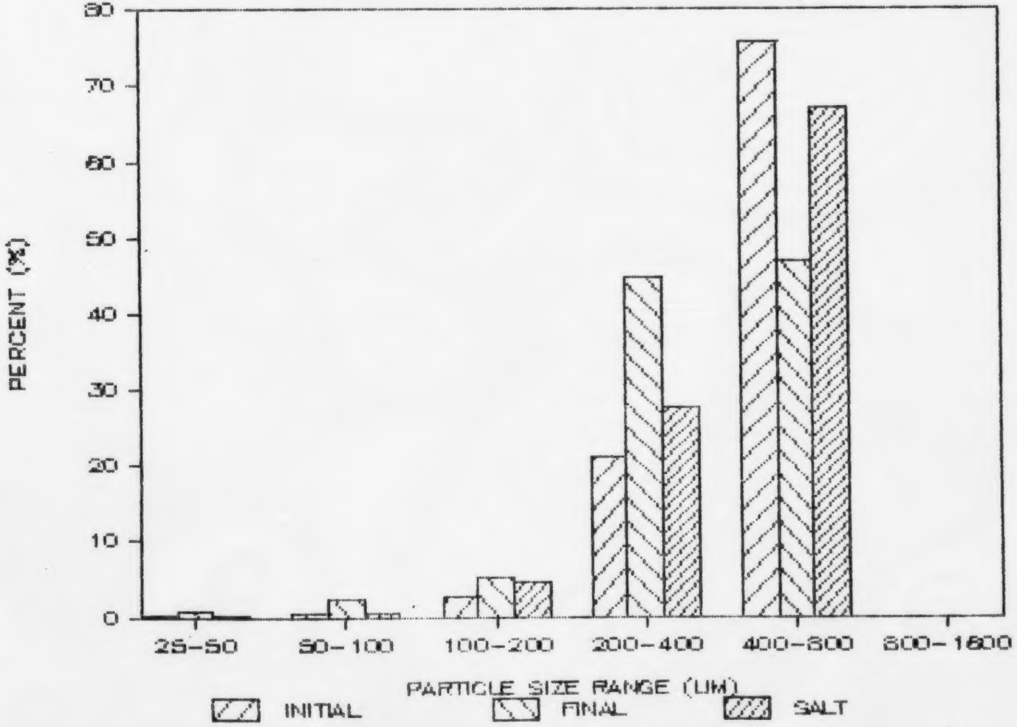

FIGURE 5.22

AVERAGE PARTICLE DISTRIBUTION BY COUNT

SURFACE:DRY TURBULENCE:HIGH WS:9.5 M/S

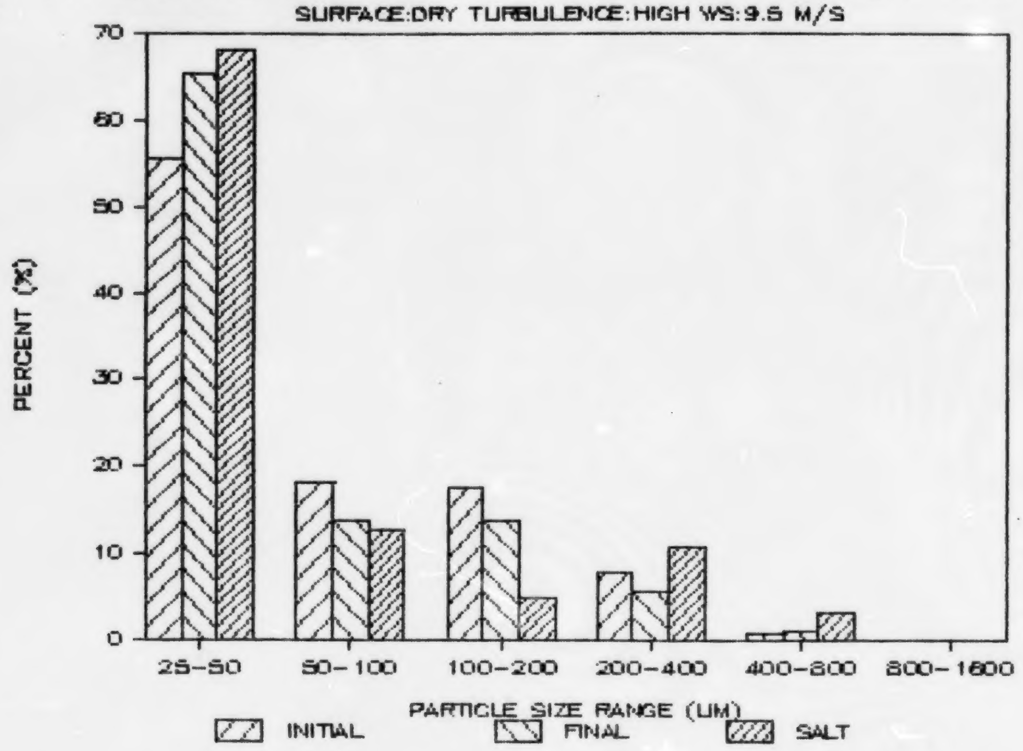

AVERAGE PARTICLE DISTRIBUTION BY WEIGHT

SURFACE:DRY TURBULENCE:HIGH WS:9.5 M/S

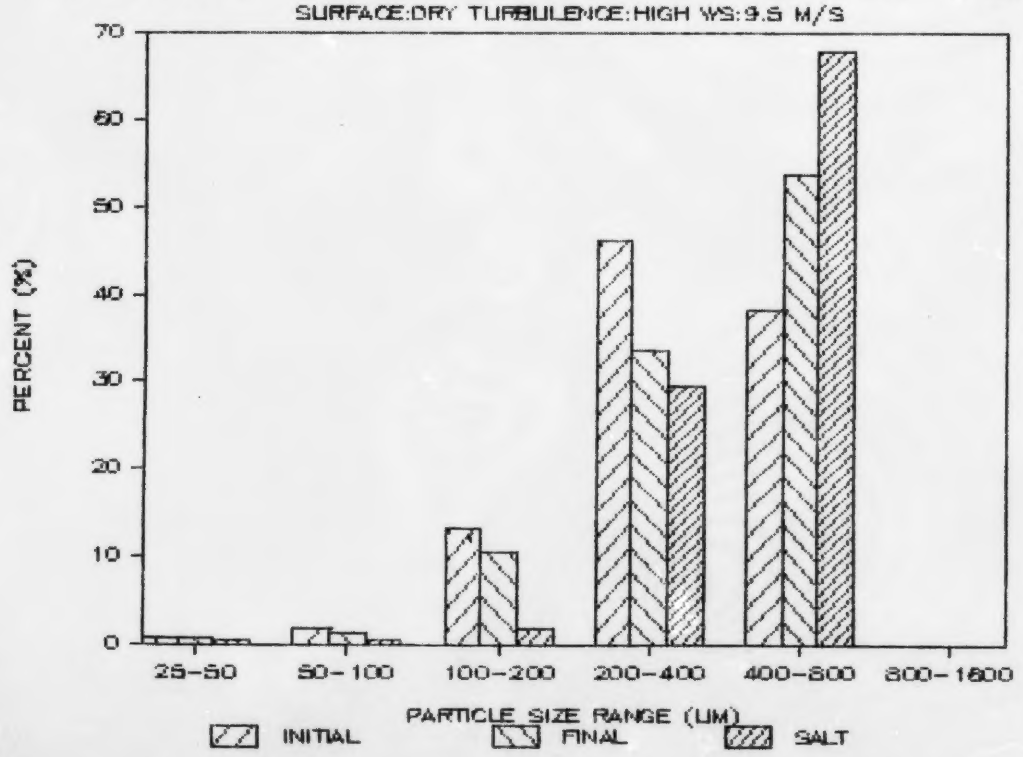

FIGURE 5.23

AVERAGE PARTICLE DISTRIBUTION BY COUNT

SURFACE:WET TURBULENCE:LOW WIND:4.5M/S

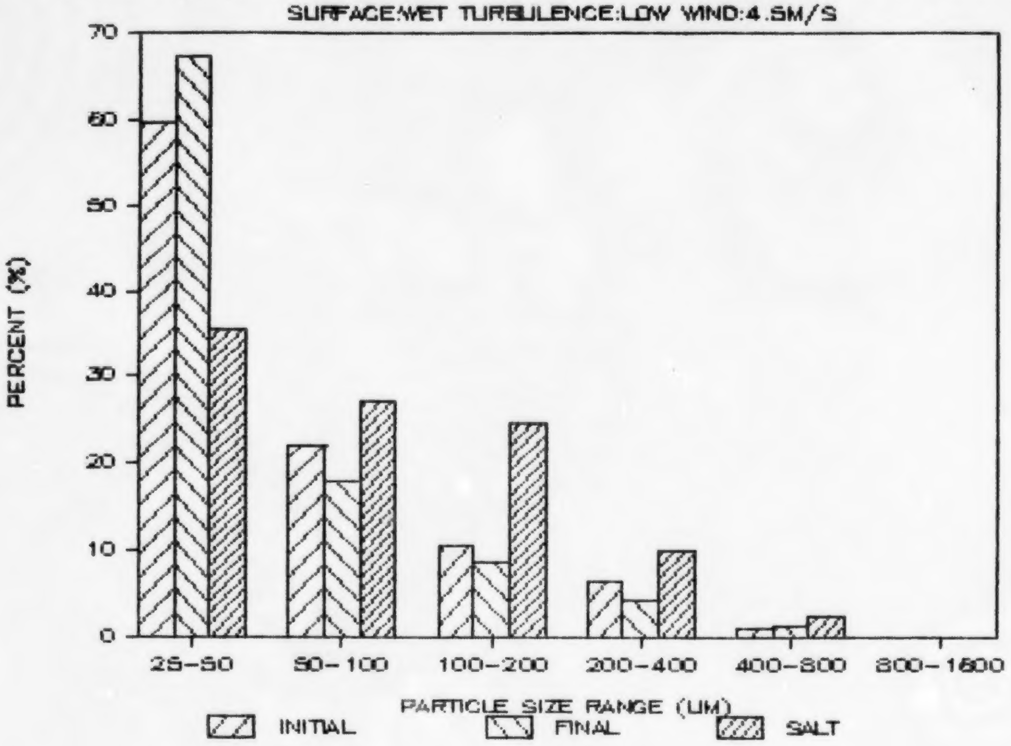

AVERAGE PARTICLE DISTRIBUTION BY WEIGHT

SURFACE:WET TURBULENCE:LOW WS:4.5 M/S

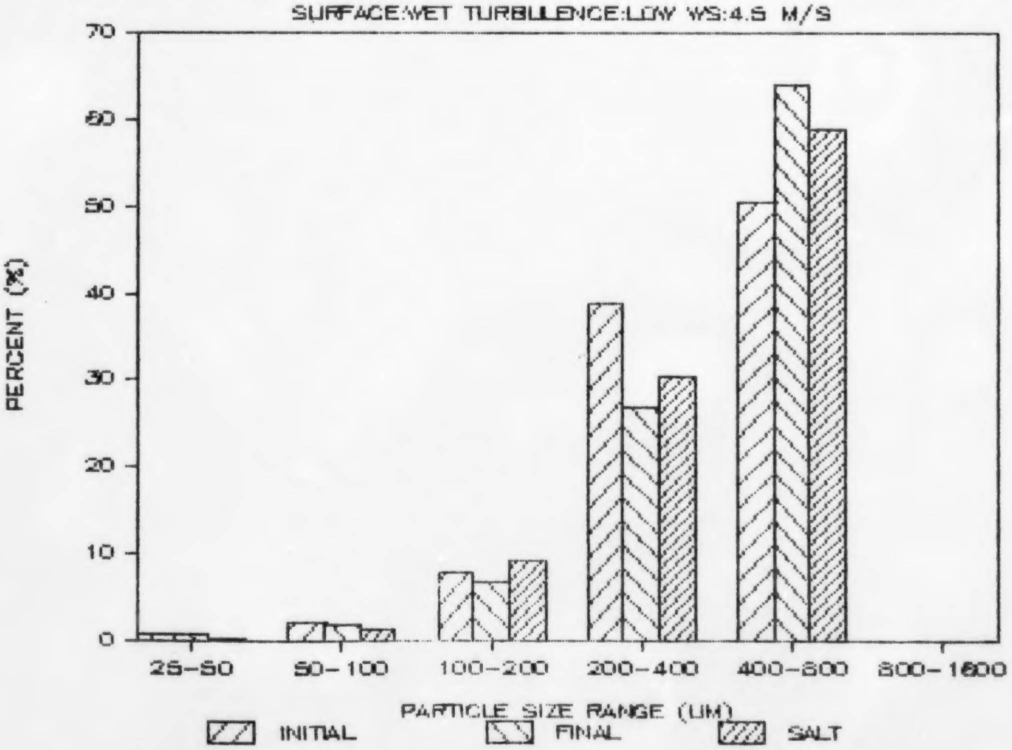

FIGURE 5.24

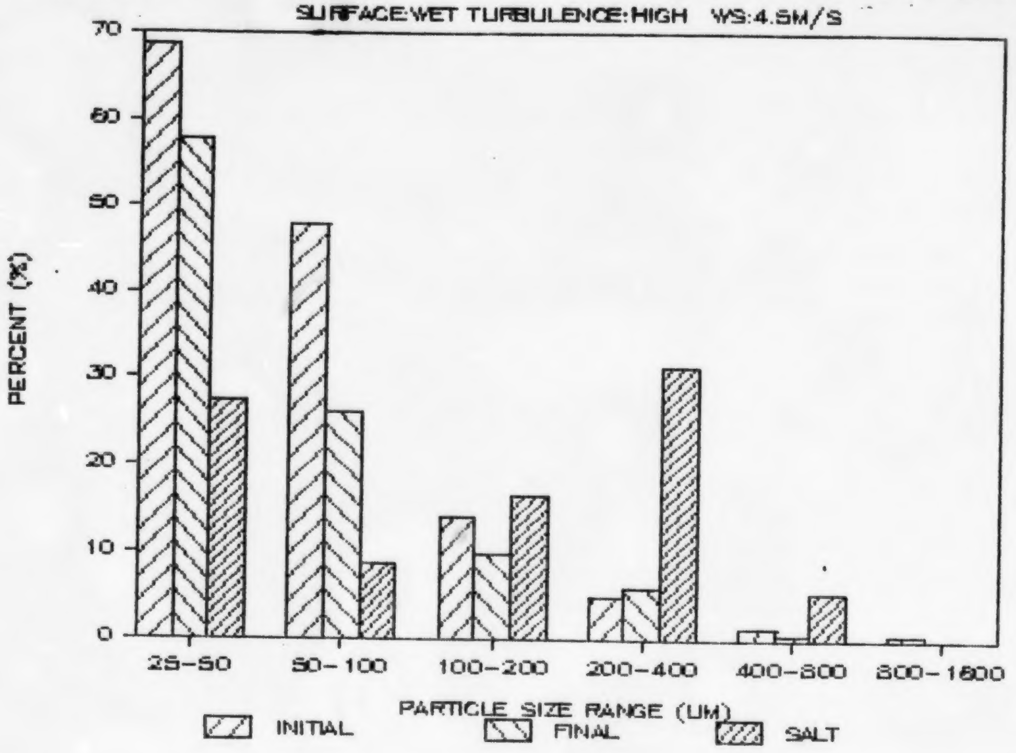
AVERAGE PARTICLE DISTRIBUTION BY COUNT

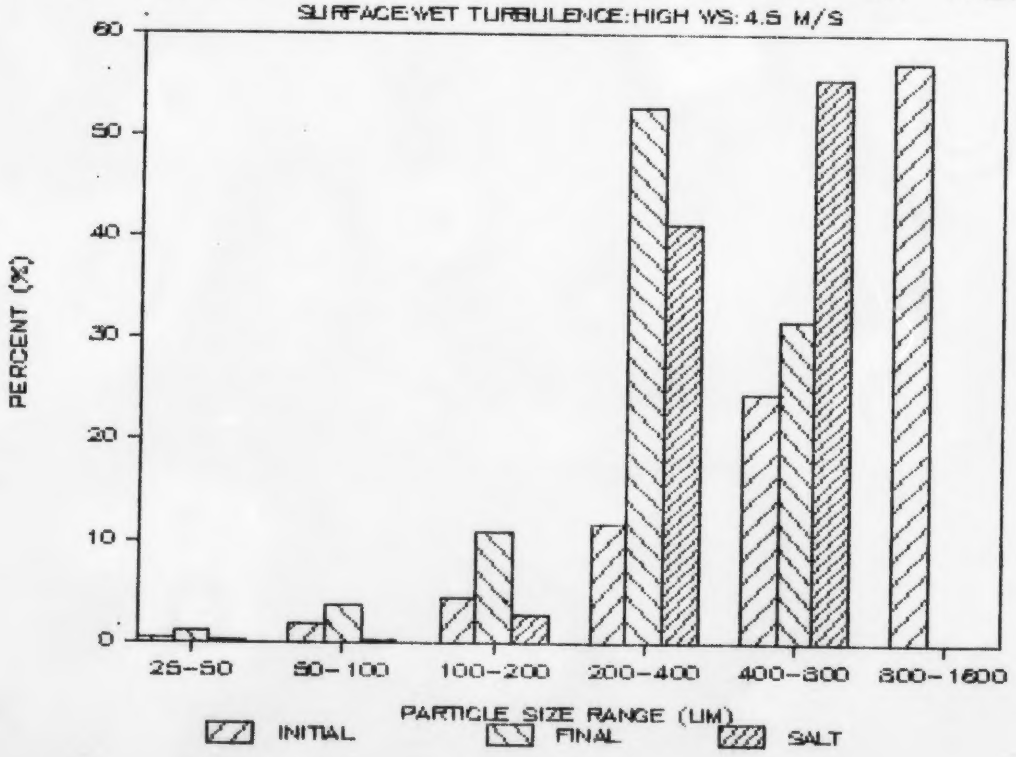
AVERAGE PARTICLE DISTRIBUTION BY WEIGHT

FIGURE 5.25

AVERAGE PARTICLE DISTRIBUTION BY COUNT

SURFACE:WET TURBULENCE:LOW WS:7.5 M/S

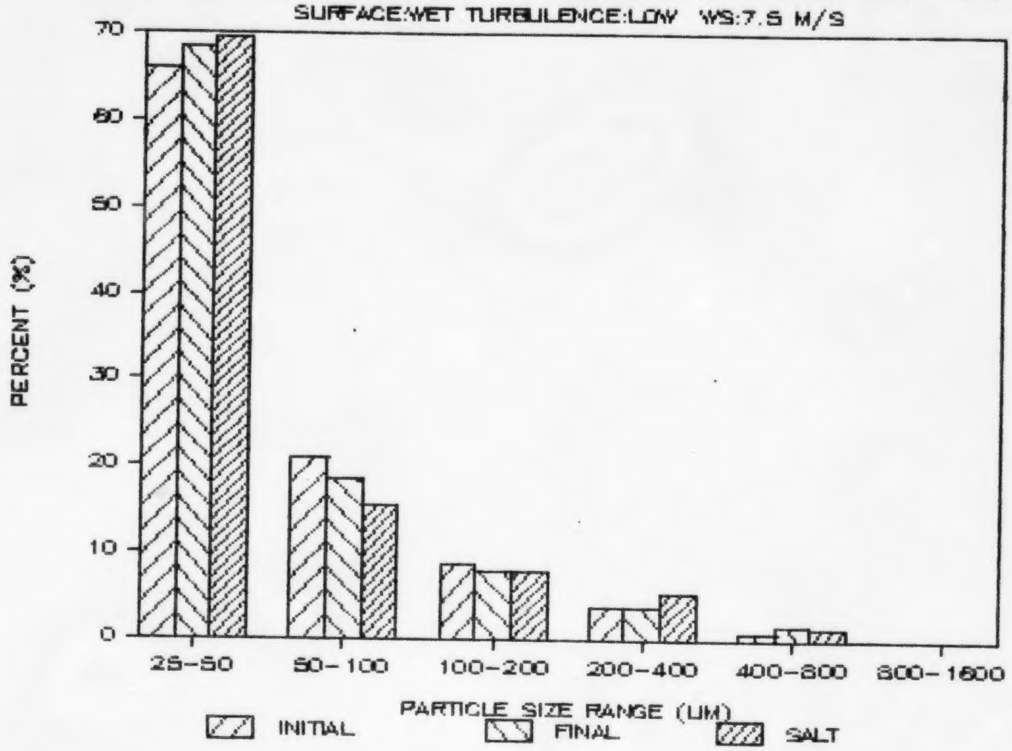

AVERAGE PARTICLE DISTRIBUTION BY WEIGHT

SURFACE:WET TURBULENCE:LOW WS:7.5 M/S

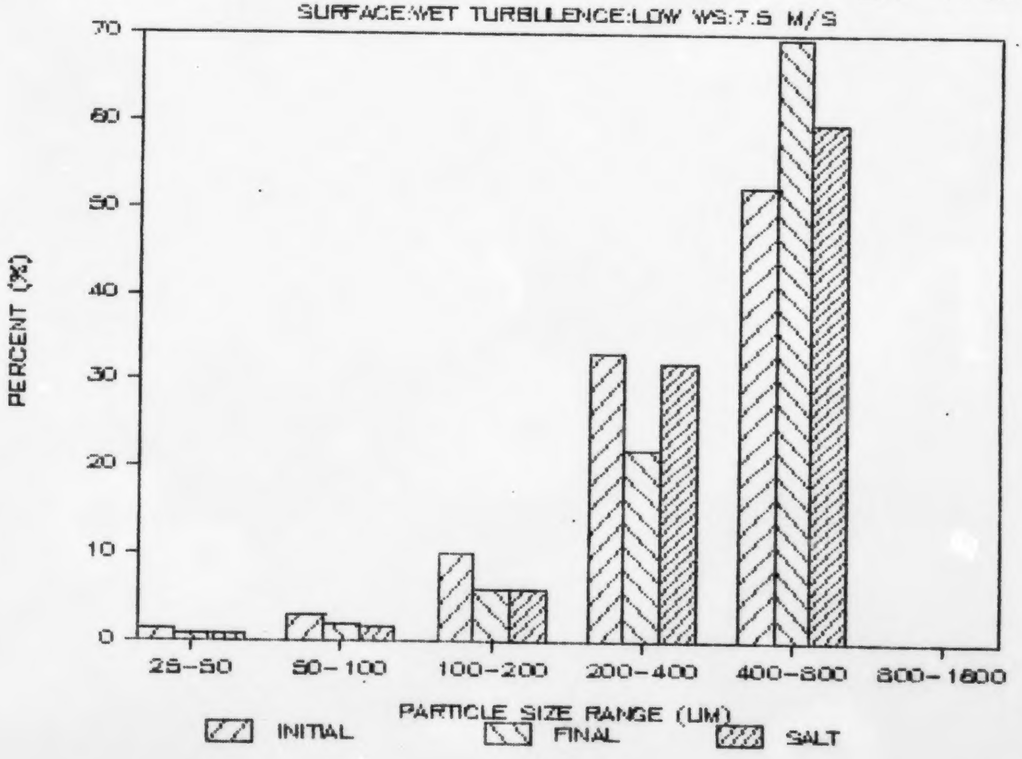

FIGURE 5.26

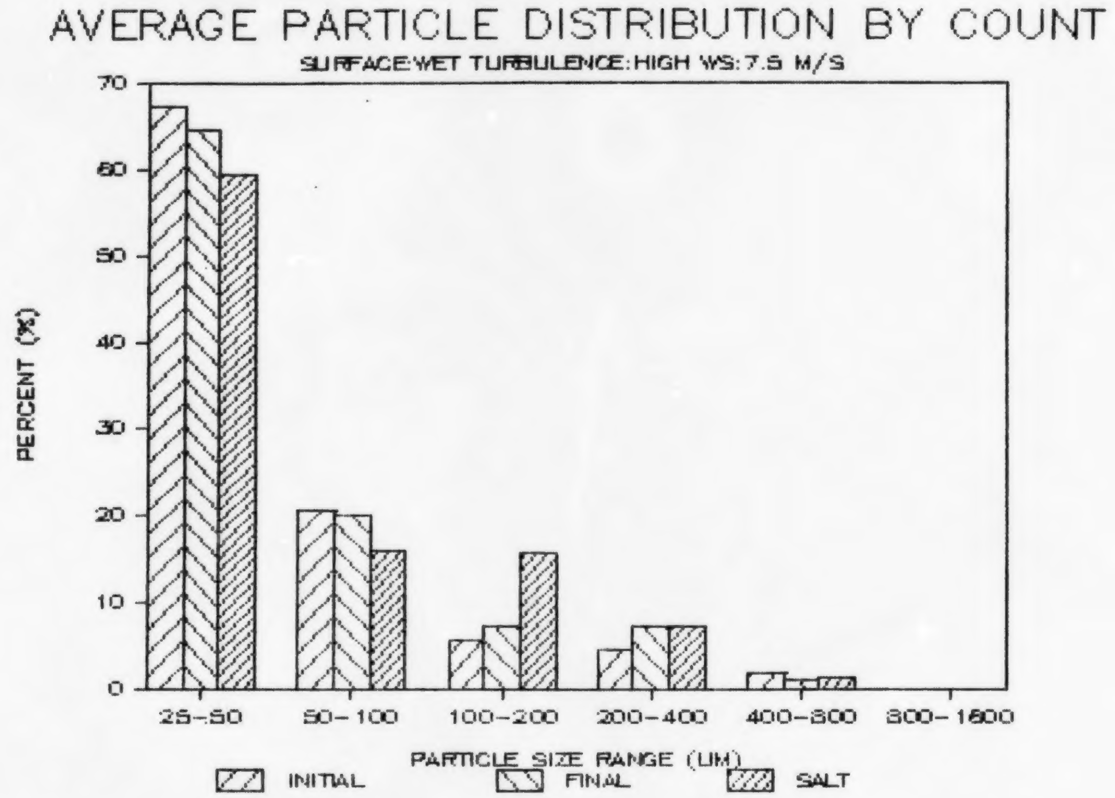

AVERAGE PARTICLE DISTRIBUTION BY COUNT

SURFACE:WET TURBULENCE:HIGH WS:7.5 M/S

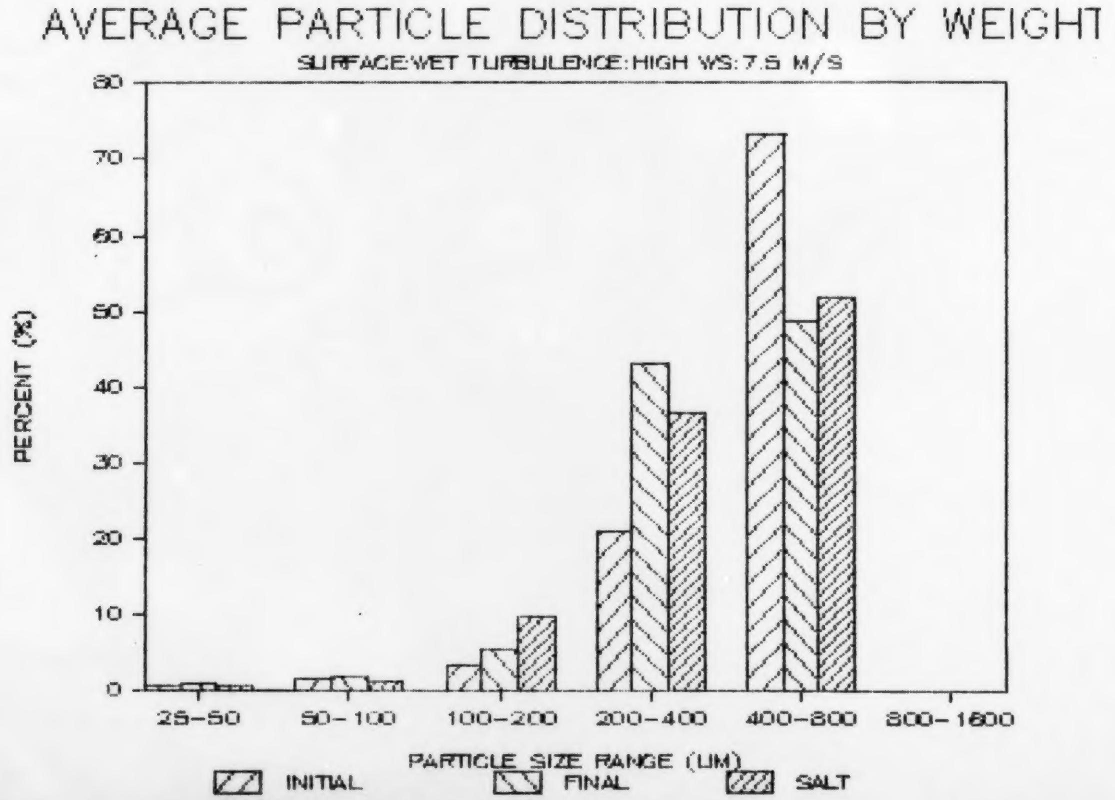

AVERAGE PARTICLE DISTRIBUTION BY WEIGHT

SURFACE:WET TURBULENCE:HIGH WS:7.5 M/S

FIGURE 5.27

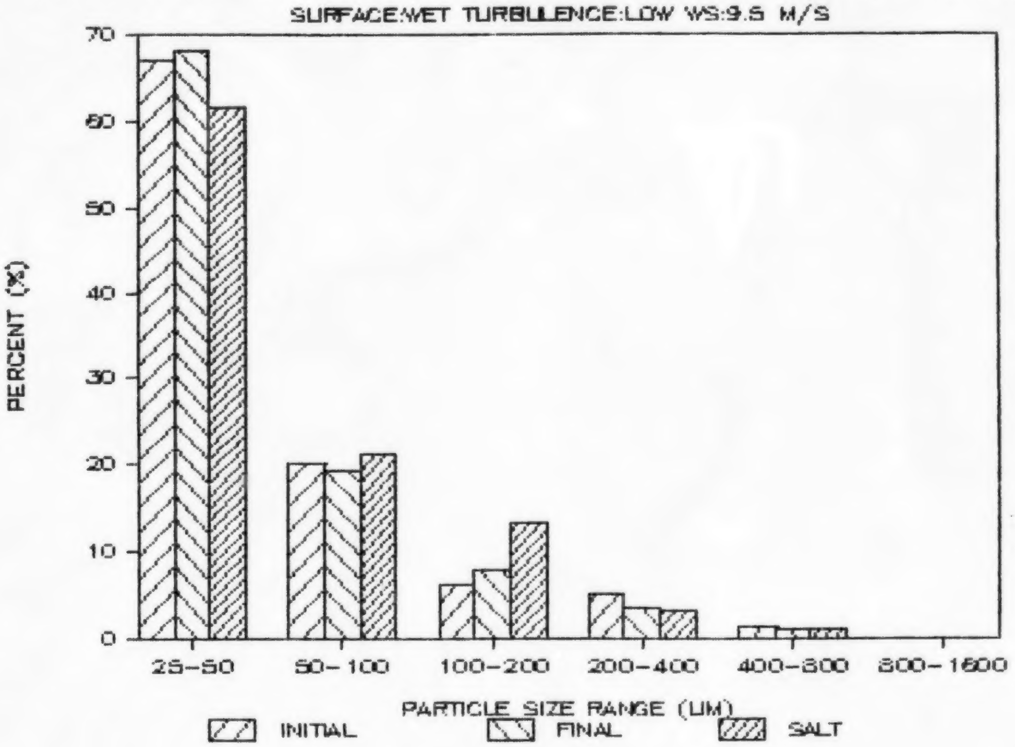

AVERAGE PARTICLE DISTRIBUTION BY COUNT

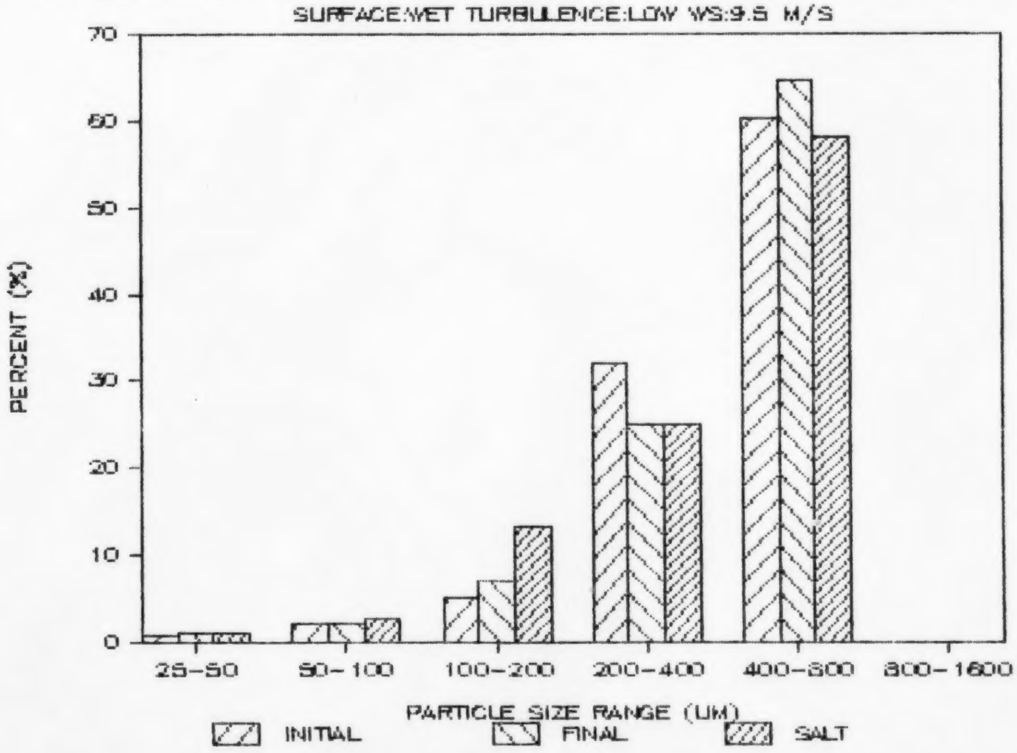

AVERAGE PARTICLE DISTRIBUTION BY WEIGHT

FIGURE 5.28

AVERAGE PARTICLE DISTRIBUTION BY COUNT

SURFACE:WET TURBULENCE:HIGH WS:9.5 M/S

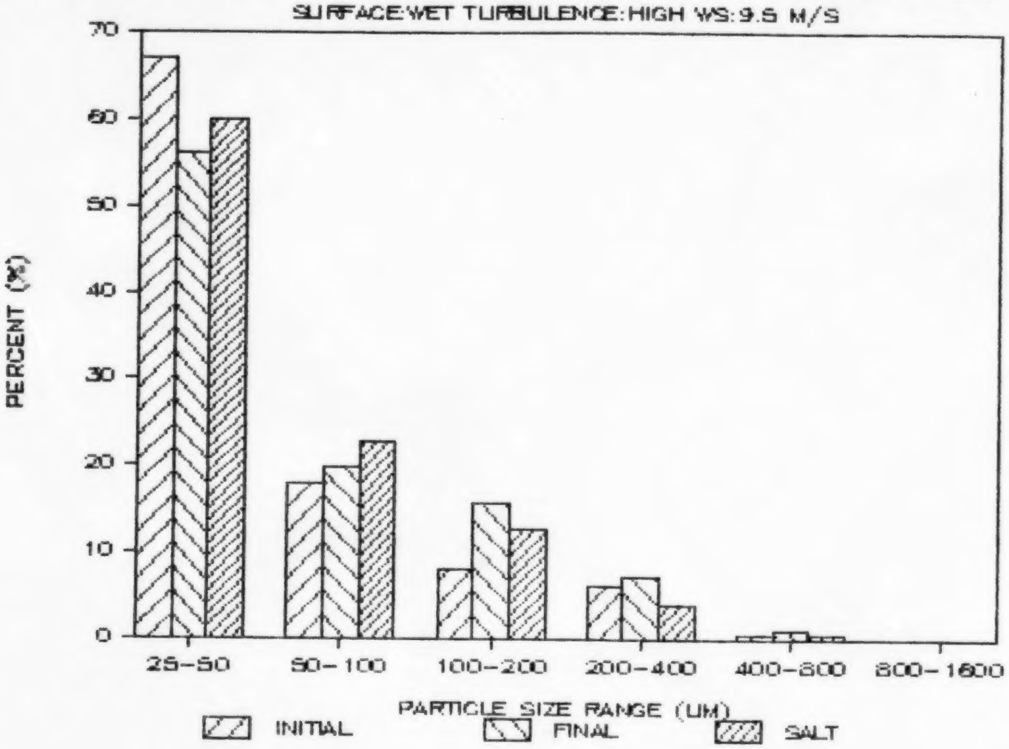

AVERAGE PARTICLE DISTRIBUTION BY WEIGHT

SURFACE:WET TURBULENCE:HIGH WS:9.5 M/S

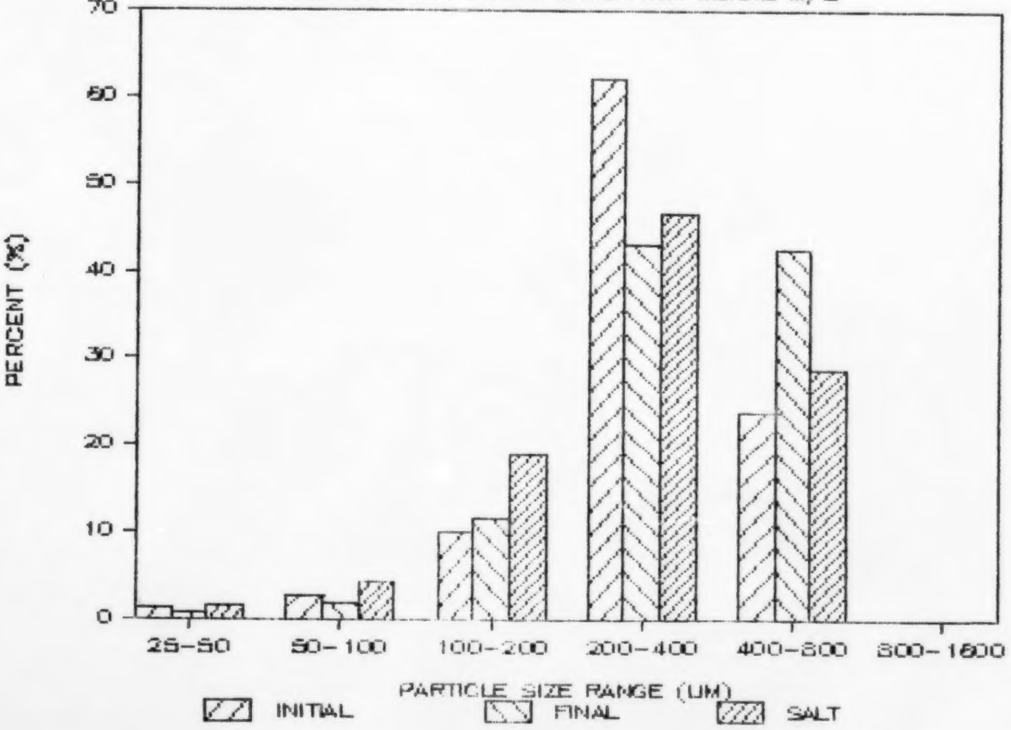

FIGURE 5.29

Median Particle Size (by weight) vs. u*

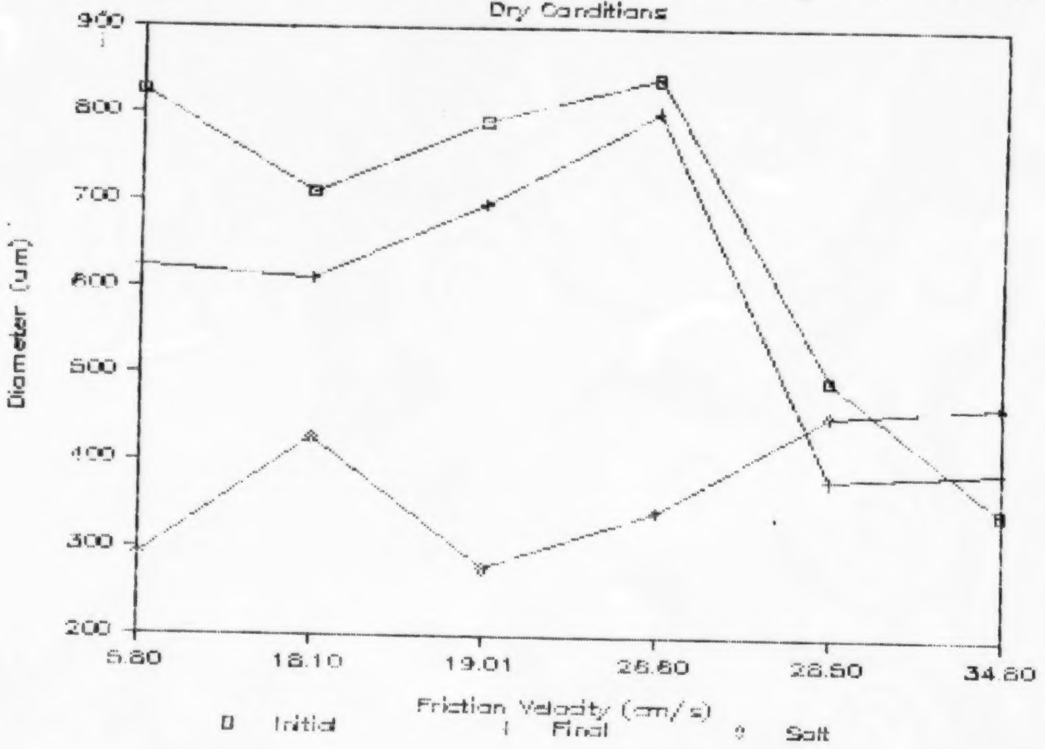

Median Particle Size (by weight) vs. u*

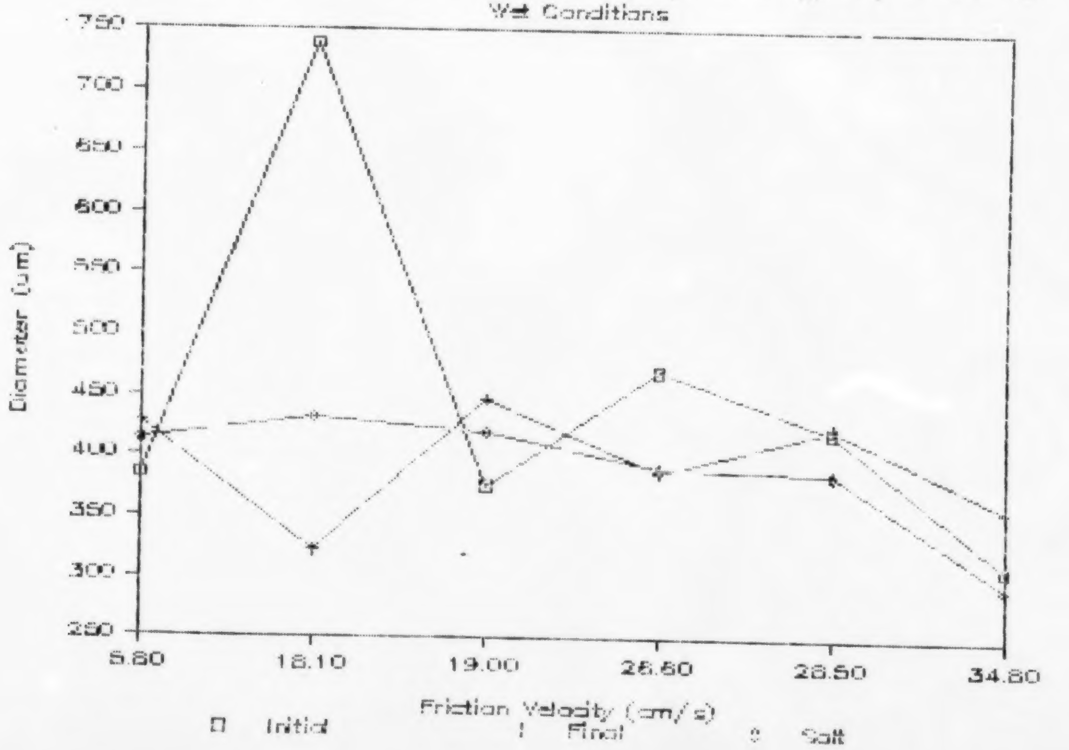

FIGURE 5.30

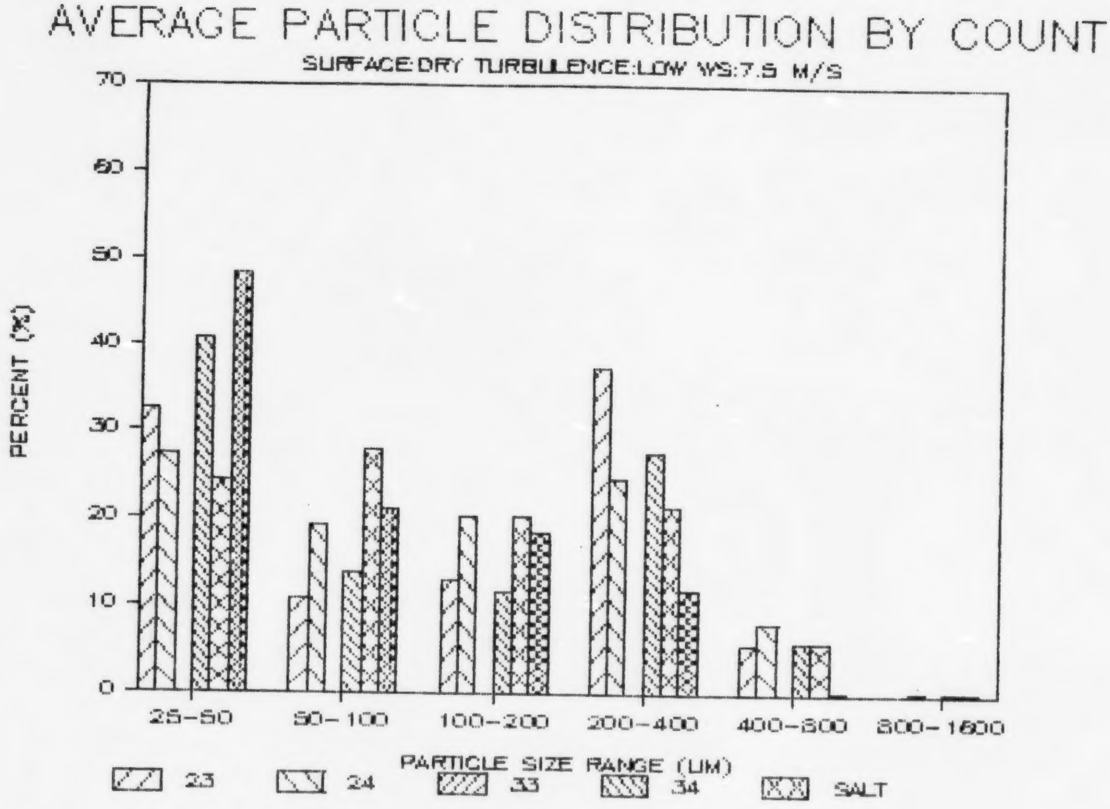
AVERAGE PARTICLE DISTRIBUTION BY COUNT
SURFACE:DRY TURBULENCE:LOW WS:7.5 M/S
PERCENT (%)
70
60
50
40
30
20
10
0
25–50
50–100
100–200
200–400
400–800
800–1600
PARTICLE SIZE RANGE (UM)
23
24
33
34
SALT

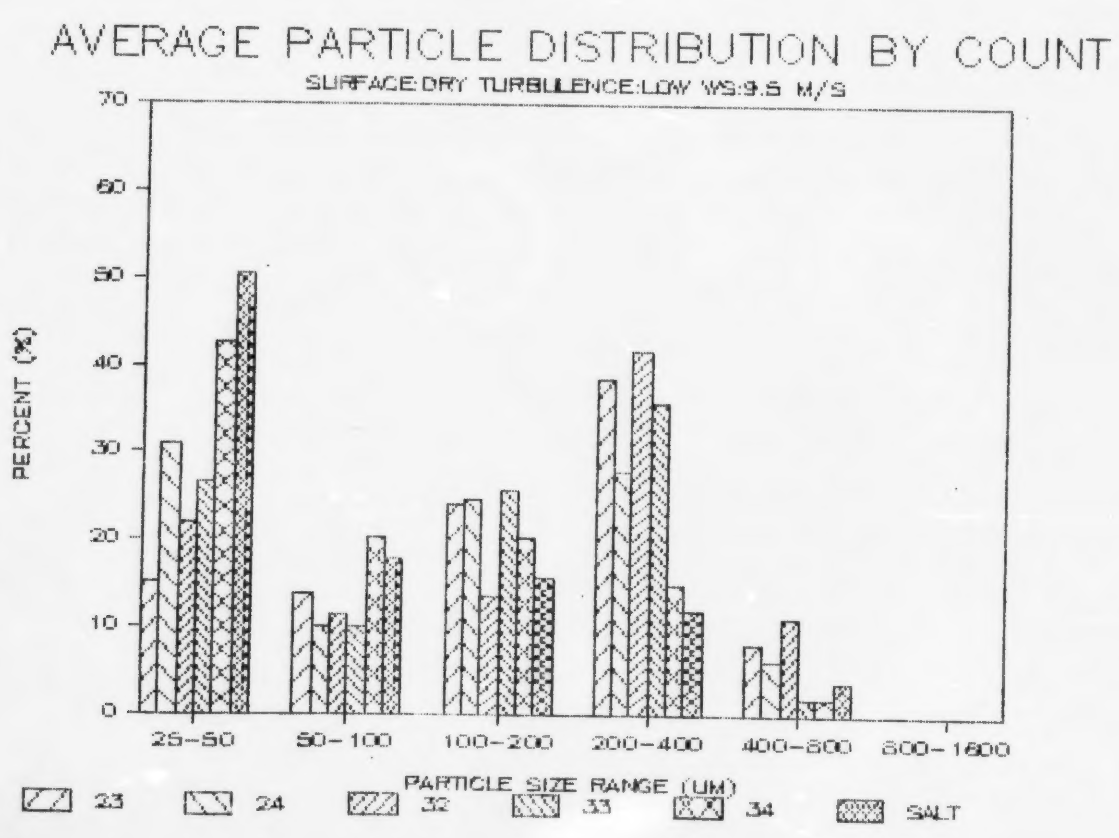
AVERAGE PARTICLE DISTRIBUTION BY COUNT
SURFACE:DRY TURBULENCE:LOW WS:9.5 M/S
PERCENT (%)
70
60
50
40
30
20
10
0
25–50
50–100
100–200
200–400
400–800
800–1600
PARTICLE SIZE RANGE (UM)
23
24
32
33
34
SALT

FIGURE 5.31

AVERAGE PARTICLE DISTRIBUTION BY COUNT

SURFACE:DRY TURBULENCE:HIGH WS:7.5 M/S

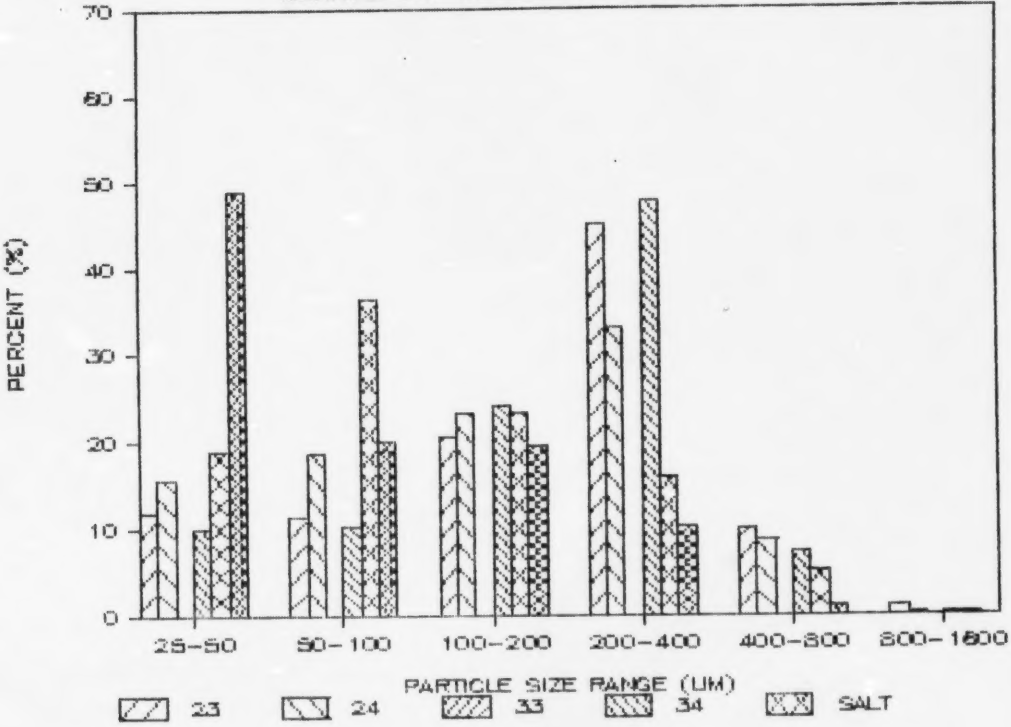

AVERAGE PARTICLE DISTRIBUTION BY COUNT

SURFACE:DRY TURBULENCE:HIGH WS:9.5 M/S

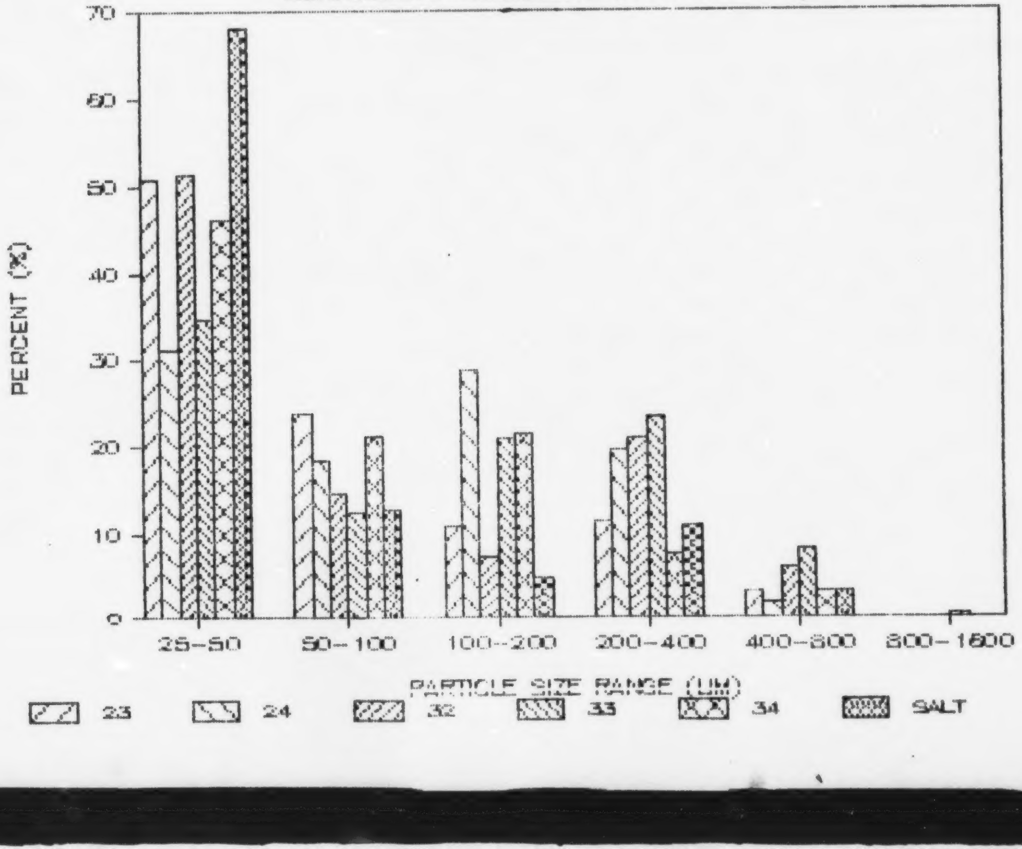

FIGURE 5.32

AVERAGE PARTICLE DISTRIBUTION BY COUNT

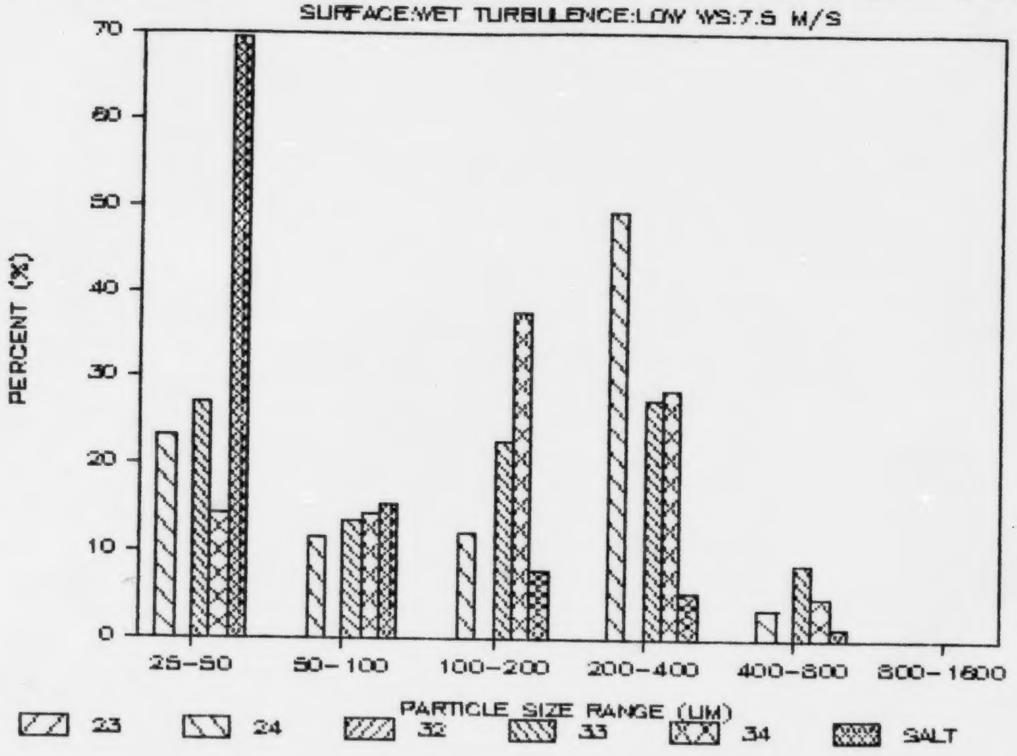

AVERAGE PARTICLE DISTRIBUTION BY COUNT

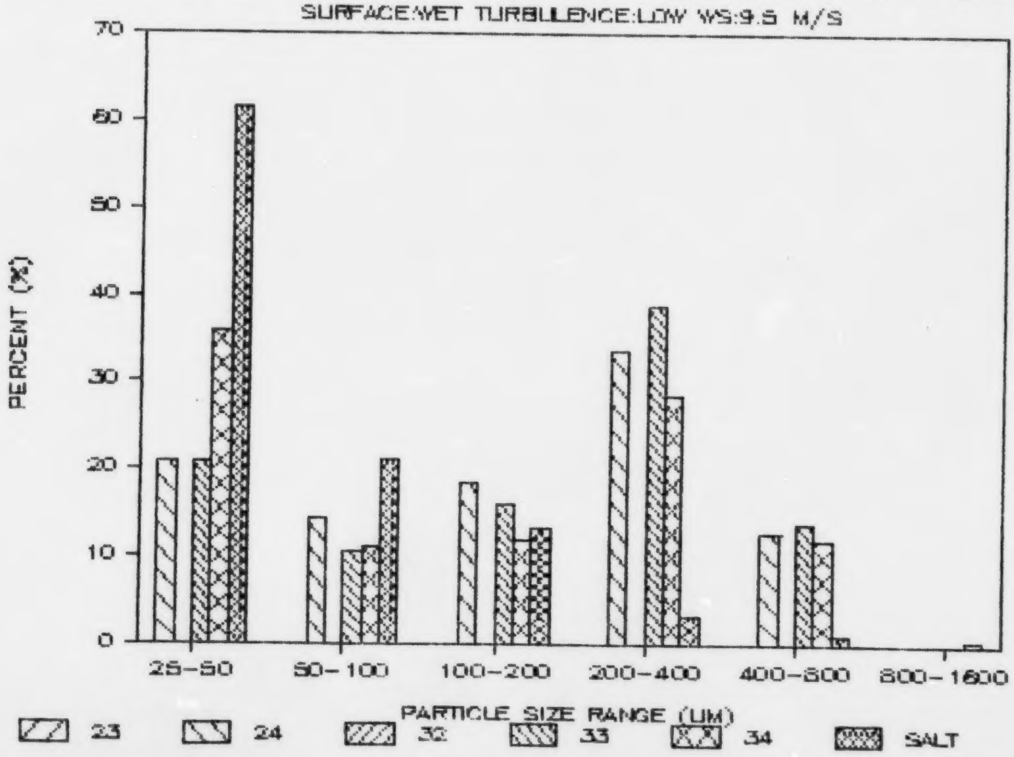

FIGURE 5.39

AVERAGE PARTICLE DISTRIBUTION BY COUNT

SURFACE:WET TURBULENCE:HIGH WS:7.5 M/S

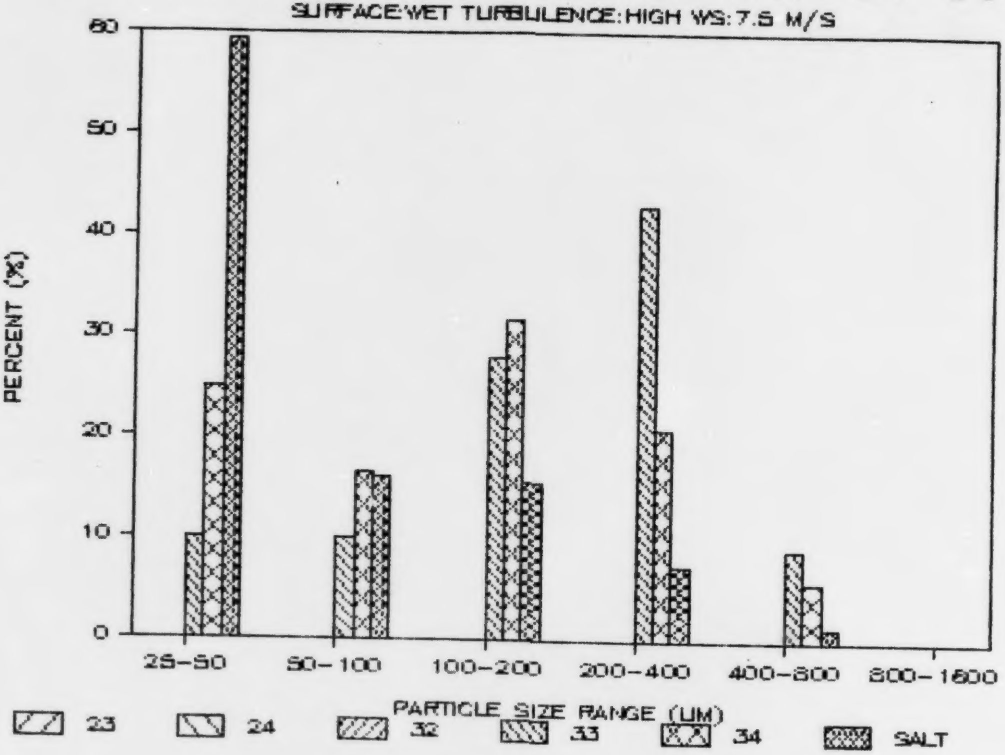

AVERAGE PARTICLE DISTRIBUTION BY COUNT

SURFACE:WET TURBULENCE:HIGH WS:9.5 M/S

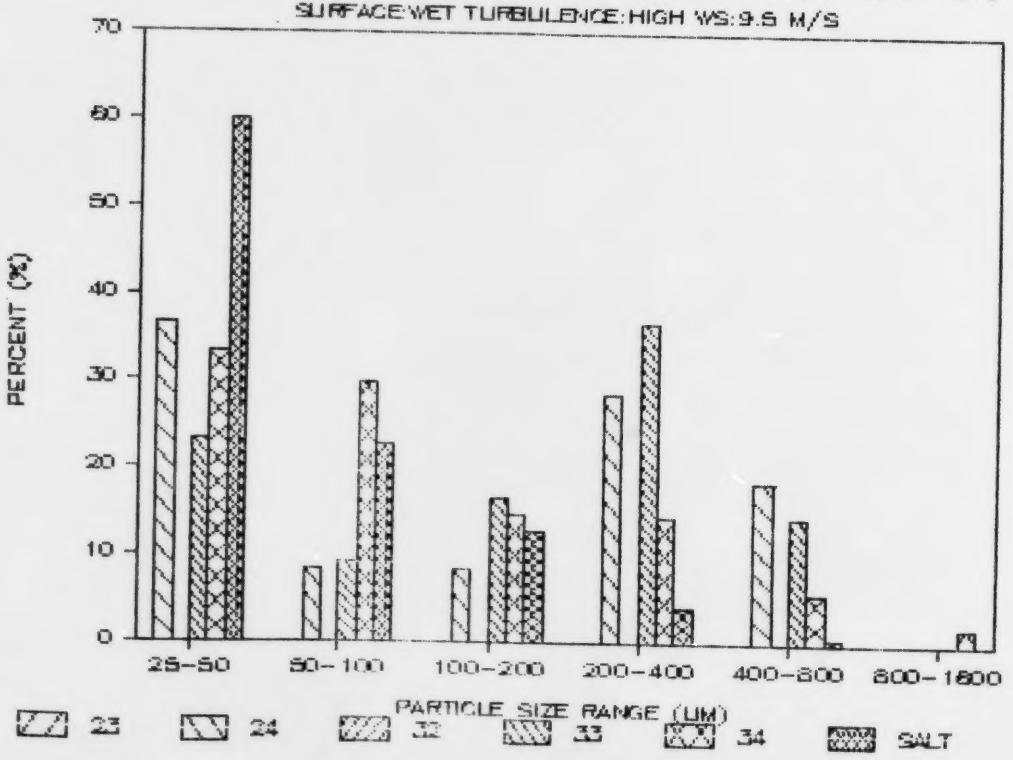

FIGURE 5.34 MEAN VERTICAL FLUX PROFILES FOR

MEAN VALUES FOR TURBULENCE LOW SURFACE DRY NOMINAL WIND 4.5 M/S

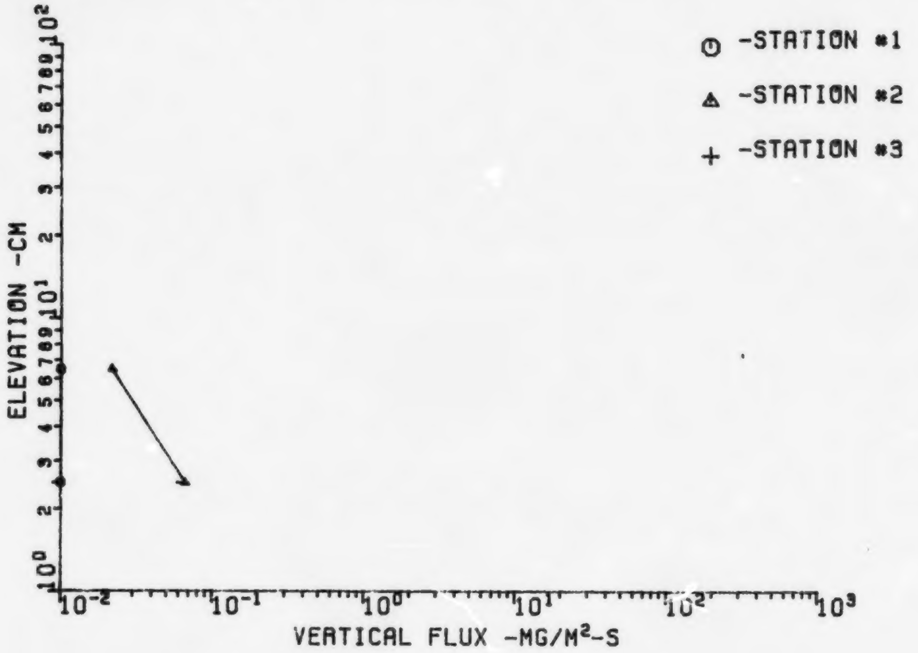

MEAN VALUES FOR TURBULENCE HIGH SURFACE DRY NOMINAL WIND 4.5 M/S

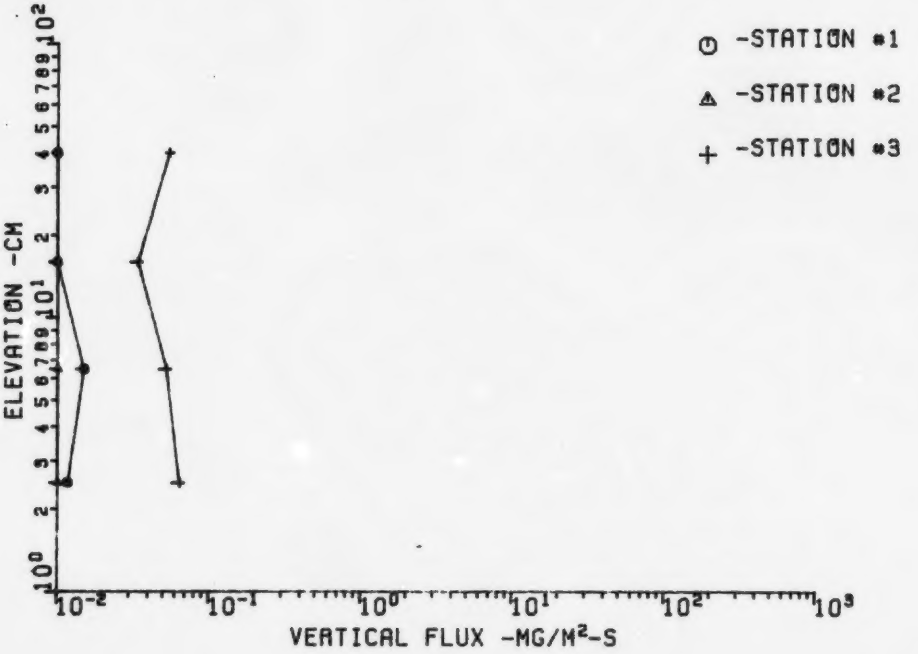

FIGURE 5.35 MEAN VERTICAL FLUX PROFILES FOR

MEAN VALUES FOR TURBULENCE LOW   SURFACE DRY   NOMINAL WIND 7.5 M/S

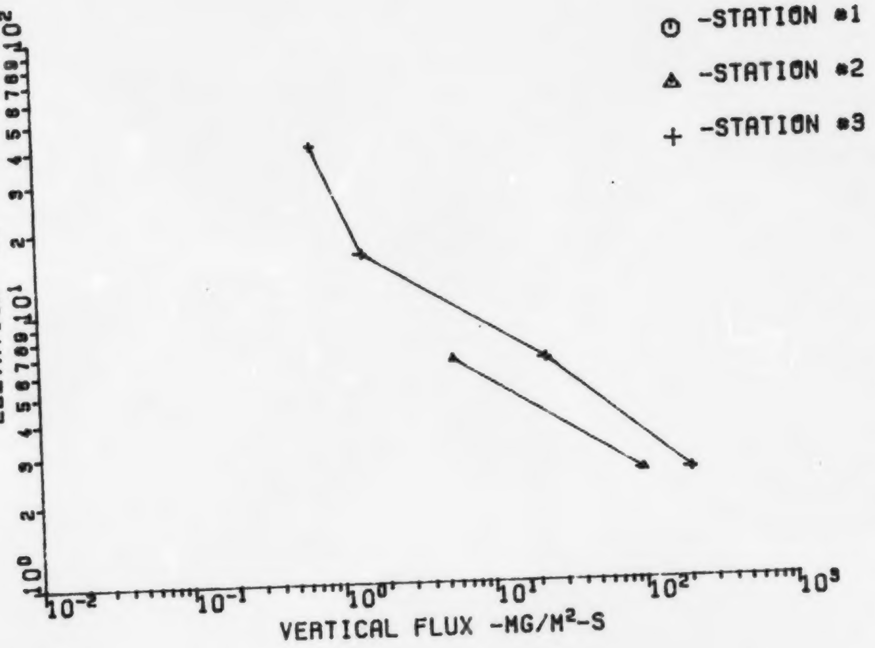

MEAN VALUES FOR TURBULENCE HIGH   SURFACE DRY   NOMINAL WIND 7.5 M/S

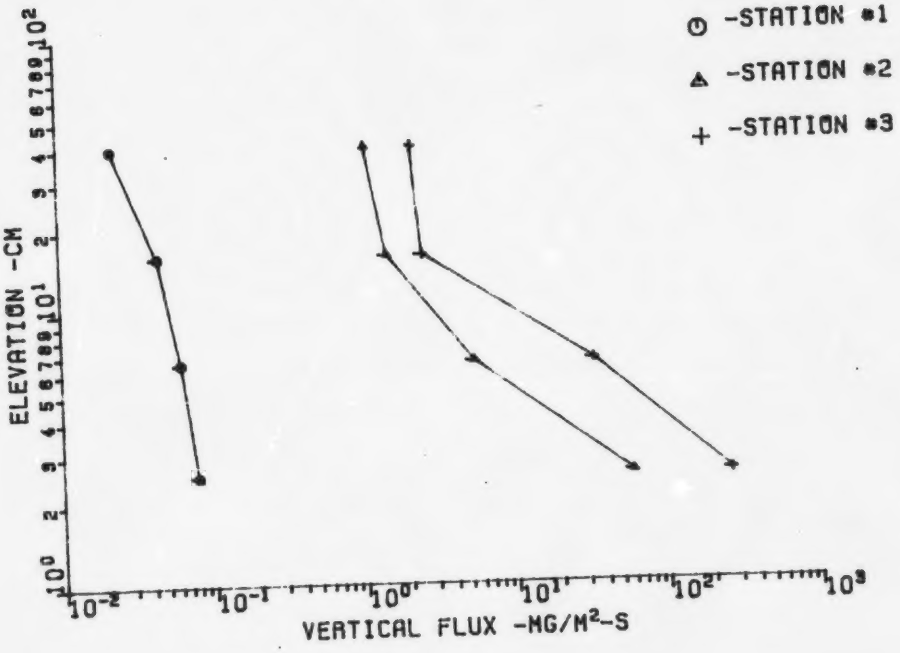

FIGURE 5.36 MEAN VERTICAL FLUX PROFILES FOR

TURBULENCE LOW   SURFACE DRY   NOMINAL WIND 9.5 M/S   REP # 1

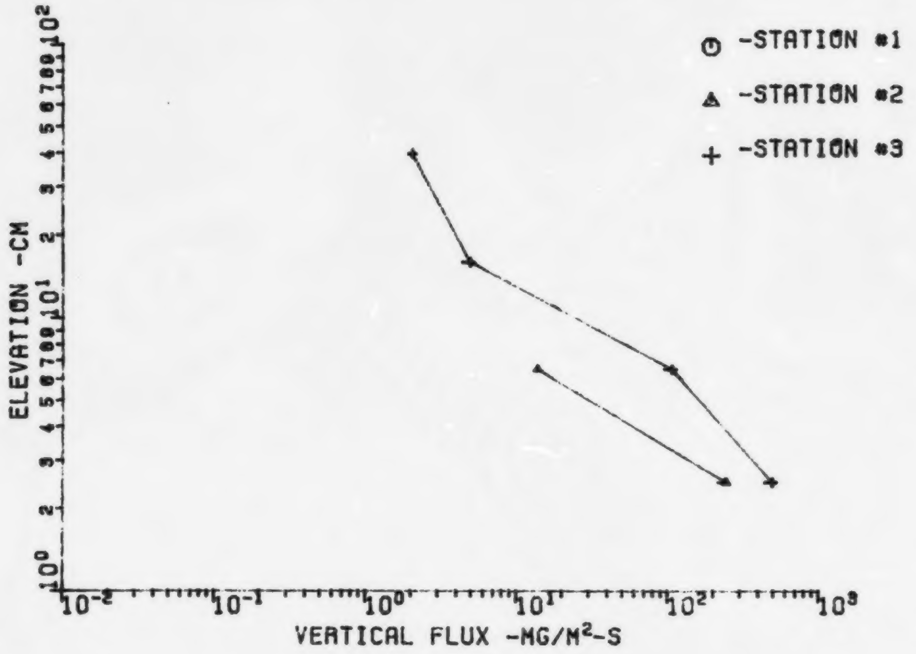

TURBULENCE HIGH   SURFACE DRY   NOMINAL WIND 9.5 M/S   REP # 1

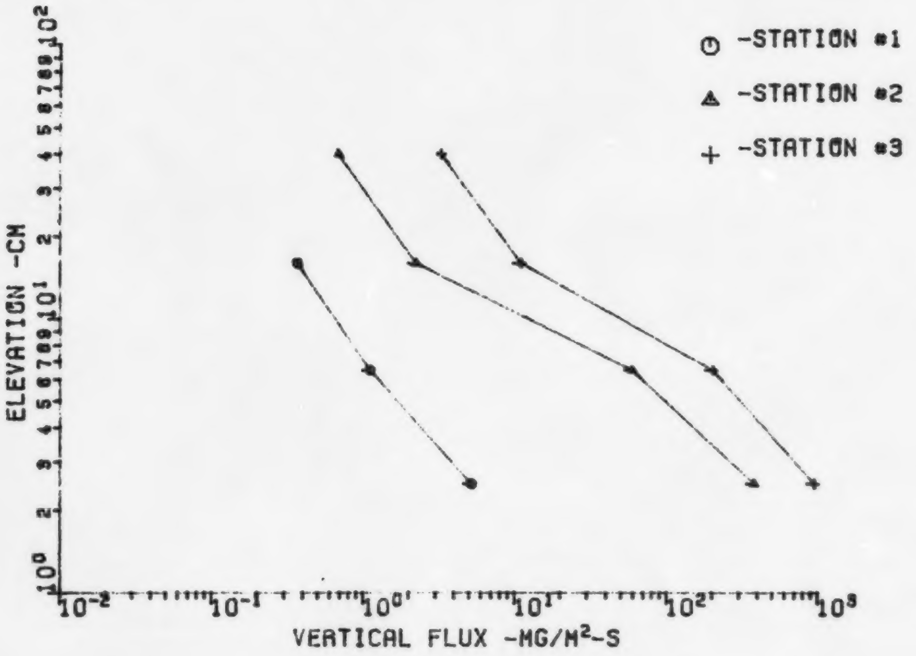

FIGURE 5.37 MEAN VERTICAL FLUX PROFILES FOR

MEAN VALUES FOR TURBULENCE LOW SURFACE WET NOMINAL WIND 4.5 M/S

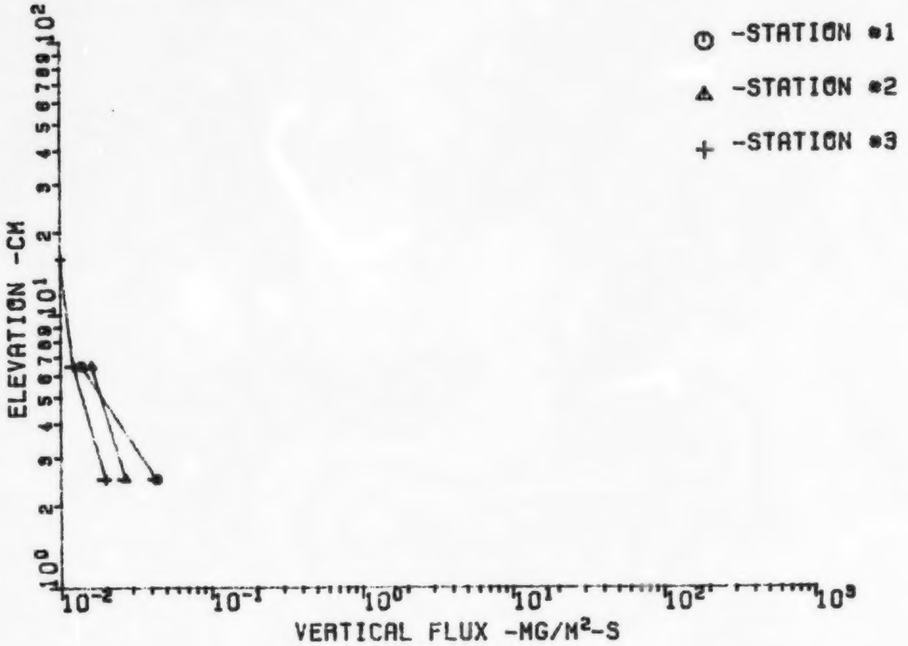

MEAN VALUES FOR TURBULENCE HIGH SURFACE WET NOMINAL WIND 4.5 M/S

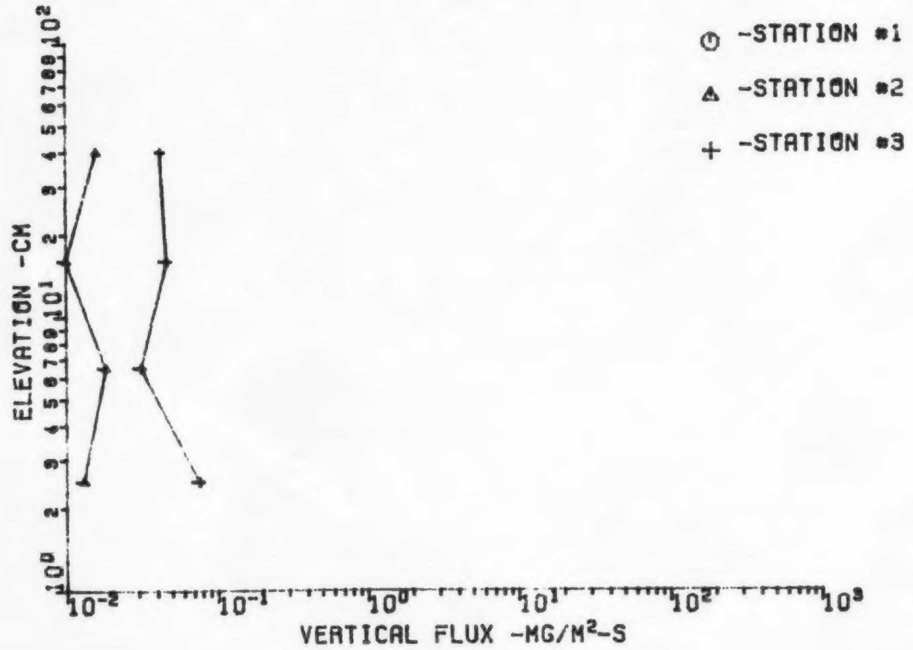

FIGURE 5.38 MEAN VERTICAL FLUX PROFILES FOR

MEAN VALUES FOR TURBULENCE LOW SURFACE WET NOMINAL WIND 7.5 M/S

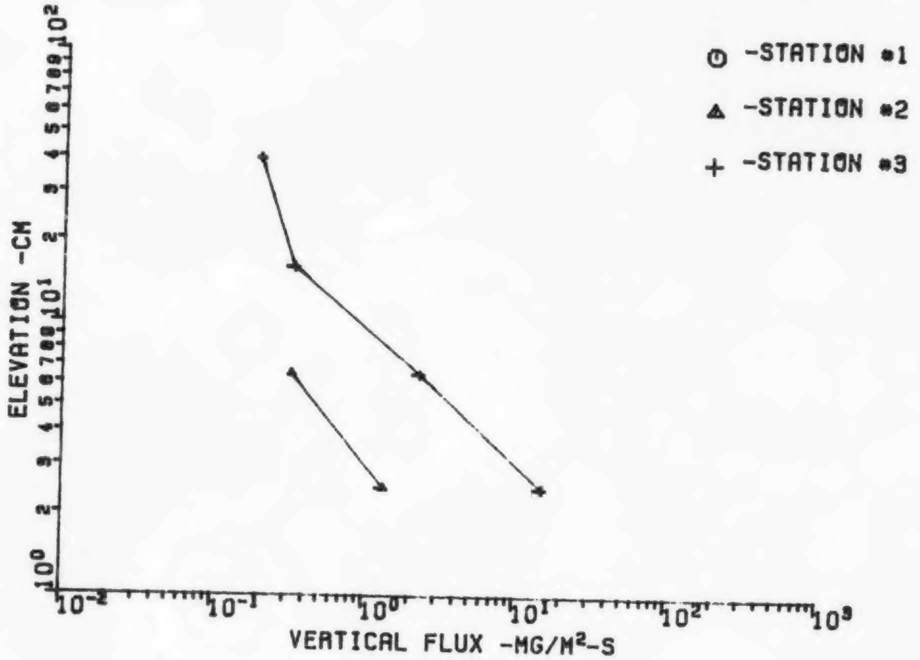

TURBULENCE HIGH SURFACE WET NOMINAL WIND 7.5 M/S REP # 2

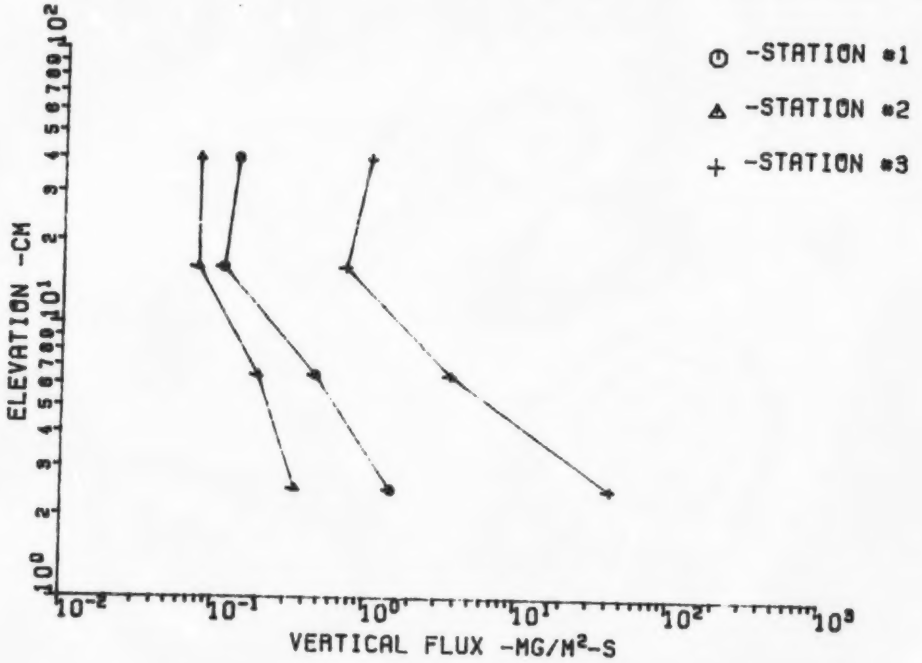

FIGURE 5.39 MEAN VERTICAL FLUX PROFILES FOR

TURBULENCE LOW SURFACE WET NOMINAL WIND 9.5 M/S REP * 1

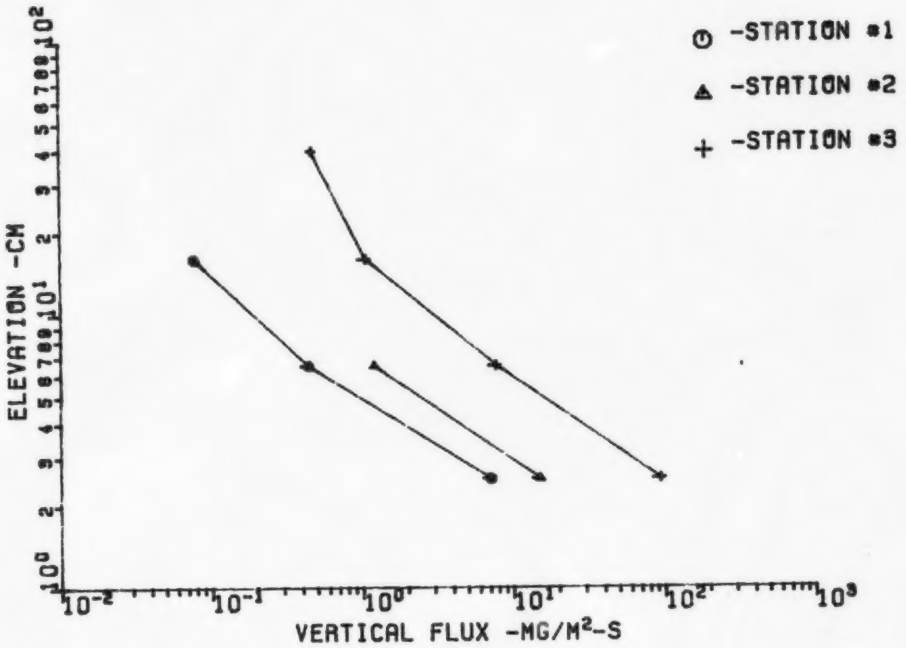

TURBULENCE HIGH SURFACE WET NOMINAL WIND 9.5 M/S REP * 1

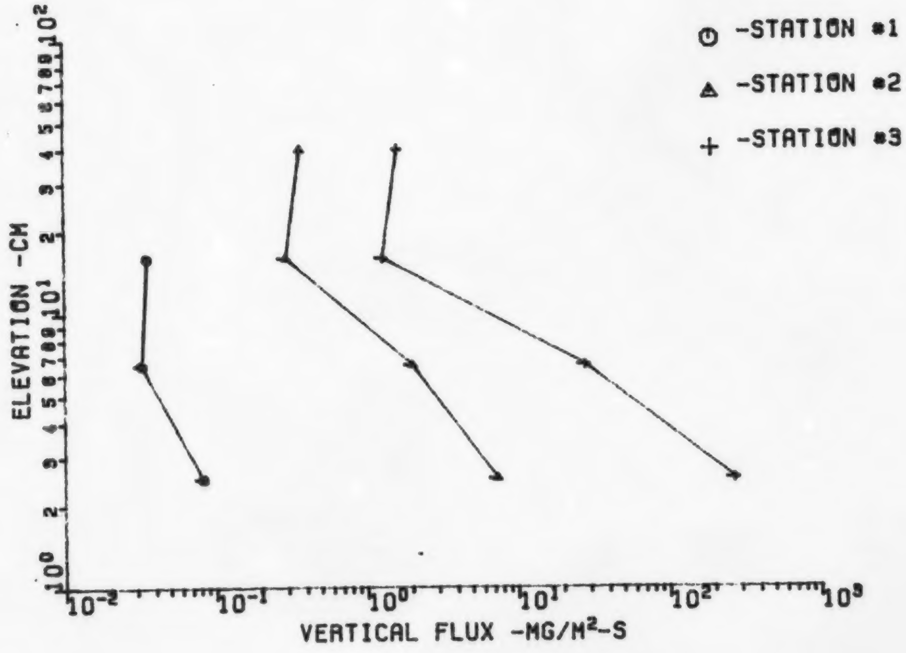

FIGURE 5.40 DRY VERTICAL FLUX @ 2.5 CM VS. U_*

VERTICAL FLUX OVER TAILINGS PILE: TRANSITION PLUS STEADY STATE REGIONS

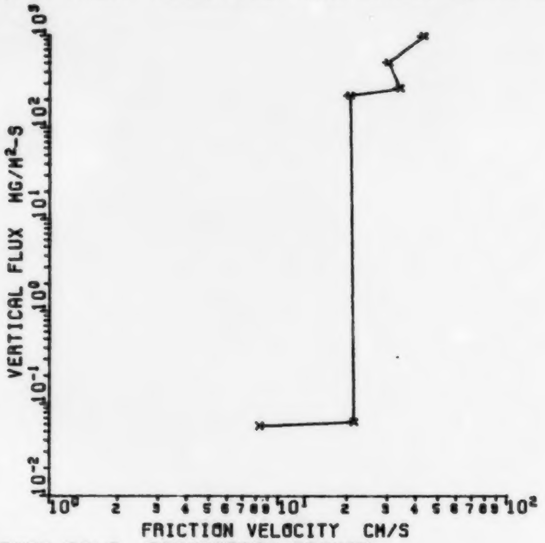

VERTICAL FLUX OVER TAILINGS PILE: TRANSITION REGION

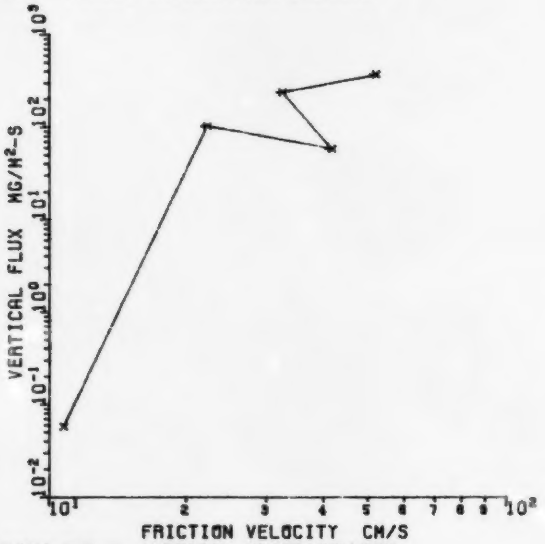

VERTICAL FLUX OVER TAILINGS PILE: STEADY STATE REGION

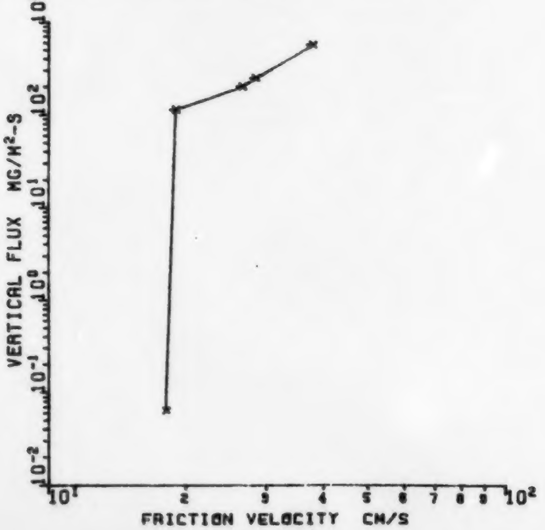

FIGURE 5.41 WET VERTICAL FLUX @2.5 CM VS. U*

VERTICAL FLUX OVER TAILINGS PILE: TRANSITION PLUS STEADY STATE REGIONS

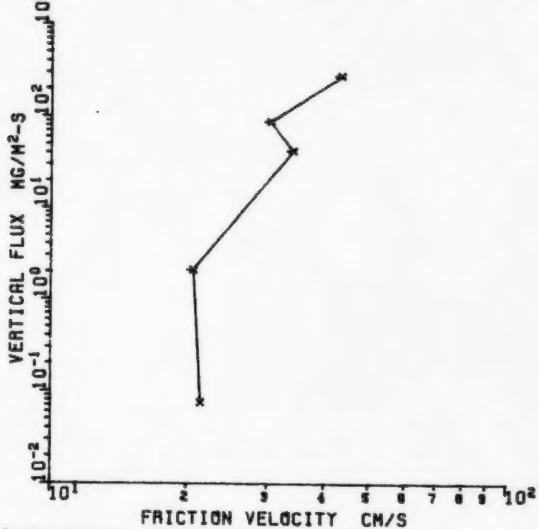

VERTICAL FLUX OVER TAILINGS PILE: TRANSITION REGION

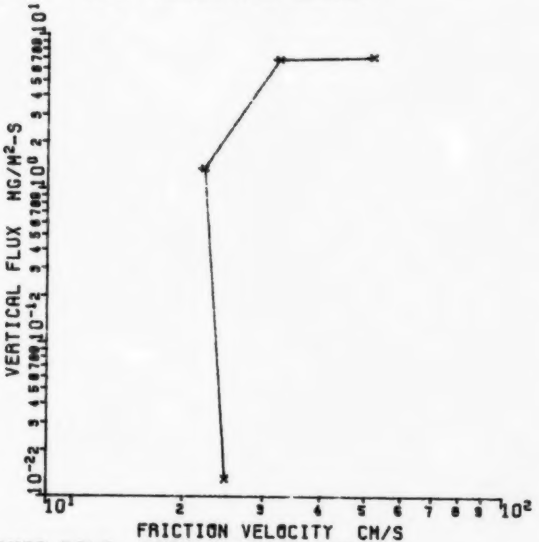

VERTICAL FLUX OVER TAILINGS PILE: STEADY STATE REGION

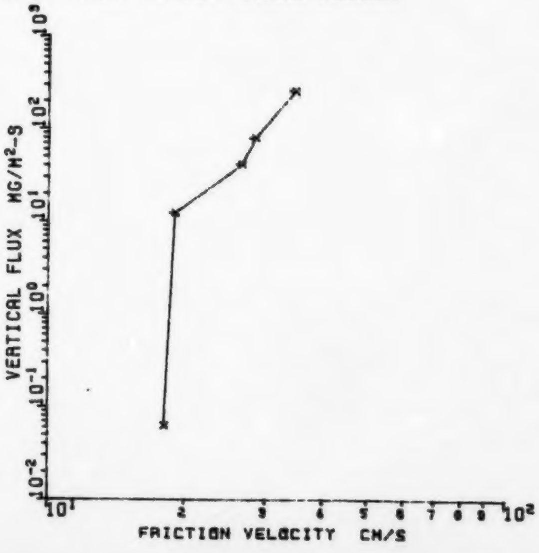

FIGURE 5.42 DRY VERTICAL FLUX, SALTATION FLUX AND SUSPENSION FACTOR VS. U*

VERTICAL FLUX OVER TAILINGS PILE: STEADY STATE REGION

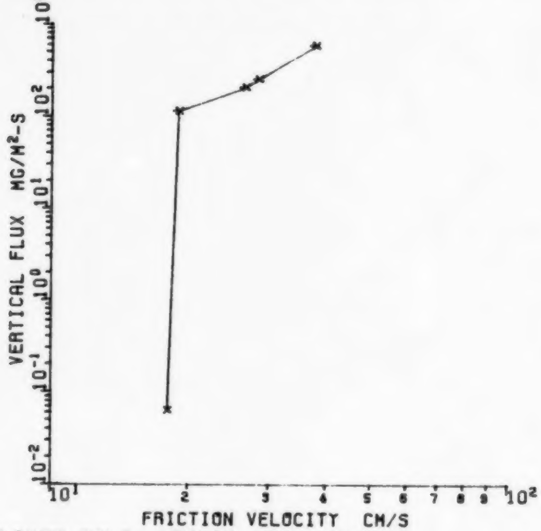

SALTATION RATE OVER TAILINGS PILE: STEADY STATE REGION

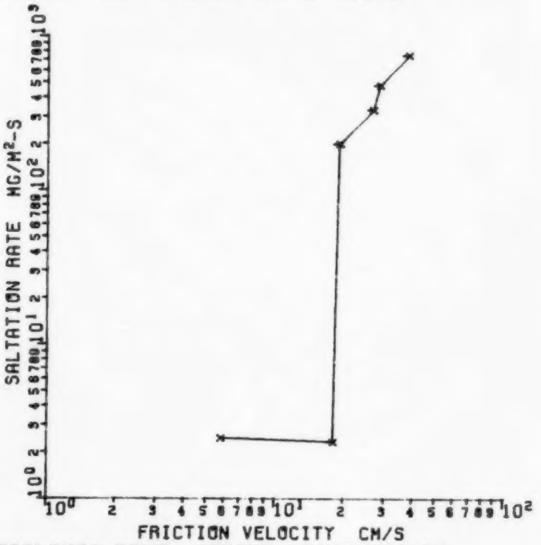

SUSPENSION FACTOR OVER TAILINGS PILE: STEADY STATE REGION

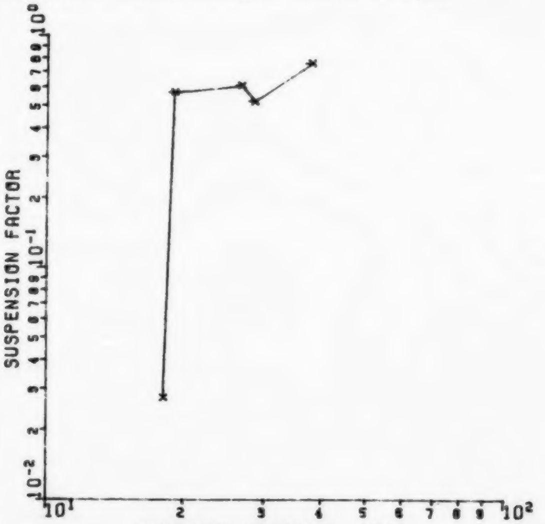

FIGURE 5.43 WET VERTICAL FLUX, SALTATION FLUX AND SUSPENSION FACTOR VS. U*

VERTICAL FLUX OVER TAILINGS PILE: STEADY STATE REGION

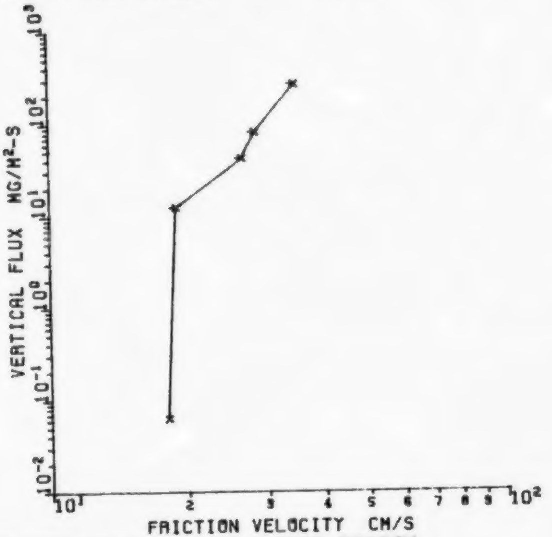

SALTATION RATE OVER TAILINGS PILE: STEADY STATE REGION

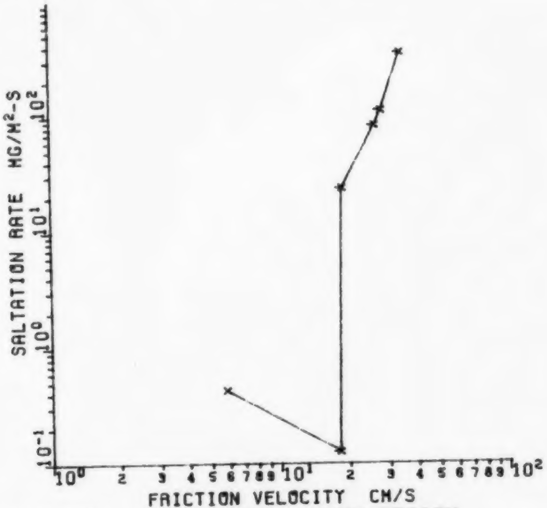

SUSPENSION FACTOR OVER TAILINGS PILE: STEADY STATE REGION

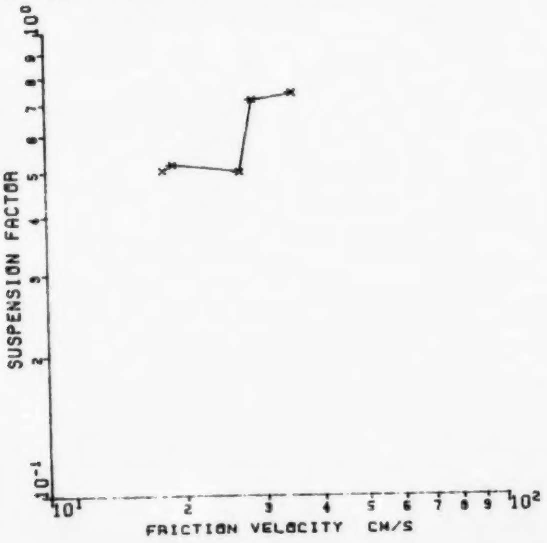

FIGURE 5.44

NET VERTICAL FLUX OVER DRY TAILINGS PILE: STEADY STATE REGION

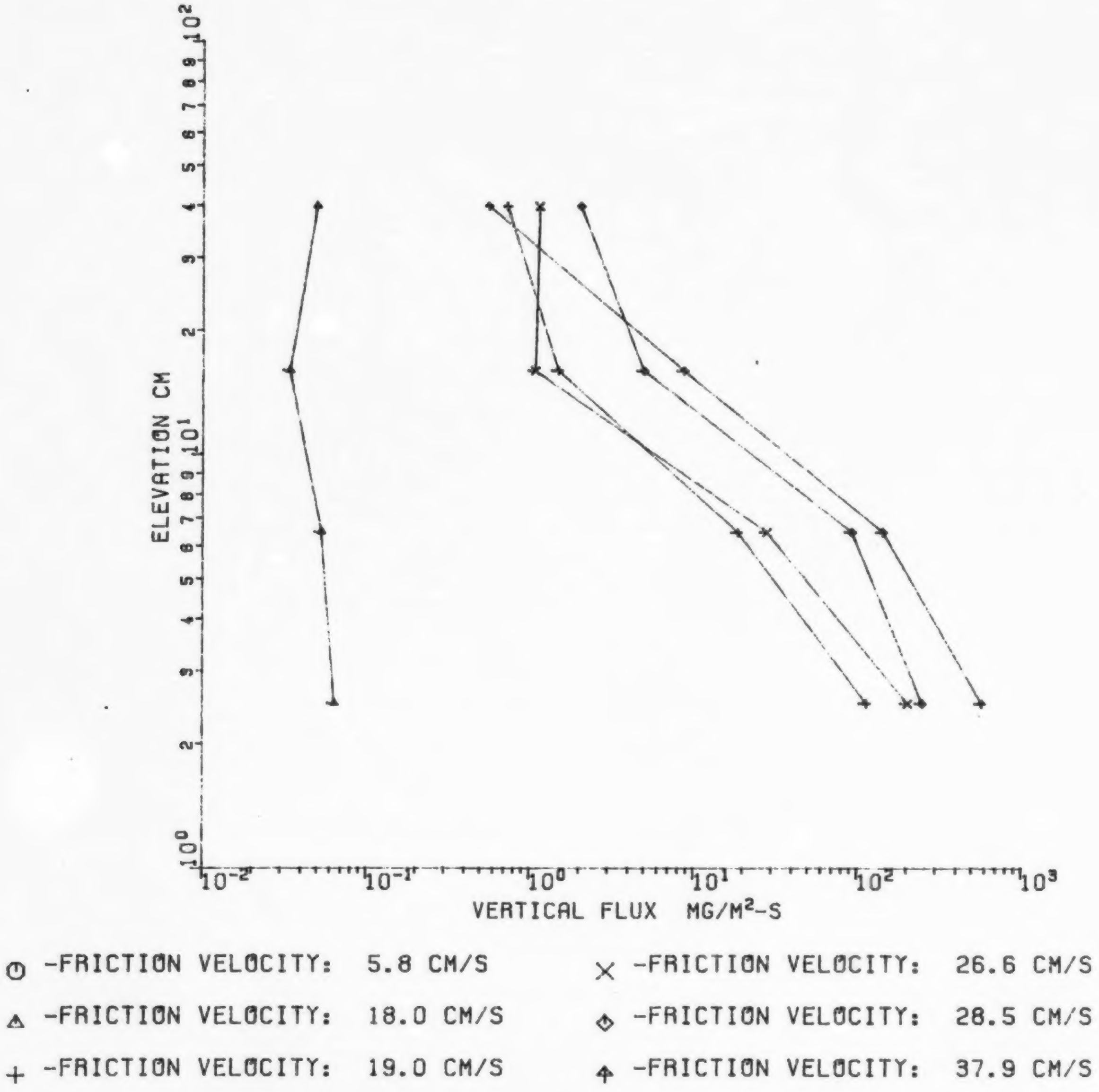

FIGURE 5.45

NET VERTICAL FLUX OVER WET TAILINGS PILE: STEADY STATE REGION

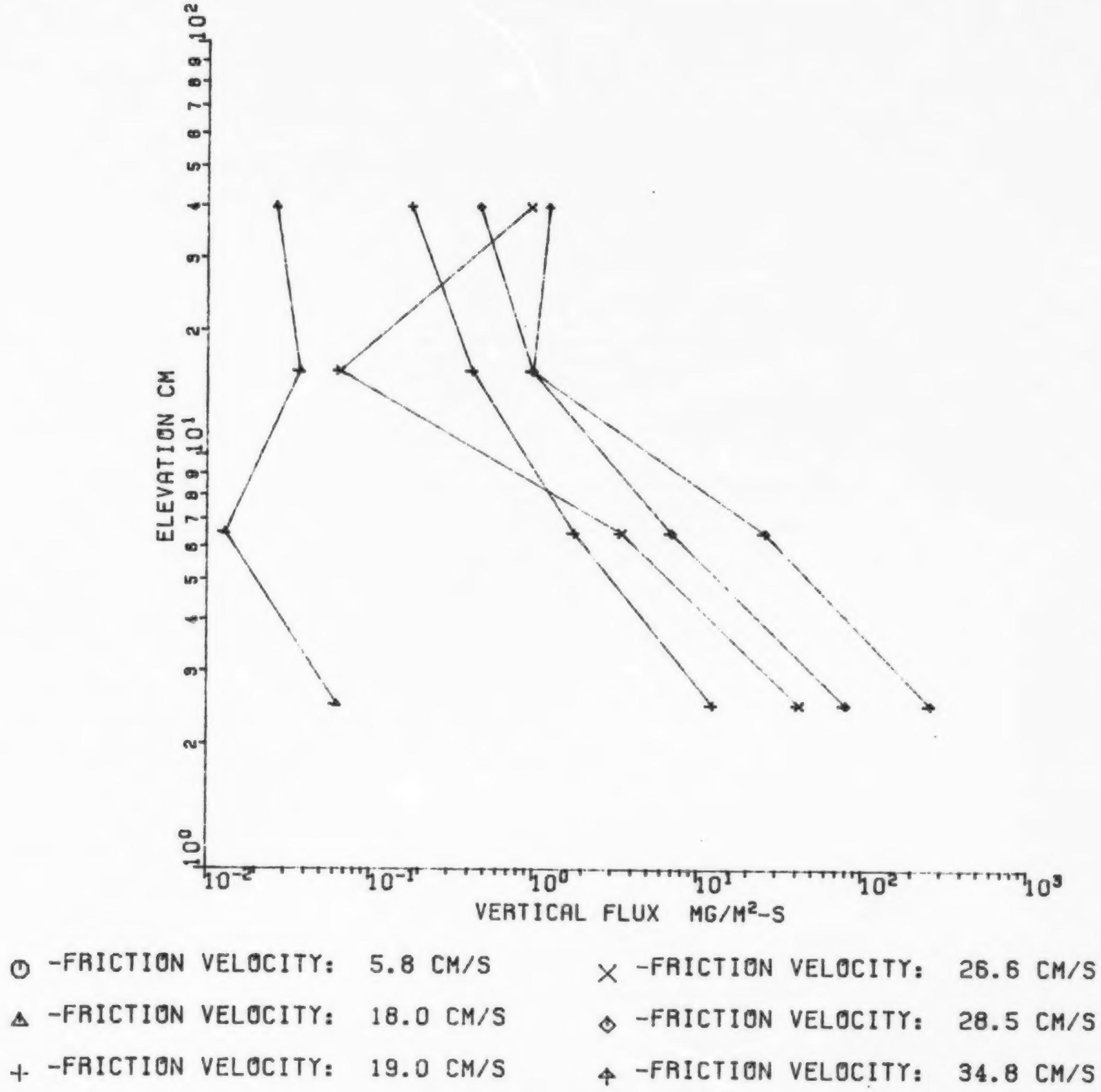

FIGURE 5.46

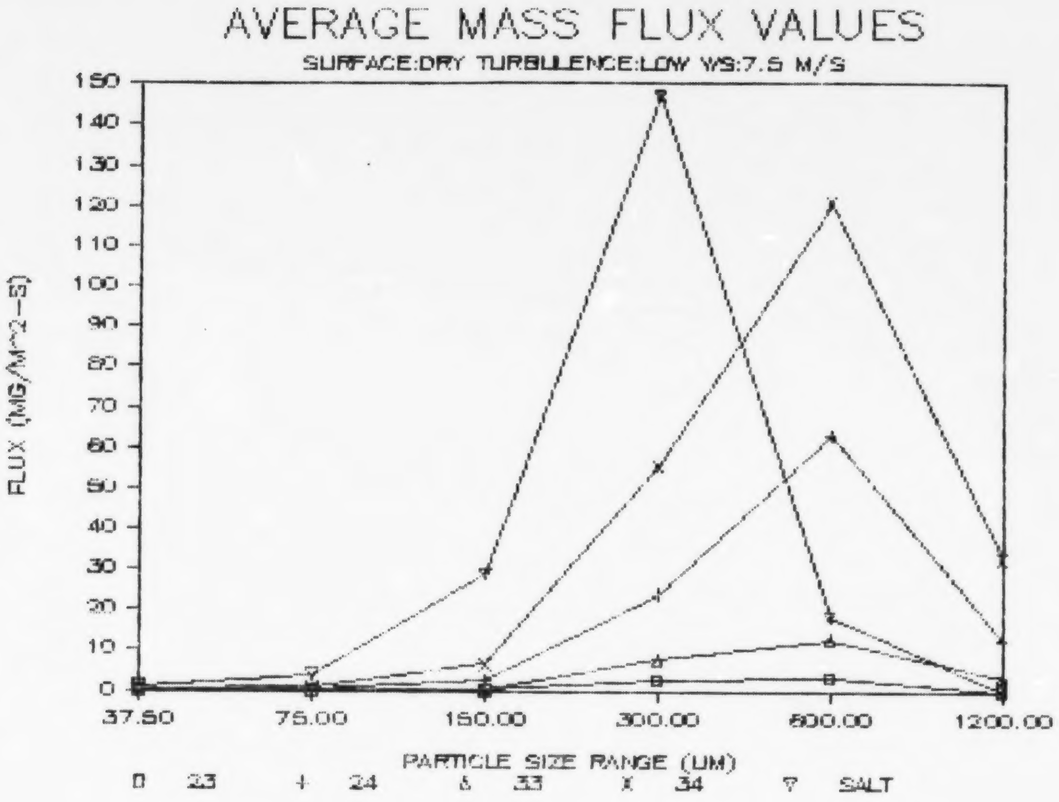
AVERAGE MASS FLUX VALUES
SURFACE:DRY TURBULENCE:LOW WS:7.5 M/S

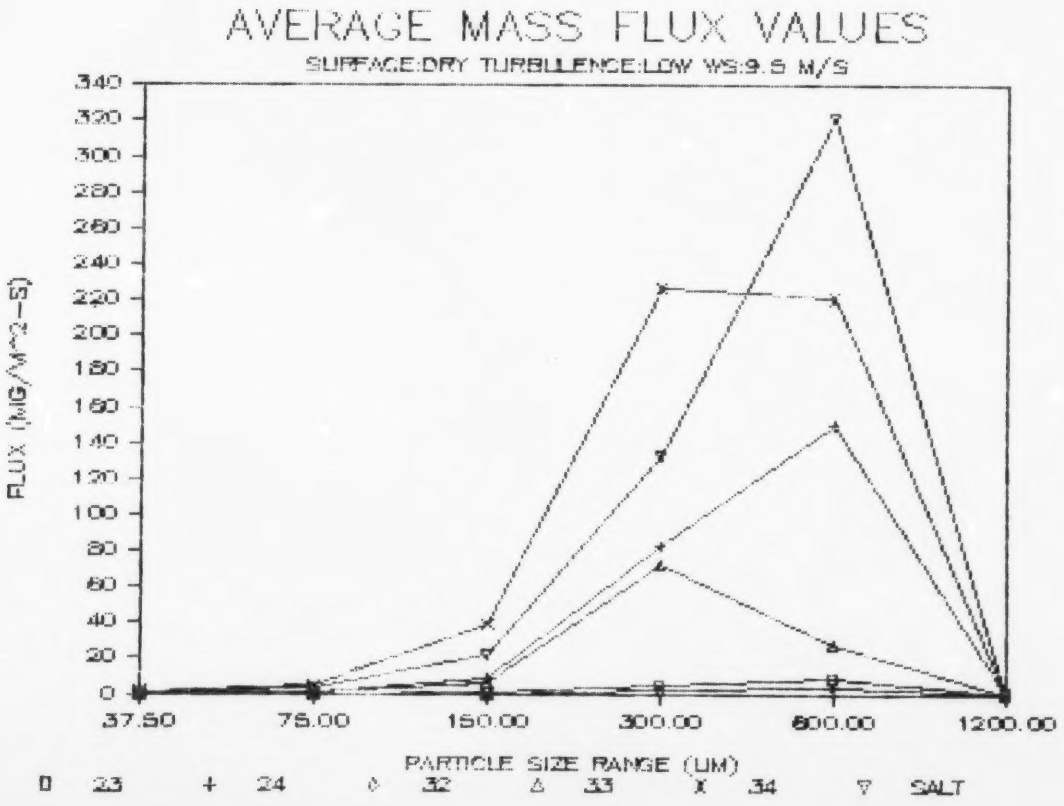
AVERAGE MASS FLUX VALUES
SURFACE:DRY TURBULENCE:LOW WS:9.5 M/S

FIGURE 5.47

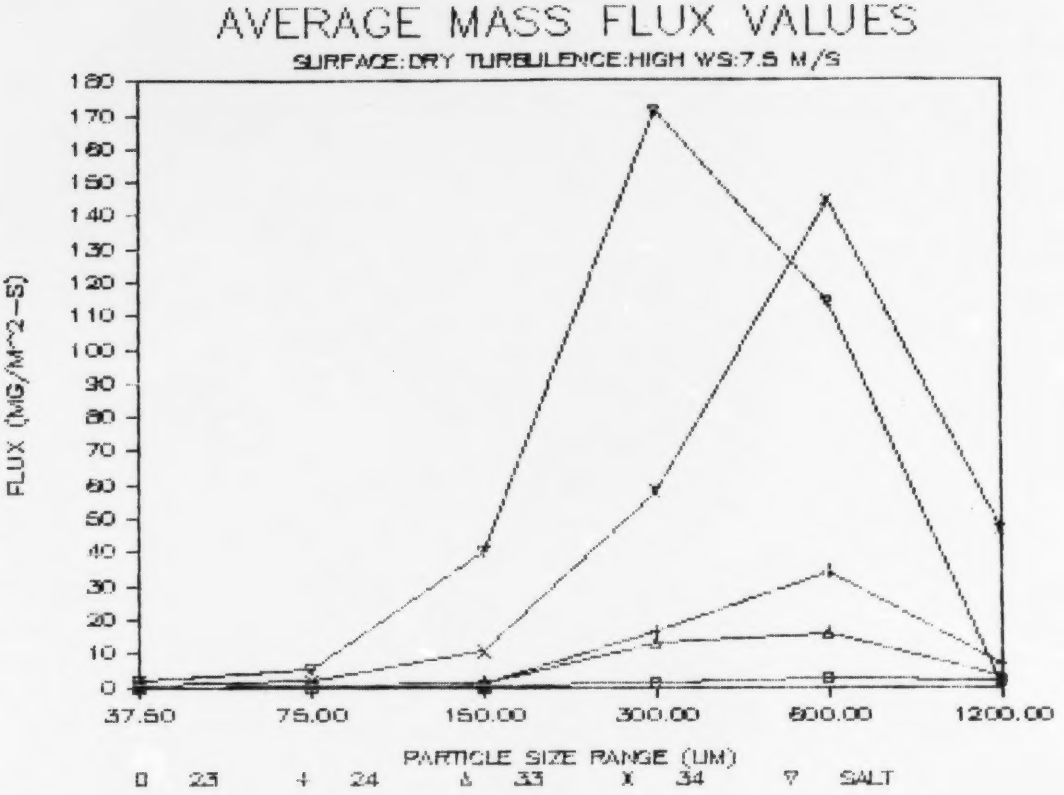
AVERAGE MASS FLUX VALUES
SURFACE:DRY TURBULENCE:HIGH WS:7.5 M/S
FLUX (MG/M^2-S)
180
170
160
150
140
130
120
110
100
90
80
70
60
50
40
30
20
10
0
37.50
75.00
150.00
300.00
600.00
1200.00
PARTICLE SIZE RANGE (UM)
□ 23
+ 24
△ 33
X 34
▽ SALT

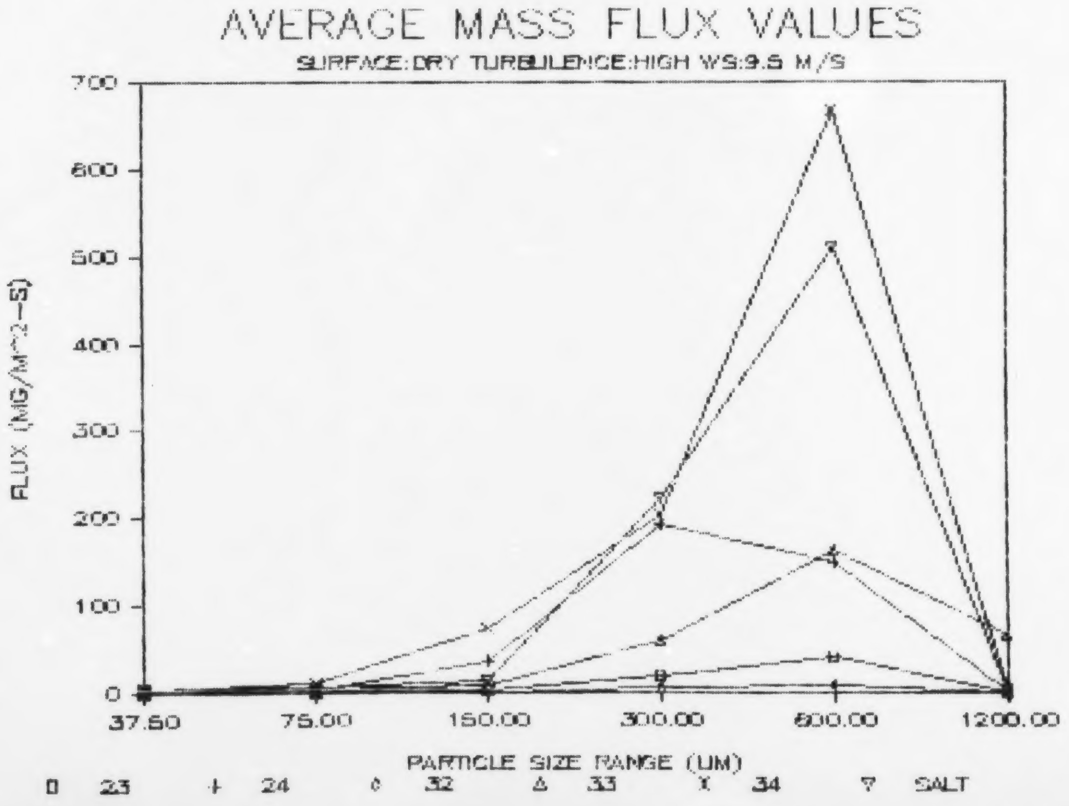
AVERAGE MASS FLUX VALUES
SURFACE:DRY TURBULENCE:HIGH WS:9.5 M/S
FLUX (MG/M^2-S)
700
600
500
400
300
200
100
0
37.50
75.00
150.00
300.00
600.00
1200.00
PARTICLE SIZE RANGE (UM)
□ 23
+ 24
◇ 32
△ 33
X 34
▽ SALT

FIGURE 5.48

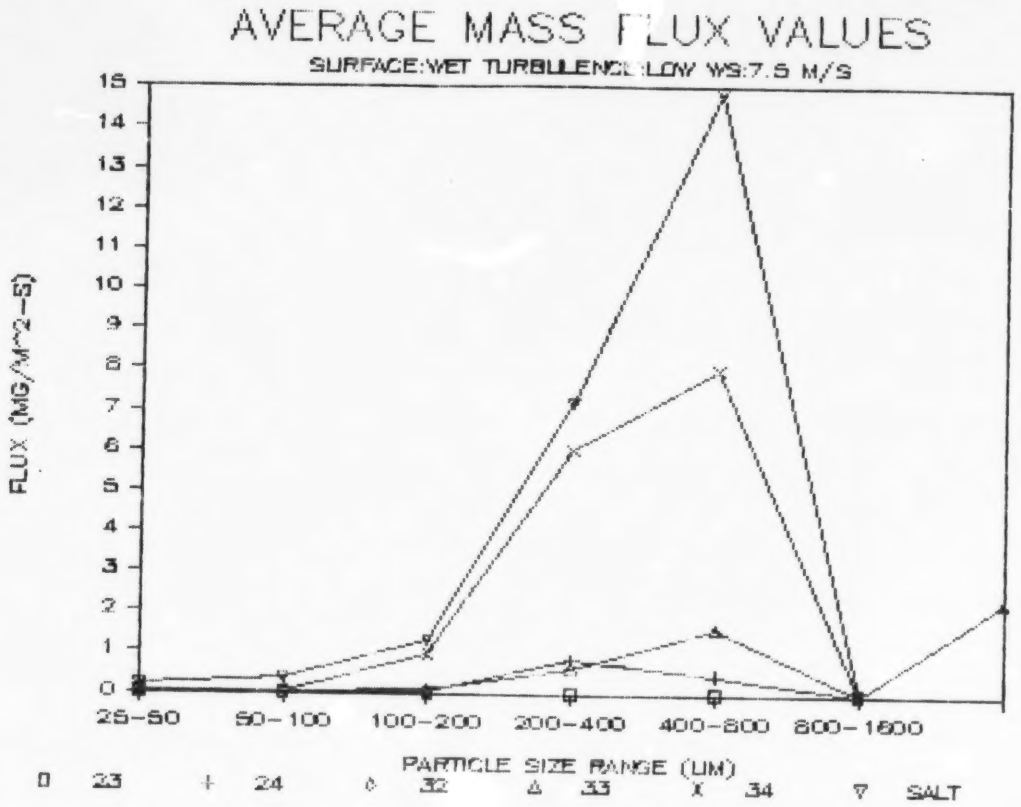
AVERAGE MASS FLUX VALUES
SURFACE:WET TURBULENCE:LOW WS:7.5 M/S
FLUX (MG/M^2-S)
15
14
13
12
11
10
9
8
7
6
5
4
3
2
1
0
25-50
50-100
100-200
200-400
400-800
800-1600
PARTICLE SIZE RANGE (UM)
□ 23
+ 24
◊ 32
△ 33
X 34
▽ SALT

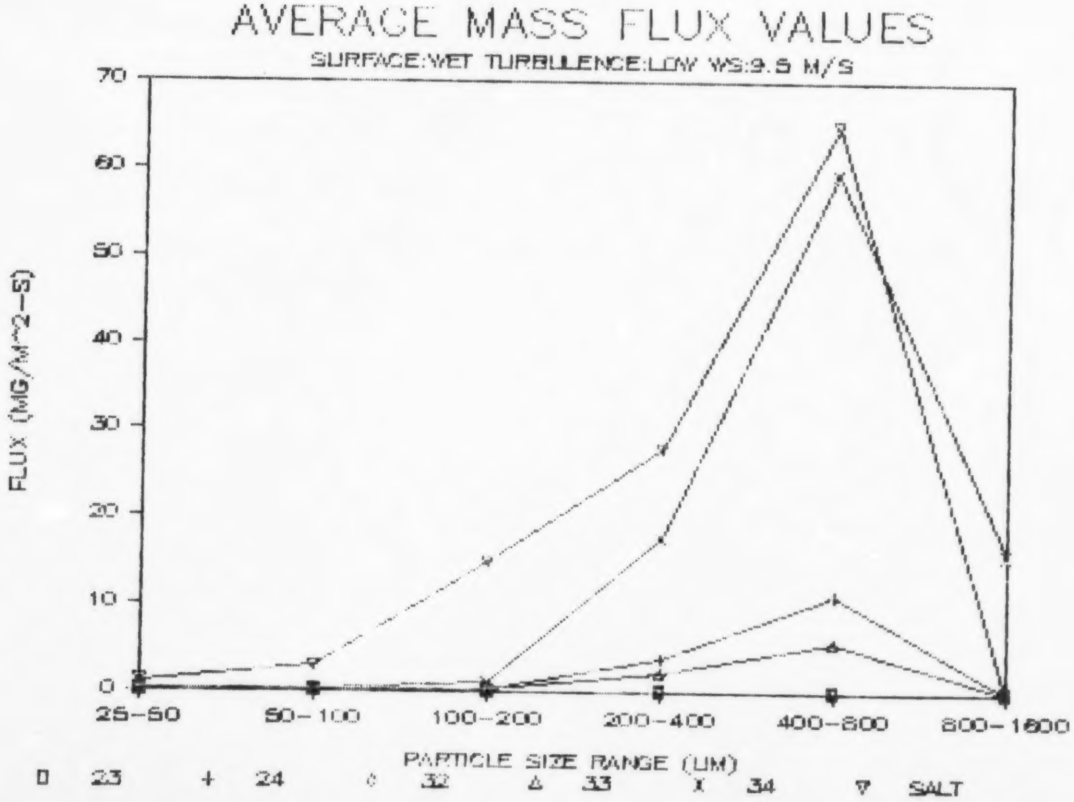
AVERAGE MASS FLUX VALUES
SURFACE:WET TURBULENCE:LOW WS:9.5 M/S
FLUX (MG/M^2-S)
70
60
50
40
30
20
10
0
25-50
50-100
100-200
200-400
400-800
800-1600
PARTICLE SIZE RANGE (UM)
□ 23
+ 24
◊ 32
△ 33
X 34
▽ SALT

FIGURE 5.49

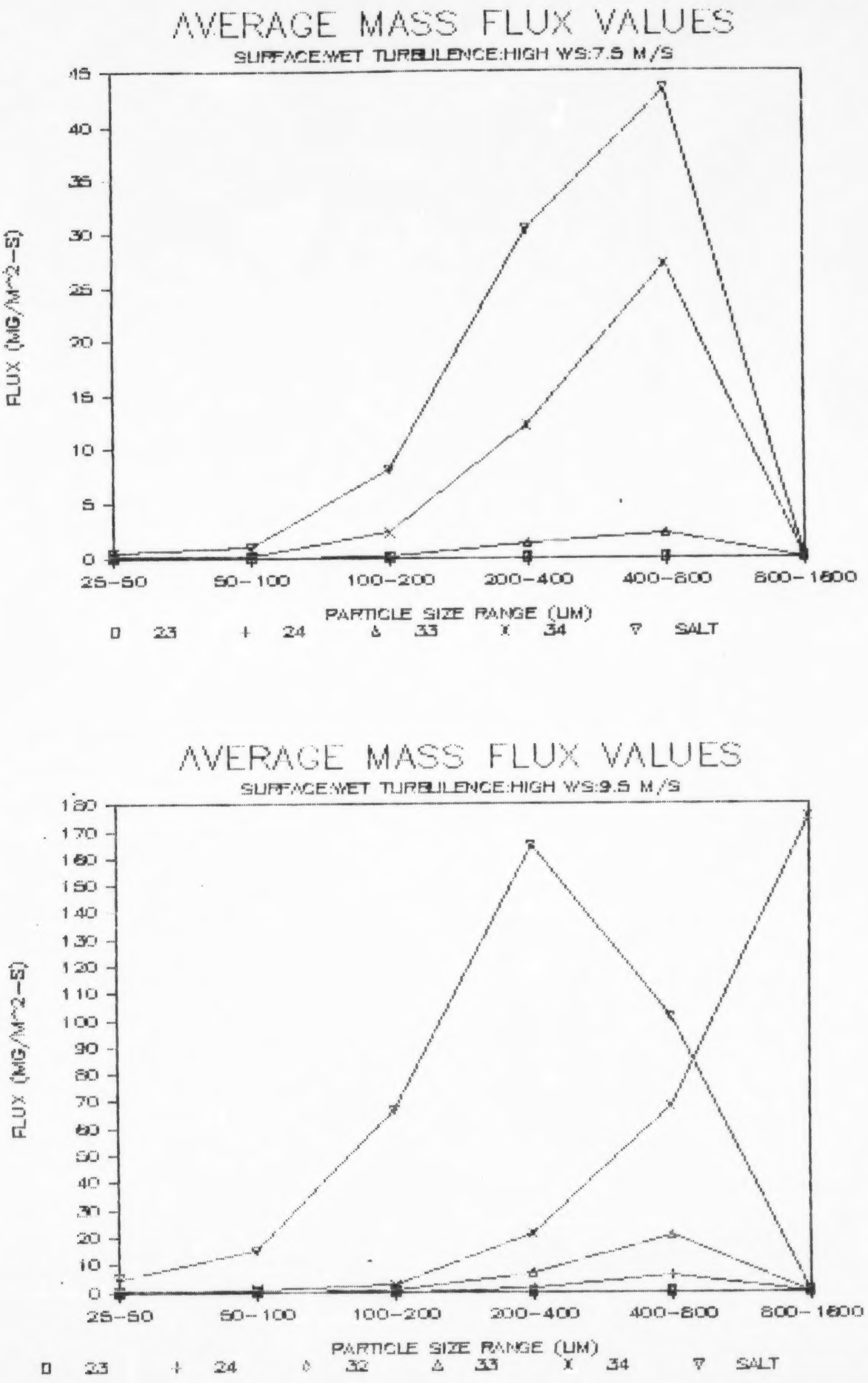

AVERAGE MASS FLUX VALUES

SURFACE:WET TURBULENCE:HIGH WS:7.5 M/S

AVERAGE MASS FLUX VALUES

SURFACE:WET TURBULENCE:HIGH WS:9.5 M/S

FIGURE 5.50

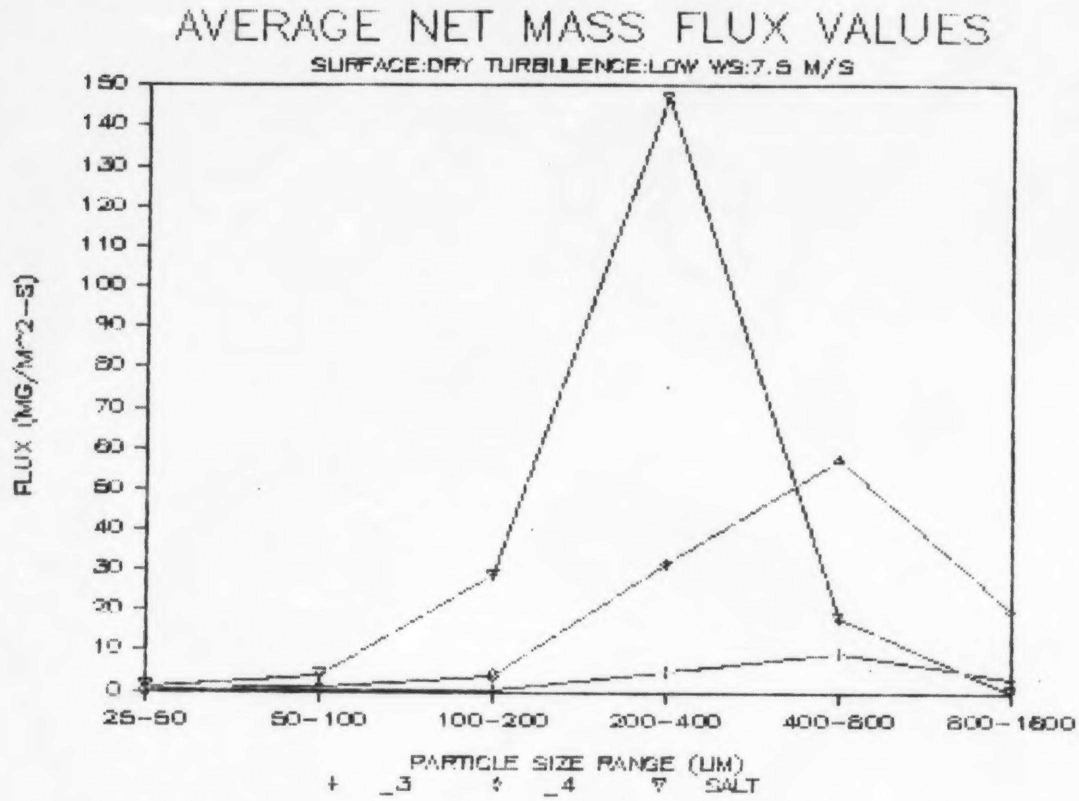

AVERAGE NET MASS FLUX VALUES
SURFACE:DRY TURBULENCE:LOW WS:7.5 M/S
FLUX (MG/M^2-S)
0
10
20
30
40
50
60
70
80
90
100
110
120
130
140
150
25-50
50-100
100-200
200-400
400-800
800-1600
PARTICLE SIZE RANGE (UM)
+ _3
◇ _4
▽ SALT

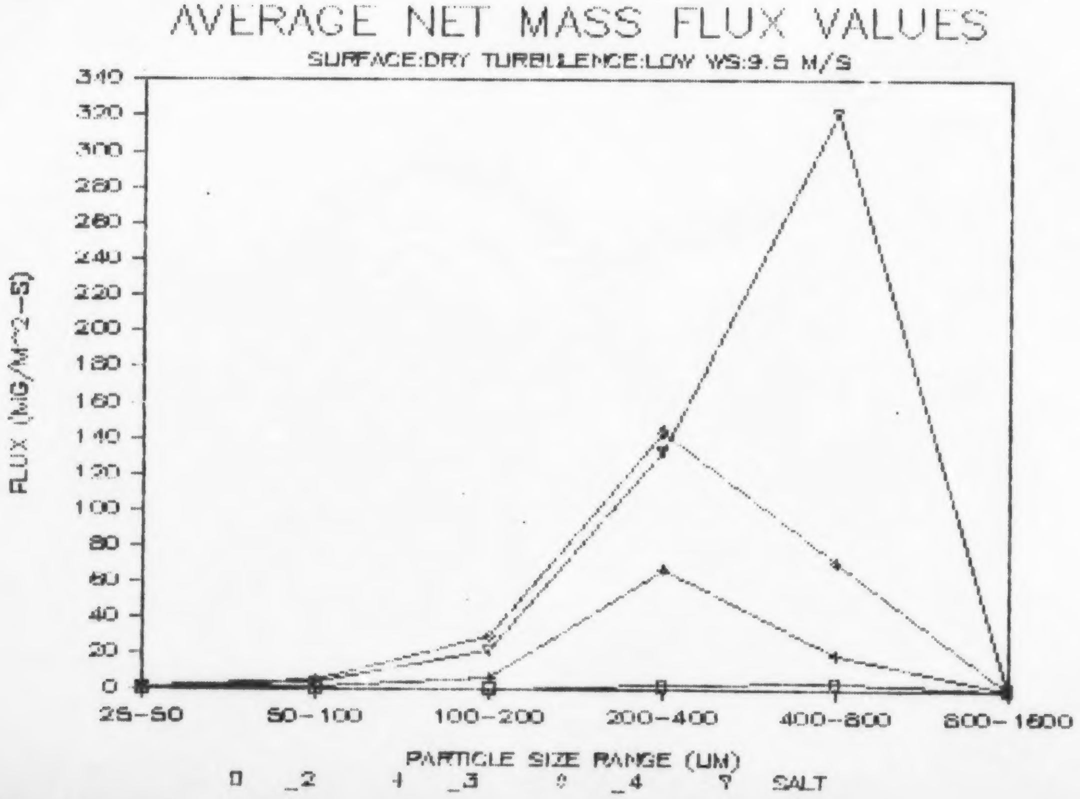

AVERAGE NET MASS FLUX VALUES
SURFACE:DRY TURBULENCE:LOW WS:9.5 M/S
FLUX (MG/M^2-S)
0
20
40
60
80
100
120
140
160
180
200
220
240
260
280
300
320
340
25-50
50-100
100-200
200-400
400-800
800-1600
PARTICLE SIZE RANGE (UM)
□ _2
+ _3
◇ _4
▽ SALT

FIGURE 5.51

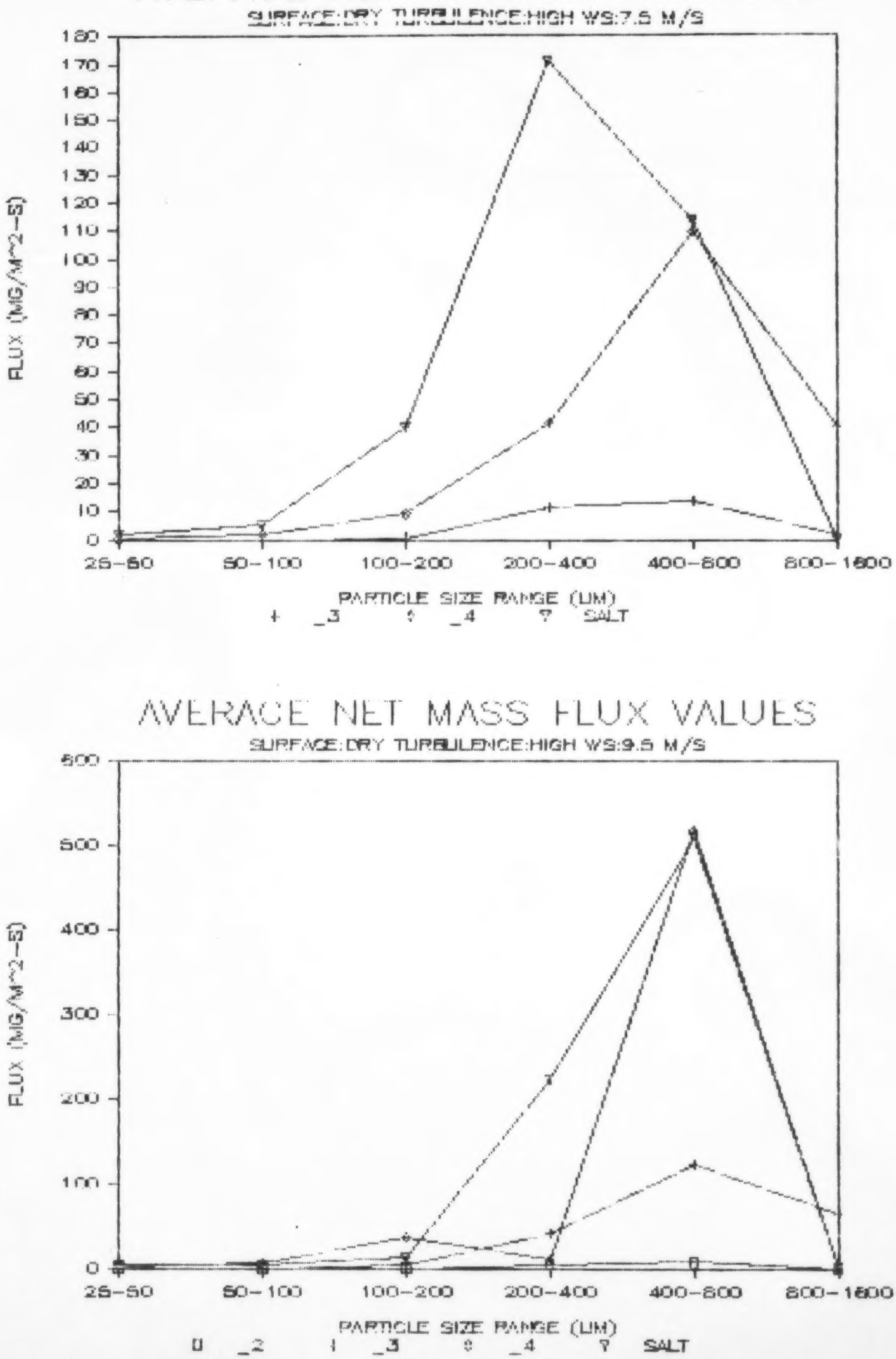
AVERAGE NET MASS FLUX VALUES
SURFACE:DRY TURBULENCE:HIGH WS:7.5 M/S

AVERAGE NET MASS FLUX VALUES
SURFACE:DRY TURBULENCE:HIGH WS:9.5 M/S

FIGURE 5.52

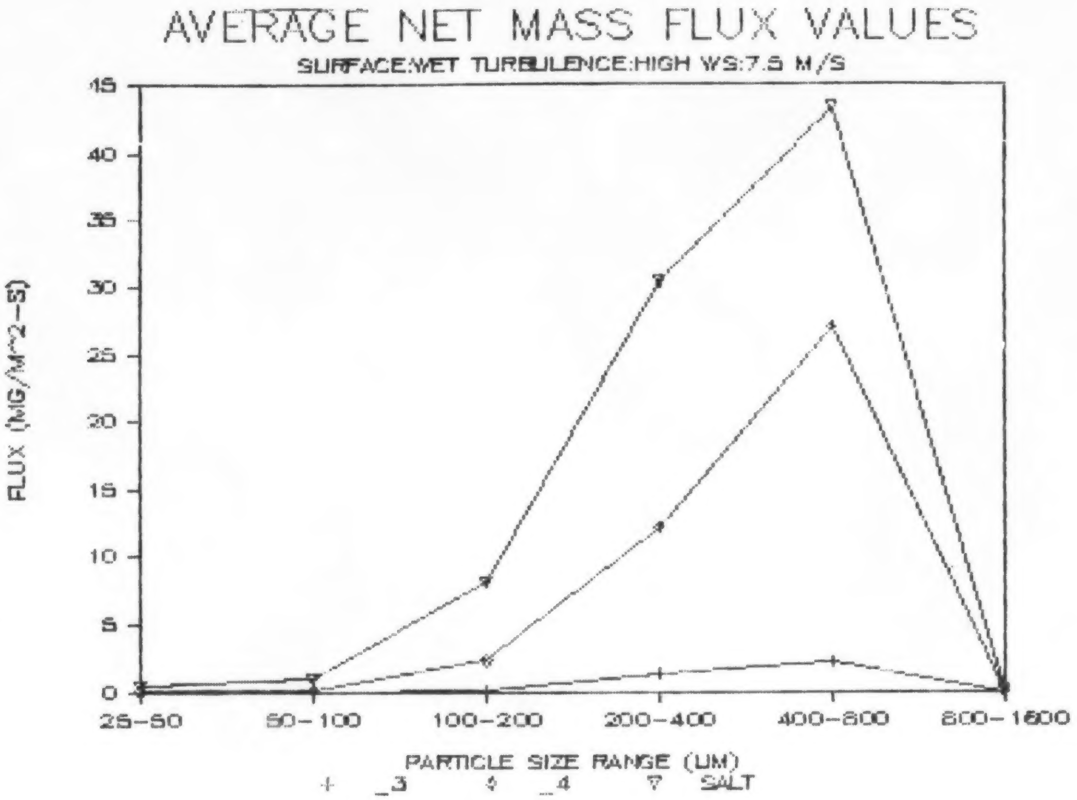
AVERAGE NET MASS FLUX VALUES
SURFACE:WET TURBULENCE:HIGH WS:7.5 M/S
FLUX (MG/M^2-S)
45
40
35
30
25
20
15
10
5
0
25-50
50-100
100-200
200-400
400-800
800-1600
PARTICLE SIZE RANGE (UM)
+ _3
◇ _4
▽ SALT

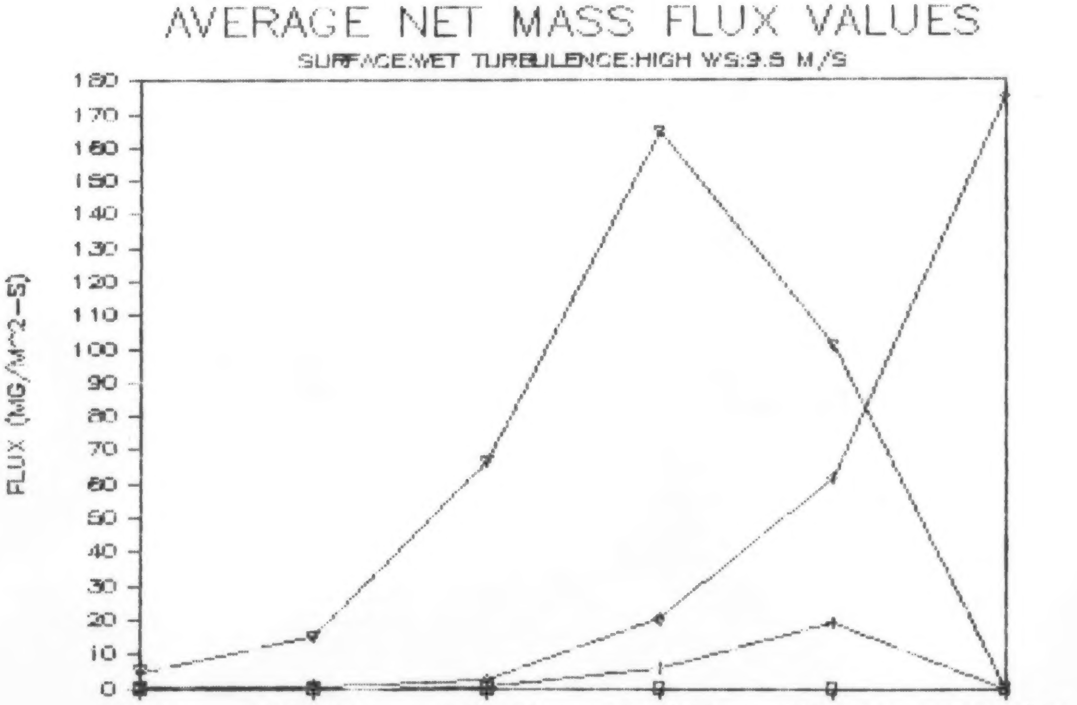
AVERAGE NET MASS FLUX VALUES
SURFACE:WET TURBULENCE:HIGH WS:9.5 M/S
FLUX (MG/M^2-S)
180
170
160
150
140
130
120
110
100
90
80
70
60
50
40
30
20
10
0
25-50
50-100
100-200
200-400
400-800
800-1600
PARTICLE SIZE RANGE (UM)
□ _2
+ _3
◇ _4
▽ SALT

FIGURE 5.53

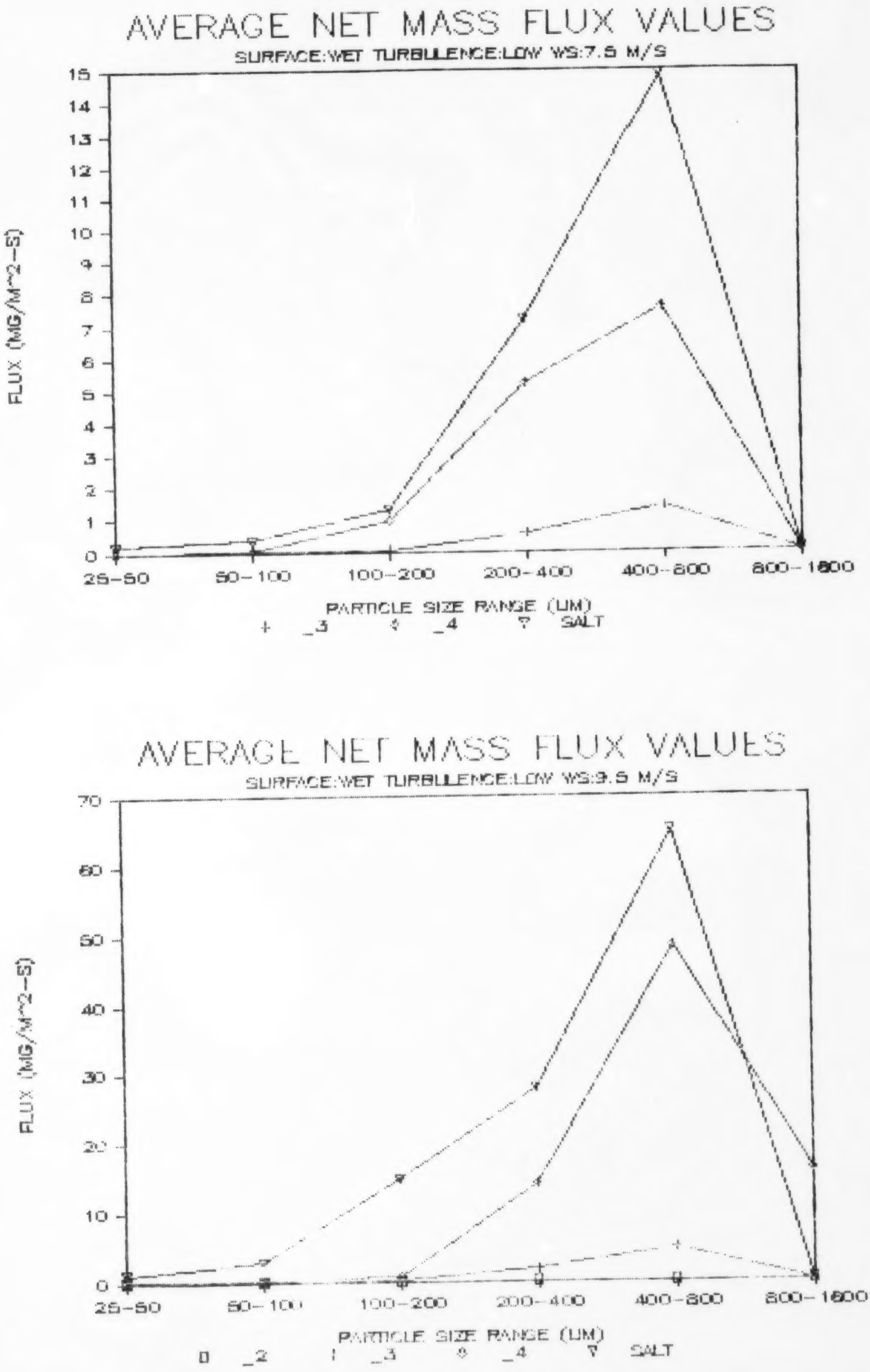
AVERAGE NET MASS FLUX VALUES

SURFACE:WET TURBULENCE:LOW WS:7.5 M/S

AVERAGE NET MASS FLUX VALUES

SURFACE:WET TURBULENCE:LOW WS:9.5 M/S